Institute for
Theoretical Physics
University of Cologne

Exploring Matter-Antimatter Asymmetry in a Rotating Universe

Inaugural-Dissertation
zur
Erlangung des Doktorgrades
der Mathematisch-Naturwissenschaftlichen Fakultät
der Universität zu Köln

vorgelegt von

Tatevik Vardanyan

angenommen im Jahr 2025

Abstract

This thesis investigates the potential role of spatial anisotropies and global rotation in addressing the observed matter-antimatter asymmetry in the universe.

The standard cosmological model, ΛCDM, faces several unresolved puzzles, including CMB anomalies, dark matter, and the matter-antimatter asymmetry. The CMB anomalies suggest deviations from isotropy, prompting the exploration of more general anisotropic models. Additionally, current solutions to dark matter and matter-antimatter asymmetry imply the need for extensions beyond the Standard Model. Given these issues, it is crucial to question the accuracy of the FLRW geometry in ΛCDM. This thesis explores the rotating Bianchi IX universe, motivated by the BKL conjecture and the potential role of global rotation in cosmological angular momentum generation, in an effort to investigate the anisotropic effects of geometry on the particle spectrum.

The Weyl and Dirac spinor fields are studied within the Bianchi IX universe, considering a range of models, from the axisymmetric Bianchi IX universe to the more general rotating Bianchi IX model. The Hamiltonian for spinor fields in this background is formulated, and the corresponding equations of motion for Weyl and Dirac spinors are derived. The field equations are solved in a fixed background as an initial step toward understanding the particle spectrum in such spacetimes. This approach sets the stage for future refinements using the adiabatic approximation and the WKB approximation. Generalized spinor spherical harmonics are obtained using analogies with the asymmetric "ideal" top. Building on previous work on the diagonal Bianchi IX model, we generalize this approach for spinor fields in a broader Bianchi IX framework.

Our work builds on earlier studies of Weyl spinors and the phenomenon of level crossing, which results in the creation of neutrinos instead of antineutrinos in an axisymmetric Bianchi IX universe as the universe evolves toward isotropy. We extend this analysis to a broader class of models, examining how these effects manifest in more general rotating and anisotropic cosmological backgrounds. While Weyl fermions do not describe neutrinos in nature, the mathematical framework developed here is useful for analyzing the Dirac equations in this context.

For Dirac fermions in the axisymmetric Bianchi IX model, we find that the energy spectrum is significantly influenced by the spin orientation, resulting in spin-dependent enhancements or suppressions for both particles and antiparticles. The inclusion of global rotation introduces further contributions due to the coupling between particle spin and the universe's rotational motion. Specifically, rotational contributions to the energy spectrum cause energy shifts with opposite effects for particles and antiparticles. Depending on the alignment of the spin with the universe's rotation, energy levels are either increased or decreased, leading to complex modifications in the energy structure.

This spin-angular velocity coupling uncovers previously unexplored mechanisms that could contribute to the observed asymmetry between matter and antimatter—effects absent in homogeneous and isotropic models.

Therefore, these results underscore the importance of background anisotropies in the search for an explanation of the matter-antimatter asymmetry and encourage further investigation in this direction. The next logical step in this research is to solve the equations in a time-dependent background, beginning with the adiabatic approximation and later employing the WKB approximation to account for more realistic conditions. Furthermore, the analysis could be extended to include interactions within quantum electrodynamics (QED), enabling the exploration of whether these geometric effects influence particle creation and annihilation processes. These efforts could provide valuable insights into the role of geometric effects in fundamental interactions, contributing to our understanding of the mechanisms driving the matter-antimatter asymmetry in the Universe.

Zusammenfassung

Diese Dissertation untersucht die potenzielle Rolle von räumlichen Anisotropien und globaler Rotation im Universum zur Erklärung der beobachteten Materie-Antimaterie-Asymmetrie.

Das Standard-Kosmologiemodell, ΛCDM, steht vor mehreren ungelösten Rätseln, einschließlich Anomalien im kosmischen Mikrowellenhintergrund (CMB), dunkler Materie und der Materie-Antimaterie-Asymmetrie. Die CMB-Anomalien deuten auf Abweichungen von der Isotropie hin, was die Untersuchung allgemeinerer anisotroper Modelle anregt. Darüber hinaus implizieren die aktuellen Lösungen für dunkle Materie und Materie-Antimaterie-Asymmetrie die Notwendigkeit von Erweiterungen über das Standardmodell hinaus. Angesichts dieser Probleme ist es entscheidend, die Genauigkeit der FLRW-Geometrie im Rahmen von ΛCDM zu hinterfragen. Diese Dissertation untersucht das rotierende Bianchi-IX-Universum, das durch die BKL-Vermutung und die potenzielle Rolle der globalen Rotation in der Erzeugung von kosmologischem Drehimpuls motiviert ist, um die anisotropen Effekte der Geometrie auf das Teilchenspektrum zu untersuchen.

Die Weyl- und Dirac-Spinorfelder werden im Kontext des Bianchi-IX-Universums untersucht. Es wird eine Reihe von Modellen betrachtet, vom achsensymmetrischen Bianchi-IX-Universum bis hin zum allgemeineren rotierenden Bianchi-IX-Modell. Der Hamiltonoperator für Spinorfelder in diesem Hintergrund wird formuliert, und die entsprechenden Bewegungsgleichungen für Weyl- und Dirac-Spinoren werden abgeleitet. Die Feldgleichungen werden in einem festen Hintergrund als erster Schritt zur Untersuchung des Teilchenspektrums in solchen Raumzeiten gelöst. Dieser Ansatz bildet die Grundlage für zukünftige Verfeinerungen unter Verwendung der adiabatischen Näherung und der WKB-Näherung. Verallgemeinerte spinorische sphärische Harmonien werden unter Verwendung von Analogien mit dem asymmetrischen „idealen“ Kegel erhalten. Aufbauend auf früheren Arbeiten zum diagonalen Bianchi-IX-Modell verallgemeinern wir diesen Ansatz für Spinorfelder in einem breiteren Bianchi-IX-Rahmen.

Unsere Arbeit baut auf früheren Studien von Weyl-Spinoren und dem Phänomen des Levelcrossings auf, das zur Entstehung von Neutrinos anstelle von Antineutrinos in einem achsensymmetrischen Bianchi-IX-Universum führt, während sich das Universum in Richtung Isotropie entwickelt. Wir erweitern diese Analyse auf eine breitere Klasse von Modellen und untersuchen, wie diese Effekte in allgemeineren rotierenden und anisotropen kosmologischen Hintergründen auftreten. Während Weyl-Fermionen in der Natur keine Neutrinos beschreiben, ist der hier entwickelte mathematische Rahmen nützlich, um die Dirac-Gleichungen in diesem Kontext zu analysieren.

Für Dirac-Fermionen im achsensymmetrischen Bianchi-IX-Modell stellen wir fest,

dass das Energiespektrum erheblich von der Spinorientierung beeinflusst wird, was zu spinabhängigen Verstärkungen oder Abschwächungen sowohl für Teilchen als auch für Antiteilchen führt. Die Einbeziehung globaler Rotation führt zu weiteren Beiträgen aufgrund der Kopplung zwischen Teilchenspin und der Rotationsbewegung des Universums. Insbesondere verursachen die rotatorischen Beiträge zum Energiespektrum Energieverschiebungen mit gegensätzlichen Effekten für Teilchen und Antiteilchen. Abhängig von der Ausrichtung des Spins mit der Rotation des Universums werden die Energieniveaus entweder erhöht oder verringert, was zu komplexen Änderungen in der Energiestruktur führt. Diese Kopplung von Spin und Winkelgeschwindigkeit zeigt bislang unerforschte Mechanismen auf, die zur beobachteten Asymmetrie zwischen Materie und Antimaterie im Universum beitragen könnten – Effekte, die in homogenen und isotropen Modellen fehlen.

Daher unterstreichen diese Ergebnisse die Bedeutung von Hintergrundanisotropien in der Suche nach einer Erklärung der Materie-Antimaterie-Asymmetrie und regen zu weiteren Untersuchungen in diese Richtung an. Der nächste logische Schritt in dieser Forschung besteht darin, die Gleichungen in einem zeitabhängigen Hintergrund zu lösen, beginnend mit der adiabatischen Näherung und später unter Verwendung der WKB-Näherung, um realistischere Bedingungen zu berücksichtigen. Darüber hinaus könnte die Analyse auf die Einbeziehung von Wechselwirkungen im Rahmen der Quanten-Elektrodynamik (QED) ausgeweitet werden, um zu untersuchen, ob diese geometrischen Effekte die Erzeugung und Vernichtung von Teilchen beeinflussen. Diese Bemühungen könnten wertvolle Einblicke in die Rolle geometrischer Effekte in fundamentalen Wechselwirkungen bieten und unser Verständnis der Mechanismen erweitern, welche die Materie-Antimaterie-Asymmetrie im Universum antreiben.

Notation and Conventions

Mathematical Symbols

$:=$	Definition.
$\approx$	Approximately equal to.
$\propto$	Proportional to.
$\sim$	Asymptotically equal to.
$\equiv$	Identical by definition.
$\gtrsim$	Greater than or approximately equal to.
$\in$	Element of a set.
$\forall$	"For all" (universal quantifier).
$(.,.)$	Scalar product.
$[.,.]$	Commutator: $[A,B] = AB - BA$.
$\{.,.\}$	Anticommutator: $\{A,B\} = AB + BA$.
$\langle . . \rangle$	Correlation function.
$\wedge$	Wedge product.
∂_μ	Partial derivative with respect to coordinate x^μ.
$\mathbb{R}$	Set of real numbers.
$(.)^*$	Complex conjugation.
$(.)^T$	Transpose of a matrix.
$(.)^\dagger$	Hermitian adjoint (complex conjugate transpose).

Conventions

- We adopt natural units: $\hbar = c = 1$.
- The metric signature convention used is $(-,+,+,+)$.
- Greek indices $(\mu, \nu, \ldots)$ denote spacetime components and run as $\mu = 0, 1, 2, 3$.
- Latin indices $(i, j, \ldots)$ denote spatial components and run as $i = 1, 2, 3$.
- Greek indices with a hat, i.e., $\hat{\alpha}, \hat{\beta}$, refer to the local inertial frame.
- Einstein summation convention is assumed, i.e., $\sum_i A_i B^i$ is written as $A_i B^i$.

Content

1 Introduction and motivation

There are four fundamental forces in Nature. Three of them—the strong, electromagnetic, and weak forces—are described by quantum field theory and form the basis of the Standard Model of particle physics. The gravitational force, on the other hand, is described by Einstein's General Theory of Relativity (GR), which is a classical theory. These two theories together provide the theoretical framework for cosmology, which aims to study the origin, evolution, and large-scale structure of the universe.

General Relativity is an extremely successful theory that has passed numerous observational tests across both astrophysical and cosmological scales. These include phenomena such as the deflection of light, the perihelion precession, gravitational redshift, and cosmic expansion. Recent exciting developments include the direct detection of gravitational waves by LIGO [1] and the imaging of a black hole's shadow [2]. Despite its success, GR faces a breakdown due to the occurrence of spacetime singularities under general conditions, as predicted by the Hawking-Penrose singularity theorems [3], [4]. Singularities occur in black holes and, in cosmology, at the beginning of the evolution of the Universe, known as the Big Bang singularity. Thus, GR fails to describe the physics in the early Universe at high-energy scales near the Big Bang singularity.

It is expected that singularities can be avoided in a fundamental quantum gravity (QG) theory [5]. However, since a complete QG theory is not yet available, the only framework we can currently rely on to describe physical interactions in the early Universe is Quantum Field Theory (QFT) in curved spacetime. Unfortunately, this theory itself faces several conceptual and technical challenges, including issues with renormalization, the ambiguity of the vacuum state due to the lack of Poincaré invariance, and the fundamental definition of a particle in curved spacetime [6]. The study of particle production and interactions in the early Universe is, therefore, only possible through the use of various approximations, which will be discussed in this thesis in Sec. 3.

The ΛCDM model is the leading cosmological framework, providing the foundation for our understanding of the evolution of the Universe. Its success is evident in its remarkable agreement with observational data, including measurements of the Cosmic Microwave Background (CMB) from WMAP [7] and Planck [8], as well as large-scale structure observations from the Sloan Digital Sky Survey (SDSS) [9], among others.

The Standard Model of Cosmology (ΛCDM model) describes the universe as consisting of approximately 5% ordinary baryonic matter, 26% cold dark matter (CDM), and 69% dark energy (Λ, the cosmological constant) [8]. It assumes the geometry of the Universe to be homogeneous and isotropic, based on the validity of the cosmological principle, and is described by Friedmann-Lemaître-Robertson-Walker (FLRW) cosmological models, particularly a flat model [79].

Furthermore, as part of its framework, the ΛCDM model incorporates a phase of inflation, which is assumed to have occurred around 10^{-34} seconds after the Big Bang, during which the Universe underwent exponential expansion. Inflation solves key problems, such as the horizon problem and the flatness problem, and provides a mechanism for generating the initial density fluctuations that serve as the seeds for the large-scale structure of the Universe today [11], [12], [13].

The standard model of cosmology, the ΛCDM model, is remarkably successful in describing a wide range of observations. However, several persistent and significant challenges remain within this framework, suggesting that new physics may be required beyond the standard cosmological model [14]. To explore this in more detail, we first examine the key puzzles that arise within the ΛCDM model in the next section, followed by a discussion on these challenges and their implications.

1.1 Puzzles in the Standard Model of Cosmology

Among the unresolved issues of ΛCDM are the *nature of dark matter and dark energy*, *CMB anomalies*, the *Hubble tension*, the *matter-antimatter asymmetry*, and others [8]. In addition, the cold dark matter model, which forms the foundation of the ΛCDM framework, also faces several challenges on small scales, which will be discussed in detail in the next section.

The Hubble tension refers to the disagreement between local measurements of the Hubble constant and its value inferred from the CMB [15]. Extensive discussions of this issue and possible resolutions based on different cosmological models, including dynamical dark energy, primordial magnetic fields, modified gravity, and other alternatives, can be found in review articles [16], [17]. In this section, we will focus specifically on CMB anomalies, dark matter, and the matter-antimatter asymmetry, providing a brief overview of these issues. Later, in Sec. 1.2, these puzzles will be addressed from a geometric perspective, which motivates the problem explored in this thesis.

1.1.1 Cosmic Microwave Background anomalies

In the early Universe, matter was extremely hot and dense. As the Universe expanded, it cooled down, leading to a sequence of phase transitions that shaped its thermal history. A detailed description of these phase transitions can be found in [18], [19], [20], and [21]. The light nuclei were created during Big Bang Nucleosynthesis (at ~ 200 s), the theoretical framework for which was initially developed by Gamow et al. in the 1940s [22]. At this stage, the universe was too hot for electrons to be bound to nuclei to form neutral atoms. This process became possible much later, when the universe had cooled further and transitioned from radiation domination to matter domination. Around 380,000 years after the Big Bang, when the temperature had dropped to approximately 3000 K, protons and electrons combined to form neutral hydrogen atoms. As a result, the photons, which were interacting with electrons via Thomson scattering, decoupled from the matter and began to free-stream. These decoupled photons, now known as the CMB photons, retain the characteristic blackbody radiation spectrum (as a result of being in thermal equilibrium with the matter) from the time of decoupling. Additionally, the temperature spectrum of the CMB exhibits anisotropies on the order of 10^{-5}, providing evidence for fluctuations in the primordial matter density.

The CMB spectrum was first detected by Arno Penzias and Robert Wilson in 1965 [23]. Since then, increasingly precise observations have been made by missions such as the Cosmic Background Explorer (COBE) [24], the Wilkinson Microwave Anisotropy Probe (WMAP) [7], and Planck [8]. These missions have not only refined our understanding of the CMB but also revealed unexpected features in the data at large angular scales. Notable anomalies include the *alignment of the lowest multipole moments* with each other and with the motion and geometry of the Solar System, a *hemispherical power asymmetry*, *parity asymmetry*, and the presence of *cold spots* (for a detailed discussion, see [14], [25], [26] and the references therein). These anomalies challenge the expected statistical isotropy and Gaussianity of the CMB temperature fluctuations[1].

The CMB temperature anisotropies[2], $\Delta T(\hat{n})$, where the unit vector $\hat{n}$ denotes a direction in the sky, are measured relative to the mean CMB temperature, $\bar{T} = 2.7\,\mathrm{K}$. These anisotropies can be expanded in terms of spherical harmonics as

$$\Theta(\hat{n}) = \frac{\Delta T(\hat{n})}{\bar{T}} = \sum_{\ell m} a_{\ell m} Y_{\ell m}(\hat{n}), \tag{1.1}$$

where $a_{\ell m}$ are the expansion coefficients, also known as multipole moments, and $Y_{\ell m}(\hat{n})$ are the standard spherical harmonics on a 2-sphere. The multipole number ℓ corresponds to different angular scales of the temperature anisotropies and takes integer values $\ell \geq 0$. Specifically, $\ell = 0, 1, 2, 3, ...$ correspond to the monopole, dipole, quadrupole, and octupole, respectively. The monopole and dipole components are not of cosmological interest, as the variance of the monopole is undefined and the dipole is primarily influenced by our motion through the universe. Therefore, in anisotropy studies, analyses typically focus on the multipoles with $\ell \geq 2$. The magnetic quantum numbers take values $m = -\ell, -\ell + 1, \ldots, +\ell$.

The statistical properties of CMB anisotropies are analyzed using the two-point correlation function, which quantifies the relationships between temperature fluctuations

[1]Statistical isotropy follows from the cosmological principle, a fundamental assumption of the standard cosmological model, while Gaussianity arises from inflation, which is an integral part of the ΛCDM framework.

[2]A more detailed discussion of the CMB temperature anisotropies can be found in the standard literature, see, for example, [27] and [28].

at different points on the sky. Statistical isotropy implies that the expectation values of all two-point correlation functions are invariant under arbitrary rotations of the sky. As a result, the two-point correlation function depends only on the angular separation θ between two points, with $\cos\theta = \hat{n}_1 \cdot \hat{n}_2$. This function can then be expanded in terms of Legendre polynomials as follows:

$$C(\theta) = \left\langle \Theta(\hat{n}_1)\Theta(\hat{n}_2) \right\rangle = \frac{1}{4\pi} \sum_{\ell} (2\ell+1) C_\ell P_\ell(\cos\theta), \tag{1.2}$$

which leads to the following relation

$$\left\langle a^*_{\ell m} a_{\ell' m'} \right\rangle = C_\ell \, \delta_{\ell\ell'} \delta_{mm'}, \tag{1.3}$$

where C_l is known as the angular power of the multipole ℓ.

Having briefly introduced the necessary mathematical concepts, we now return to the discussion of CMB anomalies. Given the complexity and technical nature of the topic, we will focus on highlighting the key aspects of these anomalies and discussing their significance, without delving into the technical details.

Lack of large-angle CMB temperature correlations

It has been observed that the two-point angular correlation function $C(\theta)$, as given by (1.2), is suppressed at large angular scales, it nearly vanishing for angular separations $\theta \gtrsim 60°$. Additionally, the angular power spectrum shows suppression at low-ℓ values, particularly with a heavily suppressed quadrupole, a mildly suppressed octupole, and unsuppressed higher multipoles. These anomalies cannot be adequately explained within the framework of the standard model of cosmology. One possible explanation for the lack of power at large scales is the finite topology of the Universe [16].

Quadrupole-octupole alignment

In the standard ΛCDM model, the orientations and shapes of the multipole moments in harmonic space are expected to be random and independent. However, observations show that the quadrupole ($\ell = 2$) and octopole ($\ell = 3$) are unexpectedly planar and aligned with each other[3].

Even more strikingly, the quadrupole and octopole planes are not only aligned with each other but are also unexpectedly perpendicular to the Ecliptic plane and aligned

[3]An alternative approach to analyzing large-angle anomalies involves using multipole vectors, as introduced in [29]. These vectors offer a different representation compared to spherical harmonics, providing a more convenient tool for studying these anomalies.

with the CMB dipole [26]. No known systematics or foreground contamination has been identified to account for these violations of statistical isotropy. The alignment of these low-order multipoles suggests the presence of a *preferred direction* in the CMB temperature anisotropy, challenging the assumption of statistical isotropy in the standard cosmological model.

Hemispherical asymmetry

A hemispherical power asymmetry has been detected, where the CMB temperature anisotropies are larger in one hemisphere of the sky than in the other. Notably, the plane that maximizes this asymmetry is approximately aligned with the Ecliptic plane. Proposed explanations for this anomaly include models involving a superhorizon perturbation or asymmetric initial states of quantum perturbations [25]. However, no convincing systematic or cosmological explanation has yet accounted for why one ecliptic hemisphere exhibits less power than the other.

Parity Asymmetry

In the CMB angular power spectrum, odd ℓ multipoles exhibit excess power compared to even ℓ multipoles on the largest angular scales ($2 < \ell < 30$). This contradicts the predictions of the ΛCDM model, which expects power to be equally distributed between even and odd modes.

The parity asymmetry appears to be correlated with the lack of power at large angular scales. Furthermore, the direction that maximizes this parity asymmetry is also close to the direction of the hemispherical asymmetry [14]. As a result, it remains unclear whether the parity asymmetry is an independent anomaly or a byproduct of another underlying anomaly.

Cold spot

The Cold Spot was discovered in the southern hemisphere of the CMB sky, located at the galactic coordinates $(l, b) = (209°, -57°)$. The Cold Spot is an unusually large, roughly circular region with a radius of about five degrees. It exhibits a significant temperature decrement, with a mean temperature of $\Delta T \approx -100\,\mu K$ relative to the average CMB temperature [25]. It represents a statistical anomaly in the large-angle fluctuations of the CMB, indicating non-Gaussian features. This observation contradicts the Gaussianity assumption predicted by the standard ΛCDM model.

Providing a theoretical explanation for a localized feature appearing in a non-special location in the sky is challenging. In this context, Bianchi cosmological models, which are homogeneous yet anisotropic, have been proposed as a potential explanation for the Cold Spot. Other possible explanations include large statistical fluctuations, an artifact of inflation, multiple voids, the universe's rotation axis, cosmic textures, and more [14], [25].

To summarize, several anomalies in the CMB data appear to contradict the predictions of the standard ΛCDM model. While some studies suggest that these anomalies could be the result of statistical flukes [30], the fact that multiple sets of them are statistically independent makes it highly unlikely that all of these anomalies arose simultaneously by chance. Furthermore, anomalies on large scales cannot be attributed to experimental systematics or foreground contamination. Instead, the most plausible explanation is that they have a cosmological origin, with non-trivial cosmic topology or anisotropic geometry being the only currently promising frameworks [16]. Further clarification of the nature of these anomalies can be achieved through new CMB observations, such as CMB polarization studies, large-scale structure surveys, and other cosmological probes.

1.1.2 Dark matter

There is strong evidence for the existence of dark matter, inferred from various gravitational effects, including galaxy rotation curves, gravitational lensing, the dynamics of galaxy clusters, and cluster collisions, as well as from cosmic microwave background data. Below, we will briefly describe these observations, along with the properties and proposed models of dark matter, focusing on cold dark matter (CDM), which forms the foundation of the ΛCDM model. Finally, we will conclude by discussing the challenges faced by the CDM model. For further details, see the review papers [31], [32] and references therein.

Galactic rotation curves

The rotational velocity of stars and gas orbiting the centers of galaxies is expected to decrease as the radius increases. For a spherically concentrated mass $M(r)$, the orbital velocity follows the relation

$$v(r) = \sqrt{GM(r)/r}. \tag{1.4}$$

If all the mass is enclosed at the center, the orbital velocity behaves as $v(r) \sim r^{1/2}$. However, as shown in Fig. 1, as the radius increases, $v(r) \sim r$, meaning the rotation curve remains flat, contrary to the expected behavior. This discrepancy was first discovered by Vera Rubin and Kent Ford in the 1970 [33].

To account for this behavior, the most straightforward explanation is that galaxies contain far more mass than is visible from the stellar objects in the galactic disks, implying the presence of a large, spherically distributed dark matter halo extending well beyond the visible boundaries of the galaxy.

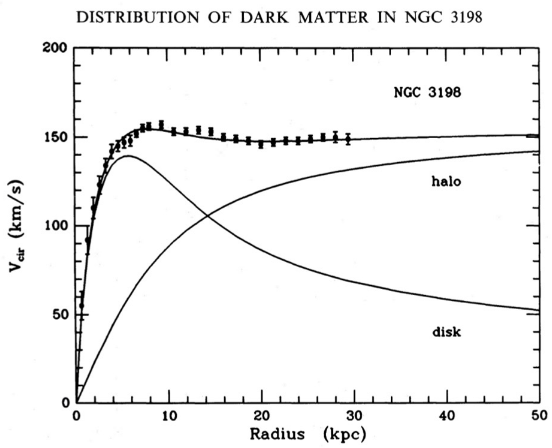

Figure 1: Galactic rotation curve of NGC 3198, illustrating the contribution of the dark matter halo required to match the observed data [31].

Mass of Galaxy Clusters: Virial Theorem and Gravitational Lensing

For a stationary, bound system—such as a cluster of galaxies—the Virial Theorem, which relates the system's kinetic energy T and potential energy V, should hold. Specifically,

$$2\langle T\rangle + \langle V\rangle = 0. \tag{1.5}$$

This is used to estimate the mass of galaxy clusters by relating the velocity dispersion of galaxies to the gravitational potential. However, the mass calculated using the Virial Theorem was significantly higher than the mass of the visible matter. In addition, another method for estimating the mass of galaxy clusters is gravitational lensing, where the gravitational field of a cluster deflects the light from background objects. The weak lensing data from the Sloan Digital Sky Survey (SDSS) [9] revealed that galaxies, including the Milky Way, are larger and more massive than previously thought. Consequently, mass estimates based on gravitational lensing also indicate the presence of additional mass beyond what is accounted for by visible matter. Moreover, this approach suggests that dark matter extends to even greater distances than those inferred from rotation curves. For instance, in the Milky Way, visible matter extends up to 10 kpc, while the dark matter halo is believed to reach 100 kpc based on rotation curve analysis. However, lensing data suggests that it may extend even further, up to 200 kpc from the centers of galaxies [34].

Collisions of clusters

A collision of two galaxy clusters, known as the Bullet Cluster, was detected by NASA's Chandra X-ray Observatory and is shown in Fig. 2. The gas from the two clusters interacts, slows down, and exhibits a characteristic shock wave (depicted in pink). In contrast, the dark matter component (shown in blue) passes through unaffected, as it only interacts gravitationally. The dark matter is detected through gravitational lensing.

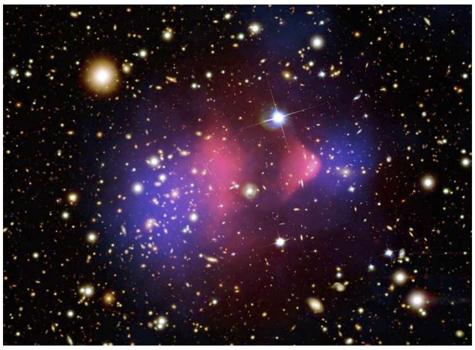

Figure 2: A collision of galaxy clusters forming the Bullet Cluster. The gas is shown in pink, while the dark matter distribution is inferred from gravitational lensing and depicted in blue [32].

Cosmic microwave background

The evidence for dark matter also comes from the Cosmic Microwave Background (CMB) data, first detected by COBE in 1992 and later refined by WMAP and Planck. Analyzing these data within the framework of the ΛCDM model leads to the conclusion that dark matter must be present in the Universe and is approximately five times more abundant than baryonic matter [8].

Properties of Dark Matter

Based on the observed phenomena, dark matter is expected to have the following properties: its interactions with Standard Model particles must be extremely weak, with interactions with baryonic matter occurring solely through gravity. Additionally, dark matter must be nearly *collisionless*, exhibiting very weak self-interactions, as evidenced by observations of the Bullet Cluster.

Moreover, dark matter must be *non-relativistic*, or "cold", behaving like a collection of non-relativistic particles attracted by gravity. This is crucial for the growth of small perturbations in the CMB and for dark matter to accumulate and form the galactic halos of galaxies, consistent with observations.

Furthermore, observations from the Cosmic Microwave Background (CMB) indicate that baryonic matter makes up only 5% of the total energy density of the universe, with the remaining component attributed to dark matter, which must therefore be non-baryonic. This conclusion is further supported by Big Bang Nucleosynthesis (BBN), which accurately predicts the abundances of light elements (H, He, Li, D) based on the total baryonic density. Additionally, large-scale structure formation models require non-baryonic dark matter to drive the necessary growth of cosmic structures [35]. These observations place strict upper bounds on the amount of baryonic matter in the universe and strongly suggest that dark matter is non-baryonic[4] [36].

Finally, dark matter has to be *stable* because its presence is observed in the early universe and persists to the present day. Its stability is essential, as cosmological simulations and CMB observations rely on dark matter to explain the growth of density perturbations and the distribution of galaxies. If dark matter does decay, the process must occur at an extremely slow rate.

Models of Dark Matter

If dark matter is composed of particles, its models can be classified based on the thermal velocities of these particles. Dark matter is categorized as *cold* (non-relativistic), *hot* (relativistic), or *warm* (intermediate between the two). This classification plays a crucial role in structure formation, as the velocity of dark matter particles affects how cosmic structures grow and evolve over time [37], [38].

The hot dark matter model, composed of massive and relativistic particles such as neutrinos, would result in a very different formation of structures in the universe. It would prevent the formation of small-scale structures like galaxies. Consequently, this would significantly affect the formation and distribution of galaxies, deviating from the observations we currently see. Observations of the CMB and large-scale structure surveys favor the cold dark matter (CDM) model, which forms the basis of the standard cosmological model, ΛCDM [8]. However, the CDM model also faces certain challenges[5], which we will briefly discuss below.

Since CDM particles must be massive, non-relativistic, weakly interacting, and stable, no Standard Model particles satisfy these requirements. Consequently, a remarkably wide range of candidates has been proposed for the CDM model. Among the many possibilities are Weakly Interacting Massive Particles (WIMPs), axions (hypothetical particles motivated by the strong CP problem in quantum chromodynamics

[4]However, some models propose that dark matter could have a baryonic nature. One such model involves MACHOs (Massive Compact Halo Objects), which consist of ordinary baryonic matter in the form of faint stars, stellar remnants, black holes, or mirror matter [32].

[5]The Warm Dark Matter (WDM) model is considered to address some of these challenges; however, it also introduces its own set of difficulties [39].

(QCD)), sterile neutrinos, supersymmetric particles, primordial black holes, Kaluza-Klein particles from higher-dimensional theories, and numerous other exotic candidates (see, e.g., [40]). The vast and diverse range of proposed candidates underscores the complexity of identifying the true nature of dark matter.

Finally, let us also mention that, alternatively, some approaches attempt to explain the effects attributed to dark matter without introducing additional matter, instead suggesting that the theory of gravity itself must be modified. Numerous theories have been developed to alter gravity in a way that eliminates the need for dark matter and dark energy. These include Modified Newtonian Dynamics (MOND), Tensor-Vector-Scalar Gravity (TeVeS), f(R) Gravity, and Generalized Einstein-Aether Theory (GEA), among others. However, most of these alternative gravity models struggle to fully account for the observed effects of dark matter, with MOND being the only approach that could still be considered a relevant theory in this context (see, e.g., the review article [41]).

Problems of Cold Dark Matter (CDM) model

The CDM model has been a successful framework for predicting and explaining the large-scale structure of the Universe. However, it faces several challenges at smaller scales, particularly those below approximately 1 Mpc. Among the most well-known issues are the *Cusp/Core problem*, *Missing Satellites*, *Too Big to Fail*, and the *angular momentum catastrophe*, which are briefly explained below. A detailed discussion of the issues and possible solutions to some of the problems can be found in [42], [43], and the references therein.

The observed dark matter-dominated galaxies are found to be less dense and less cuspy than predicted by the CDM model. This discrepancy is known as the "cusp/core" (CC) problem. Various approaches have been proposed to address this issue, one of which is fuzzy dark matter (FDM), or fuzzy cold dark matter (FCDM). FDM consists of ultra-light bosonic particles that, due to their extremely small mass, behave more like waves than traditional particles, hence the term "fuzzy" [44].

The "missing satellite problem" (MSP) refers to the discrepancy between the number of small galaxies and dwarf galaxy satellites in the Local Group[6] predicted by the CDM model and what is actually observed. The observed number of these galaxies is significantly lower than the predictions made by the CDM model.

Furthermore, the "Too Big To Fail" (TBTF) problem refers to the prediction by CDM simulations that massive dark matter halos should host bright galaxies or large satellite galaxies, a prediction that contradicts observations. Halos of this mass are

[6]The Local Group refers to a galaxy group that includes the Milky Way and its neighboring galaxies, which are all gravitationally bound to each other.

generally expected to form bright galaxies or large satellites, so the fact that they are missing presents a significant challenge to our understanding.

The angular momentum catastrophe refers to the discrepancy between the angular momentum distributions observed in galaxy formation simulations and those seen in actual galaxies. In [45], the authors demonstrated that the angular momentum distributions of dwarf galaxy disks are clearly distinct from those of the dark matter halos. In the standard picture of structure formation, the angular momentum of protogalaxies is thought to arise from cosmological torques. Since both dark and baryonic matter experience the same tidal forces, it is expected that they should exhibit similar angular momentum distributions. Thus, understanding the angular momentum distribution of disk galaxies remains a significant challenge for the current model of galaxy formation.

In conclusion, while the ΛCDM model has been successful in describing the formation and evolution of large-scale structures in the Universe, it faces significant unresolved challenges at smaller scales. Moreover, as previously mentioned, no Standard Model particle can account for cold dark matter (CDM), requiring the consideration of physics beyond the Standard Model—an area for which no direct evidence has been found so far. This highlights the limitations of the ΛCDM model and underscores the need to reassess our understanding of it.

1.1.3 Matter-antimatter asymmetry

Qunatum Field Theory, which forms the foundation of the Standard Model of particle physics, predicts the existence of antiparticles and describes the processes of pair creation and annihilation, which are symmetric with respect to particles and antiparticles. Therefore, the fact that we observe a matter-dominated universe, with an almost complete absence of antimatter[7], remains an unresolved issue in modern cosmology.

In the early stages, the Universe was hot, with an equilibrium maintained between particle pair creation and annihilation processes. As the Universe expanded and the plasma cooled, matter and antimatter annihilated each other, leaving behind a small excess of matter. The study of matter-antimatter asymmetry primarily focuses on baryon asymmetry because it is directly observable, leaves a clear imprint on cosmological data, and is crucial for explaining the current structure and composition of the Universe, as it is the main contributor to its matter density (apart from dark matter and dark energy). Additionally, leptons (such as neutrinos and electrons) also exhibit an asymmetry, though directly measuring it is challenging [48]. The asymmetry of

[7]Some theories suggest that the Universe may not have a fundamental matter-antimatter asymmetry. Instead, it could be composed of separate regions dominated by either matter or antimatter, or a homogeneous blend of both. If this were true, we would expect to detect γ-rays from matter-antimatter annihilation processes. However, observational evidence does not support these scenarios [46], [47].

electrons is indirectly inferred from baryon asymmetry[8].

The baryon asymmetry of the Universe (BAU) is characterized by a parameter baryon-to-photon ratio, denoted by η. It is defined as the ratio of the number of baryons to the number of photons in the early Universe, i.e., $\eta = N_B/N_\gamma$. This parameter can be measured in two independent ways: from the power spectrum of temperature fluctuations in the Cosmic Microwave Background (CMB) and from the abundances of light elements in the intergalactic medium, as predicted by Big Bang Nucleosynthesis (BBN) (see, e.g., [49] for a detailed discussion). The result from Big Bang Nucleosynthesis (BBN) is given in [50], while the value inferred from the Cosmic Microwave Background (CMB) is reported in [51]. The measured values for η from both methods[9] are consistent, giving $\eta \sim 10^{-10}$. Thus, after the Universe cooled down, matter and antimatter annihilated, leaving behind an excess of baryons—roughly one baryon for every 10 billion photons. Therefore, the vast matter-antimatter asymmetry observed in the Universe today was an extremely small quantity in the early Universe.

The generation of baryon asymmetry (referred to as Baryogenesis) is possible if the following three Sakharov conditions are satisfied [52]:

- Baryon number (B) violation,
- C (charge conjugation symmetry) and CP (C and parity) violation,
- Deviation from thermal equilibrium.

The first condition is evident: if the Universe starts with a baryon number of zero, it cannot evolve into a state with a nonzero baryon number $B \neq 0$ without baryon number-violating interactions. Additionally, if C and CP symmetries hold, any process that generates an excess of baryons will be accompanied by another process producing an equal number of antibaryons, preventing a net baryon asymmetry. Hence, the second condition is required. Finally, since thermal equilibrium is a time-translation invariant state, the creation of baryon asymmetry would be impossible if the system started with a vanishing baryon number.

The Standard Model (SM) fulfills all the necessary conditions for baryogenesis [53]. In [54], 't Hooft demonstrated that while baryon and lepton numbers are conserved in perturbative theory, non-perturbative effects at very high temperatures can violate these symmetries. These effects, known as sphaleron processes, are key to baryon number violation. Additionally, CP violation occurs through weak interactions and quark Yukawa couplings [55], while the expansion of the Universe ensures departure

[8]Due to the charge neutrality of the Universe, the number of electrons must be equal to the number of protons.

[9]These methods measure η at different stages of the Universe's evolution, which helps to constrain cosmological models and test their validity, especially the ΛCDM model.

from equilibrium. However, these effects within the SM are too weak to account for the observed baryon asymmetry, making successful baryogenesis unlikely within the Standard Model alone. As a result, extensions of the Standard Model are explored as potential solutions, often introducing new sources of CP violation and baryon number violation. These modifications give rise to various baryogenesis scenarios, such as models with an extended Higgs sector or the Minimal Supersymmetric Standard Model (MSSM), as discussed in the literature [56]. This class of mechanisms is broadly known as Electroweak Baryogenesis.

In addition, several beyond Standard Model mechanisms have been proposed to explain the origin of baryon asymmetry. Notable among them are Grand Unified Theory (GUT) Baryogenesis, the Affleck-Dine Mechanism in supersymmetric (SUSY) theories, Baryogenesis via Leptogenesis and gravitational baryogenesis[10]. While these mechanisms offer potential solutions to the baryon asymmetry problem, they face significant theoretical and observational challenges that remain unresolved. For a more detailed discussion of these approaches and their limitations, see [49], [56], [58], [59], and references therein.

In conclusion, the matter-antimatter asymmetry remains a major unresolved problem in modern cosmology. While various attempts to extend the Standard Model or explore physics beyond the Standard Model have been proposed, none are currently supported by observational evidence.

[10]This approach suggests that a CP-violating coupling between the Ricci scalar and the baryon number current can generate the observed baryon asymmetry in an expanding universe. For further details, see, e.g., [57].

1.2 Addressing cosmological puzzles from a geometric perspective

As outlined in the previous section, the standard cosmological model, ΛCDM, encounters various difficulties. In particular, when it comes to anomalies in the CMB, homogeneous and isotropic FLRW models fail to provide satisfactory explanations—unless these anomalies can be attributed to statistical effects or background contamination, which is considered unlikely based on prior discussion. Consequently, these anomalies hint at a deviation from isotropy on large scales, opening the door to exploring more general homogeneous but anisotropic models as a possible resolution to these issues.

Furthermore, since no particles within the Standard Model meet the necessary conditions for cold dark matter, as previously discussed, alternative candidates beyond the Standard Model must be considered, though these particles have yet to be observed. In addition, while the cold dark matter model successfully accounts for most expected properties of dark matter and aligns well with large-scale structure observations, it faces significant challenges on smaller scales, prompting a reconsideration of the model.

Finally, to explain the matter-antimatter asymmetry, the Sakharov conditions for successful baryogenesis must be satisfied. In this context, Standard Model physics is insufficient to produce the necessary asymmetry to resolve the problem, and once again, solutions must be sought in physics beyond the Standard Model.

Given these substantial difficulties, the natural first question is whether the foundational assumptions of the FLRW geometry in the ΛCDM model are correct. Could it be that the simplicity of such a highly symmetric geometry is the cause of these challenges? In fact, as stated by Gerard 't Hooft in [54]:

> *"When one attempts to construct a realistic model of nature, one is often confronted with the difficulty that most simple models have too much symmetry."*

This suggests that the highly symmetric nature of the FLRW geometry may not be an accurate reflection of the true structure of the Universe. Consequently, the first step in addressing these cosmological puzzles would be to relax the isotropy assumption, as suggested by the CMB anomalies, and to develop cosmological models based on more general geometries, testing them against observational data.

How might the assumption of a homogeneous and anisotropic model of the universe contribute to resolving the puzzles of matter-antimatter asymmetry and the nature of dark matter? As mentioned at the beginning of this chapter, within the framework of QFT in curved spacetime, there are inherent challenges in defining the concept of a particle and establishing an unambiguous vacuum. These challenges can be addressed using approximations, e.g. adiabatic approximation. In the FLRW geometry, the only gravitational effect that enters into the particle physics discussion compared to

Minkowski spacetime, is the expansion of the universe, which leads to the redshifting of particles. However, in anisotropic models, the geometric effects are expected to be more complex. To assess the impact of geometric anisotropy on particles and their interactions, it is essential to derive the equations of motion for the relevant fields in the given anisotropic background. These equations must then be solved under an appropriate approximation, followed by quantization to understand how anisotropic geometric dynamics affect the system. If a suitable anisotropic model is chosen, it may reveal an asymmetry between particles and antiparticles—potentially providing an explanation for the observed matter-antimatter asymmetry, without relying on the mechanisms typically proposed in particle physics[11]. The objective of this thesis is to explore this possibility.

Moreover, in the framework of the ΛCDM model, dark matter plays a crucial role in the growth of the initial perturbations, which serve as the seeds for large-scale structures. It has been shown that without a significant amount of dark matter, there would not be sufficient gravitational attraction to facilitate the formation of the large-scale structures we observe today. The process of structure formation in the ΛCDM model is discussed in great detail in [35]. In the context of a homogeneous anisotropic model, the evolution of the initial perturbations differs from that in FLRW models (see, e.g., [60] and references therein), thereby impacting the structure formation. Consequently, anisotropic gravitational effects may account for some of the phenomena typically attributed to dark matter. However, as discussed earlier, certain observations supporting the existence of dark matter, such as the collision of the Bullet Cluster, would be challenging to explain solely through anisotropic effects, without invoking the presence of actual dark matter.

Furthermore, since the mechanism responsible for the matter-antimatter asymmetry remains unknown, and given that electric charge is conserved in GR, particles and antiparticles are expected to be produced in equal amounts. If a fundamental asymmetry between particles and antiparticles were induced by the spatial anisotropy of the universe—for instance, a suppression of antiparticles—matter and antimatter could coexist without undergoing complete annihilation. This idea is highly speculative and provides a heuristic perspective that requires rigorous investigation. A definitive conclusion can only be reached through detailed studies of Quantum Electrodynamics within a specific anisotropic cosmological model.

Now, the question arises: which homogeneous, anisotropic model of the universe should be considered? We will explore this in the next section.

[11]Such effects have been studied for Weyl neutrinos by Gibbons in [61], [62] within an axisymmetric Bianchi IX universe. In this thesis, we will analyze these results in detail and extend the discussion to Dirac spinors.

1.3 Why rotating Bianchi IX universe?

There exist various homogeneous, anisotropic cosmological models, which are classified and described in detail in Chap. 2. To investigate the possible effects proposed above, we adopt the Bianchi IX model, which represents a *finite* universe and, in general, allows for *global rotation*. The following section presents arguments to justify this choice.

BKL conjecture

As discussed previously, singularities inevitably arise in GR, making the study of their nature a key area of investigation in theoretical physics. The Big Bang singularity is not a consequence of the symmetry of the FLRW framework but rather a generic feature of Einstein's field equations [63]. In the 1946, Lifshitz [64] examined the gravitational stability of non-static isotropic universe models. He concluded that space's isotropy cannot be maintained as the universe evolves towards singularities. Later, in a series of influential works [65], [66], Vladimir Belinsky, Isaak Khalatnikov, and Evgeny Lifshitz (BKL) proposed a conjecture about the behavior of spacetime near a singularity. Their prediction highlighted highly chaotic and oscillatory dynamics when approaching to singularity that are dominated by time-dependent factors rather than spatial variations. As a result, different spatial points effectively decouple, and the behavior of the universe becomes similar to that of the general Bianchi IX model. The dynamics of the diagonal Bianchi IX model were independently studied by Misner [67], who proposed that the oscillations in the Bianchi IX model could potentially resolve the "horizon problem". These studies were later generalized to symmetric and general Bianchi IX models by Ryan [68], [69].

In addition, the BKL conjecture has important applications in quantum gravity, particularly in the study of singularities and quantum gravitational effects near them. It has been explored in various quantum gravity approaches, such as canonical quantum gravity [70] and loop quantum gravity [71], along with other related studies.

Thus, a more realistic cosmological model would be to consider an initially homogeneous and anisotropic universe. In this case, as suggested by the BKL conjecture, a general Bianchi IX universe, which later evolved toward the isotropic FLRW universe that we observe today. This is important, as the initial anisotropies could potentially be responsible for the resolution of cosmological puzzles, as argued in the previous section. The question remains, however, how exactly the isotropization of such a universe could take place.

Isotropization

One possible mechanism for the isotropization of initially homogeneous, anisotropic models is an inflationary phase. A general discussion on whether inflation can occur in such universes and, if so, whether it leads to isotropization can be found in [60] and references therein. The isotropization of the Bianchi IX model driven by a scalar field with an exponential potential of the form proportional to $e^{k\varphi}$ is examined in [72]. It has been shown that for $k < \sqrt{2}$, a set of continuously expanding anisotropic Bianchi IX models exists that undergo isotropization. Conversely, for $k > \sqrt{2}$, initially expanding Bianchi IX models do not evolve toward an continuously expanding isotropic state.

The claim of the inflationary epoch that it can evolve the universe from generic initial conditions to a homogeneous and isotropic state relies on the validity of the "cosmic no-hair conjecture", proposed by Gibbons and Hawking [73] and Hawking and Moss [74]. This conjecture states that all expanding universe models with a positive cosmological constant asymptotically approach the de Sitter solution[12]. In [75], Wald examined the cosmic no-hair conjecture within the framework of homogeneous cosmological models, showing that all initially expanding Bianchi models, with the exception of type IX, tend to approach the de Sitter solution on a rapidly exponential timescale. For type IX cosmologies, similar behavior is observed, given that the cosmological constant is large enough, which lends further support to the "cosmic no-hair conjecture".

Finally, another factor contributing to the damping of anisotropy is cosmological particle creation, as discussed in, e.g., [77].

Thus, given that the initial dynamics near the Big Bang are described by the Bianchi IX metric, and assuming successful isotropization occurs (provided certain conditions are satisfied), with the evolving geometry approaching the FLRW model observed today, this model can be considered a reasonable choice for study.

[12]The Cosmic No-Hair Conjecture has significant implications for quantum gravity, as quantum gravitational effects could offer a more nuanced understanding of isotropization. Fundamental discussions on this topic are available in the literature (see, e.g., [5], [76]).

Angular momentum generation in cosmological context

Another motivating factor for considering the rotating Bianchi IX universe is its relevance to the question of how galaxies acquired angular momentum. The generation of angular momentum in the cosmological context remains a crucial unresolved issue in modern astrophysics and cosmology. Several approaches have been proposed to explain this phenomenon. For more details, see e.g., [78], [79], and the references therein:

- One explanation involves the role of primordial turbulence. The idea is that turbulence in the intergalactic medium, caused by the initial density fluctuations in primordial gas, could have contributed to the formation of rotating structures such as galaxies. However, this model faces significant challenges, as turbulence likely couldn't have been maintained for long enough against the dissipation processes to contribute meaningfully to angular momentum.

- Another proposed mechanism is the tidal torques from neighboring proto-galaxies, known as Tidal torque theory. This theory suggests that angular momentum in forming galaxies arises from tidal interactions between collapsing regions of the universe and surrounding mass distributions. However, this idea is only valid in the linear regime when density perturbations were small. Additionally, it struggles to explain the observed relation $J \propto M^{5/3}$, which is commonly seen in galaxies.

- Finally, global rotation could play a key role. In this scenario, the Coriolis force within galactic frames could naturally induce rotation as galaxies form, leading to the generation of angular momentum.

This last approach was initially proposed by G. Gamow [80], K. Gödel [81], and C. B. Collins and S. W. Hawking [82]. However, a more detailed study was carried out by Li-Xin Li, who in his paper [78] explores the theoretical implications of a rotating universe on the formation of galaxies. Specifically, he examines how global rotation could influence angular momentum, structure formation, and the evolution of cosmic objects. Li also argued that the empirical relation between angular momentum and the mass of a galaxy, $J \propto M^{5/3}$, can be explained by global rotation. The role of global rotation has been further studied by [83], [84], [85], and others.

Observations indicate the presence of angular momentum on unexpectedly large scales. Specifically, galaxy filaments have been found to exhibit rotation, and when these filaments are stacked together, they continue to display coherent spinning motion [86]. Additionally, some galaxy clusters have also been observed to rotate [87]. Theoretically, a galaxy cluster can acquire angular momentum through either an off-axis merger or a global rotation of the universe. However, studies have not found strong evidence of recent mergers in the clusters suspected to be rotating. This absence of merger signatures suggests that global rotation may be a plausible explanation for their angular momentum.

While tidal torques remain the dominant explanation for angular momentum generation in cosmic structures, tidal torque theory is most effective at smaller scales, such as galaxies, during the early stages of structure formation. For larger structures, however, it struggles to account for the observed rotation. This limitation makes the hypothesis of global rotation in the early universe an intriguing alternative.

To summarize, considering the observations and theoretical challenges discussed, the Bianchi IX cosmological model provides a valuable framework for exploring fundamental cosmological puzzles and understanding the origin of large-scale rotation. By examining potential deviations from the standard ΛCDM model due to anisotropy and global rotation, this approach offers a fresh perspective on the limitations of the highly symmetric underlying geometry. In doing so, it may reveal new insights into cosmic dynamics and the role of rotation in shaping the universe's large-scale structure.

Of course, in the pursuit of constructing a realistic cosmological model, one must remain consistent with CMB observations. If a global rotation exists, its angular velocity is constrained by CMB limits to approximately $\omega \sim 10^{-12}$ rad yr^{-1} [88]. Moreover, ongoing research continues to explore Bianchi models in the context of CMB anomalies (see, e.g., [89], [90]), with the latter specifically discussing an axisymmetric Bianchi IX model as a potential solution to certain CMB anomalies. A comprehensive overview of observational and theoretical anisotropic models can be found in [60].

Finally, studying the physics of spin-1/2 particles in a rotating Bianchi IX universe can reveal many unexpected and interesting effects that are absent in FLRW models. Kamenshchik and Teryaev [91] have conducted research on the motion of Dirac particles in the Bianchi IX model, where particles are treated as classical objects (with further references on Dirac particles in general gravitational fields available there). They demonstrated that anisotropies induce spin precession, which becomes chaotic due to the oscillatory approach to a singularity. The authors showed showed that this could lead to helicity flips in fermions during the early universe, potentially resulting in the production of sterile particles that may contribute to dark matter. Therefore, observing such effects arising within classical discussions suggests that even more nuanced phenomena, such as those arising from spin-angular velocity coupling due to the rotation of the universe, may emerge in a more fundamental theory. By considering quantum field theory in the Bianchi IX model and quantizing the field to introduce particles, we can explore these effects more thoroughly. In this thesis, we carry out these calculations and show that indeed, such effects do appear.

1.4 Structure of the thesis

This thesis is structured as follows: Chapter 2 begins with an overview of homogeneous and anisotropic models in cosmology, introducing the mathematical and conceptual frameworks essential for understanding these spacetimes, with particular emphasis on the Bianchi IX model. Chapter 3 examines the foundational aspects of QFT in curved spacetime, beginning with the established framework of QFT in Minkowski spacetime. It reviews the key concepts and equations that govern spinor fields, with a focus on Dirac and Weyl spinors. The chapter then extends the formulation of spinor fields to curved spacetime, utilizing the vierbein formalism. The chapter concludes with a discussion on cosmological particle creation in an expanding universe. Moving to Chapter 4, the focus is on the Hamiltonian formulation of the spinor field within the Bianchi IX universe. The ADM decomposition of spacetime serves as the foundation for expressing the gravitational dynamics in a Hamiltonian framework. The Lagrangian and Hamiltonian densities for both the gravitational and spinor components of the system are derived, setting the stage for further analysis. The equations of motion for the Weyl and Dirac spinor fields are obtained, providing the groundwork for their quantization in the following chapters. Chapter 5 examines the properties of the SO(3) group, the symmetry group of the Bianchi IX universe. Since the study focuses on spinor fields, investigating the representations of the SO(3) group is essential for analyzing the behavior of spinors in this context. In Chapter 6, the correspondence between the asymmetric rotor and the fixed Bianchi IX model is explored. This correspondence allows the application of the energy eigenbasis of the asymmetric rotor, derived from quantum mechanics, to the study of spinor fields in the Mixmaster universe. Chapter 7 presents the solutions and quantization of the left-handed Weyl and Dirac field equations within the fixed Bianchi IX universe. Given the complexity of the Bianchi IX model, a fixed background enables the analytic solution of the field equations. This approach facilitates a detailed examination of the effects of background anisotropies and rotation on the particle and antiparticle energy spectra. The chapter begins by discussing a range of Bianchi IX models, starting with the simplest, the axisymmetric case, and gradually progressing to more complex models. This progression allows for an exploration of key features and geometric contributions. The thesis concludes with Chapter 8, summarizing the key findings and offering an outlook on potential future research directions.

2 Spatially homogeneous anisotropic models

In this chapter, we begin with a general discussion on homogeneous and anisotropic models in cosmology, providing the mathematical and conceptual tools necessary to understand these spacetimes. We will then focus on the Bianchi IX model, discussing key details that lay the groundwork for a later exploration of the spinor field in this universe.

Key sources in the literature, such as [60] and [92–94], provide a detailed exposition of homogeneous anisotropic cosmological models and serve as a foundation for our discussion. Additionally, works by Jantzen [95–97] offer valuable insights into spatially homogeneous spacetimes from a group-theoretical perspective. His contributions have been instrumental in understanding the role of symmetry groups in classifying spatially homogeneous cosmological models and analyzing their dynamical behavior, particularly within the Hamiltonian formalism.

2.1 Lie groups of isometries and spatial homogeneity

The transformations that leave the metric g of the manifold $\mathcal{M}$ invariant are called isometries. These are generated by Killing vectors ξ, which satisfy

$$\mathcal{L}_\xi \, g = 0, \tag{2.1}$$

where $\mathcal{L}_\xi$ denotes the Lie derivative with respect to ξ. The set of Killing vectors $\{\xi_a\}$ on the manifold forms a Lie algebra. Consequently, they satisfy the following relation

$$[\xi_a, \xi_b] = C^c{}_{ab} \; \xi_c, \tag{2.2}$$

where $C^c{}_{ab}$ are called *structure constants.* The Jacobi identity expressed in terms of these constants reads

$$C^a{}_{c[b} C^c{}_{d\,f]} = 0. \tag{2.3}$$

The isometries generated by the Killing vectors ξ_a, for $a = 1, 2, ..., r$, form a Lie group G, known as the isometry (or symmetry) group of the manifold $\mathcal{M}$. To explicitly indicate the dimension of the group in the notation, this Lie group is typically denoted by G_r.

The *orbit* of a fixed point x, where $x \in \mathcal{M}$, is the set of all the points on the manifold $\mathcal{M}$ that can be reached by the action of the group G on x. Let us denote it by $\mathcal{O}_x$. The orbit forms a submanifold of $\mathcal{M}$ and is referred to as a *homogeneous* or *invariant subspace.*

If $\mathcal{O}_x = \mathcal{M}$, the group G is said to act transitively on the orbit. Furthermore, if the transformation from the point $x \in \mathcal{M}$ to any other point in the orbit is unique, the group is called *simply transitive*. Conversely, if the transformation is not unique, the group is said to be *multiply transitive*.

Spatially homogeneous spacetimes can be constructed by considering a four-dimensional manifold $\mathcal{M}$ that is invariant under a three-dimensional simply transitive Lie group G_3. This group generates three-dimensional homogeneous hypersurfaces. These cosmological models, known as *Bianchi models*, are classified based on the algebraic properties of the Lie algebra associated with G_3, as discussed in the next section.

The only spatially homogeneous cosmological model that is not a Bianchi model is the Kantowski-Sachs model, which is invariant under a G_4 group that contains no transitive G_3.

2.2 The classification of three-dimensional Lie algebras

The classification of three-dimensional Lie algebras was originally introduced by Luigi Bianchi. In the literature, however, the classification is often described using the Schücking-Behr approach, rather than Bianchi's original method. The historical development of the Bianchi classification of homogeneous cosmological models and the contributions of various authors are presented in [98].

To provide the classification, the structure constants are first decomposed under the action of the general linear group $GL(3,\mathbb{R})$ as follows [97], [99]:

$$C^k_{ij} = \varepsilon_{ijl} n^{kl} + a_m \delta^{mk}_{ij}, \tag{2.4}$$

where

$$a_m = \frac{1}{2} C^k_{mk}, \quad \text{and} \quad a_m n^{mk} = 0. \tag{2.5}$$

Next, one can introduce a parameter h via the following relation,

$$a_i a_j = \frac{1}{2} h\, \epsilon_{ikl} \epsilon_{jmn} n^{km} n^{ln}. \tag{2.6}$$

As a symmetric matrix, $\{n^{kl}\}$ can be diagonalized,

$$\{n^{kl}\} = \mathrm{diag}\left(n^{(1)}, n^{(2)}, n^{(3)}\right), \quad a_m = a\delta^3_m, \quad a \geq 0, \tag{2.7}$$

with

$$a^2 = h\, n^{(1)} n^{(2)}, \quad a\, n^{(3)} = 0. \tag{2.8}$$

It is now possible to classify all three-dimensional Lie algebras (and hence the spatially homogeneous model universes) by the values of a and $n^{(i)}$. The various spatially homogeneous models are referred to as the Bianchi types. These Bianchi symmetry types can be further divided into two symmetry classes, A and B, depending on whether a

is zero or not.

Class	**Bianchi type**	$n^{(1)}$	$n^{(2)}$	$n^{(3)}$	a	h
A	I	0	0	0	0	—
	II	0	0	1	0	—
	VI_0	1	-1	0	0	0
	VII_0	1	1	0	0	0
	VIII	1	1	-1	0	0
	IX	1	1	1	0	0
B	V	0	0	0	1	—
	IV	1	0	0	1	—
	$\mathrm{III}\equiv\mathrm{VI}_{-1}$	1	-1	0	1	-1
	$\mathrm{VI}_{h\neq 0,-1}$	1	-1	0	a	$-a^2$
	$\mathrm{VII}_{h\neq 0}$	1	1	0	a	a^2

Table 1: Bianchi classification of three-dimensional Lie algebras in the Schücking-Behr approach. Canonical structure constants for different Bianchi types.

The Bianchi types I, V, and IX include the FLRW universes as special cases, with $\mathcal{K} = 0, -1, +1$, respectively [60], [100]. Later, we will focus on Bianchi type IX and discuss the details of this model in the upcoming sections.

2.3 The line element of Bianchi-type models

As we discussed earlier, the three-dimensional simply transitive Lie group generates three-dimensional homogeneous hypersurfaces Σ (i.e., the orbits) in a four-dimensional manifold $\mathcal{M}$. Therefore, it is possible to choose a one-parameter family of these homogeneous spacelike hypersurfaces that fill the manifold, allowing the spacetime manifold to be expressed as a product $\mathcal{M} = \mathbb{R} \times \Sigma$. This enables the line element of any spatially homogeneous spacetime to be written as follows

$$ds^2 = -dt^2 + dl^2, \tag{2.9}$$

where dl^2 is the line element of the homogeneous hypersurface labeled by the parameter t.

Invariant basis

The simplest way to express the spatial metric is to introduce an *invariant basis* $\{e_i\}$ (where $i = 1, 2, 3$), a basis that is invariant under the action of the symmetry group. Therefore, the Lie derivative of the invariant vectors along the Killing vectors must vanish, i.e.,

$$\mathcal{L}_{\xi_i} e_j = [\xi_i, e_j] = 0. \tag{2.10}$$

The invariant vectors are tangent to each hypersurface, and their structure coefficients are constant on each homogeneous hypersurface. These invariant vector fields, therefore, generate a transformation group that is isomorphic to the original Lie group. Let us consider a homogeneous hypersurface with three Killing vectors ξ_i, which satisfy the following commutation relations,

$$[\xi_i, \xi_j] = C^k_{ij} \xi_k, \tag{2.11}$$

where C^k_{ij} are the structure constants of the group. The invariant basis $\{e_i\}$ can be constructed by taking the vectors e_i at a given point P_0 on the hypersurface, then choosing $e_i(P_0) = \xi_i(P_0)$ and requiring that the conditions (2.10) be satisfied. The obtained invariant vectors e_i satisfy the following commutation relations,

$$[e_i, e_j] = -C^k_{ij} e_k. \tag{2.12}$$

The 1-forms σ^i dual to this basis obey the following relations

$$d\sigma^k = \frac{1}{2} C^k_{ij}\, \sigma^i \wedge \sigma^j. \tag{2.13}$$

To complete the discussion on the invariant basis, let us point out that the action of the group on the manifold can be either left or right. The left-action of the group leads to a left-invariant (or left-homogeneous) Riemannian manifold Σ with a left-invariant spatial metric and left-invariant Killing vectors generating the isometries [95].

If a group acts simply transitively on the manifold, then the orbit and the group are diffeomorphic, and the left action of the group on the manifold corresponds to left translation on the group. Let us recall that for a group acting on itself from the left, i. e., under left-translations L_g, $g_1 \to g g_1$, and that for the right translations R_g, $g_1 \to g_1 g$, where $g, g_1 \in G$. Due to the fact that these two translations commute with each other as a result of the associativity of the group multiplication, R_g is invariant under the symmetry transformations generated by L_g. Therefore, for the left-homogeneous Riemannian space Σ, the left translations L_g generate the symmetry transformations via the Killing vectors $\{\xi_i\}$, and the generators of the R_g form the invariant basis $\{e_i\}$.

The spatial metric

The line element of the homogeneous hypersurface can be given as follows:

$$dl^2 = h_{ij} \sigma^i \sigma^j, \tag{2.14}$$

where h_{ij} is the three-metric and σ^i are the 1-forms dual to the invariant basis e_i. The 1-forms can be expressed in terms of coordinates via $\sigma^i = e^i{}_\alpha dx^\alpha$, where $e^i{}_\alpha$ is a matrix.

Therefore, the line element can be written as

$$dl^2 = h_{ij}(e^i{}_\alpha dx^\alpha)(e^j{}_\beta dx^\beta). \tag{2.15}$$

The time dependence in dl^2 can be treated using different approaches [60]:

- *Metric approach:* Only the spatial metric h_{ij} depends on time.
- *Automorphism approach:* Time dependence is included in both the spatial metric h_{ij} and the basis vectors e_i.
- *Orthonormal tetrad approach:* By introducing an orthonormal basis, the metric simplifies to $g_{\mu\nu} = \eta_{\mu\nu}$, making the basis vectors and structure coefficients time-dependent.

We will adopt the automorphism approach throughout this thesis, with a detailed discussion in the context of the Bianchi IX model.

Automorphism approach

First, we define the automorphism group of the Lie algebra g with respect to the basis $\{e_i\}$, denoted as $\mathrm{Aut}_e(g)$. This group, which is a subgroup of the general linear group $\mathrm{GL}(n, \mathbb{R})$, consists of transformations of the basis $\{e_i\}$ by elements $A \in \mathrm{GL}(n, \mathbb{R})$ that preserve the structure constants [95].

Thus, considering a transformation of the basis $\{e_i\}$ by an element $A \in \mathrm{GL}(n, \mathbb{R})$, we write

$$\bar{e}_i = A^{-1\,j}{}_i\, e_j \equiv A_i{}^j e_j, \tag{2.16}$$

and it can be shown that the structure constants of the basis $\bar{e}_i$

$$\bar{C}^k_{ij} = A^k{}_l C^l_{mn} A^{-1\,m}{}_i\, A^{-1\,n}{}_j = C^k_{ij}. \tag{2.17}$$

The special automorphism group, defined as $\mathrm{SAut}_e(g) = \{A \in \mathrm{Aut}_e(g) |\ \det A = 1\}$, is used instead of $\mathrm{Aut}_e(g)$ in studies of Lagrangian and Hamiltonian formulations of homogeneous cosmologies, as it ensures the invariance of the volume element under frame transformations [101].

The action of $\mathrm{SAut}_e(g)$ on the hypersurface Σ induces a decomposition of the three-metric into diagonal and off-diagonal components,

$$h = A^T \bar{h} A, \quad A \in \mathrm{SAut}_e(g), \tag{2.18}$$

where $\bar{h}$ is the diagonal metric. Both $\bar{h}$ and matrix A are time-dependent.

2.4 Bianchi IX model

The symmetry group of the Bianchi IX model is the rotation group SO(3), with the structure constants given by $C^k_{ij} = -\varepsilon_{ijk}$. The topology of this model is a 3-sphere, S^3.

For the Bianchi IX model, $\mathrm{SAut}_e(g) = \mathrm{Aut}_e(g) = \mathrm{SO}(3, \mathbb{R})$, so the spatial metric can be diagonalized via the rotation group, which coincides with the symmetry group of the homogeneous space. The relation (2.18) for the Bianchi IX model then reads

$$h_{ij} = R_i{}^k R_j{}^l \bar{h}_{kl} = \bar{h}_{kl} R^k{}_i R^l{}_j, \tag{2.19}$$

where R is the rotation matrix, $R \in \mathrm{SO}(3)$, which, when parametrized by Euler angles, is given by (5.4). This decomposition significantly simplifies the dynamical equations. Furthermore, the diagonal metric $\bar{h}_{kl}$ can be parametrized by Misner variables α, β_+, β_- [67], [102] as follows:

$$\bar{h}_{kl} = e^{2\alpha} \mathrm{diag}\left(e^{2\beta_+ + 2\sqrt{3}\beta_-}, e^{2\beta_+ - 2\sqrt{3}\beta_-}, e^{-4\beta_+} \right), \tag{2.20}$$

where the parameters α, β_+ and β_- are functions of time, describing the evolution of the spatial volume and the shape of the universe, respectively. The parameters $\beta_\pm$ are known as the *anisotropy factors*.

Thus, the dynamics are described by two sets of three variables: one set parametrizing the diagonal metric, $\{\alpha, \beta_+, \beta_-\}$, and another set specifying the diagonalizing matrix R, which are the Euler angles $\{\phi, \theta, \psi\}$.

Three cases for a Bianchi IX universe can be distinguished [100]:

- *Diagonal (or non-rotating) case:* In this case, the metric is diagonal, i.e., $h_{ij} = \bar{h}_{ij}$. This model of the universe is also known as the Mixmaster universe.

- *Symmetric (non-tumbling) case:* In this case, there is a rotation around only one axis, so h_{ij} has one off-diagonal term. Considering a rotation around the z-axis, we have $R \equiv R_z(\phi)$, and the metric becomes

$$h = R_z^T(\phi) \bar{h} R_z(\phi). \tag{2.21}$$

- *General case:* In this case, the metric h_{ij} is a general 3×3 matrix, given by (2.19) with a rotation matrix defined in (5.4).

Note that the closed FLRW model is a special case of the diagonal Bianchi IX, with $\beta_+ = \beta_- = 0$. In addition, the Bianchi IX model also contains the axisymmetric Bianchi IX universe as a special case, for which the space exhibits axial symmetry in addition to invariance under SO(3). The axisymmetric Bianchi IX line element is recovered by setting $\beta_- = 0$ in (2.20). Thus, for this model, the dynamical variables are only α and β_+.

Finally, we note that D. H. King [103] has demonstrated that any Bianchi type-IX universe can be interpreted as a closed FLRW universe with superimposed circularly polarized gravitational waves, where the longest wavelength fits into the closed universe.

Invariant basis

The invariant basis (which is right-invariant for left-homogeneous space) has to satisfy the commutation relations (2.12). For the Bianchi IX model with structure constants $C^k_{ij} = -\varepsilon_{ijk}$, it reads

$$[e_i, e_j] = \varepsilon_{ijk} e_k. \tag{2.22}$$

The construction of the invariant basis is presented in detail in Appendix A.2. The invariant basis in terms of the Euler angles in zyz-convention is given by

$$\begin{aligned} e_1 &= \sin\psi \frac{\partial}{\partial\theta} + \cos\psi \left(\cot\theta \frac{\partial}{\partial\psi} - \frac{1}{\sin\theta}\frac{\partial}{\partial\phi} \right), \\ e_2 &= \cos\psi \frac{\partial}{\partial\theta} - \sin\psi \left(\cot\theta \frac{\partial}{\partial\psi} - \frac{1}{\sin\theta}\frac{\partial}{\partial\phi} \right), \\ e_3 &= \frac{\partial}{\partial\psi}. \end{aligned} \tag{2.23}$$

The Killing vectors, which form a left-invariant basis, $\xi_i \equiv \tilde{e}_i$, are related to the right-invariant basis by the matrix adjoint representation of the Lie group [97]. In our case, the adjoint group of SO(3) is the group SO(3) itself.Therefore, the matrices of the adjoint representation are the rotation matrices $R \in \mathrm{SO}(3)$, given by (5.4). Thus, the left- and right-invariant bases are related by

$$\tilde{e}_j = R^i{}_j e_i. \tag{2.24}$$

Using this relation, one can obtain the left-invariant basis, which has the form

$$\begin{aligned} \tilde{e}_1 &= -\sin\phi \frac{\partial}{\partial\theta} - \cos\phi \left(\cot\theta \frac{\partial}{\partial\phi} - \frac{1}{\sin\theta}\frac{\partial}{\partial\psi} \right) \\ \tilde{e}_2 &= \cos\phi \frac{\partial}{\partial\theta} - \sin\phi \left(\cot\theta \frac{\partial}{\partial\phi} - \frac{1}{\sin\theta}\frac{\partial}{\partial\psi} \right) \\ \tilde{e}_3 &= \frac{\partial}{\partial\phi}, \end{aligned} \tag{2.25}$$

and satisfies the commutation relations

$$[\tilde{e}_i, \tilde{e}_j] = -\varepsilon_{ijk} \tilde{e}_k. \tag{2.26}$$

Finally, it is easy to show that

$$[\tilde{e}_i, e_j] = 0, \quad \text{for} \quad \forall\, i, j. \tag{2.27}$$

One-forms

To calculate the one-forms $\{\sigma^i\}$ dual to the basis $\{e_i\}$, we first express both in terms of the coordinates

$$e_\nu = \sigma_\nu{}^\tau \partial_\tau, \quad \text{and} \quad \sigma^\nu = \sigma^\nu{}_\mu \, dx^\mu, \tag{2.28}$$

where

$$\sigma^\nu{}_\mu \, \sigma_\nu{}^\tau = \delta^\tau_\mu. \tag{2.29}$$

Using the above relations and coordinates $(x^0, x^1, x^2, x^3) = (t, \phi, \theta, \psi)$, one-forms dual to the basis (2.23) can be expressed as

$$\begin{aligned}
\sigma^0 &= dt, \\
\sigma^1 &= -\cos\psi \sin\theta d\phi + \sin\psi d\theta, \\
\sigma^2 &= \sin\psi \sin\theta d\phi + \cos\psi d\theta, \\
\sigma^3 &= \cos\theta d\phi + d\psi.
\end{aligned} \tag{2.30}$$

Moreover, the wedge product takes the form

$$\sigma^1 \wedge \sigma^2 \wedge \sigma^3 = -\sin\theta d\phi \wedge d\theta \wedge d\psi = \sin\theta d\theta \wedge d\phi \wedge d\psi. \tag{2.31}$$

Finally, it can be shown that the following relations hold for the one-forms corresponding to the left-invariant and right-invariant bases [97]

$$R^{-1} dR = \mathcal{J}_a \sigma^a, \quad \text{and} \quad dR\, R^{-1} = \mathcal{J}_a \tilde{\sigma}^a, \tag{2.32}$$

where $R \in \mathrm{SO}(3)$ and $\mathcal{J}_a$ are the generators of the rotation group SO(3), given by (5.11).

3 Quantum Field Theory in curved spacetime

In this section, we will explore the foundations of quantum field theory (QFT) in curved spacetime, beginning with the standard framework of QFT in Minkowski spacetime. We start by reviewing the essential concepts and equations governing spinor fields, with particular focus on Dirac and Weyl spinors, which are central to the study of fermionic fields in quantum field theory.

Extending the formulation of spinor fields to curved spacetime presents a challenge, as the concept of a spinor is inherently tied to Lorentz invariance, which is not manifest in general curved spacetimes. To address this, we utilize the vierbein formalism, which allows us to relate the curved spacetime metric to a locally flat frame. This enables the construction of a Lorentz-invariant Lagrangian for spinor fields in curved spacetime, ensuring the proper definition and behavior of spinors in such a setting.

We conclude this section with a discussion of cosmological particle creation in an expanding universe, which provides a natural transition to our study of spinor fields in the Bianchi IX universe. In this context, we will investigate how the structure of the universe influences the dynamics of Weyl and Dirac spinors.

Throughout this section, we follow the standard treatments and methodologies presented in established textbooks on quantum field theory in Minkowski spacetime [104–108] and in curved spacetime [6], [109], [110].

3.1 Spinor field in Minkowski spacetime

The Lagrangian density[13] of the Dirac spinor field in Minkowski spaectime is given by

$$\mathcal{L} = \bar{\Psi}(i\gamma^\mu \partial_\mu - m)\Psi, \tag{3.1}$$

where $\bar{\Psi} = \Psi^\dagger \gamma^0$. From the Euler-Lagrange equation we derive the Dirac equation

$$(i\gamma^\mu \partial_\mu - m)\Psi = 0. \tag{3.2}$$

The matrices γ^μ satisfy the anticommutation rules

$$\{\gamma^\mu, \gamma^\nu\} = -2\eta^{\mu\nu}, \tag{3.3}$$

where the sign convention is $(-, +, +, +)$. We use the gamma matrices in the *Weyl (or chiral) representation*, among other possible choices such as the Dirac and Majorana

[13]For convenience, we will refer to it simply as the Lagrangian.

representations, as it best suits our analysis; hence, they take the form

$$\gamma^0 = \begin{pmatrix} 0 & I \\ I & 0 \end{pmatrix}, \quad \gamma^i = \begin{pmatrix} 0 & \sigma_i \\ -\sigma_i & 0 \end{pmatrix}, \quad \gamma^5 = \begin{pmatrix} -I & 0 \\ 0 & I \end{pmatrix}, \tag{3.4}$$

with the Pauli matrices given by

$$\sigma_1 = \begin{pmatrix} 0 & 1 \\ 1 & 0 \end{pmatrix}, \quad \sigma_2 = \begin{pmatrix} 0 & -i \\ i & 0 \end{pmatrix}, \quad \sigma_3 = \begin{pmatrix} 1 & 0 \\ 0 & -1 \end{pmatrix}. \tag{3.5}$$

The Klein-Gordon equation is satisfied by each component of the Dirac spinor Ψ. Indeed, acting on the Dirac equation (3.2) with the operator $(i\gamma^\nu\partial_\nu + m)$ leads to the Klein-Gordon equation, namely

$$(i\gamma^\nu\partial_\nu + m)(i\gamma^\mu\partial_\mu - m)\Psi = -(\gamma^\mu\gamma^\nu\partial_\mu\partial_\nu + m^2)\Psi = (\partial_\mu\partial^\mu - m^2)\Psi = 0, \tag{3.6}$$

where we used

$$\gamma^\mu\gamma^\nu\partial_\mu\partial_\nu = \frac{1}{2}\{\gamma^\mu, \gamma^\nu\}\partial_\mu\partial_\nu = -\partial_\mu\partial^\mu. \tag{3.7}$$

Introducing the notation

$$\sigma^\mu = (I, \sigma^i), \quad \bar{\sigma}^\mu = (I, -\sigma^i), \quad \mu = 0, 1, 2, 3, \tag{3.8}$$

we can express γ^μ as

$$\gamma^\mu = \begin{pmatrix} 0 & \sigma^\mu \\ \bar{\sigma}^\mu & 0 \end{pmatrix}. \tag{3.9}$$

The Dirac spinor representation of the Lorentz group is reducible. It decomposes into two irreducible representations: left-handed and right-handed spinor representations, which act on two-component spinors. Therefore, the spinor Ψ can be written in the following form

$$\Psi = \begin{pmatrix} \Psi_L \\ \Psi_R \end{pmatrix}, \tag{3.10}$$

where Ψ_L and Ψ_R are known as the left-handed and right-handed Weyl spinors, respectively. In terms of these spinors, the Dirac Lagrangian takes the form

$$\mathcal{L} = i\Psi_R^\dagger\sigma^\mu\partial_\mu\Psi_R + i\Psi_L^\dagger\bar{\sigma}^\mu\partial_\mu\Psi_L - m\left(\Psi_R^\dagger\Psi_L + \Psi_L^\dagger\Psi_R\right). \tag{3.11}$$

Hence, we see that the mass m couples the left-handed and right-handed spinors. For the massless case we can write

$$\mathcal{L} = \mathcal{L}_L + \mathcal{L}_R, \tag{3.12}$$

where

$$\mathcal{L}_L = i\Psi_L^\dagger \bar{\sigma}^\mu \partial_\mu \Psi_L, \tag{3.13}$$

and

$$\mathcal{L}_R = i\Psi_R^\dagger \sigma^\mu \partial_\mu \Psi_R. \tag{3.14}$$

These are the Lagrangians for the left-handed and right-handed spinors, respectively.

Furthermore, the Dirac Hamiltonian density reads

$$\mathcal{H} = \bar{\Psi}\left(-i\gamma^i \partial_i + m\right)\Psi. \tag{3.15}$$

In terms of the Ψ_L and Ψ_R spinors it takes the form

$$\mathcal{H} = i\Psi_L^\dagger \sigma^i \partial_i \Psi_L - i\Psi_R^\dagger \sigma^i \partial_i \Psi_R + m\left[\Psi_R^\dagger \Psi_L + \Psi_L^\dagger \Psi_R\right]. \tag{3.16}$$

For the massless case, we get

$$\mathcal{H} = \mathcal{H}_L + \mathcal{H}_R, \tag{3.17}$$

where

$$\mathcal{H}_L = i\Psi_L^\dagger \sigma^i \partial_i \Psi_L, \tag{3.18}$$

and

$$\mathcal{H}_R = -i\Psi_R^\dagger \sigma^i \partial_i \Psi_R. \tag{3.19}$$

Finally, in terms of the Weyl spinors, the Dirac equation reads

$$\begin{pmatrix} -m & i\sigma^\mu \partial_\mu \\ i\bar{\sigma}^\mu \partial_\mu & -m \end{pmatrix} \begin{pmatrix} \Psi_L \\ \Psi_R \end{pmatrix} = 0, \tag{3.20}$$

which leads to two equations

$$i\bar{\sigma}^\mu \partial_\mu \Psi_L = m\Psi_R, \tag{3.21}$$

and

$$i\sigma^\mu \partial_\mu \Psi_R = m\Psi_L. \tag{3.22}$$

For the massless fermions, we obtain the Weyl equations

- *Left-handed*:

$$i\bar{\sigma}^\mu \partial_\mu \Psi_L = 0, \tag{3.23}$$

- *Right-handed*:

$$i\sigma^\mu \partial_\mu \Psi_R = 0. \tag{3.24}$$

In the following sections, we will explore the solutions to the Weyl and Dirac equations, as well as the quantization of the corresponding spinor fields.

3.1.1 Weyl spinor field

The discovery of neutrino oscillations provided definitive evidence that neutrinos have mass, ruling out the possibility of them being purely massless Weyl fermions. Consequently, neutrinos are expected to be either Dirac or Majorana particles[14]. However, for our study, we discuss the Weyl spinors not as for its relevance in the true nature of neutrinos rather for the relevance for its formalism which serves as a foundational framework for understanding more general spinor fields. In Nature, neutrinos are observed to be left-handed[15], meaning that in weak interactions, neutrinos are predominantly left-handed, while antineutrinos are right-handed, making the left-handed Weyl equation a natural starting point for our analysis. By studying the Weyl field in detail, we lay the groundwork for later discussions on massive spinor fields.

Solution

Separating the temporal and spatial components in the left-handed Weyl equation (3.23), we obtain

$$\partial_0 \Psi_L(x) = \sigma^i \partial_i \Psi_L(x). \tag{3.25}$$

Let us look for the solution to this equation by separating the variables into temporal and spatial parts, i.e.

$$\Psi_L(x) = N(t)\Psi_L(\mathbf{x}), \tag{3.26}$$

where $N(t)$ is a function of t and $\Psi_L(\mathbf{x})$ is a spinor[16]. Substituting this into the Weyl equation, we obtain

$$i\frac{1}{N(t)}\partial_0 N(t) = i\frac{1}{\Psi_L(\mathbf{x})}\sigma^i \partial_i \Psi_L(\mathbf{x}). \tag{3.27}$$

Since the left side of the equation depends only on time and the right side only on space, both sides can be set equal to a constant E. Hence, we get

$$i\frac{1}{N(t)}\partial_0 N(t) = E, \quad \to \quad N(t) = e^{-iEt}. \tag{3.28}$$

[14]Dirac neutrinos are fermions with mass, described by four-component spinors that include both left- and right-handed components. Majorana neutrinos, also massive, are described by a four-component spinor, but with the restriction that they are equal to their own charge conjugates, making them their own antiparticles.

[15]Both Dirac and Majorana neutrinos can have left- and right-handed components, with the mass term linking the two; however, only the left-handed component interacts with the weak force [106].

[16]We use the notation $\vec{x} = \mathbf{x}$.

and

$$\left(i\sigma^i\partial_i - E\right)\Psi_L(\mathbf{x}) = 0. \tag{3.29}$$

To solve this equation, we can apply a Fourier expansion and seek solutions of the following form,

$$\Psi_p(\mathbf{x}) = w_L(p)e^{\pm i\mathbf{p}\cdot\mathbf{x}} \equiv w_L(p)e^{\pm ip_ix^i}, \tag{3.30}$$

where $w_L(p)$ are two-spinors.

Substituting this into (3.29) leads to

$$\left(\pm\sigma^i p_i + E\right) w_L(p) = 0. \tag{3.31}$$

Using the Pauli matrices (3.5) explicitly, we obtain

$$\begin{pmatrix} \pm E + p_3 & p_1 - ip_2 \\ p_1 + ip_2 & \pm E - p_3 \end{pmatrix} w_L(p) = 0. \tag{3.32}$$

It is straightforward to show that from this one gets $E^2 = p_1^2 + p_2^2 + p_3^2 = |\mathbf{p}|^2$. Introducing $\varepsilon_p = |\mathbf{p}| > 0$, we can write the energy eigenvalues as $E = \pm\varepsilon_p$.

Furthermore, to find the eigenspinors we can look for the solutions by the following form,

$$w_L(p) = \begin{bmatrix} f_1(p) \\ f_2(p) \end{bmatrix}. \tag{3.33}$$

Substituting this into (3.32), we get two solutions:

$$f_1(p) = \frac{(p_1 - ip_2)}{(-\varepsilon_p - p_3)} f_2(p), \tag{3.34}$$

and

$$f_2(p) = \frac{(p_1 + ip_2)}{(-\varepsilon_p + p_3)} f_1(p). \tag{3.35}$$

The two independent solutions can be given as

- The positive frequency solution[17]

$$\Psi_p^{(+)} = w_L^1(p)e^{-ip\cdot x} := u_L(p)e^{i(\varepsilon_p t - \mathbf{p}\cdot\mathbf{x})}, \tag{3.36}$$

[17] Note that the sign in the exponent $e^{ip\cdot x}$ differs from standard QFT textbooks, for example, [106], due to a different choice of metric signature.

- The negative frequency solution

$$\Psi_p^{(-)} = w_L^2(p)e^{ip\cdot x} := v_L(p)e^{i(-\varepsilon_p t+\mathbf{p}\cdot\mathbf{x})}, \tag{3.37}$$

where u_L and v_L are the eigenspinors[18].

The eigenspinors satisfy the following normalization and orthogonality conditions:

$$u_L^\dagger(p)u_L(p) = v_L^\dagger(p)v_L(p) = 1, \tag{3.38}$$

and

$$u_L^\dagger(p)u_L(\tilde{p}) = v_L^\dagger(p)v_L(\tilde{p}) = u_L^\dagger(p)v_L(\tilde{p}) = 0, \tag{3.39}$$

where $\tilde{p}_\mu = (-\varepsilon_p, -\mathbf{p})$.

Thus, using the relations (3.34) and (3.35), along with the orthonormalization conditions above, the positive and negative frequency solutions take the forms

$$\Psi_p^{(+)}(x) = u_L(p)e^{-ip\cdot x} = \frac{1}{\sqrt{2\varepsilon_p(\varepsilon_p - p_z)}}\begin{pmatrix} -\varepsilon_p + p_z \\ p_x + ip_y \end{pmatrix} e^{i(\varepsilon_p t-\mathbf{p}\cdot\mathbf{x})}, \tag{3.40}$$

and

$$\Psi_p^{(-)}(x) = v_L(p)e^{ip\cdot x} = \frac{1}{\sqrt{2\varepsilon_p(\varepsilon_p + p_z)}}\begin{pmatrix} -p_x + ip_y \\ \varepsilon_p + p_z \end{pmatrix} e^{i(-\varepsilon_p t+\mathbf{p}\cdot\mathbf{x})}. \tag{3.41}$$

Finally, the general solution can be expressed as a linear combination of the positive and negative energy solutions as follows:

$$\Psi_L(x) = \int \frac{d^3p}{(2\pi)^3}\left[a(\mathbf{p})\Psi_p^{(+)}(x) + b^*(\mathbf{p})\Psi_p^{(-)}(x)\right]. \tag{3.42}$$

Quantization

The field is quantized by taking $a(\mathbf{p})$ and $b(\mathbf{p})$ as operators,

$$\Psi_L(x) = \int \frac{d^3p}{(2\pi)^3}\left[a(\mathbf{p})u_L(p)e^{-ip\cdot x} + b^\dagger(\mathbf{p})v_L(p)e^{ip\cdot x}\right], \tag{3.43}$$

$$\Psi_L^\dagger(x) = \int \frac{d^3p}{(2\pi)^3}\left[a^\dagger(\mathbf{p})u_L^\dagger(p)e^{ip\cdot x} + b(\mathbf{p})v_L^\dagger(p)e^{-ip\cdot x}\right], \tag{3.44}$$

[18]Later, we will show that these spinors are indeed left-handed, thus justifying the name.

and requiring the following anticommutation relations to hold:

$$\{a(\mathbf{p}), a^\dagger(\mathbf{q})\} = (2\pi)^3\delta^{(3)}(\mathbf{p}-\mathbf{q}), \quad \{b(\mathbf{p}), b^\dagger(\mathbf{q})\} = (2\pi)^3\delta^{(3)}(\mathbf{p}-\mathbf{q}), \tag{3.45}$$

We define the vacuum state by

$$a(\mathbf{p})|0\rangle = b(\mathbf{p})|0\rangle = 0. \tag{3.46}$$

The operator $a^\dagger(\mathbf{p})$ creates a neutrino, and $b^\dagger(\mathbf{p})$ creates an antineutrino, the helicities of which are discussed below.

Helicity

For the Dirac spinor, the helicity operator, which is the projection of angular momentum along the direction of momentum, is defined by

$$h = \frac{i}{2}\varepsilon_{ijk}p^i\Sigma^{jk} = \frac{1}{2}p_i\begin{pmatrix}\sigma^i & 0\\ 0 & \sigma^i\end{pmatrix}, \tag{3.47}$$

where the Lorentz group generators are

$$\Sigma^{ij} = -\frac{i}{2}\epsilon^{ijk}\begin{pmatrix}\sigma^k & 0\\ 0 & \sigma^k\end{pmatrix}. \tag{3.48}$$

Therefore, the helicity operator acting on the Weyl spinors is

$$h = \frac{1}{2|\mathbf{p}|}\sigma^i p_i \equiv \frac{1}{2\varepsilon_p}\sigma^i p_i. \tag{3.49}$$

It is easy to show that the solutions of the Weyl equation are helicity eigenstates. Indeed, let us first write the positive and negative frequency solutions in a general form,

$$\Psi_p^{(\pm)} = w_L(p)e^{\pm ip\cdot x}. \tag{3.50}$$

Substituting this into the left-handed Weyl equation (3.23), we obtain

$$\left[\bar{\sigma}^0 p_0 + \bar{\sigma}^i p_i\right] w_L(p)e^{\pm ip\cdot x} = 0, \tag{3.51}$$

which leads to

$$Ip_0 w_L(p) = \sigma^i p_i w_L(p). \tag{3.52}$$

Recalling the definition (3.49), and rewriting the above equation in terms of the helicity operator, we obtain the eigenvalue equation

$$hw_L(p) = \lambda w_L(p), \tag{3.53}$$

where the eigenvalues are $\lambda = \frac{1}{2|\mathbf{p}|}p_0$. Since $p_0 = -\varepsilon_p$, the helicity eigenvalue is $-\frac{1}{2}$, and thus we have

$$h\Psi_p^{(\pm)} = -\frac{1}{2}\Psi_p^{(\pm)}. \tag{3.54}$$

Therefore, as indicated by the name, we have shown that this is indeed a left-handed spinor. The solutions of the right-handed Weyl equation are also eigenstates of the helicity operator, with the corresponding helicity eigenvalue of $+\frac{1}{2}$.

One can prove that the Weyl operator of the left-handed spinor field (3.43) annihilates a negative helicity particle and creates a positive helicity antiparticle. Hence, it can be shown that $a^\dagger(\mathbf{p})$ creates a neutrino with negative helicity, and $b^\dagger(\mathbf{p})$ creates an antineutrino with positive helicity:

$$ha^\dagger(\mathbf{p})|0\rangle = -\frac{1}{2}a^\dagger(\mathbf{p})|0\rangle, \quad \text{and} \quad hb^\dagger(\mathbf{p})|0\rangle = \frac{1}{2}b^\dagger(\mathbf{p})|0\rangle. \tag{3.55}$$

Explicit and detailed calculations can be found in [111].

Hamiltonian

To complete this section, let us express the Hamiltonian in terms of creation and annihilation operators. Recalling the left-handed Hamiltonian

$$H_L = i\int d^3x\, \Psi_L^\dagger \sigma^i \partial_i \Psi_L, \tag{3.56}$$

and inserting (3.43) and (3.44), we can express the Hamiltonian in terms of creation and annihilation operators as

$$H_L = \int \frac{d^3p}{(2\pi)^3}\, \varepsilon_p \Big\{a^\dagger(\mathbf{p})a(\mathbf{p}) + b^\dagger(\mathbf{p})b(\mathbf{p}) - \delta^3(0)\Big\}, \tag{3.57}$$

where the delta function evaluated at zero, $\delta^3(0)$, represents an infinite vacuum energy contribution arising from the integral over all momentum modes. To remove this unphysical divergence, normal ordering is applied [106].

3.1.2 Dirac spinor field

As we have shown, the Dirac equation (3.20) in the Weyl basis leads to two separate equations,

$$i\sigma^\mu \partial_\mu \Psi_R = m\Psi_L, \tag{3.58}$$

and

$$i\bar{\sigma}^\mu \partial_\mu \Psi_L = m\Psi_R. \tag{3.59}$$

Let us now proceed with the solution of these equations.

Solution

Separating the temporal and spatial parts of the spinor field, we can seek solutions of the following form:

$$\Psi(t, \mathbf{x}) = N(t)w(\mathbf{x}) = N(t)\begin{pmatrix} w_L \\ w_R \end{pmatrix}, \tag{3.60}$$

where the four-spinor w can be expressed in terms of the left-handed and right-handed Weyl spinors. Substituting the above decomposition into equations (3.58) and (3.59), we obtain

$$\begin{aligned} Ew_L &= i\sigma^i\partial_i w_L + mw_R, \\ Ew_R &= -i\sigma^i\partial_i w_R + mw_L, \end{aligned} \tag{3.61}$$

where E is a constant introduced by

$$i\frac{\partial_t N(t)}{N(t)} = E \quad \rightarrow \quad N(t) = e^{-iEt}. \tag{3.62}$$

Furthermore, using the Fourier expansion

$$\begin{pmatrix} w_L \\ w_R \end{pmatrix} = \begin{pmatrix} w_L^p \\ w_R^p \end{pmatrix} e^{\pm ip_i x^i}, \tag{3.63}$$

and substituting this into the equations (3.61) leads to

$$\begin{aligned} \left(-E \pm \sigma^i p_i\right) w_R^p + mw_L^p &= 0, \\ \left(-E \mp \sigma^i p_i\right) w_L^p + mw_R^p &= 0. \end{aligned} \tag{3.64}$$

From the above relations, we deduce:

$$\left(-E \mp \sigma^i p_i\right)\left(-E \pm \sigma^i p_i\right) - m^2 = 0, \tag{3.65}$$

which leads to the following energy eigenvalues:

$$E = \pm(m^2 + |\mathbf{p}|^2)^{1/2} := \pm\varepsilon_p. \tag{3.66}$$

To calculate the eigenspinors w_p, let us first consider the rest frame where $p_i = 0$. In this case, the energy eigenvalues are $E = \pm m$. Substituting this into equation (3.64), we obtain two independent solutions:

$$u_s \equiv w_p^1(p_i = 0) = \begin{pmatrix} \xi_s \\ \xi_s \end{pmatrix}, \quad v_s \equiv w_p^2(p_i = 0) = \begin{pmatrix} \eta_s \\ -\eta_s \end{pmatrix}, \tag{3.67}$$

where the two-component spinors ξ_s and η_s are given by

$$\{\xi_s, \eta_s\} = \left\{ \begin{pmatrix} 1 \\ 0 \end{pmatrix}, \begin{pmatrix} 0 \\ 1 \end{pmatrix} \right\}, \quad s = 1, 2. \tag{3.68}$$

Then, it is straightforward to show that the general eigenspinors of equation (3.64) take the form

$$u_s(p) = \begin{pmatrix} \sqrt{p \cdot \sigma}\, \xi_s \\ \sqrt{p \cdot \bar{\sigma}}\, \xi_s \end{pmatrix} \tag{3.69}$$

and

$$v_s(p) = \begin{pmatrix} \sqrt{p \cdot \sigma}\, \eta_s \\ -\sqrt{p \cdot \bar{\sigma}}\, \eta_s \end{pmatrix}, \tag{3.70}$$

which satisfy the following normalization conditions,

$$\bar{u}_r(p) u_s(p) = 2m\delta_{rs}, \quad \text{and} \quad \bar{v}_r(p) v_s(p) = -2m\delta_{rs}. \tag{3.71}$$

Hence, the positive- and negative-frequency solutions are given by

$$\Psi_p^{s(+)}(x) = u_s(p) e^{ip\cdot x}, \tag{3.72}$$

and

$$\Psi_p^{s(-)}(x) = v_s(p) e^{-ip\cdot x}. \tag{3.73}$$

Quantization

The spinor field can be expanded as

$$\Psi(x) = \sum_{s=1,2} \int \frac{d^3p}{(2\pi)^3} \frac{1}{\sqrt{2\varepsilon_p}} \left[a_{\mathbf{p}}^s u_s(p) e^{-ip\cdot x} + b_{\mathbf{p}}^{s\,\dagger} v_s(p) e^{ip\cdot x} \right], \tag{3.74}$$

and similarly,

$$\bar{\Psi}(x) = \sum_{s=1,2} \int \frac{d^3p}{(2\pi)^3} \frac{1}{\sqrt{2\varepsilon_p}} \left[a_{\mathbf{p}}^{s\,\dagger} \bar{u}_s(p) e^{ip\cdot x} + b_{\mathbf{p}}^s \bar{v}_s(p) e^{-ip\cdot x} \right], \tag{3.75}$$

where $\varepsilon_p = \sqrt{\mathbf{p}^2 + m^2}$ is the relativistic energy.

The operators $a_{\mathbf{p}}^{s\,\dagger}$ and $a_{\mathbf{p}}^s$ are the creation and annihilation operators for a fermion, while $b_{\mathbf{p}}^{s\,\dagger}$ and $b_{\mathbf{p}}^s$ are the creation and annihilation operators for an antifermion. The index s labels the spin degrees of freedom, taking values $s = 1, 2$ for a spin-$\frac{1}{2}$ field. The spinors $u_s(p)$ and $v_s(p)$ are solutions of the Dirac equation, corresponding to fermion and antifermion states with momentum $\mathbf{p}$ and energy ε_p.

The operators satisfy the following anticommutation relations:

$$\{a^r_{\mathbf{p}}, a^{s\dagger}_{\mathbf{q}}\} = \{b^r_{\mathbf{p}}, b^{s\dagger}_{\mathbf{q}}\} = (2\pi)^3\delta^{(3)}(\mathbf{p}-\mathbf{q})\delta^{rs}. \tag{3.76}$$

The vacuum state is defined by

$$a^s_{\mathbf{p}}|0\rangle = b^r_{\mathbf{p}}|0\rangle = 0. \tag{3.77}$$

Helicity

It is important to note that, unlike Weyl spinors, the helicity of massive Dirac particles, as defined by (3.47), depends on the reference frame. The helicity of massive Dirac particles can change under Lorentz transformations because a boost to a different reference frame can reverse the momentum direction, which in turn flips the helicity. In contrast, for massless particles, helicity is Lorentz-invariant. Therefore, rather than helicity, the *chirality* of the spinor is Lorentz-invariant, making it a more fundamental quantity in relativistic quantum field theory.

Chirality is defined as the eigenvalue of the chirality operator, given by

$$\gamma^5 = i\gamma^0\gamma^1\gamma^2\gamma^3. \tag{3.78}$$

The Dirac spinor can then be decomposed into left-handed and right-handed components (which we already mentioned) using the projection operators

$$\Psi_L = P_L\Psi, \quad \Psi_R = P_R\Psi, \tag{3.79}$$

where the projection operators are

$$P_L = \frac{1-\gamma^5}{2}, \quad P_R = \frac{1+\gamma^5}{2}. \tag{3.80}$$

For massless particles, chirality and helicity are the same, since a massless particle's momentum always aligns with its spin in any reference frame.

Hamiltonian

The Hamiltonian for the Dirac field is given by

$$H = \int d^3x\ \bar{\Psi}\left(-i\gamma^i\partial_i + m\right)\Psi. \tag{3.81}$$

First, we observe that substituting the positive and negative frequency solutions into the Dirac equation leads to the following relations:

$$\begin{aligned}\left(\gamma^i p_i + m\right) u_s(p) &= -\gamma^0 p_0 u_s(p) = \varepsilon_p \gamma^0 u_s(p),\\ \left(-\gamma^i p_i + m\right) v_s(p) &= \gamma^0 p_0 v_s(p) = -\varepsilon_p \gamma^0 v_s(p).\end{aligned} \tag{3.82}$$

Next, we recall the following standard relations (see, for example, [112])

$$\begin{aligned}\bar{u}_{s'}(\mathbf{p})\gamma^0 u_s(\mathbf{p}) &= 2p^0 \delta_{ss'} = 2\varepsilon_p \delta_{ss'},\\ \bar{v}_{s'}(\mathbf{p})\gamma^0 v_s(\mathbf{p}) &= 2p^0 \delta_{ss'} = 2\varepsilon_p \delta_{ss'},\end{aligned} \tag{3.83}$$

and

$$\begin{aligned}\bar{u}_{s'}(-\mathbf{p})\gamma^0 v_s(\mathbf{p}) &= 0,\\ \bar{v}_{s'}(-\mathbf{p})\gamma^0 u_s(\mathbf{p}) &= 0.\end{aligned} \tag{3.84}$$

Substituting the field expansions (3.74) and (3.75) into the Hamiltonian (3.81), and utilizing the relations above, we obtain the following expression for the Hamiltonian:

$$H = \sum_s \int \frac{d^3p}{(2\pi)^3} \varepsilon_p \left\{ a_{\mathbf{p}}^{s\,\dagger} a_{\mathbf{p}}^s + b_{\mathbf{p}}^{s\,\dagger} b_{\mathbf{p}}^s - \delta^{(3)}(0) \right\}. \tag{3.85}$$

3.2 Spinor field in curved spacetime

To generalize the Dirac equation to curved spacetime (as well as to accelerated frames in Minkowski space), the notion of spinors must be appropriately extended. This extension can be achieved through the vierbein formalism, which provides a framework for addressing the local Lorentz invariance of the Dirac equation in a general Riemannian spacetime. By introducing vierbeins, we can translate between the curved spacetime and the locally flat tangent space, ensuring that the spinor fields transform appropriately under local Lorentz transformations. This approach allows us to formulate the Dirac equation in a manner consistent with general relativity, while preserving its fundamental structure.

In constructing this section, we rely on the comprehensive treatments provided in the textbooks by Parker and Toms [110], Birrell and Davies [6], and Grib et al. [113], alongside the insightful lecture notes by Saharian [114], all of which address key aspects of spinors in curved spacetime.

Vierbein Formalism

The vierbein (or tetrad) is a set of four linearly independent vector fields that form an orthonormal basis for the tangent space at each point of a four-dimensional curved spacetime. The vierbein, denoted by $\hat{h}^{\hat{\alpha}}{}_{\mu}(x)$, relates the curved spacetime metric to the flat Minkowski metric, i.e. by use of vierbein, the spacetime dependence is shifted into the vierbeins.

The metric can be expressed via

$$g_{\mu\nu}(x) = \eta_{\hat{\alpha}\hat{\beta}} \hat{h}^{\hat{\alpha}}{}_{\mu}(x) \hat{h}^{\hat{\beta}}{}_{\nu}(x), \tag{3.86}$$

where $\eta_{\hat{\alpha}\hat{\beta}}$ is the Minkowski metric with signature $(-, +, +, +)$. Note that μ, ν are the spacetime indices and $\hat{\alpha}, \hat{\beta}$ are the local inertial frame indices.

Introducing one-forms $\chi^{\hat{\alpha}}(x)$ of the local orthonormal frame by

$$\chi^{\hat{\alpha}}(x) = \hat{h}^{\hat{\alpha}}{}_{\mu}(x) dx^{\mu}, \tag{3.87}$$

the line element in the curved spacetime can be written as

$$ds^2 = g_{\mu\nu}(x) dx^{\mu} dx^{\nu} = \eta_{\hat{\alpha}\hat{\beta}}\, \chi^{\hat{\alpha}}(x) \chi^{\hat{\alpha}}(x). \tag{3.88}$$

The tetrad $\hat{h}^{\hat{\alpha}}{}_{\mu}(x)$ satisfies the relations

$$\hat{h}_{\hat{\alpha}}{}^{\mu} \hat{h}_{\hat{\beta}\mu} = \eta_{\hat{\alpha}\hat{\beta}}, \quad \hat{h}^{\hat{\alpha}}{}_{\mu} \hat{h}_{\hat{\beta}}{}^{\mu} = \delta^{\hat{\alpha}}{}_{\hat{\beta}}, \quad \hat{h}^{\hat{\alpha}}{}_{\mu} \hat{h}_{\hat{\alpha}\nu} = g_{\mu\nu}, \tag{3.89}$$

where we introduced $\hat{h}_{\hat{\alpha}}{}^{\mu}$, which is the reciprocal tetrad (also known as dual tetrad or inverse vierbein).

Additionally, the following duality relations hold:

$$\hat{h}_{\hat{\alpha}}{}^{\mu} \hat{h}^{\hat{\alpha}}{}_{\nu} = \delta^{\mu}{}_{\nu}, \quad \hat{h}_{\hat{\alpha}}{}^{\mu} \hat{h}^{\hat{\beta}}{}_{\mu} = \delta^{\hat{\alpha}}{}_{\hat{\beta}}. \tag{3.90}$$

The generalized gamma matrices in curved spacetime are defined by

$$\gamma^{\mu}(x) = \hat{h}_{\hat{\alpha}}{}^{\mu}(x) \gamma^{\hat{\alpha}}, \tag{3.91}$$

where the $\gamma^{\hat{\alpha}}$ are the gamma matrices in Minkowski spacetime, which satisfy the following anticommutation relations:

$$\{\gamma^{\hat{\alpha}}, \gamma^{\hat{\beta}}\} = -2\eta^{\hat{\alpha}\hat{\beta}}. \tag{3.92}$$

Therefore, in curved spacetime, the generalized gamma matrices satisfy

$$\{\gamma^{\mu}(x), \gamma^{\nu}(x)\} = -2g^{\mu\nu}(x). \tag{3.93}$$

The covariant derivative acting on the spinor is defined by

$$\nabla_{\mu}\Psi = (\partial_{\mu} + \Gamma_{\mu})\Psi, \tag{3.94}$$

with the connection Γ_μ given by

$$\Gamma_\mu(x) = \frac{1}{2}\hat{h}_{\hat{\alpha}\nu}\left(\nabla_\mu \hat{h}_{\hat{\beta}}^{\ \nu}\right)\Sigma^{\hat{\alpha}\hat{\beta}}, \tag{3.95}$$

where $\Sigma^{\hat{\alpha}\hat{\beta}}$ are the generators of the Lorentz group and, as such, have the form

$$\Sigma^{\hat{\alpha}\hat{\beta}} = \frac{1}{4}\left[\gamma^{\hat{\alpha}}, \gamma^{\hat{\beta}}\right]. \tag{3.96}$$

Moreover, the covariant derivative of the tetrad is given by

$$\nabla_\mu \hat{h}_{\hat{\beta}}^{\ \nu} = \partial_\mu \hat{h}_{\hat{\beta}}^{\ \nu} + \Gamma^\nu_{\mu\sigma}\hat{h}_{\hat{\beta}}^{\ \sigma}. \tag{3.97}$$

Dirac equation

Finally, we can write the action for a Dirac spinor field in curved spacetime as

$$S = \int d^4x\sqrt{-g}\mathcal{L}, \tag{3.98}$$

with the Lagrangian density

$$\mathcal{L}_D(x) = \sqrt{-g}\bar{\Psi}\left(i\gamma^\mu\nabla_\mu - m\right)\Psi, \tag{3.99}$$

where $\bar{\Psi} = \Psi^\dagger\gamma^{\hat{0}}$.

Variation of the action S with respect to $\bar{\Psi}$ yields the covariant Dirac equation in curved spacetime

$$\left(i\gamma^\mu\nabla_\mu - m\right)\Psi = 0. \tag{3.100}$$

To calculate the *second-order equation* for the Dirac spinor field, let us apply the operator $(-i\gamma^\nu\nabla_\nu - m)$ on the Dirac equation, which leads to

$$\left(-i\gamma^\nu\nabla_\nu - m\right)\left(i\gamma^\nu\nabla_\mu - m\right)\Psi = \left[(\gamma^\mu\nabla_\mu)^2 + m^2\right]\Psi = 0. \tag{3.101}$$

It can be shown that (first demonstrated by Schrödinger in 1931)

$$(\gamma^\mu\nabla_\mu)^2\Psi = \gamma^\mu\gamma^\nu\nabla_\mu\nabla_\nu\Psi = -\left(\nabla_\mu\nabla^\mu + \frac{1}{8}R_{\lambda\sigma\mu\nu}\gamma^\mu\gamma^\nu\gamma^\lambda\gamma^\sigma\right)\Psi, \tag{3.102}$$

and

$$R_{\mu\nu\lambda\sigma}\gamma^\mu\gamma^\nu\gamma^\lambda\gamma^\sigma = 2R. \tag{3.103}$$

Therefore, the second-order equation satisfied by each spinor component reads

$$\left[\nabla_\mu\nabla^\mu + R/4 - m^2\right]\Psi = 0. \tag{3.104}$$

Finally, to complete the discussion, let us also mention the energy-momentum tensor for the Dirac field, which takes the form

$$T_{\mu\nu} = \frac{i}{2}\left[\bar{\Psi}\gamma_{(\mu}\nabla_{\nu)}\Psi - (\nabla_{(\mu}\bar{\Psi})\gamma_{\nu)}\Psi\right]. \tag{3.105}$$

3.3 Particle creation in curved spacetime

The classical fields in Minkowski spacetime can be extended to curved spacetime. A particular example is the Dirac field, as explored in the previous section.

Quantum field theory in curved spacetime can be formulated by extending the formal canonical quantization scheme used in Minkowski spacetime to a curved background. The construction of a vacuum state, Fock space, and other related structures can proceed in the same manner as in Minkowski spacetime. However, in curved spacetime, the formalism introduces an inherent ambiguity.

In Minkowski spacetime, the Poincaré group symmetries guarantee the existence of a unique vacuum state. A natural set of mode solutions emerges from the preferred coordinate system (t, x, y, z), and the invariance under Lorentz transformations ensures that this vacuum remains consistent across all inertial frames.

In contrast, the lack of invariance under the Poincaré group in curved spacetime (and for non-inertial frames) means there is no global inertial frame or timelike Killing vector field. This absence of Poincaré symmetry introduces ambiguities in defining the vacuum. This issue has been extensively discussed in the literature and covered in standard textbooks such as [6], [110], [113] and [115].

As a consequence of the vacuum ambiguity in curved spacetime, particle creation arises as a fundamental phenomenon. A notable example is Hawking radiation, where quantum fluctuations near a black hole's event horizon generate particle-antiparticle pairs, with one falling into the black hole and the other escaping as radiation [116], [117]. This provides a heuristic picture of the process, illustrating how quantum effects near the event horizon can lead to the emission of radiation.

Another important example of particle creation occurs in the context of the expanding universe. In this area, Leonard Parker made pioneering contributions to the study of particle creation in curved spacetime, particularly through his work on quantum field theory in cosmological settings [118], [119]. This is a subject we will delve into further in the subsequent sections.

In this section, we begin by examining the quantization of the Dirac spinor field in curved spacetime. Then we introduce the Bogoliubov transformations, which provides a framework for analyzing particle creation by relating different mode expansions of the quantum field.

Building on this, we explore various approaches to defining a particle concept in curved spacetime and examine particle creation in an expanding universe. Finally, we provide a preliminary discussion on the Bianchi IX model, laying the groundwork for a more detailed analysis of particle creation in this highly anisotropic cosmological setting presented in Chap. 7.

3.3.1 Canonical quantization of spinor field

The canonical quantization procedure starts with the construction of a complete orthonormal set of solutions of the classical field, in this case the Dirac spinor field. We denote by $\left\{\psi_J^{(+)}, \psi_J^{(-)}\right\}$ a set of solutions of the Dirac equation in curved spacetime[19].

The set obeys the following orthonormalization conditions:

$$\left(\psi_J^{(+)}, \psi_{J'}^{(+)}\right) = \delta_{JJ'}, \quad \left(\psi_J^{(-)}, \psi_{J'}^{(-)}\right) = \delta_{JJ'}, \quad \left(\psi_J^{(+)}, \psi_{J'}^{(-)}\right) = 0, \tag{3.106}$$

The index J denotes the set of quantum numbers used to label the modes (e.g., momentum and spin). Thus, the spinor field can be expanded as[20]

$$\Psi = \sum_J \left[a_J \psi_J^{(+)} + b_J^\dagger \psi_J^{(-)}\right]. \tag{3.107}$$

Moreover, since the choice of modes is not generally unique in curved spacetime, we can also introduce another orthonormalized set, $\{\chi_{J'}^{(+)}, \chi_{J'}^{(-)}\}$, in which the spinor field can be expanded,

$$\Psi = \sum_{J'} \left[\tilde{a}_{J'} \chi_{J'}^{(+)} + \tilde{b}_{J'}^\dagger \chi_{J'}^{(-)}\right]. \tag{3.108}$$

To quantize the field, we treat the expansion coefficients as operators and impose the following anticommutation relations:

$$\left\{a_J, a_{J'}^\dagger\right\} = \left\{\tilde{a}_J, \tilde{a}_{J'}^\dagger\right\} = \delta_{JJ'}, \quad \left\{b_J, b_{J'}^\dagger\right\} = \left\{\tilde{b}_J, \tilde{b}_{J'}^\dagger\right\} = \delta_{JJ'}, \tag{3.109}$$

with all other anticommutators vanishing.

The vacuum states corresponding to each set can be introduced as follows:

$$\begin{aligned} a_J|0\rangle &= b_J|0\rangle = 0, \quad \langle 0|0\rangle = 1, \\ \tilde{a}_J|\tilde{0}\rangle &= \tilde{b}_J|\tilde{0}\rangle = 0, \quad \langle \tilde{0}|\tilde{0}\rangle = 1. \end{aligned} \tag{3.110}$$

[19]This notation should not be confused with the positive- and negative-frequency solutions defined in Minkowski spacetime. Here, we use it merely to label independent solutions, without implying a frequency interpretation. In curved spacetime, as discussed earlier, the concepts of positive- and negative-frequency modes are not globally well-defined due to the absence of a timelike Killing vector field. However, as we will see later, within certain approximations, it is possible to recover an approximate notion of positive- and negative-frequency solutions.

[20]We assume summation over discrete indices and integration over continuous indices, with both cases symbolically denoted by Σ_J.

The particle and antiparticle number operators are defined as follows: For the first set,

$$N_J = a_J^\dagger a_J, \quad \bar{N}_J = b_J^\dagger b_J, \tag{3.111}$$

and for the second set

$$\tilde{N}_J = \tilde{a}_J^\dagger \tilde{a}_J, \quad \tilde{\bar{N}}_J = \tilde{b}_J^\dagger \tilde{b}_J. \tag{3.112}$$

Bogoliubov transformation

Since both sets are complete, we can write the following expansion relations:

$$\psi_J^{(-)} = \sum_{J'} \left[\alpha_{JJ'} \chi_{J'}^{(-)} - \beta_{JJ'} \chi_{J'}^{(+)} \right], \tag{3.113}$$

and

$$\psi_J^{(+)} = \sum_{J'} \left[\alpha_{JJ'}^* \chi_{J'}^{(+)} + \beta_{JJ'}^* \chi_{J'}^{(-)} \right]. \tag{3.114}$$

Here, $\alpha_{JJ'}$ and $\beta_{JJ'}$ are matrices. These relations are known as Bogoliubov transformations.

Using the above relations, we can also relate the operators from one expansion to those in the other. The following relations are then obtained [113]:

$$\begin{aligned} a_J &= \sum_{J'} \left[\alpha_{JJ'} \ \tilde{a}_{J'} + \beta_{JJ'} \ \tilde{b}_{J'}^\dagger \right], \\ b_J &= \sum_{J'} \left[\alpha_{JJ'} \ \tilde{b}_{J'} - \beta_{JJ'} \ \tilde{a}_{J'}^\dagger \right], \end{aligned} \tag{3.115}$$

and

$$\begin{aligned} a_J^\dagger &= \sum_{J'} \left[\alpha_{JJ'}^* \ \tilde{a}_{J'}^\dagger + \beta_{JJ'}^* \ \tilde{b}_{J'} \right], \\ b_J^\dagger &= \sum_{J'} \left[\alpha_{JJ'}^* \ \tilde{b}_{J'}^\dagger - \beta_{JJ'}^* \ \tilde{a}_{J'} \right]. \end{aligned} \tag{3.116}$$

Introducing the matrices $\boldsymbol{\alpha} = \{\alpha_{J'J}\}$ and $\boldsymbol{\beta} = \{\beta_{J'J}\}$, they satisfy the relations

$$\boldsymbol{\alpha}\boldsymbol{\alpha}^\dagger + \boldsymbol{\beta}\boldsymbol{\beta}^\dagger = \mathbf{I}, \quad \boldsymbol{\alpha}\boldsymbol{\beta}^T = \boldsymbol{\beta}\boldsymbol{\alpha}^T, \tag{3.117}$$

which follows from the orthonormality of the sets. It can be shown that the annihilation operator of one vacuum, when acting on the other vacuum state, leads to

$$a_J|\tilde{0}\rangle = \sum_{J'} \left[\alpha_{JJ'} \ \tilde{a}_{J'} + \beta_{JJ'} \ \tilde{b}_{J'}^\dagger \right] |\tilde{0}\rangle = \sum_{J'} \beta_{JJ'} \ \tilde{b}_{J'}^\dagger |\tilde{0}\rangle \neq 0. \tag{3.118}$$

In addition, the expectation value of particle number in another vacuum state is

$$\langle\tilde{0}|N_J|\tilde{0}\rangle = \langle\tilde{0}|\bar{N}_J|\tilde{0}\rangle = \sum_{J'} |\beta_{JJ'}|^2, \tag{3.119}$$

which implies that the vacuum state of the χ_J modes contains $\sum_{J'} |\beta_{JJ'}|^2$ particles in the ψ_J modes.

3.3.2 Cosmological particle creation

The evolution of the universe's metric has been shown to lead to particle creation. As discussed above, in curved spacetime, the concept of the vacuum is not unique, and as a result, the notion of particles becomes ambiguous. To provide a clear definition of particles and the vacuum in such a setting, certain approximations or assumptions must be made when addressing cosmological particle creation.

- *Asymptotic Minkowski regions*

  A common approximation in studying particle creation in an expanding universe is to assume that spacetime behaves like Minkowski space in the distant past and future. Specifically, in cosmological models such as a flat FLRW universe, spacetime is assumed to approach Minkowski space as the scale factor $a(t)$ behaves as $a(t) \sim a_1,$ as $t \to -\infty$, and $a(t) \sim a_2,$ as $t \to \infty$. This simplification allows for the definition of the Minkowski vacuum in the "in" and "out" states, providing a well-defined notion of particles in these asymptotic regions. The effect of particle creation then arises from a Bogoliubov transformation between the initial and final states, with the number of created particles depending on the expansion rate.

  One should note that this assumption has several limitations. For example, it does not apply to models of the universe with compact topologies, such as the Bianchi IX model discussed below, where asymptotic Minkowski regions do not exist.

- *Static regions*

  In scenarios where no asymptotic Minkowski regions exist, such as in non-flat geometries, one can instead assume the presence of "in" and "out" static regions. This means that the metric remains *static* for $t < t_i$ and $t > t_f$, while it varies with time in the intermediate region $t_i < t < t_f$. Under this assumption, one can unambiguously define the past and future vacuum states, $|0_{\text{in}}\rangle$ and $|0_{\text{out}}\rangle$, corresponding to the mode decomposition in the respective static regions [115], [61].

In a static spacetime, the absence of time dependence in the metric allows for a separation of variables in the field equations. The solutions can be decomposed into a product of a temporal part and a spatial part

$$\Psi(x,t) = \Psi_E(x)e^{-iEt}, \tag{3.120}$$

where $\Psi_E(x)$ is a function of the spatial coordinates, and the factor e^{-iEt} represents the time evolution with a well-defined energy E.

- *Instantaneous Hamiltonian diagonalization*

  In a nonstationary gravitational field, where a universal definition of particles does not exist, one can describe a quantized field using a quasiparticle interpretation, with the quasiparticles' definition evolving over time. This approach relies on Hamiltonian diagonalization, a method that has been thoroughly explored and applied by A.A. Grib and his collaborators; further details can be found in [113].

  Nevertheless, this method has faced strong criticism from Fulling [120], who points out that its direct application often leads to conceptual ambiguities, resulting in infinite particle densities and a non-renormalizable energy-momentum tensor.

- *Adiabatic approximation*

  In quantum field theory in curved spacetime, the adiabatic approximation assumes a slowly expanding universe, ensuring a well-defined notion of particles at all times. This approach is particularly useful when static in and out regions do not exist, as suggested by modern cosmology.

  The approximation holds when the relative change in a mode's frequency is small compared to the universe's expansion rate, leading to minimal particle creation. When this condition is violated, wave coupling and mode mixing occur, resulting in particle production.

  To refine the understanding of particle production beyond the leading-order adiabatic approximation, one can employ the method of successive WKB approximations [6], [121],[122]. This method provides higher-order corrections to the adiabatic expansion and allows for a more accurate treatment of cases where the background evolution is more rapid. In principle, this approach yields arbitrarily precise approximations to the exact solution by systematically incorporating additional corrections.

Throughout this thesis, we will adopt the assumption of static regions to study spinor creation in the Bianchi IX model. While this assumption is admittedly artificial, it serves as a crucial first step in understanding the general features of particle production in such spacetimes. A more complete and precise analysis must be developed using the adiabatic approximation and further refinements based on the WKB approximation, which provide a systematic framework for handling time-dependent backgrounds. However, a detailed exploration of these methods will be left for future considerations.

4 Hamiltonian formulation of spinor field in a Bianchi IX universe

The Hamiltonian approach, as outlined in [92] and [100], offers a powerful method for analyzing the dynamics of Bianchi type models. In this chapter, we focus on the Hamiltonian formulation of the spinor field in the Bianchi IX universe.

We begin with the ADM decomposition of the spacetime, which provides the foundation for expressing the gravitational dynamics in a Hamiltonian framework [5]. Additionally, we construct an orthonormal frame, which is essential for the proper formulation of the Dirac field in curved spacetime. Next, we derive the Lagrangian and Hamiltonian densities for both the gravitational and spinor parts of the system, laying the groundwork for the subsequent analysis. The study of the Bianchi IX model coupled to a *homogeneous* spinor field has been explored in [123], and later extended in [124], where the Wheeler-DeWitt equation for the spinor field in the context of Bianchi IX is analyzed[21]. Here, since our focus is on the quantization of the spinor field for particle creation, we do not impose the restriction of homogeneity on the spinor field. In addition, we derive the equations of motion for the Weyl and Dirac spinor fields within the Bianchi IX universe. This serves as a preparatory step for the quantization of these fields, which will be explored in detail in the following chapters.

4.1 ADM decomposition

The Hamiltonian formulation of General Relativity begins with the ADM decomposition, which involves breaking a four-dimensional spacetime manifold $(\mathcal{M}, g)$ into a family of three-dimensional spacelike Cauchy hypersurfaces parameterized by a global time function t. The evolution of these hypersurfaces provides a way to analyze the dynamics of spacetime.

To implement this foliation, we introduce a global time function t and a vector field t^μ, which represents the 'flow of time' and satisfies the condition

$$t^\mu \nabla_\mu t = 1. \tag{4.1}$$

The vector field t^μ can be decomposed into its normal and tangential components

[21]Moreover, the Hamiltonian formulation provides an effective way to explore the quantum aspects of the Bianchi IX model, particularly leading to the Wheeler-DeWitt equation, which is central to quantum cosmology. The dynamics of the Bianchi IX model near the singularity, within the framework of quantum cosmology, have been discussed in [70]. This work contributes valuable insights into the behavior of the model in the quantum regime, especially as it approaches the singularity.

relative to the hypersurfaces as follows:

$$t^\mu = N n^\mu + N^\mu, \tag{4.2}$$

where N is the lapse function, N^μ is the shift vector, and n^μ is the unit normal vector to the hypersurface, satisfying $n^\mu n_\mu = -1$.

The spatial geometry of the hypersurface is described by the induced metric $h_{\mu\nu}$, which is related to the spacetime metric $g_{\mu\nu}$ by

$$h_{\mu\nu} = g_{\mu\nu} + n_\mu n_\nu. \tag{4.3}$$

With this decomposition, the four-metric $g_{\mu\nu}$ can be expressed in terms of the ADM variables as

$$g_{\mu\nu} = \begin{pmatrix} N_a N^a - N^2 & N_b \\ N_c & h_{ab} \end{pmatrix}. \tag{4.4}$$

The corresponding line element takes the form

$$ds^2 = g_{\mu\nu} dx^\mu dx^\nu = -(N^2 - N_i N^i) dt^2 + 2 N_i dx^i dt + h_{ij} dx^i dx^j. \tag{4.5}$$

4.1.1 The line element of Bianchi IX

As discussed in Sec. 2.3, in spatially homogeneous models, it is often more convenient to use the invariant basis rather than the coordinate basis. In such spaces, the ADM line element then reads

$$ds^2 = -N^2 dt^2 + h_{ij} \left(N^i dt + \sigma^i\right) \left(N^j dt + \sigma^j\right). \tag{4.6}$$

The one-forms $\{\sigma^i\}$, which are dual to the invariant basis, can be expressed in terms of the coordinates $\{x^i\}$ as $\sigma^i = \sigma^i{}_j \, dx^j$.

The induced three-metric h_{ij} for the Bianchi IX model, discussed in detail in Sec. 2.4, is given by

$$h_{ij} = \bar{h}_{kl} R^k{}_i R^l{}_j, \tag{4.7}$$

where R is the rotation matrix. The diagonal three-metric, expressed in terms of the Misner variables α, β_+ and β_-, takes the form

$$\bar{h}_{kl} = \left[\mathrm{diag}\left(e^{\tilde{\beta}_1}, e^{\tilde{\beta}_2}, e^{\tilde{\beta}_3}\right)\right]_{kl} \quad \text{with} \quad \tilde{\beta}_k = 2(\beta_k + \alpha), \tag{4.8}$$

where

$$\beta_1 = \beta_+ + \sqrt{3}\beta_-, \quad \beta_2 = \beta_+ - \sqrt{3}\beta_-, \quad \beta_3 = -2\beta_+. \tag{4.9}$$

It is also convenient to introduce functions

$$b^k = e^{\tilde{\beta}_k/2}, \tag{4.10}$$

and rewrite the metric as

$$h_{ij} = b^m b^n \delta_{kl} R^k{}_i R^l{}_j, \quad \text{where} \quad m = k, \quad n = l. \tag{4.11}$$

This will be particularly useful in constructing the orthonormal frame for the Bianchi IX model in the next section.

4.1.2 Orthonormal frame

The study of spinor fields in curved spacetime is facilitated by the use of the vierbein formalism, which requires the introduction of an orthonormal frame. This is discussed in detail in Sec. 3.2.

Let us first outline the general procedure for obtaining the orthonormal frame, based on the method presented in [96]. Following this, we will present the explicit construction of the orthonormal frame for the Bianchi IX model.

The metric of the manifold $(\mathcal{M}, g)$ can be expressed in terms of the vierbein as

$$g_{\mu\nu}(x) = \eta_{\hat{\alpha}\hat{\beta}} \hat{h}^{\hat{\alpha}}{}_{\mu}(x) \hat{h}^{\hat{\beta}}{}_{\nu}(x). \tag{4.12}$$

Introducing the one-forms $\chi^{\hat{\alpha}}(x)$ of the local orthonormal frame via

$$\chi^{\hat{\alpha}}(x) = \hat{h}^{\hat{\alpha}}{}_{\mu}(x) dx^{\mu}, \tag{4.13}$$

the line element in the curved spacetime can be written as

$$ds^2 = \eta_{\hat{\alpha}\hat{\beta}}\, \chi^{\hat{\alpha}}(x) \chi^{\hat{\alpha}}(x) = -\left(\chi^{\hat{0}}\right)^2 + \delta_{\hat{i}\hat{j}} \chi^{\hat{i}} \chi^{\hat{j}}, \tag{4.14}$$

where we separated the temporal and spatial parts.

Let us recall the ADM line element for a spatially homogeneous spacetime, given by (4.6). Then, the three-metric h_{ij} can be expressed in terms of the vierbein as follows

$$h_{ij}(x) = \delta_{\hat{i}\hat{j}}\, h^{\hat{i}}{}_i(x) h^{\hat{j}}{}_j(x), \tag{4.15}$$

where we introduced

$$h^{\hat{i}}{}_{i} = \hat{h}^{\hat{i}}{}_j\, \sigma^j{}_i, \tag{4.16}$$

using the relations $\sigma^i = \sigma^i{}_j\, dx^j$.

Hence, the one-forms of the orthonormal frame, given in (4.13), can be expressed as

$$\chi^{\hat{0}} = N dt, \quad \chi^{\hat{i}} = h^{\hat{i}}{}_i (N^i dt + \sigma^i). \tag{4.17}$$

Furthermore, the orthonormal basis $\bar{e}_{\hat{i}}$ can be related to the invariant basis e_i through

$$\bar{e}_{\hat{0}} = \frac{1}{N}(\partial_t - N^i e_i), \quad \bar{e}_{\hat{i}} = h_{\hat{i}}{}^i \, e_i. \tag{4.18}$$

Orthonormal frame in Bianchi IX

For the three-metric h_{ij} of Bianchi IX, given by (4.11), the orthonormal one-forms take the following form

$$\chi^{\hat{0}} = N(t) dt, \quad \chi^{\hat{i}} = b^k R^{\hat{i}}{}_i \left(N^i dt + \sigma^i\right) \quad \text{where} \quad k = \hat{i}, \tag{4.19}$$

where

$$h^{\hat{i}}{}_i = b^k R^{\hat{i}}{}_i, \quad h^{\hat{0}}{}_0 = N, \quad h^{\hat{0}}{}_i = 0, \quad h^{\hat{i}}{}_0 = b^k R^{\hat{i}}{}_i N^i. \tag{4.20}$$

For convenience, we will work in the $N^i = 0$ gauge throughout this chapter. Hence, using the relations (3.90), the inverses in this gauge are given by

$$h_{\hat{i}}{}^i = (b^k)^{-1} R^i{}_{\hat{i}}, \quad h_{\hat{0}}{}^0 = \frac{1}{N}, \quad h_{\hat{0}}{}^i = 0, \quad h_{\hat{i}}{}^0 = 0. \tag{4.21}$$

4.2 Lagrangian

The total action for a spinor field in curved spacetime consists of the sum of the Einstein-Hilbert action and the Dirac field action. In the following sections, we will examine both the gravitational and spinor components, deriving their respective Lagrangian densities using the ADM decomposition of spacetime.

4.2.1 Gravitational Lagrangian

The Einstein-Hilbert action has the following form

$$S_{EH} = \frac{1}{16\pi G} \int_M d^4x \sqrt{-g}\, R - \frac{1}{8\pi G} \int_{\partial M} d^3x \sqrt{h} K. \tag{4.22}$$

After the ADM decomposition, the Einstein-Hilbert action takes the form

$$S_{EH} = \frac{1}{16\pi G} \int_\Sigma \sigma^1 \wedge \sigma^2 \wedge \sigma^3 \int dt N \sqrt{h} \big(K_{ij} K^{ij} - K^2 + {}^{(3)}R\big), \tag{4.23}$$

where the quantity ${}^{(3)}R$ denotes the Ricci scalar on the hypersurface. The wedge product, as given by (2.31), is defined over the ranges of the Euler angles $0 \le \phi \le 2\pi$, $0 \le \theta \le \pi$ and $0 \le \psi \le 2\pi$.

The second fundamental form K_{ij}, which describes the embedding of the Cauchy hypersurface Σ into the manifold $(\mathcal{M}, g)$, can be expressed in terms of the lapse function and shift vector as

$$K_{ij} = \frac{1}{2N}(\dot{h}_{ij} - D_i N_j - D_j N_i), \tag{4.24}$$

where D_i denotes the spatial covariant derivative. The trace of the extrinsic curvature is given by $K = h^{ij} K_{ij}$ with $K^{ij} = h^{im} h^{jl} K_{ml}$.

Hence, the gravitational Lagrangian density takes the form[22]

$$\mathcal{L}_G = N\sqrt{h}\big(K_{ij}K^{ij} - K^2 + {}^{(3)}R\big). \tag{4.25}$$

In the $N_i = 0$ gauge, it will be given by

$$\mathcal{L}_G = \frac{\sqrt{h}}{4N}\left[\dot{h}_{ij} h^{im} h^{jl} \dot{h}_{ml} - \left(h^{ij}\dot{h}_{ij}\right)^2\right] + N\sqrt{h}\,{}^{(3)}R. \tag{4.26}$$

Bianchi IX model

Recalling that the three-metric of the Bianchi IX model is given by (4.7), its inverse metric takes the form

$$h^{ij} = R^i{}_m R^j{}_n \bar{h}^{mn}, \tag{4.27}$$

where

$$\bar{h}^{mn} = (b^k b^l)^{-1}\delta^{mn}, \quad k = m, \quad l = n. \tag{4.28}$$

The calculation of the time derivative of the three-metric leads to

$$\dot{h}_{ij} = \left(\dot{\bar{h}}_{kl} + \bar{h}_{nl}\,\omega^n{}_k + \bar{h}_{kp}\,\omega^p{}_l\right) R^k{}_i R^l{}_j, \tag{4.29}$$

where we introduced the "angular velocity" matrix ω defined by

$$\omega^k{}_n = \dot{R}^k{}_i R^i{}_n. \tag{4.30}$$

It can be shown that ω is an *antisymmetric matrix.* Indeed, this follows from the fact that

$$RR^T = I \tag{4.31}$$

by taking time derivative

$$\dot{R}R^T + R\dot{R}^T = 0, \tag{4.32}$$

[22]For convenience, we adopt units such that $\frac{1}{16\pi G} = 1$.

to find

$$\omega = -\omega^T. \tag{4.33}$$

Therefore, as an antisymmetric matrix, ω can be written as follows:

$$\omega = \begin{pmatrix} 0 & \omega^1{}_2 & -\omega^3{}_1 \\ -\omega^1{}_2 & 0 & \omega^2{}_3 \\ \omega^3{}_1 & -\omega^2{}_3 & 0 \end{pmatrix}. \tag{4.34}$$

Using the rotation matrix R given by (A.18), the definition (4.30) leads to the following components:

$$\begin{aligned} \omega^2{}_3 &= \sin\psi\dot{\theta} - \sin\theta\cos\psi\dot{\phi}, \\ \omega^3{}_1 &= \sin\psi\sin\theta\dot{\phi} + \cos\psi\dot{\theta}, \\ \omega^1{}_2 &= \dot{\psi} + \cos\theta\dot{\phi}. \end{aligned} \tag{4.35}$$

The Lagrangian density (4.26) can be written in terms of kinetic and potential parts as follows:

$$\mathcal{L}_G = T_G - V_G, \tag{4.36}$$

where the *kinetic term* is

$$T_G = N\sqrt{h}\big(K_{ij}K^{ij} - K^2\big) = \frac{\sqrt{h}}{4N}\left[\dot{h}_{ij}h^{im}h^{jl}\dot{h}_{ml} - \left(h^{ij}\dot{h}_{ij}\right)^2\right], \tag{4.37}$$

since this term is quadratic in the "velocities", i.e., the time derivatives of the metric components, and the *potential term* is

$$V_G = -Ne^{3\alpha}\,{}^{(3)}R. \tag{4.38}$$

This term depends only on the spatial metric and not on its time derivatives, which identifies it as the potential term.

The calculations yield the following results for the kinetic part:

- *Diagonal case:* The three metric is $h_{ij} = \bar{h}_{ij}$. We denote the kinetic term by T^{d}, which is given by

$$T^{\mathrm{d}} = 6\frac{e^{3\alpha}}{N}\left(-\dot{\alpha}^2 + \dot{\beta}_+^2 + \dot{\beta}_-^2\right). \tag{4.39}$$

- *Symmetric case:* There is rotation only about one axis, hence the three-metric is $h = R_z^T(\phi)\bar{h}R_z(\phi)$. We denote the kinetic term by T^{s}, which is given by

$$T^{\mathrm{s}} = \frac{e^{3\alpha}}{N}\left[6\left(-\dot{\alpha}^2 + \dot{\beta}_+^2 + \dot{\beta}_-^2\right) + 2\dot{\phi}^2\sinh^2\left(2\sqrt{3}\beta_-\right)\right], \tag{4.40}$$

where $(\omega^1{}_2)^2 = \dot{\phi}^2$. We can write it as

$$T^{\rm s} = T^{\rm d} + 2\frac{e^{3\alpha}}{N}\sinh^2\left(2\sqrt{3}\beta_-\right)(\omega^1{}_2)^2. \tag{4.41}$$

- *General case:* The kinetic term denoted by $T^{\rm g}$ takes the form

$$T^{\rm g} = T^{\rm d} + T^{\rm rot}, \tag{4.42}$$

where we introduced

$$T^{\rm rot} = 2\tfrac{e^{3\alpha}}{N}\left[\sinh^2\left(2\sqrt{3}\beta_-\right)(\omega^1{}_2)^2 + \sinh^2\left(3\beta_+ - \sqrt{3}\beta_-\right)(\omega^2{}_3)^2 + \sinh^2\left(3\beta_+ + \sqrt{3}\beta_-\right)(\omega^3{}_1)^2\right]. \tag{4.43}$$

Thus, we obtained for the kinetic part has a contribution from anisotropy factors as well as the rotation.

Let us study the rotation part further. First we recall the rotational kinetic energy of a rigid body as given by (6.12) below. Comparing this with the rotational kinetic energy T^{top}, it is easy to notice that we can introduce the "moments of inertia" as follows:

$$\begin{aligned} I_1 &= 4\sinh^2\left(3\beta_+ - \sqrt{3}\beta_-\right), \\ I_2 &= 4\sinh^2\left(3\beta_+ + \sqrt{3}\beta_-\right), \\ I_3 &= 4\sinh^2\left(2\sqrt{3}\beta_-\right). \end{aligned} \tag{4.44}$$

In addition, comparing (4.35) and (6.6) below, we see that

$$\Omega_1 = \omega^2{}_3, \quad \Omega_2 = \omega^3{}_1, \quad \Omega_3 = \omega^1{}_2. \tag{4.45}$$

Therefore, the rotational contribution to the kinetic term, $T^{\rm rot}$, corresponds to the kinetic energy of an asymmetric top, namely

$$T^{\rm rot} = \frac{e^{3\alpha}}{N}\left[\frac{1}{2}I_1\Omega_1^2 + \frac{1}{2}I_2\Omega_2^2 + \frac{1}{2}I_3\Omega_3^2\right]. \tag{4.46}$$

However, in this case, the "moments of inertia" are time-dependent.

Following this, the calculation of the potential term (4.38) for the Bianchi IX metric yields

$$V_G(\alpha, \beta_+, \beta_-) = \frac{N}{2}e^{\alpha}\left\{e^{-8\beta_+} + 2e^{4\beta_+}\left[\cosh\left(4\sqrt{3}\beta_-\right) - 1\right] - 4e^{-2\beta_+}\cosh\left(2\sqrt{3}\beta_-\right)\right\}. \tag{4.47}$$

Finally, the Lagrangian density for the general Bianchi IX model takes the form

$$\mathcal{L}_G = \frac{e^{3\alpha}}{N}\left\{6\left(-\dot{\alpha}^2 + \dot{\beta}_+^2 + \dot{\beta}_-^2\right) + \frac{1}{2}I_1\Omega_1^2 + \frac{1}{2}I_2\Omega_2^2 + \frac{1}{2}I_3\Omega_3^2\right\} + V_G(\alpha, \beta_+, \beta_-). \quad (4.48)$$

Dynamics of Bianchi IX

The potential, $V_G(\alpha, \beta_+, \beta_-)$, in the Bianchi IX model, first discussed by Misner [67] in his study of Mixmaster dynamics, plays a fundamental role in shaping the anisotropic evolution of the universe. For fixed values of α, this potential consists of three exponentially steep walls that form valleys, confining the system's motion and leading to chaotic behavior.

Near the singularity ($\alpha \to -\infty$), as the universe point moves through phase space, it undergoes successive bounces off the potential walls. This results in a highly non-linear, ergodic-like evolution characterized by an infinite series of Kasner epochs. The chaotic nature of the Bianchi IX model aligns with the BKL conjecture, which posits that, near a singularity, the universe's evolution is dominated by local anisotropic oscillations [65].

Finally, as the universe approaches isotropy[23], the anisotropy factors β_+ and β_- vanish, causing the potential to effectively disappear and the anisotropic oscillations to fade.

4.2.2 Spinor Lagrangian

Let us begin the discussion by recalling the essential concepts and equations from Sec. 3.2, where we provided a detailed analysis of the Dirac field in curved spacetime.

The Lagrangian density of the Dirac field in curved spacetime is given by

$$\mathcal{L}_D = \sqrt{-g}\bar{\Psi}\left(i\gamma^\mu\nabla_\mu - m\right)\Psi. \quad (4.49)$$

where $\bar{\Psi} = \Psi^\dagger\gamma^{\hat{0}}$ and the generalized gamma matrices are given by

$$\gamma^\mu = \hat{h}_{\hat{\alpha}}{}^{\mu}\gamma^{\hat{\alpha}}, \quad (4.50)$$

which satisfy the following anticommutation relations

$$\{\gamma^\mu, \gamma^\nu\} = -2g^{\mu\nu}, \quad \text{and} \quad \left\{\gamma^{\hat{\alpha}}, \gamma^{\hat{\beta}}\right\} = -2\eta^{\hat{\alpha}\hat{\beta}}. \quad (4.51)$$

[23]The isotropization mechanisms have been explained in Sec. 1.3.

The covariant derivative acting on the Dirac spinor has the form

$$\nabla_\mu \Psi = (\partial_\mu + \Gamma_\mu)\Psi. \tag{4.52}$$

The connection Γ_μ is given in (3.95), which can be rewritten as

$$\Gamma_\mu = \frac{1}{2}\kappa_{\hat{\alpha}\hat{\beta}\mu}\Sigma^{\hat{\alpha}\hat{\beta}}, \tag{4.53}$$

where we introduced

$$\kappa_{\hat{\alpha}\hat{\beta}\mu} := \hat{h}_{\hat{\alpha}\nu}\left(\nabla_\mu \hat{h}_{\hat{\beta}}^{\ \nu}\right). \tag{4.54}$$

Hence, the Lagrangian density of the spinor field can be written as follows:

$$\mathcal{L}_D(x) = \sqrt{-g}\bar{\Psi}\left(i\hat{h}_{\hat{\rho}}^{\ \mu}\gamma^{\hat{\rho}}\partial_\mu + \frac{i}{2}\kappa_{\hat{\alpha}\hat{\beta}\hat{\rho}}\gamma^{\hat{\rho}}\Sigma^{\hat{\alpha}\hat{\beta}} - m\right)\Psi, \tag{4.55}$$

where

$$\kappa_{\hat{\alpha}\hat{\beta}\hat{\rho}} = \hat{h}_{\hat{\rho}}^{\ \mu}\kappa_{\hat{\alpha}\hat{\beta}\mu}. \tag{4.56}$$

Let us recall the following definitions from differential geometry in a non-coordinate basis (for further details, see [60], [92]). Consider a basis $\{e_\alpha\}$ that satisfies the commutation relations

$$[e_\alpha, e_\beta] = \gamma^\rho{}_{\alpha\beta}e_\rho. \tag{4.57}$$

The basis vector can be expressed in terms of coordinates by $e_\alpha = \sigma_\alpha{}^\mu\partial_\mu$. Then the Ricci rotation coefficients can be defined by

$$\Gamma^\alpha{}_{\beta\gamma} = \sigma^\alpha{}_\nu\sigma_\beta{}^\nu{}_{;\mu}\sigma_\gamma{}^\mu. \tag{4.58}$$

Additionally, introducing $\gamma_{\alpha\beta\rho} = g_{\alpha\tau}\gamma^\tau{}_{\beta\rho}$, we can express the connection components in terms of the commutation coefficients as follows:

$$\Gamma_{\rho\alpha\beta} = \frac{1}{2}(\gamma_{\beta\rho\alpha} + \gamma_{\alpha\rho\beta} - \gamma_{\rho\alpha\beta}). \tag{4.59}$$

Using the above quantities for our specific case, we can write

$$\kappa_{\hat{\alpha}\hat{\beta}\hat{\rho}} = \Gamma_{\hat{\alpha}\hat{\beta}\hat{\rho}} = \frac{1}{2}(\gamma_{\hat{\rho}\hat{\alpha}\hat{\beta}} + \gamma_{\hat{\beta}\hat{\alpha}\hat{\rho}} - \gamma_{\hat{\alpha}\hat{\beta}\hat{\rho}}), \tag{4.60}$$

where $\gamma^{\hat{\sigma}}{}_{\hat{\alpha}\hat{\beta}}$ are the commutation coefficients of the orthonormal basis $\{\bar{e}_{\hat{\alpha}}\}$, namely

$$[\bar{e}_{\hat{\alpha}}, \bar{e}_{\hat{\beta}}] = \gamma^{\hat{\sigma}}{}_{\hat{\alpha}\hat{\beta}}\,\bar{e}_{\hat{\sigma}}. \tag{4.61}$$

Hence, to be able to calculate the $\kappa_{\hat{\alpha}\hat{\beta}\hat{\rho}}$ for the Bianchi IX metric, first we have to determine the commutation coefficients of the orthonormal frame. In addition, the one-forms $\{\chi^{\hat{\alpha}}\}$, dual to the basis $\{\bar{e}_{\hat{\alpha}}\}$ satisfy the following equation:

$$d\chi^{\hat{\alpha}} = -\frac{1}{2}\gamma^{\hat{\alpha}}{}_{\hat{\beta}\hat{\gamma}}\chi^{\hat{\beta}} \wedge \chi^{\hat{\gamma}}. \tag{4.62}$$

Recalling the explicit form of $\{\chi^{\hat{\alpha}}\}$ given in (4.19),

$$\chi^{\hat{0}} = N(t)\, dt, \quad \chi^{\hat{i}} = b^n R^{\hat{i}}{}_i \left(N^i dt + \sigma^i\right), \quad \text{where} \quad n = \hat{i}, \tag{4.63}$$

and substituting it into (4.62), we can determine the commutation coefficients of the orthonormal frame.

First, considering the right-hand side of (4.62), let us calculate the wedge products:

- For $\hat{\beta} = \hat{\gamma} = 0$
$$\chi^{\hat{\beta}} \wedge \chi^{\hat{\gamma}} = \chi^{\hat{0}} \wedge \chi^{\hat{0}} = 0. \tag{4.64}$$

- For $\hat{\beta} = 0$, $\hat{\gamma} = \hat{l}$, where $\hat{l} = 1, 2, 3$,
$$\chi^{\hat{0}} \wedge \chi^{\hat{l}} = N b^k R^{\hat{l}}{}_l\, dt \wedge \sigma^l, \quad k = \hat{l}. \tag{4.65}$$

- For $\hat{\beta} = \hat{j}$, $\hat{\gamma} = \hat{l}$, , where $\hat{j}, \hat{l} = 1, 2, 3$,
$$\chi^{\hat{j}} \wedge \chi^{\hat{l}} = b^m b^k \left(R^{\hat{j}}{}_j N^j R^{\hat{l}}{}_l - R^{\hat{j}}{}_l R^{\hat{l}}{}_j N^j\right) dt \wedge \sigma^l + b^m b^k R^{\hat{j}}{}_j R^{\hat{l}}{}_l\, \sigma^j \wedge \sigma^l, \tag{4.66}$$
where $\hat{j} = m$, $\hat{l} = k$.

Next, let us calculate $d\chi^{\hat{\alpha}}$:

- For $\hat{\alpha} = 0$:
$$d\chi^{\hat{0}} = \dot{N}(t) dt \wedge dt = 0, \tag{4.67}$$
which leads to
$$\gamma^{\hat{0}}{}_{\hat{\beta}\hat{\gamma}} = 0 \quad \text{for any } \hat{\beta}, \hat{\gamma}. \tag{4.68}$$

- For $\hat{\alpha} = \hat{i}$, with $\hat{i} = 1, 2, 3$:
$$d\chi^{\hat{i}} = -b^n R^{\hat{i}}{}_r (\mathcal{J}_a)^r{}_i N^i(t) dt \wedge \sigma^a + \left(\dot{b}^n R^{\hat{i}}{}_i + b^n \dot{R}^{\hat{i}}_i\right) dt \wedge \sigma^i + b^n R^{\hat{i}}{}_q (\mathcal{J}_b)^q{}_i \sigma^b \wedge \sigma^i, \tag{4.69}$$
where $n = \hat{i}$, and $a, b = 1, 2, 3$ and we used the relation (2.32), i.e.
$$dR^{\hat{i}}{}_i = R^{\hat{i}}{}_r (\mathcal{J}_a)^r{}_i \sigma^a. \tag{4.70}$$

Substituting the relations (4.69) and (4.66) into the equation (4.68) leads to

$$-\gamma^{\hat{i}}{}_{\hat{j}\hat{l}} b^m b^k R^{\hat{j}}{}_j R^{\hat{l}}{}_l = b^n R^{\hat{i}}{}_q (\mathcal{J}_j)^q{}_l, \tag{4.71}$$

and

$$\gamma^{\hat{i}}{}_{\hat{0}\hat{l}} N b^k R^{\hat{l}}{}_l + \gamma^{\hat{i}}{}_{\hat{j}\hat{l}} b^m b^k \left(R^{\hat{j}}{}_j N^j R^{\hat{l}}{}_l - R^{\hat{j}}{}_l R^{\hat{l}}{}_j N^j \right) = b^n R^{\hat{i}}{}_r (\mathcal{J}_l)^r{}_i N^i(t) - \left(\dot{b}^n R^{\hat{i}}{}_l + b^n \dot{R}^{\hat{i}}_l \right). \tag{4.72}$$

Using

$$(\mathcal{J}_a)^b{}_c = -\varepsilon_{abc}, \tag{4.73}$$

and recalling the relation for the determinant of a matrix A with elements $\{a_{ij}\}$, given by

$$\varepsilon_{i_1 i_2 \ldots i_n} a_{i_1 j_1} a_{i_2 j_2} \ldots a_{i_n j_n} = \det(A) \varepsilon_{j_1 j_2 \ldots j_n}, \tag{4.74}$$

the first equation leads to the following result

$$\gamma^{\hat{i}}{}_{\hat{l}\hat{j}} = b^n (b^m)^{-1} (b^k)^{-1} \varepsilon_{\hat{i}\hat{j}\hat{l}}. \tag{4.75}$$

Then, substituting this into (4.72), further simplifications lead to

$$\gamma^{\hat{i}}{}_{\hat{0}\hat{l}} = \frac{(b^k)^{-1}}{N} \left[b^n R^{\hat{i}}{}_q (\mathcal{J}_j)^q{}_l N^j - \left(\dot{b}^n R^{\hat{i}}{}_l + b^n \dot{R}^{\hat{i}}_l \right) \right] R^l{}_{\hat{l}}, \tag{4.76}$$

where $n = \hat{i},\ m = \hat{j},\ k = \hat{l}$.

Using the obtained relations (4.68), (4.75) and (4.76), we can finally calculate the term $\frac{i}{2}\kappa_{\hat{\alpha}\hat{\beta}\hat{\rho}}\gamma^{\hat{\rho}}\Sigma^{\hat{\alpha}\hat{\beta}}$, which enters in the Dirac Lagrangian. These calculations are carried out in Appendix A.3.

Substituting the terms $\frac{i}{2}\kappa_{\hat{\alpha}\hat{\beta}\hat{\rho}}\gamma^{\hat{\rho}}\Sigma^{\hat{\alpha}\hat{\beta}}$ given in (A.75) into the Lagrangian (4.55), we finally obtain

$$\begin{aligned}\mathcal{L}_D = N e^{3\alpha} \bar{\Psi} \Bigg\{ & i \left(\gamma^\mu \partial_\mu - \frac{3}{2N} \dot{\alpha} \gamma^{\hat{0}} \right) + \frac{i}{2} e^{-\alpha} \left[e^{-4\beta_+} + e^{2\beta_+ + 2\sqrt{3}\beta_-} + e^{2\beta_+ - 2\sqrt{3}\beta_-} \right] \gamma^{\hat{1}} \Sigma^{\hat{2}\hat{3}} \\ & - \frac{i}{N} \Big[\cosh\left(2\sqrt{3}\beta_-\right) \omega^{\hat{1}}{}_{\hat{2}} \gamma^{\hat{0}} \Sigma^{\hat{1}\hat{2}} + \cosh\left(3\beta_+ + \sqrt{3}\beta_-\right) \omega^{\hat{3}}{}_{\hat{1}} \gamma^{\hat{0}} \Sigma^{\hat{3}\hat{1}} \\ & + \cosh\left(3\beta_+ - \sqrt{3}\beta_-\right) \omega^{\hat{2}}{}_{\hat{3}} \gamma^{\hat{0}} \Sigma^{\hat{2}\hat{3}} \Big] - m \Bigg\} \Psi. \end{aligned} \tag{4.77}$$

where the first term of the Lagrangian, expressed in terms of the invariant-basis, reads

$$\gamma^\mu \partial_\mu = \hat{h}_{\hat{\rho}}{}^\mu \gamma^{\hat{\rho}} \partial_\mu = h_{\hat{\rho}}{}^0 \gamma^{\hat{\rho}} e_0 + h_{\hat{\rho}}{}^i \gamma^{\hat{\rho}} e_i = \frac{1}{N} \gamma^{\hat{0}} \partial_0 + h_{\hat{i}}{}^i \gamma^{\hat{i}} e_i, \tag{4.78}$$

and where we have used the relation (4.16) and $\hat{\rho} = 0, 1, 2, 3$ and $\hat{\imath} = 1, 2, 3$.

Furthermore, for convenience, let us introduce a function defined by

$$F(\alpha, \beta_+, \beta_-) := \frac{1}{2} e^{-\alpha} \left[e^{-4\beta_+} + e^{2\beta_+ + 2\sqrt{3}\beta_-} + e^{2\beta_+ - 2\sqrt{3}\beta_-} \right]. \tag{4.79}$$

Also, recalling the relations (4.44) for the "moments of inertia", we can write

$$\begin{aligned} \cosh\left(3\beta_+ - \sqrt{3}\beta_-\right) &= \left(1 + \frac{I_1}{4}\right)^{\frac{1}{2}}, \\ \cosh\left(3\beta_+ + \sqrt{3}\beta_-\right) &= \left(1 + \frac{I_2}{4}\right)^{\frac{1}{2}}, \\ \cosh\left(2\sqrt{3}\beta_-\right) &= \left(1 + \frac{I_3}{4}\right)^{\frac{1}{2}}. \end{aligned} \tag{4.80}$$

Finally, using "angular velocities" $\{\Omega_i\}$ as introduced in (4.45), the Hamiltonian can be rewritten as follows

$$\begin{aligned} \mathcal{L}_D = N e^{3\alpha} \bar{\Psi} \Bigg\{ & i \left(\frac{1}{N} \gamma^{\hat{0}} \partial_0 + h_{\hat{\imath}}{}^{i} \gamma^{\hat{\imath}} e_i - \frac{3}{2N} \dot{\alpha} \gamma^{\hat{0}} \right) + i F(\alpha, \beta_+, \beta_-) \gamma^{\hat{1}} \Sigma^{\hat{2}\hat{3}} - m \\ & - \frac{i}{N} \Bigg[\left(1 + \frac{I_3}{4}\right)^{\frac{1}{2}} \Omega_3 \gamma^{\hat{0}} \Sigma^{\hat{1}\hat{2}} + \left(1 + \frac{I_2}{4}\right)^{\frac{1}{2}} \Omega_2 \gamma^{\hat{0}} \Sigma^{\hat{3}\hat{1}} + \left(1 + \frac{I_1}{4}\right)^{\frac{1}{2}} \Omega_1 \gamma^{\hat{0}} \Sigma^{\hat{2}\hat{3}} \Bigg] \Bigg\} \Psi. \end{aligned} \tag{4.81}$$

Thus, in the Bianchi IX model, the Lagrangian includes the following contributions: the spinor–"angular velocity" coupling term, $\propto \Omega_i \gamma^{\hat{0}} \Sigma^{\hat{\jmath}\hat{k}}$, which arises from the model's rotation; the geometry–spinor coupling potential, $\propto F(\alpha, \beta_+, \beta_-) \gamma^{\hat{1}} \Sigma^{\hat{2}\hat{3}}$, resulting from its anisotropy; and a spinor coupling to $\dot{\alpha}$, which describes the evolution of the spatial volume. The latter, unsurprisingly, also appears in isotropic cosmological models.

4.3 Hamiltonian

The total Lagrangian density can be expressed as

$$\mathcal{L} = \mathcal{L}_G + \mathcal{L}_D, \tag{4.82}$$

where $\mathcal{L}_G$ represents the gravitational contribution, as defined in equation (4.48), and $\mathcal{L}_D$ denotes the spinor contribution, given in equation (4.77).

To obtain the canonical Hamiltonian density, we first identify the conjugate coordinates and introduce the corresponding conjugate momenta. For a Lagrangian density that depends on the generalized coordinates and their velocities,

$$\mathcal{L} = \mathcal{L}(X_i, \dot{X}_i), \tag{4.83}$$

the conjugate momenta are defined as

$$P_{X_i} = \frac{\partial \mathcal{L}}{\partial \dot{X}_i}. \tag{4.84}$$

By applying the Legendre transformation, the canonical Hamiltonian density is given by

$$\mathcal{H} = \sum_i P_{X_i} \dot{X}_i - \mathcal{L}. \tag{4.85}$$

The total Hamiltonian takes the form

$$H = \int_\Sigma \sigma^1 \wedge \sigma^2 \wedge \sigma^3 \, \mathcal{H} = \int_\Sigma \sigma^1 \wedge \sigma^2 \wedge \sigma^3 \left[N\mathcal{H}_0 + N^i H_i \right], \tag{4.86}$$

where $\mathcal{H}_0$ is the Hamiltonian constraint, and H_i represents the diffeomorphism constraint.

Gravitational Hamiltonian density

For the gravitational part, there are six independent variables: the Misner variables α, β_+, β_-, and the Euler angles ϕ, θ, ψ. Then, the Hamiltonian density $\mathcal{H}$ can be determined by

$$\mathcal{H} = \dot{\alpha} P_\alpha + \dot{\beta}_+ P_{\beta_+} + \dot{\beta}_- P_{\beta_-} + \dot{\psi} P_\psi + \dot{\theta} P_\theta + \dot{\phi} P_\phi - \mathcal{L}_G. \tag{4.87}$$

Hence, the calculations of the conjugate momenta of variables α, β_+, β_- from the Lagrangian density (4.48) lead to

$$\begin{aligned} P_\alpha &= \frac{\partial \mathcal{L}}{\partial \dot{\alpha}} = -12 \frac{e^{3\alpha}}{N} \dot{\alpha}, \\ P_{\beta_\pm} &= \frac{\partial \mathcal{L}}{\partial \dot{\beta}_\pm} = 12 \frac{e^{3\alpha}}{N} \dot{\beta}_\pm, \end{aligned} \tag{4.88}$$

and for the conjugate momenta of Euler angles we get

$$\begin{aligned} P_\psi &= \frac{\partial \mathcal{L}}{\partial \dot{\psi}} = \frac{e^{3\alpha}}{N} I_3 \Omega_3, \\ P_\theta &= \frac{\partial \mathcal{L}}{\partial \dot{\theta}} = \frac{e^{3\alpha}}{N} \left[I_2 \Omega_2 \cos\psi + I_1 \Omega_1 \sin\psi \right], \\ P_\phi &= \frac{\partial \mathcal{L}}{\partial \dot{\phi}} = \frac{e^{3\alpha}}{N} \left[I_3 \Omega_3 \cos\theta + I_2 \Omega_2 \sin\theta \sin\psi - I_1 \Omega_1 \sin\theta \cos\psi \right]. \end{aligned} \tag{4.89}$$

First, let us express $\dot{\phi}$, $\dot{\theta}$ and $\dot{\psi}$ in terms of $\Omega_1, \Omega_2, \Omega_3$ using (4.35),

$$\begin{aligned}
\dot{\phi} &= \frac{1}{\sin\theta}\left(\sin\psi\,\Omega_2 - \cos\psi\,\Omega_1\right), \\
\dot{\theta} &= \cos\psi\,\Omega_2 + \sin\psi\,\Omega_1, \\
\dot{\psi} &= \Omega_3 - \cot\theta\left(\sin\psi\,\Omega_2 - \cos\psi\,\Omega_1\right).
\end{aligned} \tag{4.90}$$

Next, from (4.89) we obtain Ω_i in terms of the conjugate momenta P_ψ, P_θ and P_ϕ, which is given by

$$\begin{aligned}
\Omega_1 &= \frac{Ne^{-3\alpha}}{I_1\sin\theta}\left[P_\theta\sin\theta\sin\psi - \cos\psi\left(P_\phi - P_\psi\cos\theta\right)\right], \\
\Omega_2 &= \frac{Ne^{-3\alpha}}{I_2\sin\theta}\left[P_\theta\sin\theta\cos\psi + \sin\psi\left(P_\phi - P_\psi\cos\theta\right)\right], \\
\Omega_3 &= \frac{Ne^{-3\alpha}}{I_3}P_\psi.
\end{aligned} \tag{4.91}$$

Then, we introduce the "angular momenta" L_i, defined as follows

$$L_i = \frac{e^{3\alpha}}{N}\,I_i\,\Omega_i, \quad i = 1, 2, 3, \tag{4.92}$$

It is easy to see from (4.89) that, in terms of angular momenta, the conjugate momenta of the Euler angles are given by

$$\begin{aligned}
P_\psi &= \frac{e^{3\alpha}}{N}L_3, \\
P_\theta &= \frac{e^{3\alpha}}{N}\left[L_2\cos\psi + L_1\sin\psi\right], \\
P_\phi &= \frac{e^{3\alpha}}{N}\left[L_3\cos\theta + L_2\sin\theta\sin\psi - L_1\sin\theta\cos\psi\right].
\end{aligned} \tag{4.93}$$

Thus, using the relations obtained above and (4.88), the canonical Hamiltonian density takes the following form:

$$\mathcal{H} = \frac{Ne^{-3\alpha}}{24}\left(-P_\alpha^2 + P_{\beta_+}^2 + P_{\beta_-}^2\right) + N\left(\frac{L_1^2}{2I_1} + \frac{L_2^2}{2I_2} + \frac{L_3^2}{2I_3}\right) + V_G(\alpha, \beta_+, \beta_-). \tag{4.94}$$

Finally, let us point out that to simplify the calculations, we previously assumed a gauge in which the shift vector N_i vanishes. However, when this assumption is relaxed, N_i simply appears as a Lagrange multiplier for the diffeomorphism constraint, $H_i \approx 0$ (see, e.g., [70], [124]).

Including the spinor field

Recalling the Dirac spinor field Lagrangian given by (4.81), we note that it contains terms proportional to Ω_i. Therefore, the conjugate momenta of the Euler angles, given by (4.89), acquire additional contributions from the spinor field.

These calculations are technically intricate and have been discussed in detail by Damour [124], where a homogeneous spinor field is considered. Since a full treatment of this topic is beyond the scope of this thesis, we refer the reader to that work for a more thorough discussion.

4.4 Equations of motion for spinor fields

The Dirac equation in Bianchi IX model can be derived from the Euler-Lagrange equation, where the Lagrangian is given by (4.77). The Dirac equation takes the form

$$\Bigg\{ i\left(\gamma^\mu \partial_\mu - \frac{3}{2N}\dot{\alpha}\gamma^{\hat{0}}\right) + iF(\alpha, \beta_+, \beta_-)\gamma^{\hat{1}}\Sigma^{\hat{2}\hat{3}} - m \\ - \frac{i}{N}\left[\left(1 + \frac{I_3}{4}\right)^{\frac{1}{2}} \Omega_3\, \gamma^{\hat{0}}\Sigma^{\hat{1}\hat{2}} + \left(1 + \frac{I_2}{4}\right)^{\frac{1}{2}} \Omega_2\, \gamma^{\hat{0}}\Sigma^{\hat{3}\hat{1}} + \left(1 + \frac{I_1}{4}\right)^{\frac{1}{2}} \Omega_1\, \gamma^{\hat{0}}\Sigma^{\hat{2}\hat{3}}\right]\Bigg\}\Psi = 0. \tag{4.95}$$

For the diagonal and symmetric Bianchi IX cases the equations simplify to:

- *Diagonal case*

$$\left\{ i\left(\gamma^\mu \partial_\mu - \frac{3}{2N}\dot{\alpha}\gamma^{\hat{0}}\right) + iF(\alpha, \beta_+, \beta_-)\gamma^{\hat{1}}\Sigma^{\hat{2}\hat{3}} - m \right\}\Psi = 0. \tag{4.96}$$

- *Symmetric case*

$$\left\{ i\left(\gamma^\mu \partial_\mu - \frac{3}{2N}\dot{\alpha}\gamma^{\hat{0}}\right) + iF(\alpha, \beta_+, \beta_-)\gamma^{\hat{1}}\Sigma^{\hat{2}\hat{3}} - m - \frac{i}{N}\left(1 + \frac{I_3}{4}\right)^{\frac{1}{2}} \Omega_3\, \gamma^{\hat{0}}\Sigma^{\hat{1}\hat{2}} \right\}\Psi = 0. \tag{4.97}$$

It is easy to see that the Dirac equation in the closed FLRW model can be recovered from (4.96) by setting the function $F(\alpha, \beta_+, \beta_-)$ equal to zero, as obtained by Parker [125].

Equations in terms of Pauli matrices

The above equations are obtained without fixing any specific representation for $\gamma^{\hat{\alpha}}$ matrices. As in Chapter 3, by giving the gamma matrices in the Weyl representation and using the notation in (3.8), the gamma matrices can be expressed as

$$\gamma^{\hat{\alpha}} = \begin{pmatrix} 0 & \sigma^{\hat{\alpha}} \\ \bar{\sigma}^{\hat{\alpha}} & 0 \end{pmatrix}. \tag{4.98}$$

In addition, by recalling the explicit calculations for the products $\gamma^{\hat{\rho}}\Sigma^{\hat{\alpha}\hat{\beta}}$ obtained in (A.68–A.73) and substituting them into equation (4.95), we can write

$$\begin{pmatrix} -m & D_R \\ D_L & -m \end{pmatrix} \Psi = 0, \tag{4.99}$$

where we introduced

$$\begin{aligned} D_R &= i h_{\hat{\alpha}}{}^{\mu} \sigma^{\hat{\alpha}} e_{\mu} - \frac{3i}{2N}\dot{\alpha} + \frac{1}{2}F(\alpha, \beta_+, \beta_-) - \frac{1}{2N}\sum_{\hat{\imath}} \left(1 + \frac{I_{\hat{\imath}}}{4}\right)^{\frac{1}{2}} \Omega_{\hat{\imath}} \sigma^{\hat{\imath}}, \\ D_L &= i h_{\hat{\alpha}}{}^{\mu} \bar{\sigma}^{\hat{\alpha}} e_{\mu} - \frac{3i}{2N}\dot{\alpha} - \frac{1}{2}F(\alpha, \beta_+, \beta_-) - \frac{1}{2N}\sum_{\hat{\imath}} \left(1 + \frac{I_{\hat{\imath}}}{4}\right)^{\frac{1}{2}} \Omega_{\hat{\imath}} \sigma^{\hat{\imath}}. \end{aligned} \tag{4.100}$$

Writing the Dirac spinor in terms of Weyl spinors, the equation (4.99) leads to the following two equations

$$\left[i h_{\hat{\alpha}}{}^{\mu} \sigma^{\hat{\alpha}} e_{\mu} - \frac{3i}{2N}\dot{\alpha} + \frac{1}{2}F(\alpha, \beta_+, \beta_-) - \frac{1}{2N}\sum_{\hat{\imath}} \left(1 + \frac{I_{\hat{\imath}}}{4}\right)^{\frac{1}{2}} \Omega_{\hat{\imath}} \sigma^{\hat{\imath}} \right] \Psi_R = m\Psi_L, \tag{4.101}$$

and

$$\left[i h_{\hat{\alpha}}{}^{\mu} \bar{\sigma}^{\hat{\alpha}} e_{\mu} - \frac{3i}{2N}\dot{\alpha} - \frac{1}{2}F(\alpha, \beta_+, \beta_-) - \frac{1}{2N}\sum_{\hat{\imath}} \left(1 + \frac{I_{\hat{\imath}}}{4}\right)^{\frac{1}{2}} \Omega_{\hat{\imath}} \sigma^{\hat{\imath}} \right] \Psi_L = m\Psi_R. \tag{4.102}$$

Weyl equations

Setting $m = 0$, we obtain the Weyl equations

- *Left-handed spinor*:

$$\left[ih_{\hat{\alpha}}{}^{\mu}\bar{\sigma}^{\hat{\alpha}}e_{\mu} - \frac{3i}{2N}\dot{\alpha} - \frac{1}{2}F(\alpha,\beta_{+},\beta_{-}) - \frac{1}{2N}\sum_{\hat{l}}\left(1+\frac{I_{\hat{l}}}{4}\right)^{\frac{1}{2}}\Omega_{\hat{l}}\sigma^{\hat{l}}\right]\Psi_{L} = 0, \tag{4.103}$$

- *Right-handed spinor*:

$$\left[ih_{\hat{\alpha}}{}^{\mu}\sigma^{\hat{\alpha}}e_{\mu} - \frac{3i}{2N}\dot{\alpha} + \frac{1}{2}F(\alpha,\beta_{+},\beta_{-}) - \frac{1}{2N}\sum_{\hat{l}}\left(1+\frac{I_{\hat{l}}}{4}\right)^{\frac{1}{2}}\Omega_{\hat{l}}\sigma^{\hat{l}}\right]\Psi_{R} = 0. \tag{4.104}$$

We will discuss the solutions of the Weyl and Dirac equations and their physical consequences for the matter-antimatter asymmetry in Sec. 7.1 and Sec. 7.2, respectively.

5 Group SO(3)

The symmetry group of the Bianchi IX model is the SO(3) group. In this chapter, we will explore the details of the SO(3) group that are relevant to the current work. Since we are considering a spinor field in the Bianchi IX universe, it is also necessary to examine the representations of the group, as they are crucial for studying the behavior of spinor fields in this context. In this chapter, we build upon foundational material from sources such as [126–129], incorporating these ideas into the discussion.

5.1 Parametrization and Lie algebra of SO(3)

Let us consider the set of all rotations in three-dimensional Euclidean space, $\mathbb{R}^3$, about a fixed point. The product of two rotations results in another rotation, and each rotation has an inverse. Additionally, there exists an identity rotation, namely the unit matrix, which corresponds to a rotation by a zero angle. Therefore, the set of all rotations forms a group, known as SO(3).

By fixing an orthonormal basis in three-dimensional space $\mathbb{R}^3$, the rotations can be represented by matrices that transform, for example, the x, y, z frame to the x', y', z' frame, maintaining the same origin. The transformation can be expressed as

$$x'^k = R^k{}_i \, x^i, \tag{5.1}$$

where $R^k{}_i$ is the rotation matrix (with k denoting the column index and i the row index). The rotation matrix is both orthogonal and special, meaning it satisfies the following conditions:

$$R^T R = I, \tag{5.2}$$

and

$$\det R = 1. \tag{5.3}$$

Thus, the rotation group consists of the set of all special orthogonal 3×3 matrices.

Matrices that satisfy only the condition (5.2) are called orthogonal. The orthogonal matrices generate the group O(3). For these matrices, $(\det R)^2 = 1$, which leads to $\det R = \pm 1$. Therefore, the orthogonal matrices also include reflection matrices. To exclude reflections and consider only rotations, the condition (5.3) must also be imposed. The above discussion can be generalized to higher-dimensional Euclidean spaces $\mathbb{R}^n$, for which the group is denoted as SO(n).

Parametrization of the rotation group

The parametric representation of the rotation group in three-dimensional space can be expressed in terms of Euler angles $\{\phi, \theta, \psi\}$. Throughout this thesis, the zyz-convention will be used[24]. Details on rotations in different conventions are discussed in Appendix A.1.

A rotation R can be expressed as a product of three successive rotations as follows

$$R = R_z(\psi) R_y(\theta) R_z(\phi), \tag{5.4}$$

where

$$R_z(\phi) = \begin{pmatrix} \cos\phi & \sin\phi & 0 \\ -\sin\phi & \cos\phi & 0 \\ 0 & 0 & 1 \end{pmatrix}, \tag{5.5}$$

$$R_y(\theta) = \begin{pmatrix} \cos\theta & 0 & -\sin\theta \\ 0 & 1 & 0 \\ \sin\theta & 0 & \cos\theta \end{pmatrix}, \tag{5.6}$$

$$R_z(\psi) = \begin{pmatrix} \cos\psi & \sin\psi & 0 \\ -\sin\psi & \cos\psi & 0 \\ 0 & 0 & 1 \end{pmatrix}. \tag{5.7}$$

The first rotation is performed around the z-axis of the initial coordinate system by an angle ϕ. Next, the system is rotated by an angle θ around the intermediate y-axis, followed by a rotation by ψ about the new z-axis. The ranges of the angles are $0 \leq \phi \leq 2\pi$, $0 \leq \theta \leq \pi$ and $0 \leq \psi \leq 2\pi$.

Generators of the group

The group SO(3) is a continuous group since the group elements depend on parameters (in this case angles) which can vary continuously and assume an infinite number of values and hence there are an infinite number of group elements. It is easy to notice that the group elements are infinitely differentiable with respect to the parameters. Mathematician Sophus Lie showed that the study of such groups (known as Lie groups) reduces to the study of the group elements in the neighborhood of the identity element.

[24]The reason for this choice will be explained later in Sec. 5.3.3.

Let us consider an infinitesimal rotation, which can be written as

$$R \simeq I + A, \tag{5.8}$$

where the elements of the matrix A are small quantities of the first order. Terms of the second and higher orders can be neglected.

The orthogonality condition (5.2) of rotation matrices R leads to the following relation

$$A + A^T = 0, \tag{5.9}$$

which implies that A is an antisymmetric matrix.

For the SO(3) group, three independent parameters are required to describe rotations. Thus, the antisymmetric matrix A can be written as follows [130]

$$A = \begin{pmatrix} 0 & \theta_3 & -\theta_2 \\ -\theta_3 & 0 & \theta_1 \\ \theta_2 & -\theta_1 & 0 \end{pmatrix} = \boldsymbol{\theta}\boldsymbol{\mathcal{J}}, \tag{5.10}$$

where $\boldsymbol{\theta} = (\theta_1, \theta_2, \theta_3)$ represents the infinitesimal angles of rotation around the x-, y-, and z-axes, respectively. The three real antisymmetric matrices are denoted by $\boldsymbol{\mathcal{J}} = (\mathcal{J}_1, \mathcal{J}_2, \mathcal{J}_3)$ with

$$\mathcal{J}_1 = \begin{pmatrix} 0 & 0 & 0 \\ 0 & 0 & 1 \\ 0 & -1 & 0 \end{pmatrix}, \quad \mathcal{J}_2 = \begin{pmatrix} 0 & 0 & -1 \\ 0 & 0 & 0 \\ 1 & 0 & 0 \end{pmatrix}, \quad \mathcal{J}_3 = \begin{pmatrix} 0 & 1 & 0 \\ -1 & 0 & 0 \\ 0 & 0 & 0 \end{pmatrix}, \tag{5.11}$$

where $\mathcal{J}_i$ are called *group generators*. Hence, for SO(3), there are three generators corresponding to rotations about each axis, where the x-, y-, and z-axes are denoted by 1, 2, and 3, respectively.

Any rotation in the group corresponding to larger values of the rotation angles θ_i can be generated by performing N successive infinitesimal rotations of θ_i/N. Taking the limit as $N \to \infty$, we obtain the following relation

$$R(\boldsymbol{\theta}) = \exp(\boldsymbol{\theta}\boldsymbol{\mathcal{J}}) = e^{\sum_i \theta_i \mathcal{J}_i} = e^{\theta_x \mathcal{J}_x} e^{\theta_y \mathcal{J}_y} e^{\theta_z \mathcal{J}_z}. \tag{5.12}$$

Thus, any rotation in three-dimensional space can be expressed in terms of the group generators.

It is also essential to introduce the generators as Hermitian matrices (due to their application in quantum physics). Therefore, let us define $J_i \equiv -i\mathcal{J}_i$, which, when written explicitly, read

$$J_1 = i\begin{pmatrix} 0 & 0 & 0 \\ 0 & 0 & -1 \\ 0 & 1 & 0 \end{pmatrix}, \quad J_2 = i\begin{pmatrix} 0 & 0 & 1 \\ 0 & 0 & 0 \\ -1 & 0 & 0 \end{pmatrix}, \quad J_3 = i\begin{pmatrix} 0 & -1 & 0 \\ 1 & 0 & 0 \\ 0 & 0 & 0 \end{pmatrix}. \tag{5.13}$$

Then, we can give a general rotation as

$$R = e^{i\sum_i \theta_i J_i}, \tag{5.14}$$

where J_i are the *Hermitian generators* of the SO(3) group.

Lie algebra

The commutator of two generators is itself a generator. The commutation relations between the generators define the Lie algebra

$$[\mathcal{J}_i, \mathcal{J}_j] = C_{ij}^k\, \mathcal{J}_k, \tag{5.15}$$

where C_{ij}^k are the structure constants. It is easy to notice that $C_{ij}^k = -C_{ji}^k$. The structure constants determine the Lie algebra, which, in turn, essentially determines the Lie group. Note that while a Lie group is characterized by multiplication, its Lie algebra is characterized by commutation.

For the SO(3) group, the structure constants are $C_{ij}^k = -\epsilon_{ijk}$, meaning that the following commutation relations hold[25]

$$[\mathcal{J}_i, \mathcal{J}_j] = -\epsilon_{ijk}\mathcal{J}_k. \tag{5.16}$$

Moreover, for the Hermitian generators, we have:

$$[J_i, J_j] = i\epsilon_{ijk} J_k. \tag{5.17}$$

5.2 Homomorphism of SU(2) onto SO(3)

The special unitary group, also known as SU(2), consists of the two-dimensional unitary matrices with determinant 1. Hence, considering a two-dimensional matrix

$$U = \begin{pmatrix} a & b \\ c & d \end{pmatrix}, \tag{5.18}$$

[25]Note that if we had chosen to work with clockwise rotations, the structure constants would be $\tilde{C}_{ij}^k = \epsilon_{ijk}$, with the generators $\tilde{\mathcal{K}}_i = -\mathcal{K}_i$, which is also commonly used in the literature.

the following condition must hold for the matrix to be unitary:

$$UU^\dagger = I, \tag{5.19}$$

and for it to be special, it has to satisfy

$$\det U = +1. \tag{5.20}$$

The condition (5.19) leads to the following relation between the matrix elements

$$a^* a + b^* b = 1, \tag{5.21}$$

and

$$a^* c + b^* d = 0, \tag{5.22}$$

which implies that

$$c = -b^* d / a^*. \tag{5.23}$$

In addition, (5.20) demands

$$ad - bc = 1. \tag{5.24}$$

It follows that $d = a^*$, $c = -b^*$. Thus, the unitary matrix can be expressed in a general form

$$U = \begin{pmatrix} a & b \\ -b^* & a^* \end{pmatrix}, \tag{5.25}$$

where $|a|^2 + |b|^2 = 1$.

Any two-dimensional Hermitian traceless matrix H can be written as a linear combination of the Pauli matrices, which are given by

$$\sigma_1 = \begin{pmatrix} 0 & 1 \\ 1 & 0 \end{pmatrix}, \quad \sigma_2 = \begin{pmatrix} 0 & -i \\ i & 0 \end{pmatrix}, \quad \sigma_3 = \begin{pmatrix} 1 & 0 \\ 0 & -1 \end{pmatrix}. \tag{5.26}$$

Therefore, such a matrix H can be written as [129], [131]

$$H = x\sigma_1 + y\sigma_2 + z\sigma_3 = \begin{pmatrix} z & x - iy \\ x + iy & -z \end{pmatrix}, \tag{5.27}$$

where x, y, z are real coefficients. We specifically chose to take these coefficients as the Cartesian coordinates.

Transforming the Hermitian matrix H by a unitary matrix U with $\det U = 1$ as

$$H' = UHU^\dagger, \tag{5.28}$$

the resulting matrix H' is also Hermitian and traceless. Therefore, H' can be written as a linear combination of Pauli matrices as well, i.e.,

$$H' = x'\sigma_1 + y'\sigma_2 + z'\sigma_3 = \begin{pmatrix} z' & x' - iy' \\ x' + iy' & -z' \end{pmatrix}, \tag{5.29}$$

with three real coefficients (x', y', z').

In addition, from the relations (5.28) and (5.25), we have

$$H' = \begin{pmatrix} a & b \\ -b^* & a^* \end{pmatrix} \begin{pmatrix} z & x - iy \\ x + iy & -z \end{pmatrix} \begin{pmatrix} a^* & -b \\ b^* & a \end{pmatrix}. \tag{5.30}$$

Therefore, based on the above two relations, one notices that x', y', z' are linearly related to x, y, z. Introducing the vectors $\mathbf{x} = (x, y, z)$ and $\mathbf{x}' = (x', y', z')$, the relation can be expressed in matrix form,

$$\mathbf{x}' = S\mathbf{x}. \tag{5.31}$$

Finally, taking into account the fact that $\det(H) = \det(H')$ and

$$\det(H) = -|\mathbf{x}|^2, \quad \det(H') = -|\mathbf{x}'|^2, \tag{5.32}$$

implies that the length of the vectors is the same; hence, the vector $\mathbf{x}$ is rotated into $\mathbf{x}'$, i.e., S is a rotation matrix, $S \equiv R$, which is parametrized by Euler angles and given by (5.4). Therefore, to any 2×2 unitary matrix U with $\det U = 1$, there corresponds a rotation matrix R in three-dimensional space.

Finally, it can be noted that if one had considered the matrix $-U$ instead of U in (5.28), the matrix H' would not change, and consequently, the resulting rotation matrix S would remain the same.

Thus, to sum up, there is a two-to-one homomorphism of the unitary group SU(2) onto the rotation group SO(3), or in other words, SU(2) double covers SO(3).

Unitary group elements in terms of Euler angles

The unitary matrices corresponding to the rotation matrices (parametrized by Euler angles) can be obtained from (5.31). Starting with the first rotation around the z-axis by the angle ϕ, described by the rotation matrix $R_z(\phi)$ (5.5), the corresponding unitary matrix is given by

$$U_\phi = e^{i\sigma_3\phi/2} = \begin{pmatrix} e^{i\frac{\phi}{2}} & 0 \\ 0 & e^{-i\frac{\phi}{2}} \end{pmatrix}. \tag{5.33}$$

For the second rotation around the intermediate y-axis, described by $R_y(\theta)$ (5.6), the corresponding unitary matrix reads

$$U_\theta = e^{i\sigma_2\theta/2} = \begin{pmatrix} \cos\frac{\theta}{2} & \sin\frac{\theta}{2} \\ -\sin\frac{\theta}{2} & \cos\frac{\theta}{2} \end{pmatrix}. \tag{5.34}$$

Finally, for the last rotation around the new z-axis by the angle ψ, the corresponding unitary matrix is

$$U_\psi = e^{i\sigma_3\psi/2} = \begin{pmatrix} e^{i\frac{\psi}{2}} & 0 \\ 0 & e^{-i\frac{\psi}{2}} \end{pmatrix}. \tag{5.35}$$

Therefore, the unitary matrix corresponding to the rotation $R = R_z(\psi)R_y(\theta)R_z(\phi)$ is the product of the above matrices, i.e.,

$$U = U_\psi U_\theta U_\phi = \begin{pmatrix} e^{i\frac{\phi+\psi}{2}}\cos\frac{\theta}{2} & e^{-i\frac{\phi-\psi}{2}}\sin\frac{\theta}{2} \\ -e^{i\frac{\phi-\psi}{2}}\sin\frac{\theta}{2} & e^{-i\frac{\phi+\psi}{2}}\cos\frac{\theta}{2} \end{pmatrix}. \tag{5.36}$$

Group generators

From the above parametric description, it is straightforward to obtain the SU(2) group generators in terms of Pauli matrices as $T_a = \frac{\sigma_a}{2}$, where $a = 1, 2, 3$. Hence, they are explicitly written as

$$T_1 = \frac{1}{2}\begin{pmatrix} 0 & 1 \\ 1 & 0 \end{pmatrix}, \quad T_2 = \frac{1}{2}\begin{pmatrix} 0 & -i \\ i & 0 \end{pmatrix}, \quad T_3 = \frac{1}{2}\begin{pmatrix} 1 & 0 \\ 0 & -1 \end{pmatrix}. \tag{5.37}$$

Therefore, the group elements can be given by the form

$$U = e^{i\theta_a T_a}, \tag{5.38}$$

where θ_a are the rotation parameters. Moreover, the group generators satisfy the following commutation relations,

$$[T_a, T_b] = i\varepsilon_{abc}T_c. \tag{5.39}$$

Recalling the commutation relation of the Hermitian operators of the SO(3) group (5.17), it is easy to notice that the Lie algebras of SO(3) and SU(2) are isomorphic.

5.3 Group representations

We provide a brief description of the unitary representations of the SO(3) group, focusing on functions that remain invariant under the group action and on the spinor representation of the group.

5.3.1 Irreducible representations

It has been proven that any continuous unitary representation of a compact Lie group, such as SO(3), in a Hilbert space can be expressed as a direct sum of the finite-dimensional irreducible representations of the group (see, e.g., [128]).

Let there be given a unitary representation $g \to T_g$ of the group of rotations in a Hilbert space $\mathcal{H}$. Any element of the group in a particular representation can be written as

$$T_g = e^{i\theta_k J_k}, \tag{5.40}$$

where θ_k are the continuous parameters of the group and J_k are the Hermitian generators of the group in the considered representation. The generators in an arbitrary representation form a Lie algebra, whose structure is isomorphic to that of the group's Lie algebra, that is,

$$[J_i, J_j] = i\varepsilon_{ijk} J_k. \tag{5.41}$$

Thus, the commutation relations of the group generators (5.17) hold in arbitrary representations. To analyze the eigenvectors of the Hermitian generators, we first consider the following combinations

$$J_+ = J_1 + iJ_2, \quad J_- = J_1 - iJ_2. \tag{5.42}$$

The commutators of these matrices are

$$[J_+, J_3] = -J_+, \quad [J_-, J_3] = J_-, \quad [J_+, J_-] = 2J_3. \tag{5.43}$$

For any irreducible representation J_+, J_- and J_3 define an orthogonal basis consisting of the normalized eigenvectors of J_3, given by the following equations,

$$\begin{aligned} J_+ f_m &= \alpha_{m+1} f_{m+1}, \\ J_- f_m &= \alpha_m f_{m-1}, \\ J_3 f_m &= m f_m, \end{aligned} \tag{5.44}$$

where $m = -l, -l+1, ..., l$, with l being either an integer or a half-integer, and $\alpha_m = \sqrt{(l+m)(l-m+1)}$. The eigenvectors $f_l, f_{l-1}, ... f_{-l}$ form the *canonical basis* of the representation. The number l, which corresponds to the largest eigenvalue of the

Hermitian generator J_3, is called the weight of the considered irreducible representation.

In addition, all the eigenvectors of an irreducible representation with a given weight l satisfy the eigenvalue equation for the Casimir operator $J^2 = J_1^2 + J_2^2 + J_3^2$, since it commutes with all the operators of the representation. Thus, we have

$$J^2 f = l(l+1)f. \tag{5.45}$$

Finally, we note that the general representation of the group can be expressed as a block diagonal matrix, consisting of all irreducible representations with weights ranging from $-l$ to l.

5.3.2 Spinor representation

Let us consider a first-rank spinor ψ, denoted by

$$\psi = \begin{pmatrix} \psi_1 \\ \psi_2 \end{pmatrix}. \tag{5.46}$$

Under a rotation of the frame by the rotation matrix R (5.4), the spinors transform via the unitary matrix U, as given in (5.36), namely

$$\psi' = U\psi, \tag{5.47}$$

The above transformation yields a first-rank spinor representation (a two-dimensional representation of the rotation group).

To construct the canonical basis for this representation, we need to solve the equations (5.41), where for the spinor representation, the matrices J_i correspond to the matrices T_i, $i = 1, 2, 3$, as given by (5.37).

Let us consider the equation

$$J_3 f_m = m f_m, \tag{5.48}$$

where

$$J_3 \equiv T_3 = \begin{pmatrix} \frac{1}{2} & 0 \\ 0 & -\frac{1}{2} \end{pmatrix}, \tag{5.49}$$

and f_m are the eigenspinors which can be written as

$$f_m = \begin{pmatrix} f_m^1 \\ f_m^2 \end{pmatrix}. \tag{5.50}$$

Hence, the solutions of the equation (5.48) are

$$f_{\frac{1}{2}} = \begin{pmatrix} 1 \\ 0 \end{pmatrix}, \quad f_{-\frac{1}{2}} = \begin{pmatrix} 0 \\ 1 \end{pmatrix}, \tag{5.51}$$

where m assumes two eigenvalues; $m = -\frac{1}{2}, \frac{1}{2}$.

It is straightforward to show, by solving the eigenvalue equation of the Casimir operator (5.45), that the spinor representation is an irreducible representation with weight $\frac{1}{2}$.

5.3.3 Generalized spherical harmonics

Next, we examine the functions that remain invariant under the action of the SO(3) group.

Considering a function $f(\psi, \theta, \phi)$ expressed in terms of Euler angles, it is transformed under a rotation of the coordinate frame by the action of an operator T_g as follows

$$T_g f(\psi, \theta, \phi) = f'(\psi, \theta, \phi) = f(\psi', \theta', \phi'). \tag{5.52}$$

The general representation is reducible to the irreducible representations of weight l. To study this and obtain the canonical basis, we need to follow the steps presented previously, as given in Sec. 5.3.1.

To solve the equations (5.44), we need to introduce operators J_i acting on functions. These can be defined in two ways, using the right-invariant and left-invariant bases, as given by (2.25) and (2.23), respectively.

Let us recall the commutation relations for the right- and left-invariant bases,

$$[e_i, e_j] = \varepsilon_{ijk} e_k, \quad \text{and} \quad [\tilde{e}_i, \tilde{e}_j] = -\varepsilon_{ijk} \tilde{e}_k. \tag{5.53}$$

Since the condition (5.41) must be satisfied, we can define the operators accordingly as follows

$$J_i = i e_i, \quad \tilde{J}_i = -i \tilde{e}_i. \tag{5.54}$$

Thus, recalling (2.23) and (2.25), the operators are explicitly written as

$$\begin{aligned}
J_1 &= i \left[\sin\psi \frac{\partial}{\partial\theta} + \cos\psi \left(\cot\theta \frac{\partial}{\partial\psi} - \frac{1}{\sin\theta} \frac{\partial}{\partial\phi} \right) \right], \\
J_2 &= i \left[\cos\psi \frac{\partial}{\partial\theta} - \sin\psi \left(\cot\theta \frac{\partial}{\partial\psi} - \frac{1}{\sin\theta} \frac{\partial}{\partial\phi} \right) \right], \\
J_3 &= i \frac{\partial}{\partial\psi},
\end{aligned} \tag{5.55}$$

and

$$
\begin{aligned}
\tilde{J}_1 &= i\left[\sin\phi\frac{\partial}{\partial\theta} + \cos\phi\left(\cot\theta\frac{\partial}{\partial\phi} - \frac{1}{\sin\theta}\frac{\partial}{\partial\psi}\right)\right], \\
\tilde{J}_2 &= i\left[-\cos\phi\frac{\partial}{\partial\theta} + \sin\phi\left(\cot\theta\frac{\partial}{\partial\phi} - \frac{1}{\sin\theta}\frac{\partial}{\partial\psi}\right)\right], \\
\tilde{J}_3 &= -i\frac{\partial}{\partial\phi}.
\end{aligned}
\tag{5.56}
$$

One can notice that these correspond to the body-fixed and space-fixed orbital angular momenta (see, e.g., [132]). Therefore, for convenience, we will henceforth use the notation $L_i \equiv J_i$ and $\tilde{L}_i \equiv \tilde{J}_i$.

By introducing the operators $L_\pm$ via (5.42), we obtain the following sets of operators:

$$
\begin{aligned}
L_+ &= ie^{-i\psi}\left\{i\frac{\partial}{\partial\theta} + \cot\theta\frac{\partial}{\partial\psi} - \frac{1}{\sin\theta}\frac{\partial}{\partial\phi}\right\}, \\
L_- &= ie^{i\psi}\left\{-i\frac{\partial}{\partial\theta} + \cot\theta\frac{\partial}{\partial\psi} - \frac{1}{\sin\theta}\frac{\partial}{\partial\phi}\right\}, \\
L_3 &= i\frac{\partial}{\partial\psi},
\end{aligned}
\tag{5.57}
$$

and

$$
\begin{aligned}
\tilde{L}_+ &= ie^{i\phi}\left\{-i\frac{\partial}{\partial\theta} + \cot\theta\frac{\partial}{\partial\phi} - \frac{1}{\sin\theta}\frac{\partial}{\partial\psi}\right\}, \\
\tilde{L}_- &= ie^{-i\phi}\left\{i\frac{\partial}{\partial\theta} + \cot\theta\frac{\partial}{\partial\phi} - \frac{1}{\sin\theta}\frac{\partial}{\partial\psi}\right\}, \\
\tilde{L}_3 &= -i\frac{\partial}{\partial\phi}.
\end{aligned}
\tag{5.58}
$$

Finally, by calculating the Casimir operator $L^2 = \tilde{L}^2$, the equation (5.45), expressed in terms of Euler angles, reads

$$
\left[\frac{\partial^2}{\partial\theta^2} + \cot\theta\frac{\partial}{\partial\theta} + \frac{1}{\sin^2\theta}\left(\frac{\partial^2}{\partial\phi^2} - 2\cos\theta\frac{\partial}{\partial\phi}\frac{\partial}{\partial\psi} + \frac{\partial^2}{\partial\psi^2}\right) + l(l+1)\right] f = 0. \tag{5.59}
$$

The solutions of this equation are the functions[26] [129], [133]

$$
D^l_{m'm}(\phi,\theta,\psi) = e^{im'\psi} d^l_{m'm}(\theta) e^{im\phi}, \tag{5.60}
$$

where the functions $d^l_{m'm}(\theta)$ are the solutions of the following equation,

$$
\left[\frac{d^2}{d\theta^2} + \cot\theta\frac{d}{d\theta} - \frac{m^2 + m'^2 - 2mm'\cos\theta}{\sin^2\theta} l(l+1)\right] d^l_{m'm}(\theta) = 0. \tag{5.61}
$$

[26]Gel'fand et al. used the zxz-convention with clockwise rotations [128]; hence, the functions take a slightly different form compared to those presented here.

The functions in (5.60) are the matrix elements of the Wigner matrix D^l [27], which are explicitly given by

$$D^l_{m'm}(\phi,\theta,\psi) = \left[\frac{(l+m)!(l-m)!}{(l+m')!(l-m')!}\right]^{\frac{1}{2}} (\sin\theta/2)^{2l}$$
$$\times \sum_r \binom{l+m'}{r}\binom{l-m'}{r-m-m'}(-1)^{l+m'-r}e^{im\phi}(\cot\theta/2)^{2r-m-m'}e^{im'\psi}. \tag{5.62}$$

The eigenvalue equations (5.44) can be explicitly written as

$$\begin{aligned} L_+ D^l_{-nm} &= \alpha_{n+1} D^l_{-(n+1)\,m}, \\ L_- D^l_{-nm} &= \alpha_n D^l_{-(n-1)\,m}, \\ L_3 D^l_{-nm} &= n D^l_{-nm}, \end{aligned} \tag{5.63}$$

and

$$\begin{aligned} \tilde{L}_+ D^l_{-n,m} &= \alpha_{m+1} D^l_{-n,m+1}, \\ \tilde{L}_- D^l_{-n,m} &= \alpha_m D^l_{-n,m-1}, \\ \tilde{L}_3 D^l_{-n,m} &= m D^l_{-n,m}, \end{aligned} \tag{5.64}$$

where we have replaced m' with $m' = -n$ to avoid a negative sign in the eigenvalue of the operator J_3.

The functions $D^l_{-nm}(\phi,\theta,\psi)$ will be referred to as the *generalized spherical functions*. They form a complete orthonormal basis, satisfying the following orthonormality and completeness relations:

$$\int_0^{2\pi} d\phi \int_0^{\pi} \sin\theta d\theta \int_0^{2\pi} d\psi \; \bar{D}^l_{-nm}(\phi,\theta,\psi) D^{l'}_{-n'm'}(\phi,\theta,\psi) = \frac{8\pi^2}{2l+1}\delta_{ll'}\delta_{mm'}\delta_{nn'}, \tag{5.65}$$

and

$$\sum_{lmn} \bar{D}^l_{-nm}(\phi,\theta,\psi) D^l_{-nm}(\phi',\theta',\psi') = \frac{8\pi^2}{2l+1}\delta(\phi-\phi')\delta(\cos\theta-\cos\theta')\delta(\psi-\psi'). \tag{5.66}$$

Therefore, any square-integrable function defined on S^3 can be expanded in terms of the generalized spherical functions $D^l_{-nm}(\phi,\theta,\psi)$.

[27] The zyz-convention for Euler angles have been chosen to ensure that the Wigner D-matrix elements are real, which is not the case for the zxz-convention. The zyz-convention is also preferred in quantum mechanics for the same reason.

5.4 Multiplication of representations

Let us consider two irreducible representations: a representation $g \to U_g$ with weight l_1, defined in the space R_1 with a canonical basis $\{e_{m_1}\}$, where $m_1 = -l_1, ..., l_1$, and a representation $g \to V_g$ with weight l_2, defined in the space R_2 with a canonical basis $\{f_{m_2}\}$, where $m_2 = -l_2, ..., l_2$.

The vectors e_{m_1} and f_{m_2} are the eigenvectors of J_3, satisfying the following eigenvalue equations,

$$\begin{aligned} J_3 e_{m_1} &= m_1 e_{m_1}, \quad (-l_1 \leq m_1 \leq l_1), \\ J_3 f_{m_2} &= m_2 f_{m_2}, \quad (-l_2 \leq m_2 \leq l_2). \end{aligned} \tag{5.67}$$

Then, it is evident that

$$J_3(e_{m_1} f_{m_2}) = (J_3 e_{m_1}) f_{m_2} + e_{m_1}(J_3 f_{m_2}) = (m_1 + m_2) e_{m_1} f_{m_2}. \tag{5.68}$$

Thus, the basis $\{e_{m_1} f_{m_2}\}$ in the space $R_1 \times R_2$ forms an orthonormal system of eigenvectors of J_3, with corresponding eigenvalues $m = m_1 + m_2$, where $-l_1 - l_2 \leq m \leq l_1 + l_2$.

The product of irreducible representations with weights l_1 and l_2 can also be decomposed into another set of bases, namely, irreducible representations of weight l, where $|l_1 - l_2| \leq l \leq l_1 + l_2$, forming a canonical basis. This will be denoted by $\{g^l_m\}$.

The canonical eigenvectors in the space of $R_1 \times R_2$ can be expressed as a linear combination of the eigenvectors $e_{m_1} f_{m_2}$ in the following manner [128],

$$g^l_m = \sum C^{lm}_{l_1 m_1; l_2 m_2} e_{m_1} f_{m_2}, \tag{5.69}$$

where $m = m_1 + m_2$. The coefficients $C^{lm}_{l_1 m_1; l_2 m_2}$ are known as the *Clebsch-Gordan coefficients*. Similarly, the eigenbasis $\{e_{m_1} f_{m_2}\}$ can be written as a linear combination of the canonical basis.

5.4.1 Addition of angular momenta

Let us discuss a specific example of the product of the representation which is the addition of angular momenta in quantum mechanics. The addition of angular momenta refers to the combination of two or more angular momenta to form a total angular momentum. This is a fundamental topic in quantum theory, and it has been studied extensively in various references such as [134–137].

We consider two angular-momentum operators $J(1)$ and $J(2)$ in different subspaces, both of which satisfy the angular-momentum commutation relations (5.41), namely

$$[J(1)_i, J(1)_j] = i\varepsilon_{ijk} J(1)_k, \quad [J(2)_i, J(2)_j] = i\varepsilon_{ijk} J(2)_k. \tag{5.70}$$

Also, we assume that the components of these angular momenta commute,

$$[J(1)_i, J(2)_j] = 0, \quad i, j = 1, 2, 3. \tag{5.71}$$

Introducing a total angular momentum operator by

$$J = J(1) + J(2), \tag{5.72}$$

it is easy to show that J itself also satisfies the angular-momentum commutation relations, i.e.

$$[J_i, J_j] = i\varepsilon_{ijk} J_k. \tag{5.73}$$

The eigenvalue equations for the Casimir operators of the angular momenta operators are

$$J(1)^2 |j_1 m_1\rangle = j_1(j_1+1)|j_1 m_1\rangle, \quad \text{and} \quad J(2)^2 |j_2 m_2\rangle = j_2(j_2+1)|j_2 m_2\rangle, \tag{5.74}$$

where $|j_1 m_1\rangle$ and $|j_2 m_2\rangle$ are the eigenvectors of the $J(1)$ and $J(2)$ angular momenta operators.

Furthermore, for the components $J(1)_3$ and $J(2)_3$, we have

$$J(1)_3 |j_1 m_1\rangle = m_1 |j_1 m_1\rangle \quad \text{and} \quad J(2)_3 |j_2 m_2\rangle = m_2 |j_2 m_2\rangle. \tag{5.75}$$

The total angular momentum J and its component $J_3 = J(1)_3 + J(2)_3$ also satisfy the eigenvalue equations of (5.45) and (5.44), respectively. Hence, as discussed in the previous section, we can choose the eigenbasis either in form of $\{e_{m_1} f_{m_2}\}$ or g^l_m. Let us now discuss these two eigenbases explicitly in detail.

Product of two eigenbasis

We denote the eigenbasis corresponding to the product of the eigenvectors as

$$|j_1 j_2; m_1 m_2\rangle = |j_1 m_1\rangle |j_2 m_2\rangle. \tag{5.76}$$

These are the simultaneous eigenvectors of the commuting operators $J(1)^2$, $J(2)^2$, $J(1)_3$ and $J(2)_3$. Thus, the following eigenvalue equations hold

$$\begin{aligned} J(1)^2 |j_1 j_2; m_1 m_2\rangle &= j_1(j_1+1)|j_1 j_2; m_1 m_2\rangle, \\ J(2)^2 |j_1 j_2; m_1 m_2\rangle &= j_2(j_2+1)|j_1 j_2; m_1 m_2\rangle, \end{aligned} \tag{5.77}$$

and

$$\begin{aligned} J(1)_3 |j_1 j_2; m_1 m_2\rangle &= m_1 |j_1 j_2; m_1 m_2\rangle, \\ J(2)_3 |j_1 j_2; m_1 m_2\rangle &= m_2 |j_1 j_2; m_1 m_2\rangle, \end{aligned} \tag{5.78}$$

where $|m_1| \leq j_1$ and $|m_2| \leq j_2$. For fixed j_1 and j_2, there are $(2j_1+1)(2j_2+1)$ eigenvectors for all different values of m_1 and m_2.

Canonical eigenbasis

Another option of eigenbasis are the simultaneous eigenvectors of the commuting operators J^2, $J(1)^2$, $J(2)^2$ and J_3. Note that only J_3 commutes with J^2; however,

$$[J^2, J(1)_3] \neq 0, \quad [J^2, J(2)_3] \neq 0. \tag{5.79}$$

Denoting the eigenvector by $|j_1 j_2; jm\rangle$, we have the following eigenvalue equations

$$\begin{aligned} J(1)^2 |j_1 j_2; jm\rangle &= j_1(j_1+1)|j_1 j_2; jm\rangle, \\ J(2)^2 |j_1 j_2; jm\rangle &= j_2(j_2+1)|j_1 j_2; jm\rangle, \end{aligned} \tag{5.80}$$

and

$$\begin{aligned} J^2 |j_1 j_2; jm\rangle &= j(j+1)|j_1 j_2; jm\rangle, \\ J_3 |j_1 j_2; jm\rangle &= m|j_1 j_2; jm\rangle, \end{aligned} \tag{5.81}$$

where $|j_1 - j_2| \leq j \leq j_1 + j_2$ and $m = m_1 + m_2$. For each value of j there are $2j+1$ values of m.

Clebsch-Gordan coefficients

As shown in (5.69), the two eigenvectors above can be expressed in terms of one another as follows

$$|j_1 j_2; jm\rangle = \sum_{m_1, m_2} \langle j_1 j_2; m_1 m_2 | j_1 j_2; jm\rangle |j_1 j_2; m_1 m_2\rangle, \tag{5.82}$$

where $C^{lm}_{l_1 m_1; l_2 m_2} \equiv \langle j_1 j_2; m_1 m_2 | jm\rangle$ are the *Clebsch-Gordan coefficients* as in (5.69). The inverse transformation can be written similarly as

$$|j_1 j_2; m_1 m_2\rangle = \sum_{m_1, m_2} \langle j_1 j_2; jm | j_1 j_2; m_1 m_2\rangle |j_1 j_2; jm\rangle. \tag{5.83}$$

Since the Clebsch-Gordan coefficients form a unitary matrix and the matrix elements are taken to be real by convention, the inverse coefficients $\langle j_1 j_2; jm | j_1 j_2; m_1 m_2\rangle$ are the same as $\langle j_1 j_2; m_1 m_2 | j_1 j_2; jm\rangle$.

The Clebsch-Gordan coefficients satisfy the following orthogonality and normalisation relations

$$\sum_{j,m} \langle j_1 j_2; m_1 m_2 | j_1 j_2; jm\rangle \langle j_1 j_2; m_1' m_2' | j_1 j_2; jm\rangle = \delta_{m_1 m_1'} \delta_{m_2 m_2'}, \tag{5.84}$$

and

$$\sum_{m_1,m_2} \big\langle j_1 j_2; m_1 m_2 | j_1 j_2; jm \big\rangle \big\langle j_1 j_2; m_1 m_2 | j_1 j_2; j' m' \big\rangle = \delta_{jj'} \delta_{mm'}. \tag{5.85}$$

Finally, let us recall that the Clebsch-Gordan coefficients can be expressed in terms of the *Wigner 3j-symbols*

$$C^{lm}_{l_1 m_1; l_2 m_2} \equiv \big\langle j_1 j_2; m_1 m_2 | j_1 j_2; jm \big\rangle = (-1)^{j_1 - j_2 + m} \sqrt{2j+1} \begin{pmatrix} j_1 & j_2 & j \\ m_1 & m_2 & -m \end{pmatrix}. \tag{5.86}$$

Addition of spin and orbital angular momenta

Let us now focus on the discussion of the addition of spin and orbital angular momenta (e.g., of an electron) by setting $J(1) = L$, where L is the orbital angular momentum, and $J(2) = S$ for the spin angular momentum[28]. In this case, we have $j_1 = l$ and $j_2 = s = \frac{1}{2}$. Additionally, we denote $m_1 = m_l$, with $|m_l| \leq l$, and $m_2 = m_s$, where $m_s = \pm\frac{1}{2}$.

The two possible eigenbases discussed above are the following:

$$\big|l\, s; m_l\, m_s\big\rangle \equiv \big|l\, m_l\big\rangle \big|s\, m_s\big\rangle \quad \text{and} \quad \big|l\, s; j\, m\big\rangle, \tag{5.87}$$

where $j = l \pm \frac{1}{2}$, and $m = m_l + m_s = m_l \pm \frac{1}{2}$. The $\big|l\, m_l\big\rangle$ are the orbital angular momentum eigenstates and it is well known that

$$\left\langle \theta, \phi \middle| l,\, m \pm \frac{1}{2} \right\rangle = Y_{l,\, m \pm \frac{1}{2}}(\theta, \phi). \tag{5.88}$$

The spinor eigenstates $\big|s\, m_s\big\rangle$ are

$$\left| \frac{1}{2}, \frac{1}{2} \right\rangle = \begin{pmatrix} 1 \\ 0 \end{pmatrix} \quad \text{and} \quad \left| \frac{1}{2}, -\frac{1}{2} \right\rangle = \begin{pmatrix} 0 \\ 1 \end{pmatrix}. \tag{5.89}$$

For this case, the relation (5.82) takes the form[29]

$$\big|l\, s; j\, m\big\rangle = \sum_{m_s = \pm\frac{1}{2}} C^{jm}_{l, m-m_s; s m_s} \big|l, m - m_s\big\rangle \big|s\, m_s\big\rangle. \tag{5.90}$$

The components of the Clebsch-Gordan coefficients are given in the Table below [137]:

[28] The spin-angular momentum components are given by (5.37), where $T_i \equiv S_i$.

[29] In the literature, it is common to use a more concise version of the notation, often written as $\big|j\, m\big\rangle$, instead of $\big|l\, s; j\, m\big\rangle$.

$j_s = \frac{1}{2}$	$m_s = \frac{1}{2}$	$m_s = -\frac{1}{2}$
$j = l + \frac{1}{2}$	$\sqrt{\frac{l+m+\frac{1}{2}}{2l+1}}$	$\sqrt{\frac{l-m+\frac{1}{2}}{2l+1}}$
$j = l - \frac{1}{2}$	$-\sqrt{\frac{l-m+\frac{1}{2}}{2l+1}}$	$\sqrt{\frac{l+m+\frac{1}{2}}{2l+1}}$

Therefore, the eigenstates given by (5.90) will take the form

$$\Big|l,\, \frac{1}{2}; j\, m\Big\rangle = \Big|l,\, \frac{1}{2}; l \pm \frac{1}{2},\, m\Big\rangle = \frac{1}{\sqrt{2l+1}} \begin{pmatrix} \pm\sqrt{l \pm m + \frac{1}{2}}|l, m - \frac{1}{2}\rangle \\ \sqrt{l \mp m + \frac{1}{2}}|l, m + \frac{1}{2}\rangle \end{pmatrix}. \tag{5.91}$$

Recalling (5.88), it is straightforward to show that the eigenfunctions of the total angular momentum are

$$\mathcal{Y}_l^{j=l\pm 1/2, m} := \Big\langle \theta, \phi \Big| l,\, \frac{1}{2}; l \pm \frac{1}{2},\, m\Big\rangle = \frac{1}{\sqrt{2l+1}} \begin{pmatrix} \pm\sqrt{l \pm m + \frac{1}{2}} Y_{l, m-\frac{1}{2}}(\theta, \phi) \\ \sqrt{l \mp m + \frac{1}{2}} Y_{l, m+\frac{1}{2}}(\theta, \phi) \end{pmatrix}. \tag{5.92}$$

These are known in the literature as *spin-angular functions* [137] or *spin spherical harmonics* [138].

5.4.2 Generalized spinor spherical harmonics

Finally, we are ready to discuss spinor fields that are invariant under the group SO(3), building on the discussion developed throughout this section.

Following the steps in 5.4 and in the discussion of addition of spin and orbital angular momenta, let us consider the product of two representations. The first representation, $g \to V_g$, has weight $l_1 = \frac{1}{2}$ and acts in the space R_1 (i.e., the spinor representation). It has a canonical basis $\{e_{m_1}\}$, where $m_1 = -\frac{1}{2}, \frac{1}{2}$. As in (5.89), let us adopt the notation $|l_1\, m_1\rangle$ for the eigenvectors of spinor representation. That is, we write $e_{\frac{1}{2}} = |\frac{1}{2}, \frac{1}{2}\rangle$ and $e_{-\frac{1}{2}} = |\frac{1}{2}, -\frac{1}{2}\rangle$.

The second representation, $g \to U_g$, has weight $l_2 = l$ and acts in the space R_1, which in this case is the space of functions. Its canonical basis is given by $f_{m_2} = D^l_{-m_2\, m}(\phi, \theta, \psi)$, where m_2 and $|m_2| \leq l$. Here, it is also convenient to introduce the notation $|l\, m\, m_2\rangle$ for the eigenvectors[30]. The eigenfunctions $D^l_{m_2\, m}(\phi, \theta, \psi)$ are related to these eigenvectors via

$$\langle \phi, \theta, \psi | l\, m\, m_2\rangle = D^l_{-m_2\, m}(\phi, \theta, \psi). \tag{5.93}$$

One possible choice for an eigenbasis is $\{e_{m_1} f_{m_2}\}$, which consists of the eigenvectors of

[30]Note that the quantum number m shouldn't be confused with $m = m_1 + m_2$. It is the eigenvalue of the space-fixed orbital angular momentum operator $\tilde{L}_3$.

the J_3 operator with eigenvalues of $n = m_1 + m_2$.

The eigenvectors are explicitly given by

$$e_{\frac{1}{2}} f_{n-\frac{1}{2}} = \left|\frac{1}{2}, \frac{1}{2}\right\rangle \left|l, m, n - \frac{1}{2}\right\rangle = \begin{pmatrix} \left|l, m, n - \frac{1}{2}\right\rangle \\ 0 \end{pmatrix}, \tag{5.94}$$

and

$$e_{\frac{1}{2}} f_{n+\frac{1}{2}} = \left|\frac{1}{2}, -\frac{1}{2}\right\rangle \left|l, m, n + \frac{1}{2}\right\rangle = \begin{pmatrix} 0 \\ \left|l, m, n + \frac{1}{2}\right\rangle \end{pmatrix}. \tag{5.95}$$

Another eigenbasis in the space $R_1 \times R_2$ consists of eigenvectors $g_m^{l+\frac{1}{2}}$, where $|m| \leq l + \frac{1}{2}$, and $g_m^{l-\frac{1}{2}}$, where $|m| \leq l - \frac{1}{2}$. The eigenvectors read explicitly

$$g_m^{l\pm\frac{1}{2}} = |j\, m\, n\rangle \equiv \left|l \pm \frac{1}{2},\ m\ , n\right\rangle = \frac{1}{\sqrt{2l+1}} \begin{pmatrix} \pm\sqrt{l \pm n + \frac{1}{2}}\left|l, m, n - \frac{1}{2}\right\rangle \\ \sqrt{l \mp n + \frac{1}{2}}\left|l, m, n + \frac{1}{2}\right\rangle \end{pmatrix}. \tag{5.96}$$

Moreover, in terms of the generalized spherical harmonics, the eigenfunctions take the form

$$\left\langle \psi, \theta, \phi \middle| l \pm \frac{1}{2}, n, m \right\rangle = \frac{1}{\sqrt{2l+1}} \begin{pmatrix} \pm\sqrt{l \pm n + \frac{1}{2}} D^l_{-(n-\frac{1}{2}),m}(\phi, \theta, \psi) \\ \sqrt{l \mp n + \frac{1}{2}} D^l_{-(n+\frac{1}{2}),m}(\phi, \theta, \psi) \end{pmatrix}, \tag{5.97}$$

which is the generalization of the spin spherical harmonics given in (5.92). Hence, we refer to these eigenfunctions as the *generalized spin spherical harmonics*.

Therefore, any spinor field defined on S^3 can be expanded in terms of generalized spin spherical harmonics.

6 Quantization of the rotation of rigid tops

In his study of the Klein-Gordon equation for a scalar field in the fixed Mixmaster universe, Bei-Lok Hu demonstrated an elegant connection [139]. He established that the eigenstates of the Helmholtz equation in this background are identical to the rotational eigenstates of an asymmetric top in quantum mechanics. This correspondence arises from the fact that the Laplace operator in the Helmholtz equation in the Mixmaster universe is mathematically equivalent to the Hamiltonian of an asymmetric top.

It has been demonstrated in quantum mechanics that the eigenstates of an asymmetric top Hamiltonian can be expressed as linear combinations of the eigenstates of the symmetric top Hamiltonian. Furthermore, considering the symmetry properties of the asymmetric top and expressing the Hamiltonian eigenstates in terms of the eigenstates of the symmetry group leads to significant simplifications when studying the eigenvalue problem of the Hamiltonian.

In Sec. 6.1 of this chapter, we will introduce the symmetry group of the asymmetric top, namely the group D_2, which is a point group. We will then explore the irreducible representations of this group, followed by a discussion of the eigenfunctions of both symmetric and asymmetric tops, building on the material presented in sources such as [135], [136], [140] and [141].

Furthermore, Hu's work was later generalized by J. S. Dowker and D. F. Pettengill in [142] to study spinor fields in a fixed Mixmaster universe. They showed that the solution to the second-order equation for the Dirac spinor field can be identified with the eigenvalue equation of the Hamiltonian for an asymmetric "ideal" top, where the "ideal" top is defined as one possessing "intrinsic spin".

Subsequently, we will generalize this approach for spinor fields in the general Bianchi IX model. Additionally, we will discuss two possible choices for the eigenbasis of the symmetric top, based on studies in Sec. 5.4.1 and Sec. 5.4.2, where the eigenbasis was derived through group-theoretical considerations. We explore these in detail in Sec. 6.3.

6.1 Point groups

Point groups play a crucial role in quantum mechanics, particularly in molecular spectroscopy. These groups consist of symmetry operations that describe the symmetry of a system, such as a molecule. The application of symmetry groups provides a powerful tool for studying the energy eigenstates of molecules without the need to explicitly solve the Schrödinger equation, which is often not feasible.

Symmetry transformations

Transformations that leave a system or body unchanged are called symmetry transformations. The three fundamental types of symmetry transformations are rotation, reflection, and improper rotation. Any other symmetry transformation can be expressed as a combination of these.

Rotation

Let us consider a symmetry transformation of rotation about the axis of symmetry by an angle $2\pi/n$. The operation of such a rotation also known as $n-$fold rotation is denoted by C_n. Repeating the rotation n times, the body returns to the initial position. Hence we can write

$$C_n{}^n = E, \tag{6.1}$$

where E is the identity operation.

Reflection

The operation of reflection in some plane is denoted by σ. Repeating the reflection operation twice results in the identity transformation, i.e.

$$\sigma^2 = E. \tag{6.2}$$

Improper rotation

An improper rotation, also known as a rotary-reflection transformation, consists of two operations: an n-fold rotation followed by a reflection in a plane perpendicular to the rotation axis. Repeating the improper rotation n times restores the body to its initial position. Notably, n can only take even values, as for odd values, the transformation simplifies to a reflection.

Denoting the improper rotation operation by a symbol S_n, it can be expressed in terms of the rotation and reflection operators as

$$S_n = C_n\sigma = \sigma C_n. \tag{6.3}$$

S_n is independent of the order of the application of rotation and reflection operations.

For a given body, the set of all symmetry transformations forms a group known as the *symmetry transformation group* or *symmetry group*. In the case of a finite-dimensional body, symmetry transformations are limited to rotations and reflections. Moreover, these transformations must ensure that at least one point of the body remains fixed, which is why such groups are called *point groups*.

$\mathbf{D_n}$ *group*

As mentioned earlier, the point group that will be used for our studies is the D_2 group which is a particular case of the dihedral group D_n.

Let us first discuss the group C_n. This group consists of rotations about the axis of symmetry of nth order and the identity element E. In addition, if we consider n axes of second order (horizontal axes) perpendicular to this nth order axis and including n rotations by an angle π (i.e. two-fold rotations) about these horizontal axes, we will obtain the group D_n. Hence, this groups has $2n$ elements.

Thus, the group D_2 has four group elements: the identity and three rotations by an angle π about three mutually perpendicular axes of the second order. The three rotation operators are denoted by C_2^a, C_2^b and C_2^2.

6.1.1 Irreducible representations of the D_2 group

Since the group D_2 is an Abelian group, all its irreducible representations are one-dimensional, which are denoted by A and B. The characters of the representations can take only ± 1 values, which are depicted in the Table 2 below. The indices a, b and c correspond to the principle axes about which the rotations are performed.

The representations A are symmetric and the B representations are antisymmetric with respect to the rotations about a symmetrical axis of the nth order. As one can see in Table 2, the representation A doesn't change the sign under the symmetry operations of the group elements, whereas the representations B do change their signs.

$\mathbf{D}_2$	E	C_2^a	C_2^b	C_2^c
A	1	1	1	1
B_a	1	1	-1	-1
B_b	1	-1	1	-1
B_c	1	-1	-1	1

Table 2: Characters of irreducible representations of D_2 group.

6.1.2 Two-valued representations of finite point groups

For the later discussion of spinors with half-integral spin, we must also consider the two-valued irreducible representations of the point groups.

Since the two-valued representations are not true representations of a group, we must adopt the following approach to obtain them [136]. First, we have to introduce a new group element Q, which is a rotation by an angle of 2π about an arbitrary axis, and demand the following conditions to be satisfied

$$C_n{}^n = Q, \quad Q^2 = C_n{}^{2n} = E. \tag{6.4}$$

Hence, the rotations C_n about the axes of symmetry yield identical transformations after being applied $2n$ times, rather than after n times.

Similarly, for the reflection in a plane we demand

$$\sigma^2 = Q, \quad \sigma^4 = E. \tag{6.5}$$

The element Q commutes with all the other elements of the group. As a result, a new set of elements is formed, which creates a group whose order is twice that of the original group. The new group is called *double point groups*.

This approach enables the introduction of two-valued representations of the point group by constructing the one-valued representations of the corresponding double group. The irreducible representations of a double point group include the one-valued irreducible representations, which are identical to those of the original point group. In addition to these one-valued representations, two-dimensional representations also arise.

As a particular case, let us consider the D_2 group and denote the corresponding double group by D_2'. The characters of the two-dimensional irreducible representation of the double group D_2', denoted by E' (not to be confused with the identity element), are given in the table below:

$\mathbf{D}_2$	E	Q	C_2^a $C_2^a Q$	C_2^b $C_2^b Q$	C_2^c $C_2^c Q$
E'	2	-2	0	0	0

Table 3: Characters of two-valued representation of D_2' group.

Application in Quantum Mechanics

In Quantum Mechanics, it is not always possible to solve the Schrödinger equation exactly. Therefore, one can study the properties of the energy eigenvalues and eigenstates of a system, particularly for more complex molecules, by utilizing the symmetry groups. The symmetry transformations leave the Hamiltonian of the system invariant, meaning that the group elements commute with the Hamiltonian. As a result, it can be shown that the energy eigenfunctions of the system can be classified according to the irreducible representations of the symmetry group.

Additionally, let us mention that the energy eigenstates corresponding to one-dimensional irreducible representations are non-degenerate, while the eigenstates associated with two-dimensional representations are two-fold degenerate [135].

6.2 Rigid tops

Since our focus is on the energy eigenstates of symmetric and asymmetric tops, we begin by reviewing the necessary concepts from classical mechanics. We will then derive the Hamiltonians for both cases, which will later be quantized.

Motion of a rigid body in classical mechanics

In general, the motion of a rigid body with respect to a fixed coordinate system involves both translations and rotations (around the center of mass). Here, we will focus specifically on the rotational aspects.

The rotational dynamics are characterized by the angular velocity, moments of inertia, and angular momentum, which will be introduced below [143], [144].

Angular velocity

Let us denote the angular velocity vector of the rotating rigid body by $\mathbf{\Omega}$. The components of the angular velocity vector along the coordinate axes, expressed in terms of the Euler angles in zyz-convention, are given by

$$\begin{aligned} \Omega_1 &= \sin\psi\dot{\theta} - \sin\theta\cos\psi\dot{\phi}, \\ \Omega_2 &= \sin\psi\sin\theta\dot{\phi} + \cos\psi\dot{\theta}, \\ \Omega_3 &= \dot{\psi} + \cos\theta\dot{\phi}, \end{aligned} \tag{6.6}$$

where Ω_1, Ω_2 and Ω_3 are the angular velocities about the x', y' and z' axes of the body-fixed frame of reference.

Angular momentum

The angular momentum vector $\mathbf{L}$ is related to the angular velocity vector $\mathbf{\Omega}$ by a linear transformation, which involves the moment of inertia tensor. The relationship is given by

$$L_i = I_{ij}\Omega_j, \quad i,j = 1,2,3, \tag{6.7}$$

where L_i are the components of the angular momentum vector and I_{ij} is the (moment of) inertia tensor, which depends on the choice of the rotation axis.

Since the moment of inertia tensor is a symmetric matrix, it can be diagonalized through an appropriate transformation, such as changing the direction of the coordinate axes. Therefore, the diagonalized tensor can be obtained as follows:

$$I^{\mathrm{d}} = RIR^T, \tag{6.8}$$

where R is a rotation matrix and I^{d} is the diagonal moment of inertia tensor given by

$$I^{\mathrm{d}} = \begin{pmatrix} I_1 & 0 & 0 \\ 0 & I_2 & 0 \\ 0 & 0 & I_3 \end{pmatrix}. \tag{6.9}$$

The directions of the coordinate axes x', y' and z' for which the moment of inertia tensor is diagonal are called the principal axes.

The angular momentum and angular velocity vector components along the principal axes are related as

$$L_1 = I_1\Omega_1, \quad L_2 = I_2\Omega_2, \quad L_3 = I_3\Omega_3. \tag{6.10}$$

Kinetic energy

Finally, another important concept needed to study the dynamics of the rotation of the rigid body is the kinetic energy. The rotational kinetic energy can be written as

$$T = \frac{1}{2} I_{ij}\Omega_i\Omega_j. \tag{6.11}$$

If the axes x', y' and z' are taken to be the principal axes of inertia, the kinetic energy simplifies to

$$T = \frac{1}{2}I_1\Omega_1^2 + \frac{1}{2}I_2\Omega_2^2 + \frac{1}{2}I_3\Omega_3^2. \tag{6.12}$$

In addition, it can be expressed in terms of the components of the angular momentum

$$T = \frac{L_1^2}{2I_1} + \frac{L_2^2}{2I_2} + \frac{L_3^2}{2I_3}. \tag{6.13}$$

6.2.1 Symmetric top

A symmetric top is a rigid body where two of the three moments of inertia are equal, $I_1 = I_2 \neq I_3$. Hence, the rotational kinetic energy of a symmetric top takes the form

$$T = \frac{1}{2}I_1\left(\Omega_1^2 + \Omega_2^2\right) + \frac{1}{2}I_3\Omega_3^2, \tag{6.14}$$

In terms of the angular momenta, the kinetic energy can be written

$$T^{\mathrm{top}} = \frac{L_1^2 + L_2^2}{2I_1} + \frac{L_3^2}{2I_3}. \tag{6.15}$$

Let us introduce the following parameters

$$a = \frac{1}{2I_1}, \quad b = \frac{1}{2I_2}, \quad c = \frac{1}{2I_3}, \tag{6.16}$$

These are known as *rotational constants*. Taking $a = b$ for the symmetric top, we can write the Hamiltonian of the symmetric top as follows:

$$H = a(L_1^2 + L_2^2) + cL_3^2, \tag{6.17}$$

or equivalently

$$H = aL^2 + (c - a)L_3^2. \tag{6.18}$$

Recalling the body-fixed angular momentum operator L_i in terms of Euler angles, as presented in equation (5.55), and explicitly substituting the operators, the Schrödinger equation for the symmetric top can be written as

$$-a\left\{\frac{\partial^2}{\partial\theta^2} + \cot\theta\frac{\partial}{\partial\theta} + \left(\frac{c}{a} + \cot^2\theta\right)\frac{\partial^2}{\partial\psi^2} + \frac{1}{\sin^2\theta}\frac{\partial^2}{\partial\phi^2} - \frac{2\cos\theta}{\sin^2\theta}\frac{\partial^2}{\partial\phi\partial\psi}\right\}\Psi = E\Psi. \tag{6.19}$$

Before discussing the solution to the above equation, let us first note that for the spherical top, where $I_1 = I_2 = I_3$, the equation simplifies to the eigenvalue equation of the Casimir (or total angular momentum) operator (5.59), with eigenvalues of

$$E = al(l+1), \tag{6.20}$$

and the orthonormalized eigenfunctions of

$$\Psi_{lnm}(\phi,\theta,\psi) = \sqrt{\frac{2l+1}{8\pi^2}}D^l_{-nm}(\phi,\theta,\psi), \tag{6.21}$$

where l take integer values and $|n|, |m| \leq l$.

To solve the equation (6.19), let us use the following ansatz:

$$\Psi(\phi,\theta,\psi) = e^{-in\psi}B(\theta)e^{im\phi}. \tag{6.22}$$

Substituting this ansatz into the equation, we obtain

$$-\left\{\frac{d^2}{d\theta^2} + \cot\theta\,\frac{d}{d\theta} - \frac{m^2 + n^2 + 2mn\cos\theta}{\sin^2\theta}\right\}B(\theta) = \left\{\frac{1}{a}\,E + \frac{a-c}{a}\,n^2\right\}B(\theta). \tag{6.23}$$

Recalling the equation (5.61), one can see that $B(\theta) = d^{(l)}_{-nm}(\theta)$ with the eigenvalues of

$$E = a\,l(l+1) + (c-a)\,n^2. \tag{6.24}$$

Thus, the eigenfunctions of the symmetric and spherical tops are the same. The difference lies in the energy eigenvalues. For the spherical top, the energy eigenvalues depend solely on the quantum number l, and the levels are $(2l+1)$-fold degenerate, corresponding to the values of n. On the other hand, for the symmetric top the energy eigenvalues depend on n^2 as well. Since the values of n with different signs correspond to the same energy eigenstate, the degeneracy is $2(2l+1)$ for $n \neq 0$.

Finally, for the convenience of future developments regarding the asymmetric and "ideal" tops, let us use the notation $|l\,m\,n\rangle$ to describe the eigenstates, as was done in (5.93), namely,

$$\Psi_{lmn}(\psi,\theta,\phi) = \sqrt{\frac{2l+1}{8\pi^2}}\langle\phi,\theta,\psi|l\,m\,n\rangle. \tag{6.25}$$

Furthermore, the eigenvalue equations for the body- and space-fixed angular momenta, given in (5.57) and (5.58), can be rewritten using this notation as

$$\begin{aligned} L_+|l\,m\,n\rangle &= \alpha_{n+1}\,|l,\,m,\,n+1\rangle, \\ L_-|l\,m\,n\rangle &= \alpha_n\,|l,\,m,\,n-1\rangle, \\ L_3|l\,m\,n\rangle &= n|l\,m\,n\rangle, \end{aligned} \tag{6.26}$$

and

$$\begin{aligned} \tilde{L}_+|l\,m\,n\rangle &= \alpha_{m+1}|l,\,m+1,\,n\rangle, \\ \tilde{L}_-|l\,m\,n\rangle &= \alpha_m|l,\,m-1,\,n\rangle, \\ \tilde{L}_3|l\,m\,n\rangle &= m|l\,m\,n\rangle. \end{aligned} \tag{6.27}$$

We conclude the discussion by noting that the Hamiltonian of the symmetric top commutes with the operators L^2, L_3 and $\tilde{L}_3$. The operators L_i act on the index n of the eigenstates $|l\,m\,n\rangle$, while the operators $\tilde{L}_i$ act on the index m.

6.2.2 Asymmetric top

An asymmetric top is a rigid body in which all three moments of inertia are distinct, i.e., $I_1 \neq I_2 \neq I_3$. Hence, the Hamiltonian has the general form

$$H = aL_1^2 + bL_2^2 + cL_3^2. \tag{6.28}$$

It is easy to observe that, unlike in the symmetric case, the Hamiltonian commutes with the operators L^2 and $\tilde{L}_3$; however, it no longer commutes with L_3. Therefore, n is no longer a good quantum number for the asymmetric top.

It can be shown that the eigenfunctions of the asymmetric rigid rotator can be expressed as linear combinations of the symmetric top eigenfunctions $|l\,m\,n\rangle$ [135].

Therefore, we can write

$$\big|l\,m\big\rangle = \sum_{n=-l}^{l} a_n^l \big|l\,m\,n\big\rangle, \tag{6.29}$$

where $\big|lm\big\rangle$ are the eigenstates of the asymmetric top. Substituting this expansion into the Schrödinger equation

$$H\big|l\,m\big\rangle = E\big|l\,m\big\rangle, \tag{6.30}$$

we get

$$\sum_n a_n \left(H_{nn'} - E\,\delta_{nn'}\right) = 0, \tag{6.31}$$

where

$$\hat{H}\big|l\,m\,n\big\rangle = \sum_{n'} H_{nn'}\big|l\,m\,n'\big\rangle. \tag{6.32}$$

Hence, we get $(2l+1)$ equations corresponding to each value of n. The roots of the secular equation

$$\det|H_{nn'} - E\delta_{nn'}| = 0, \tag{6.33}$$

are the energy eigenvalues of the asymmetric top.

However, a more convenient choice of eigenbasis can be made to simplify the calculation of the energy eigenvalues. This eigenbasis can be constructed by incorporating the symmetry properties of the asymmetric top [140], [145], [146].

Symmetry properties of the asymmetric rotator

The symmetry group of the asymmetric top is the group D_2, which as we discussed in Section 6.1, contains an identity element and three two-fold rotations C_2^a, C_2^b, C_2^c, i.e., rotations by angle π about the three principle axes of the top.

The Hamiltonian and the commutation relations of angular momenta (5.41) are invariant under the transformations of the symmetry group. Therefore, as discussed in Section 6.1, the eigenfunctions can be classified according to the irreducible representations of the symmetry group. The D_2 group has four one-dimensional irreducible representations: A, B_1, B_2, and B_3, see Table 2.

The symmetry axes of the rotations, denoted by a, b, and c, can be identified with the body-fixed axes x', y', and z', respectively[31]. The Euler angles will be transformed under the operations C_2^a, C_2^b, C_2^c as expressed in Table 4 below.

Therefore, it can be shown that the eigenstates $\big|l\,m\,n\big\rangle$ transform under the action

[31]Note that this is a specific choice. In general, there are 3! ways of relating a, b and c to the body-fixed coordinate axes. Additionally, due to the various choices of Euler angles used to describe the orientation of the body-fixed axis with respect to the space-fixed axis, the notation and operation of the two-fold rotation on the eigenbasis $\big|l\,m\,n\big\rangle$ differ in the literature, which can lead to confusion [145].

C_2^a	C_2^b	C_2^c
$-\phi$	ϕ	ϕ
$\theta+\pi$	$\theta+\pi$	θ
ψ	$-\psi$	$\psi+\pi$

Table 4: Transformation of the Euler angles under the operation of two-fold rotations.

of these operators as

$$\begin{aligned} C_2^a|l\,m\,n\rangle &= (-1)^l|l\,m\,-n\rangle, \\ C_2^b|l\,m\,n\rangle &= (-1)^{l+n}|l\,m\,-n\rangle, \\ C_2^c|l\,m\,n\rangle &= (-1)^n|l\,m\,n\rangle. \end{aligned} \tag{6.34}$$

Let us introduce the functions (for $n \neq 0$) as in [147],

$$|l\,m\,n\,x\rangle = (-1)^{max\ n,m}|l\,m\,n\rangle, \tag{6.35}$$

Then we take the following combination (known as the Wang combination)

$$|l\,m\,n\,\gamma\rangle = 2^{-1/2}\left[|l\,m\,n\,x\rangle + (-1)^\gamma|l\,m\,-n\,x\rangle\right], \tag{6.36}$$

where $\gamma = 0$ (even) and 1 (odd). Furthermore, for $n = 0$ only $\gamma = 0$ exists, i.e.,

$$|l\,m\,0\,0\rangle = |l\,m\,0\,x\rangle. \tag{6.37}$$

One can show that

$$\begin{aligned} C_2^a|l\,m\,n\,\gamma\rangle &= (-1)^{l+\gamma}|l\,m\,n\,\gamma\rangle, \\ C_2^b|l\,m\,n\,\gamma\rangle &= (-1)^{l+\gamma+n}|l\,m\,n\,\gamma\rangle, \\ C_2^c|l\,m\,n\,\gamma\rangle &= (-1)^n|l\,m\,n\,\gamma\rangle. \end{aligned} \tag{6.38}$$

Thus, the states $|l\,m\,n\,\gamma\rangle$ are simultaneous eigenstates of the C_2^a, C_2^b, C_2^c operators. The symmetry species (or the representation classes) of the eigenstates depend on the parities of n and $l+\gamma$, as shown in the Table below, where 'e' denotes the even values and 'o' denotes the odd values.

Symmetry species	Parity of n	Parity of $l+\gamma$
A	e	e
B_a	o	e
B_b	o	o
B_c	e	o

Finally, instead of (6.29), we can expand the asymmetric top eigenstates in terms of $|l\,m\,n\,\gamma\rangle$

$$|l\,m\,\gamma\rangle = \sum_n a^l_{mn,\gamma} |l\,m\,n\,\gamma\rangle. \tag{6.39}$$

In this case, the secular equation takes the form

$$\det|H_{nn',\gamma} - E\delta_{nn'}| = 0. \tag{6.40}$$

Hence, expanding the eigenstates of the asymmetric top using the basis $|l\,m\,n\,\gamma\rangle$ leads to the secular equation breaking down into four lower-degree equations, each corresponding to one of the four possible symmetry species (associated with the symmetry representations) of the eigenstates.

6.3 "Ideal" tops

As mentioned in the introduction of this chapter, the solution to the second-order equation for the Dirac spinor field in the fixed Mixmaster universe corresponds to the eigenvalue equation of the Hamiltonian for an asymmetric "ideal" top [142].

In this section, we extend our discussion to the general Bianchi IX model, which encompasses the Mixmaster (or diagonal) model as a particular case.

6.3.1 Hamiltonian of the "ideal" top

Second-order equation

First, let us recall the second-order equation for the Dirac spinor field Ψ. As we discussed in Sec. 3.2, it is given by

$$\left[\nabla_\mu \nabla^\mu + R/4 - m^2\right] \Psi = 0, \tag{6.41}$$

where the covariant derivative has the form

$$\nabla_\mu = \partial_\mu + \Gamma_\mu, \tag{6.42}$$

with the partial derivatives expressed in terms of the invariant basis: $\partial_0 = e_0$ and $\partial_i = \sigma^j{}_i e_j$. The connection is given by

$$\Gamma_\mu = \frac{1}{2}\kappa_{\hat\alpha\hat\beta\mu}\Sigma^{\hat\alpha\hat\beta}, \quad \text{where} \quad \kappa_{\hat\alpha\hat\beta\mu} = \hat{h}^{\hat\rho}{}_\mu \kappa_{\hat\alpha\hat\beta\hat\rho}. \tag{6.43}$$

Let us also recall the relation (3.103), which can be rewritten as

$$\frac{R}{4} = \frac{1}{8}R_{\mu\nu\lambda\sigma}\gamma^\mu\gamma^\nu\gamma^\lambda\gamma^\sigma = \frac{1}{2}R_{\mu\nu\lambda\sigma}\Sigma^{\mu\nu}\Sigma^{\lambda\sigma}, \tag{6.44}$$

where we introduced $\Sigma^{\mu\nu}$, defined by

$$\Sigma^{\mu\nu} = \frac{1}{4}[\gamma^\mu, \gamma^\nu]. \tag{6.45}$$

Since $\gamma^\mu = \hat{h}_{\hat{\alpha}}{}^{\mu}\gamma^{\hat{\alpha}}$, we can express $\Sigma^{\mu\nu}$ in terms of the Lorentz generators $\Sigma^{\hat{\alpha}\hat{\beta}}$ as follows:

$$\Sigma^{\mu\nu} = \frac{1}{4}[\hat{h}_{\hat{\alpha}}{}^{\mu}\gamma^{\hat{\alpha}}, \hat{h}_{\hat{\beta}}{}^{\nu}\gamma^{\hat{\beta}}] = \hat{h}_{\hat{\alpha}}{}^{\mu}\hat{h}_{\hat{\beta}}{}^{\nu}\Sigma^{\hat{\alpha}\hat{\beta}}. \tag{6.46}$$

We can write the Dirac spinor Ψ via two bispinors

$$\Psi = \begin{pmatrix} \Psi_L \\ \Psi_R \end{pmatrix}, \tag{6.47}$$

and by substituting it into (6.41), we can separate the second-order equation for each bispinor. Hence, the second-order equation for the left-handed and right-handed spinors is given by

$$\left[\nabla_\mu\nabla^\mu + \frac{1}{2}R_{\mu\nu\lambda\sigma}\Sigma^{\mu\nu}_{L,R}\Sigma^{\lambda\sigma}_{L,R} - m^2\right]\Psi_{L,R} = 0, \tag{6.48}$$

where

$$\Sigma^{\mu\nu}_{L,R} = \hat{h}_{\hat{\alpha}}{}^{\mu}\hat{h}_{\hat{\beta}}{}^{\nu}\Sigma^{\hat{\alpha}\hat{\beta}}_{L,R}, \tag{6.49}$$

and $\Sigma^{\hat{\alpha}\hat{\beta}}_{L,R}$ are generators of the Lorentz group for $(\frac{1}{2}, 0)$ and $(0, \frac{1}{2})$ representations, respectively (see, e.g., Srednicki [112] for details).

Considering a fixed general Bianchi IX model, all time-dependent parameters α, $\beta_\pm$ and $\omega^i{}_j$ are set to constants. Since the generators $\Sigma^{\hat{\alpha}\hat{\beta}}_{L,R}$ are proportional to $j_i = \frac{\sigma_i}{2}$ spin angular momentum operators, it has been shown in [142] that

$$\frac{1}{2}R_{\mu\nu\lambda\sigma}\Sigma^{\mu\nu}_{L,R}\Sigma^{\lambda\sigma}_{L,R} = \sum_i c_i \tilde{j}_i^2, \tag{6.50}$$

where c_i are constants that can be determined through careful calculations. This is a general form to express the proportionality.

Next, let us consider the first term of the second-order equation, which for the $N_i = 0$ gauge, simplifies to

$$\nabla_\mu\nabla^\mu = g^{\mu\nu}\nabla_\mu\nabla_\nu = -\frac{1}{N(t)}\partial_t^2 + g^{ij}\nabla_i\nabla_j, \tag{6.51}$$

where the three-metric g^{ij} is given in a coordinate basis. Let us relate it to the three-metric in the invariant basis $\{e_i\}$. Using the relations (2.28), we can write

$$dl^2 = g_{ij}dx^i dx^j = g_{ij}\sigma^i{}_a\sigma^j{}_b\sigma^a\sigma^b = h_{ab}\,\sigma^a\sigma^b. \tag{6.52}$$

Furthermore, the inverse three-metric in coordinate basis then is given by $g^{ij} = h^{ab}{\sigma_a}^i{\sigma_b}^j$, where the inverse three-metric of Bianchi IX has the form

$$h^{ab} = R^a{}_m R^b{}_n \bar{h}^{mn}, \tag{6.53}$$

with

$$\bar{h}^{mn} = (b^k b^l)^{-1}\delta^{mn}, \quad k = m, \quad l = n. \tag{6.54}$$

The explicit forms of functions b^k are give in (4.10).

Let us consider the spatial part of (6.51). Using the relations obtained above, we can write

$$g^{ij}\nabla_i\nabla_j = h^{ab}{\sigma_a}^i{\sigma_b}^j(\partial_i\partial_j + \partial_i\,\Gamma_j + \Gamma_i\,\partial_j + \Gamma_i\Gamma_j). \tag{6.55}$$

Substituting the inverse three-metric and using $e_a = {\sigma_a}^i\partial_i$, we obtain

$$g^{ij}\nabla_i\nabla_j = R^a{}_m R^b{}_n \bar{h}^{mn}(e_a e_b + e_a\,{\sigma_b}^j\Gamma_j + {\sigma_a}^i\Gamma_i\,e_b + {\sigma_a}^i{\sigma_b}^j\Gamma_i\Gamma_j). \tag{6.56}$$

Let us analyze the terms inside the brackets separately:

- The first term simplifies to

$$R^a{}_m R^b{}_n \bar{h}^{mn} e_a e_b = R^a{}_m R^b{}_n (b^k b^l)^{-1}\delta^{mn} e_a e_b = \sum_i e^{-\tilde{\beta}_i}\tilde{e}_i^2, \tag{6.57}$$

  where we have used the relation of the left-invariant and right-invariant bases, i.e., $\tilde{e}_m = R^a{}_m e_a$. Furthermore, since the left-invariant basis is related to the space-fixed angular momentum by (5.54), it is easy to notice that the above term is proportional to $\tilde{L}_i^2$. So, let us write

$$R^a{}_m R^b{}_n \bar{h}^{mn} e_a e_b = \sum_i \tilde{\rho}_i \tilde{L}_i^2, \tag{6.58}$$

  where $\tilde{\rho}_i$ are again constants. Note, that for the diagonal case the first term takes the form

$$\bar{h}^{mn} e_m e_n = (b^k b^l)^{-1}\delta^{mn} e_m e_n = \sum_i e^{-\tilde{\beta}_i} e_i^2 = \sum_i \rho_i L_i^2, \tag{6.59}$$

  where $\rho_i = -\tilde{\rho}_i$ and L_i are the body-fixed angular momentum components.

- Next, let us consider the last term in the brackets. For the covariant derivative acting on the $\psi_{L,R}$ we can introduce

$$\Gamma_i^{L,R} = \frac{1}{2}\kappa_{\hat{\alpha}\hat{\beta}i}\Sigma_{L,R}^{\hat{\alpha}\hat{\beta}} = \frac{1}{2}\hat{h}^{\hat{\rho}}{}_i\kappa_{\hat{\alpha}\hat{\beta}\hat{\rho}}\Sigma_{L,R}^{\hat{\alpha}\hat{\beta}} := A_i{}^{\hat{m}}j_{\hat{m}}, \tag{6.60}$$

Therefore, the last term in (6.56) is proportional to

$$R^a{}_m R^b{}_n \bar{h}^{mn}\sigma_a{}^i\sigma_b{}^j\Gamma_i\Gamma_j = \sum_i \tilde{\upsilon}_i\,\tilde{j}_i^2, \tag{6.61}$$

where spin angular momentum components in space-fixed frame, denoted by $\tilde{j}_i$ are related to the components in body-fixed frame as

$$\tilde{j}_i = R^m{}_i\, j_m. \tag{6.62}$$

For the diagonal case, we have

$$\bar{h}^{mn}\sigma_m{}^i\sigma_n{}^j\Gamma_i\Gamma_j = \sum_i \upsilon_i j_i^2. \tag{6.63}$$

- Finally, for terms $e_i\Gamma_j$ and $\Gamma_i e_j$ it is straightforward to show that

$$R^a{}_m R^b{}_n \bar{h}^{mn}(e_a\,\sigma_b{}^j\Gamma_j + \sigma_a{}^i\Gamma_i\,e_b) = \sum_i \xi_i\tilde{L}_i\tilde{j}_i, \tag{6.64}$$

where we used the fact that the orbital and spin angular momenta commute. This term corresponds to the spin-orbit coupling.

For the diagonal case, we get

$$\bar{h}^{mn}(e_m\,\sigma_n{}^j\Gamma_j + \sigma_m{}^i\Gamma_i\,e_n) = \sum_i \xi_i L_i j_i, \tag{6.65}$$

Moreover, we can introduce the total angular momentum J in the body-fixed frame and $\tilde{J}$ in the space-fixed frame as follows:

$$J_i = L_i + j_i, \quad \tilde{J}_i = \tilde{L}_i + \tilde{j}_i, \tag{6.66}$$

where the total angular momenta J and $\tilde{J}$ are related via the rotation matrices

$$\tilde{J}_i = R^m{}_i J_m. \tag{6.67}$$

The coupling term can be expressed in terms of the total angular momentum $\tilde{J}_i$

$$\tilde{L}_i \tilde{j}_i = \frac{1}{2}(\tilde{J}_i^2 - \tilde{L}_i^2 - \tilde{j}_i^2). \tag{6.68}$$

The same obviously holds in the body-fixed frame as well.

Hamiltonian

Let us substitute (6.50) and (6.56), with relations obtained above, into the second-order equation (6.48). Taking into account the separation of the temporal and spatial parts in (6.51), we get the Hamiltonian eigenvalue equation

$$H\psi_{L,R}(\psi,\theta,\phi) = (E^2 - m^2)\Psi_{L,R}(\psi,\theta,\phi), \tag{6.69}$$

with the eigenvalues of $E^2 - m^2$ and the Hamiltonian of the form

$$H = \sum_i \left(\tilde{\lambda}_i \tilde{L}_i^2 + \tilde{\mu}_i \tilde{j}_i^2 + \tilde{\nu}_i \tilde{J}_i^2 \right), \tag{6.70}$$

where $\tilde{\lambda}_i$, $\tilde{\mu}_i$, $\tilde{\nu}_i$ are constants.

For the diagonal Bianchi IX model, it will be expressed in terms of the body-fixed angular momenta, as derived in [142],

$$H = \sum_i \left(\lambda_i L_i^2 + \mu_i j_i^2 + \nu_i J_i^2 \right), \tag{6.71}$$

which is the Hamiltonian of an asymmetric top with an "intrinsic" spin, also known as an "ideal" asymmetric top.

Also, let us point out that for the symmetric "ideal" top we have

$$H = \lambda L^2 + \mu j^2 + \nu J^2, \tag{6.72}$$

where the coefficients of each angular momenta components are the same constants.

6.3.2 Symmetric "ideal" top

Body-fixed Hamiltonian

Let us note that the body-fixed Hamiltonian of the "ideal" symmetric top, given by (6.72), commutes with the operators J^2, $L^2 = \tilde{L}^2$, j^2, J_3 and $\tilde{L}_3$. The eigenstates of this Hamiltonian are the same as those obtained in Sec. 5.4.2 using a purely group-theoretical approach. As mentioned there, one can choose between two different bases. In Sec. 5.4.1, it was shown that the choice of a different basis is related to the selection of sets of operators that commute with the Hamiltonian:

- For the commuting set of the operators $L^2 = \tilde{L}^2$, j^2, L_3, j_3 and $\tilde{L}_3$, the eigenstates are

$$|l\,s; m\,(n-n_s)\,n_s\rangle = |l\,m\,(n-n_s)\rangle|s\,n_s\rangle, \tag{6.73}$$

  where $n_s = \pm\frac{1}{2}$. Hence, we have two independent basis vectors

  – $n_s = \frac{1}{2}$

$$\Big|l, m, n - \frac{1}{2}\Big\rangle\Big|\frac{1}{2}, \frac{1}{2}\Big\rangle = \begin{pmatrix} |l, m, n - \frac{1}{2}\rangle \\ 0 \end{pmatrix}, \tag{6.74}$$

  – $n_s = -\frac{1}{2}$

$$\Big|l, m, n + \frac{1}{2}\Big\rangle\Big|\frac{1}{2}, -\frac{1}{2}\Big\rangle = \begin{pmatrix} 0 \\ |l, m, n + \frac{1}{2}\rangle \end{pmatrix}. \tag{6.75}$$

- For the set of operators $J^2, L^2 = \tilde{L}^2, j^2, J_3, \tilde{L}_3$, the eigenstates are $|l\,s; j\,m\,n\rangle$, which can be expressed in terms of the previous eigenstate as follows

$$|l\,s; j\,m\,n\rangle = \sum_{n_s=\pm\frac{1}{2}} C^{jn}_{l,n-n_s;sn_s}|l, m, n - n_s\rangle|s\,n_s\rangle, \tag{6.76}$$

  where $j = l \pm \frac{1}{2}$. As we obtained in (5.96), the eigenvectors then explicitly have the form

$$|j\,m\,n\rangle \equiv \Big|l \pm \frac{1}{2}, m\,n\Big\rangle = \frac{1}{\sqrt{2l+1}} \begin{pmatrix} \pm\sqrt{l \pm n + \frac{1}{2}}|l, m, n - \frac{1}{2}\rangle \\ \sqrt{l \mp n + \frac{1}{2}}|l, m, n + \frac{1}{2}\rangle \end{pmatrix}. \tag{6.77}$$

Thus, any bispinor on a symmetric top can be expanded using the obtained eigenvectors, with the choice of either of the two bases for the expansion.

Space-fixed Hamiltonian

The Hamiltonian of the "ideal" symmetric top, expressed in terms of the space-fixed angular momentum operator, reads

$$H = \tilde{\lambda}\tilde{L}^2 + \tilde{\mu}\tilde{j}^2 + \tilde{\nu}\tilde{J}^2. \tag{6.78}$$

In this case, the Hamiltonian commutes with the operators $\tilde{J}^2$, $L^2 = \tilde{L}^2$, $\tilde{j}^2$, $\tilde{J}_3$ and L_3. Following the same steps as before, it is apparent that the eigenbasis of the space-fixed Hamiltonian can be obtained by simply exchanging the quantum numbers m and n. Thus, the two eigenstates are given by:

- For the commuting set of operators $L^2 = \tilde{L}^2$, $\tilde{j}^2$, $\tilde{L}_3$, $\tilde{j}_3$ and L_3, the eigenstates are
$$|l\, s; (m - m_s)\, n\rangle = |l\, (m - m_s)\, n\rangle|s\, m_s\rangle, \tag{6.79}$$
where $m_s = \pm\frac{1}{2}$. Then the eigenvectors take the explicit form
  - $m_s = \frac{1}{2}$
$$\left|l, m - \frac{1}{2}, n\right\rangle\left|\frac{1}{2}, \frac{1}{2}\right\rangle = \begin{pmatrix} |l, m - \frac{1}{2}, n\rangle \\ 0 \end{pmatrix}, \tag{6.80}$$
  - $m_s = -\frac{1}{2}$
$$\left|l, m + \frac{1}{2}, n\right\rangle\left|\frac{1}{2}, -\frac{1}{2}\right\rangle = \begin{pmatrix} 0 \\ |l, m + \frac{1}{2}, n\rangle \end{pmatrix}. \tag{6.81}$$

- For the set $\tilde{J}^2, L^2 = \tilde{L}^2, \tilde{j}^2, \tilde{J}_3, L_3$, the eigenstates are
$$|l\, s; j\, m\, n\rangle = \sum_{m_s = \pm\frac{1}{2}} C^{jm}_{l,m-m_s;sm_s}|l, m - m_s, n\rangle|s\, m_s\rangle, \tag{6.82}$$
which has the following explicit form
$$|j\, m\, n\rangle \equiv \left|l \pm \frac{1}{2}, m\, n\right\rangle = \frac{1}{\sqrt{2l+1}}\begin{pmatrix} \pm\sqrt{l \pm m + \frac{1}{2}}|l, m - \frac{1}{2}, n\rangle \\ \sqrt{l \mp m + \frac{1}{2}}|l, m + \frac{1}{2}, n\rangle \end{pmatrix}. \tag{6.83}$$

6.3.3 Asymmetric "ideal" top

Body-fixed Hamiltonian

The Hamiltonian of the asymmetric "ideal" top (6.71) commutes with the operators $L^2 = \tilde{L}^2, j^2, J^2, \tilde{L}_3$; however, unlike the symmetric "ideal" top, it doesn't commute with the operators L_3, j_3, J_3. Hence, n is no longer a good quantum number. It has been shown in [142] that similar to the asymmetric top, the eigenbasis of the asymmetric "ideal" top can be expressed as a linear combination of the eigenbasis of the symmetric "ideal top".

First, to be able to separately discuss the spinor components, let us introduce a spinor index μ, which takes values $\mu = 1, 2$. Thus, recalling the eigenstates of the symmetric "ideal" top, for each spinor component it can be written as follows:

- For the basis (6.76) of the symmetric ideal top, by introducing the spinor index, we have

$$\Big|j\,m\,n\Big\rangle_\mu = \sum_{j=l\pm\frac{1}{2}} C^{j,n}_{l,n+\frac{(-1)^\mu}{2};\frac{1}{2},\frac{(-1)^\mu}{2}} \Big|l, m, n + \frac{(-1)^\mu}{2}\Big\rangle_\mu . \tag{6.84}$$

  Therefore, the eigenstates of the asymmetric top (for each spinor component) can be expanded as

$$\Big|j\,m\Big\rangle_\mu = \sum_n a^j_{mn} \Big|j\,m\,n\Big\rangle_\mu . \tag{6.85}$$

  - For $\mu = 1$, it reads

$$\Big|j\,m\Big\rangle_1 = \sum_n a^j_{mn} \Big|j\,m\,n\Big\rangle_\mu = \pm \sum_n a^{l\pm\frac{1}{2}}_{mn} \left(\frac{\sqrt{l \pm n + \frac{1}{2}}}{\sqrt{2l+1}} \Big|l, m, n - \frac{1}{2}\Big\rangle \right), \tag{6.86}$$

  - For $\mu = 2$, we have

$$\Big|j\,m\Big\rangle_2 = \sum_n a^j_{mn} \Big|j\,m\,n\Big\rangle_2 = \sum_n a^{l\pm\frac{1}{2}}_{mn} \left(\frac{\sqrt{l \mp n + \frac{1}{2}}}{\sqrt{2l+1}} \Big|l, m, n + \frac{1}{2}\Big\rangle \right). \tag{6.87}$$

- For the basis (6.79), each spinor component can be expanded as

$$\Big|l\,s; m\Big\rangle_\mu = \sum_n a^l_{mn} \Big|l, m, n + \frac{(-1)^\mu}{2}\Big\rangle_\mu . \tag{6.88}$$

Space-fixed Hamiltonian

The space-fixed Hamiltonian (6.70) commutes with the operators $\tilde{J}^2$, $L^2 = \tilde{L}^2$, $\tilde{j}^2$, and L_3. It does no longer commute with the operators $\tilde{J}_3$, $\tilde{L}_3$ and $\tilde{j}_3$. Therefore, we have to sum over m quantum number.

Thus, we can expand the spinor field as follows:

- For the basis (6.82) of symmetric ideal top, introducing the spinor index μ, we have

$$\left|j\,m\,n\right\rangle_\mu = \sum_{j=l\pm\frac{1}{2}} C^{j,m}_{l,m+\frac{(-1)^\mu}{2};\frac{1}{2},\frac{(-1)^\mu}{2}} \left|l, m+\frac{(-1)^\mu}{2}, n\right\rangle_\mu. \tag{6.89}$$

  The eigenstates of the asymmetric top Hamiltonian can be given by

$$\left|j\,n\right\rangle_\mu = \sum_m \tilde{a}^j_{mn} \left|j\,m\,n\right\rangle_\mu. \tag{6.90}$$

  - For $\mu = 1$:

$$\left|j\,n\right\rangle_1 = \sum_m \tilde{a}^j_{mn}\left|j\,m\,n\right\rangle_\mu = \pm\sum_m a^{l\pm\frac{1}{2}}_{mn}\left(\frac{\sqrt{l\pm m+\frac{1}{2}}}{\sqrt{2l+1}}\left|l, m-\frac{1}{2}, n\right\rangle\right), \tag{6.91}$$

  - For $\mu = 2$:

$$\left|j\,n\right\rangle_2 = \sum_m \tilde{a}^j_{mn}\left|j\,m\,n\right\rangle_2 = \sum_m \tilde{a}^{l\pm\frac{1}{2}}_{mn}\left(\frac{\sqrt{l\mp m+\frac{1}{2}}}{\sqrt{2l+1}}\left|l, m+\frac{1}{2}, n\right\rangle\right). \tag{6.92}$$

- For the basis (6.73), each spinor component can be expanded as

$$\left|l\,s; n\right\rangle_\mu = \sum_m \tilde{a}^l_{mn}\left|l, m+\frac{(-1)^\mu}{2}, n\right\rangle_\mu. \tag{6.93}$$

Symmetry adapted basis

Finally, one can also incorporate the symmetry properties of the "ideal" asymmetric top to expand the eigenstates in terms of the eigenstates of the symmetry group operators.

As discussed in Sec.6.1.2, the point group D_2 must be extended to its double point group D_2' in order to incorporate the spinors. The group elements are provided in Table 3.

Under the action of the operators C_2^a, C_2^b and C_2^c, the eigenstates $|j\,m\,n\rangle$ are transformed as[32]

$$\begin{aligned} C_2^a|j\,m\,n\rangle &= e^{i\pi j}|j\,m\,-n\rangle, \\ C_2^b|j\,m\,n\rangle &= e^{i\pi(j+n)}|j\,m\,-n\rangle, \\ C_2^c|j\,m\,n\rangle &= e^{i\pi n}|j\,m\,n\rangle. \end{aligned} \tag{6.94}$$

We introduce a basis $|j\,m\,n\,\gamma\rangle$, which generalizes (6.36) as follows:

$$|j\,m\,n\,\gamma\rangle = 2^{-1/2}\left[|j\,m\,n\,x\rangle + (-1)^\gamma|j\,m\,-n\,x\rangle\right]. \tag{6.95}$$

The transformations of these states under the action of the D_2 group operators are given by:

- For integral j:

$$\begin{aligned} C_2^a|j\,m\,n\,\gamma\rangle &= (-1)^{j+\gamma}|j\,m\,n\,\gamma\rangle, \\ C_2^b|j\,m\,n\,\gamma\rangle &= (-1)^{j+\gamma+n}|j\,m\,n\,\gamma\rangle, \\ C_2^c|j\,m\,n\,\gamma\rangle &= (-1)^{n}|j\,m\,n\,\gamma\rangle. \end{aligned} \tag{6.96}$$

  Hence, $|j\,m\,n\,\gamma\rangle$ for integral values of j are simultaneous eigenstates of the symmetry operators (as expected). Using these states as the basis for the expansion will split the Hamiltonian into four blocks, each corresponding to one of the four irreducible representations of the D_2 group.

- For half-integral j:

$$\begin{aligned} C_2^a|j\,m\,n\,\gamma\rangle &= (-1)^{\gamma}e^{i\pi j}|j\,m\,n\,\gamma\rangle, \\ C_2^b|j\,m\,n\,\gamma\rangle &= -e^{i\pi(j+n)}(-1)^{\gamma}|j\,m\,n\,-\gamma\rangle, \\ C_2^c|j\,m\,n\,\gamma\rangle &= e^{i\pi n}|j\,m\,n\,-\gamma\rangle. \end{aligned} \tag{6.97}$$

Using the above states as a basis for the expansion, it has been shown that the Hamiltonian splits into two blocks. Furthermore, the energy eigenvalues for each block are

[32] The eigenvalues are different from the one obtained in [142], because of different choices of Euler angles.

doubly degenerate [142].

The expansion of the asymmetric "ideal" top eigenstates in terms of these eigenstates can be written as

$$\left|j\,m\,\gamma\right\rangle_{\mu} = \sum_{n} a^{j}_{mn,\gamma}\left|j\,m\,n\,\gamma\right\rangle_{\mu}. \tag{6.98}$$

This expansion, however, is not a convenient choice for solving the Weyl and Dirac equations. The reason is that in these equations, the operators L_i and $\tilde{L}_i$ appear (instead of the squares of the operators, as in the second-order equation), and these do not commute with the operators C_2^a, C_2^b and C_2^c of the D_2 group.

Therefore, throughout the thesis, the expressions (6.88) and (6.93) will be used as the most convenient choice.

7 Spinors in a Bianchi IX universe

In this chapter, we present the solutions and quantization of the left-handed Weyl and Dirac field equations, as derived in Sec. 4.4, within the context of a fixed Bianchi IX universe.

The motivation for using a fixed background is twofold. First, as discussed in detail in Sec. 3.3.2, to address particle creation due to cosmic expansion, certain assumptions must be made to unambiguously define the "in" and "out" vacuum states. We assume that the universe is static in both the past (the "in" region) and the future (the "out" region), while evolving between these two regions. Although the assumption of a fixed background is an unrealistic approximation, it still allows us to explore the unique effects of spacetime anisotropy on particle energy spectrum and particle creation processes. This approach serves as a first step in understanding the general features of particle production in such spacetimes, which can be further refined in the future using the adiabatic approximation and other advancements based on the WKB approximation.

Second, given the highly complex dynamics of the Bianchi IX model, adopting a fixed background enables analytical solutions to the field equations. This approach allows us to isolate and examine the effects of background anisotropies and rotation on the particle and antiparticle energy spectrum. Notably, intriguing and novel effects emerge, particularly asymmetries in the energy spectrum between particles and antiparticles with different spin states. These effects are especially significant for Dirac spinors in a rotating universe and will be explored in detail in Sec. 7.2.2.

We begin by considering axisymmetric Bianchi IX models as a special case of the more general Bianchi IX model. This approach allows us to first investigate the key features and contributions of geometric aspects, starting from the simplest cases and gradually progressing to the most complicated. In Sec. 7.1, we will study Weyl spinors across the range of models mentioned earlier, addressing each one separately. Additionally, we will briefly discuss the phenomenon of fermion level crossing for Weyl neutrinos, which arises due to spectral asymmetry resulting from the anisotropic geometry. This effect was originally explored by G. W. Gibbons [61] in the context of the axisymmetric Bianchi IX model. In this work, we extend this analysis to a broader range of models. Finally, in Sec. 7.2, we will focus on the Dirac spinors across these models, which constitutes the primary focus of this thesis.

7.1 Weyl spinor

Let us recall the left-handed Weyl equation for the general Bianchi IX case, previously derived in Sec. 4.4 and given by eq. (4.103), which we explicitly present here:

$$\left[ih_{\hat{\alpha}}{}^{\mu}\bar{\sigma}^{\hat{\alpha}}e_{\mu} - \frac{3i}{2N}\dot{\alpha} - \frac{1}{2}F(\alpha,\beta_+,\beta_-) - \frac{1}{2N}\sum_{\hat{l}}\left(1+\frac{I_{\hat{l}}}{4}\right)^{\frac{1}{2}}\Omega_{\hat{l}}\sigma^{\hat{l}}\right]\Psi_L = 0. \tag{7.1}$$

In this section, we solve this equation for various universe models, each addressed in its respective subsection.

7.1.1 Axisymmetric Bianchi IX model

To obtain the axisymmetric Bianchi IX model, which is the simplest case, we impose an axial symmetry on the diagonal Bianchi IX model. This symmetry assumes that the spacetime remains invariant under rotations around a specific axis. This model, fixed in time, represents a symmetric top.

As briefly mentioned in Sec. 2.4, the line element for axisymmetric Bianchi IX model can be derived by setting $\beta_- = 0$ in the line element of diagonal Bianchi IX model, which implies $\beta_1 = \beta_2 = \beta_+$ and $\beta_3 = -2\beta_+$, as defined in eq. (4.9).

Hence, the line element of axisymmetric Bianchi IX has the form[33]

$$dl^2 = e^{2(\beta_+ + \alpha)}\left[\left(\sigma^1\right)^2 + \left(\sigma^2\right)^2\right] + e^{2(-2\beta_+ + \alpha)}\left(\sigma^3\right)^2. \tag{7.2}$$

In this case, the inverse vierbein obtained in (4.21) for the general Bianchi IX model simplifies to

$$h_{\hat{i}}{}^{i} = (b^k)^{-1}\delta^{i}{}_{\hat{i}}, \quad h_{\hat{0}}{}^{0} = \frac{1}{N}, \quad h_{\hat{0}}{}^{i} = 0, \quad h_{\hat{i}}{}^{0} = 0, \quad k = \hat{i}. \tag{7.3}$$

Furthermore, to obtain the left-handed Weyl equation for the axisymmetric Bianchi IX model, we must drop the rotational contributions $\propto \Omega_{\hat{l}}$ in eq. (7.1). Additionally, it is more convenient to carry out the calculations in conformal time, which can be achieved by substituting $N = e^{\alpha}$.

Thus, the left-handed Weyl equation in the axisymmetric Bianchi IX model takes the form

$$\left[i\bar{\sigma}^{\hat{0}}\partial_{\eta} + ie^{-(\beta_{\hat{i}}+\alpha)}\bar{\sigma}^{\hat{i}}e_{\hat{i}} - i\frac{3}{2}\alpha' - \frac{1}{2}\tilde{F}(\alpha,\beta_+)\right]\Psi_L = 0, \tag{7.4}$$

where we introduced a new function by setting $\beta_- = 0$ in $F(\alpha,\beta_+,\beta_-)$, as defined in

[33]Note that σ^i here refers to the one-forms, while the Pauli matrices are denoted by $\sigma^{\hat{i}}$. These should not be confused.

(4.79), i.e.

$$\tilde{F}(\alpha, \beta_+) := F(\alpha, \beta_+, \beta_- = 0) = \frac{1}{2} e^{-\alpha} \left[e^{-4\beta_+} + 2e^{2\beta_+} \right]. \tag{7.5}$$

Solutions in the fixed background

We take β_+ and α as constants given at the specific moment of time. Recalling the notation in (3.8), where $\bar{\sigma}^{\hat{0}} = I$ and $\bar{\sigma}^{\hat{i}} = -\sigma^{\hat{i}}$, the equation for the fixed background takes the form

$$i\partial_\eta \Psi_L = \left[ie^{-(\beta_{\hat{i}}+\alpha)} \sigma^{\hat{i}} e_{\hat{i}} + \frac{1}{2} \tilde{F}(\alpha, \beta_+) \right] \Psi_L. \tag{7.6}$$

In a fixed spacetime, the absence of time dependence in the metric allows for the separation of variables in the field equations. Thus, by separating the temporal and spatial variables, we can look for solutions of the form

$$\Psi_L(\eta, \psi, \theta, \phi) = N(\eta) \Xi(\psi, \theta, \phi), \tag{7.7}$$

where $N(\eta)$ is a function of time and $\Xi(\psi, \theta, \phi)$ is a spinor. Substituting this into the equation and gathering the temporal and spatial parts on different sides, we obtain

$$i \frac{(\partial_\eta N(\eta))}{N(\eta)} = \frac{1}{\Xi(\psi, \theta, \phi)} \left[ie^{-(\beta_{\hat{i}}+\alpha)} \sigma^{\hat{i}} e_{\hat{i}} + \frac{1}{2} \tilde{F}(\alpha, \beta_+) \right] \Xi(\psi, \theta, \phi). \tag{7.8}$$

Setting each side equal to a constant E, for the temporal part we get

$$i \frac{(\partial_\eta N(\eta))}{N(\eta)} = E \quad \rightarrow \quad N(\eta) = e^{-iE\eta}, \tag{7.9}$$

and the spatial part leads to

$$\left[ie^{-(\beta_{\hat{i}}+\alpha)} \sigma^{\hat{i}} e_{\hat{i}} + \frac{1}{2} \tilde{F}(\alpha, \beta_+) \right] \Xi(\psi, \theta, \phi) = E \, \Xi(\psi, \theta, \phi). \tag{7.10}$$

Note, this is the eigenvalue equation of the operator

$$D_\eta := \left[ie^{-(\beta_{\hat{i}}+\alpha)} \sigma^{\hat{i}} e_{\hat{i}} + \frac{1}{2} \tilde{F}(\alpha, \beta_+) \right]. \tag{7.11}$$

Recalling the connection between the right-invariant angular momentum and the invariant basis, as given in (5.54), i.e.,

$$L_i = ie_i, \tag{7.12}$$

we obtain the following relations

$$i(e_{\hat{1}} - ie_{\hat{2}}) = L_{\hat{1}} - iL_{\hat{2}} = L_- \quad \text{and} \quad i(e_{\hat{1}} + ie_{\hat{2}}) = L_{\hat{1}} + iL_{\hat{2}} = L_+. \tag{7.13}$$

Then, the equation (7.10) can be written in terms of the angular momentum operators as follows:

$$\begin{pmatrix} e^{2\beta_+-\alpha}L_{\hat{3}}+\frac{1}{2}\tilde{F}(\alpha,\beta_+) & e^{-(\beta_++\alpha)}L_- \\ e^{-(\beta_++\alpha)}L_+ & -e^{2\beta_+-\alpha}L_{\hat{3}}+\frac{1}{2}\tilde{F}(\alpha,\beta_+) \end{pmatrix}\Xi = E\,\Xi. \tag{7.14}$$

In Sec. 6.3.2, we discussed the eigenbasis of the symmetric "ideal" top in detail. As mentioned, the spinor field on the symmetric top can be expanded using two possible choices of the eigenbases, given by equations (6.73) and (6.76).

Namely, the spinor Ξ can be expanded either as

$$\Xi_{nlm} = \begin{pmatrix} w_1 \\ w_2 \end{pmatrix} = \frac{1}{\sqrt{2l+1}}\begin{pmatrix} \left(f^1_{nlm}\sqrt{l+n+\frac{1}{2}} - f^2_{nlm}\sqrt{l-n+\frac{1}{2}}\right)|l,m,n-\frac{1}{2}\rangle \\ \left(f^1_{nlm}\sqrt{l-n+\frac{1}{2}} + f^2_{nlm}\sqrt{l+n+\frac{1}{2}}\right)|l,m,n+\frac{1}{2}\rangle \end{pmatrix}, \tag{7.15}$$

or

$$\Xi_{nlm} = \begin{pmatrix} w_1 \\ w_2 \end{pmatrix} = \begin{pmatrix} f^1_{nlm}|l,m,n-\frac{1}{2}\rangle \\ f^2_{nlm}|l,m,n+\frac{1}{2}\rangle \end{pmatrix}. \tag{7.16}$$

Here, f^1_{nlm}, f^2_{nlm} are the expansion coefficients and $|l\,m\,n\rangle$ are the eigenfunctions of the operators L^2, L_3, and $\tilde{L}_3$; see Sec. 6.2.1.

We will proceed with the second expansion, as it is more convenient for our calculations. Recalling the eigenvalue equations (6.26), we can calculate the following terms,

$$\begin{aligned} L_+w_1 &= f^1_{nlm}\,L_+\left|l,m,n-\frac{1}{2}\right\rangle = f^1_{nlm}\alpha_{n+\frac{1}{2}}\left|l,m,n+\frac{1}{2}\right\rangle, \\ L_-w_2 &= f^2_{nlm}\,L_-\left|l,m,n+\frac{1}{2}\right\rangle = f^2_{nlm}\alpha_{n+\frac{1}{2}}\left|l,m,n-\frac{1}{2}\right\rangle, \\ L_{\hat{3}}w_{1,2} &= f^{1,2}_{nlm}\left(n\mp\frac{1}{2}\right)\left|l,m,n\mp\frac{1}{2}\right\rangle, \end{aligned} \tag{7.17}$$

where $\alpha_n = \sqrt{(l+n)(l-n+1)}$, with $|m| \le l$ and $\left|n-\frac{1}{2}\right| \le l$ corresponding to $\left|l,m,n-\frac{1}{2}\right\rangle$, and $\left|n+\frac{1}{2}\right| \le l$ corresponding to $\left|l,m,n+\frac{1}{2}\right\rangle$.

The matrix equation (7.14) can be rewritten as two separate equations. Substituting the above results into these equations yields

$$\begin{aligned} \left[E-\frac{1}{2}\tilde{F}(\alpha,\beta_+)-e^{-(\beta_{\hat{3}}+\alpha)}\left(n-\frac{1}{2}\right)\right]f^1_{nlm} &= e^{-(\beta_{\hat{1}}+\alpha)}f^2_{nlm}\,\alpha_{n+\frac{1}{2}}, \\ \left[E-\frac{1}{2}\tilde{F}(\alpha,\beta_+)+e^{-(\beta_{\hat{3}}+\alpha)}\left(n+\frac{1}{2}\right)\right]f^2_{nlm} &= e^{-(\beta_{\hat{1}}+\alpha)}f^1_{nlm}\,\alpha_{n+\frac{1}{2}}. \end{aligned} \tag{7.18}$$

Energy eigenvalues

To calculate the energy eigenvalues, we divid in (7.18) one equation by the other. Then, simplifications lead to the following quadratic equation:

$$\begin{aligned} E^2 - \left(\tilde{F}(\alpha, \beta_+) - e^{2\beta_+ - \alpha}\right) E + \frac{1}{4}\tilde{F}^2(\alpha, \beta_+) - \frac{1}{2}\tilde{F}(\alpha, \beta_+) e^{2\beta_+ - \alpha} \\ - e^{2(2\beta_+ - \alpha)}\left(n^2 - \frac{1}{4}\right) - e^{-2(\beta_+ + \alpha)}\alpha^2_{n+\frac{1}{2}} = 0, \end{aligned} \tag{7.19}$$

which has two solutions given by

$$E_{1,2} = e^{-(\beta_+ + \alpha)}\left\{\frac{1}{4}e^{-3\beta_+} \pm \left[n^2 e^{6\beta_+} + \alpha^2_{n+\frac{1}{2}}\right]^{1/2}\right\}. \tag{7.20}$$

For convenience, let us introduce functions

$$\tilde{G}(\alpha, \beta_+) := \frac{1}{2}\left(\tilde{F}(\alpha, \beta_+) - e^{2\beta_+ - \alpha}\right) = \frac{1}{4}e^{-4\beta_+ - \alpha}, \tag{7.21}$$

and

$$\tilde{\omega}_{nl}(\alpha, \beta_+) = e^{-(\beta_+ + \alpha)}\left[n^2 e^{6\beta_+} + \alpha^2_{n+\frac{1}{2}}\right]^{1/2}, \tag{7.22}$$

Hence, the energy eigenvalues can be written

$$\begin{aligned} E_1 &= \tilde{G}(\alpha, \beta_+) - \tilde{\omega}_{nl}(\alpha, \beta_+), \\ E_2 &= \tilde{G}(\alpha, \beta_+) + \tilde{\omega}_{nl}(\alpha, \beta_+). \end{aligned} \tag{7.23}$$

The negative eigenvalues correspond to neutrinos, representing positive-frequency solutions, while the positive eigenvalues correspond to antineutrinos (see Sec. 3.1.1). One can observe that, due to the anisotropic contribution, there is spectral asymmetry, which is not present in isotropic models.

In addition, as the universe evolves and approaches isotropy (explained in detail in Sec. 4.2.1), i.e., $\beta_+ \to 0$, the energy eigenvalues simplify to:

$$E_{1,2} \to e^{-\alpha}\left\{\frac{1}{4} \pm \left[n^2 + \alpha^2_{n+\frac{1}{2}}\right]^{1/2}\right\}. \tag{7.24}$$

It is easy to observe that for certain modes, where both energy eigenvalues (7.23) are initially positive, the eigenvalue E_1 can become negative after the damping of anisotropies. As explained by G. W. Gibbons in [61], this is the cause of the fermion level crossing. We will explore this phenomenon further, along with other universe models discussed in this chapter, in Sec. 7.1.5.

Next, let us also present the eigenspinors, which were obtained from the equations (7.18) for the energy eigenvalues (7.20), and are given by the following expression[34]:

$$\Xi^{1,2}_{nlm} = \begin{pmatrix} w_1 \\ w_2 \end{pmatrix} = \begin{pmatrix} e^{-(\beta_+ + \alpha)} \left\{ n e^{3\beta_+} \pm \left[n^2 e^{6\beta_+} + \alpha^2_{n+\frac{1}{2}} \right]^{1/2} \right\} |l, m, n - \frac{1}{2}\rangle \\ \alpha_{n+\frac{1}{2}} e^{-(\beta_+ + \alpha)} |l, m, n + \frac{1}{2}\rangle \end{pmatrix} . \tag{7.25}$$

It should be noted that the energy eigenvalues (7.23) are proportional to n^2, which indicates that the energy levels are degenerate. However, in the case of rotating axisymmetric Bianchi IX, we will see that this degeneracy is lifted.

General solution

Finally, the general solution can be expressed as follows:

$$\Psi_L(\eta, \psi, \theta, \phi) = \sum_{n\,l\,m} \left[a^1_{nlm} \Xi^1_{nlm} e^{-iE_1\eta} + a^2_{nlm} \Xi^2_{nlm} e^{-iE_2\eta} \right] , \tag{7.26}$$

where a^1_{nlm} and a^2_{nlm} are the expansion coefficients. Note that, since there are no distinct positive and negative energy eigenvalues at this stage, one cannot yet identify these coefficients as creation and annihilation operators. More details on this will be presented in Sec. 7.1.5.

7.1.2 Rotating axisymmetric Bianchi IX model

We can consider a more general case: a rotating axisymmetric Bianchi IX model. Due to its axial symmetry, this model can exhibit rotation only about one axis. Hence, the three-metric for this model can be obtained by setting $\beta_- = 0$ in the three-metric of the symmetric Bianchi IX model, given by (2.21), i.e.,

$$h\big|_{\beta_-=0} = R^T_z(\phi) \bar{h}\big|_{\beta_-=0} R_z(\phi). \tag{7.27}$$

Then, the inverse vierbein can be given by

$$h_{\hat{i}}{}^{i} = (b^k)^{-1} R^i{}_{\hat{i}}(\phi), \quad h_{\hat{0}}{}^{0} = \frac{1}{N}, \quad h_{\hat{0}}{}^{i} = 0, \quad h_{\hat{i}}{}^{0} = 0, \quad k = \hat{i}, \tag{7.28}$$

where the matrix $R_z(\phi)$ is given by (5.5). Furthermore, in (7.1), we retain only Ω_3 (which corresponds to the rotation with the angle ϕ). Recalling the definition of the

[34] In the following sections, the eigenspinors will not be explicitly derived, as they are not required. However, they can be obtained in a similar manner to those presented here.

moments of inertia given by (4.44), we see that

$$I_3 = 4\sinh^2\left(2\sqrt{3}\beta_-\right) = 0. \tag{7.29}$$

Thus, the left-handed Weyl equation for the rotating axisymmetric Bianchi IX model takes the form

$$\left\{ie^{-\alpha}\bar{\sigma}^{\hat{0}}e_0 + ie^{-\alpha}e^{-\beta_k}R^i{}_{\hat{i}}\bar{\sigma}^{\hat{i}}e_i - \frac{3i}{2}\alpha' - \frac{1}{2}\tilde{F}(\alpha,\beta_+) - \frac{1}{2}e^{-\alpha}\Omega_{\hat{3}}\sigma^{\hat{3}}\right\}\Psi_L = 0. \tag{7.30}$$

Solutions in the fixed background

Considering α, β_+, and $\Omega_{\hat{3}}$ as constants, and recalling (3.8), the equation of motion takes the form

$$i\partial_\eta\Psi_L = \left\{ie^{-(\beta_k+\alpha)}R^i{}_{\hat{i}}\sigma^{\hat{i}}e_i + \frac{1}{2}\tilde{F}(\alpha,\beta_+) + \frac{1}{2}e^{-\alpha}\Omega_{\hat{3}}\sigma^{\hat{3}}\right\}\Psi_L. \tag{7.31}$$

By following the same steps as before and separating the temporal and spatial components as

$$\Psi_L(\eta,\psi,\theta,\phi) = N(\eta)\,\Xi(\psi,\theta,\phi), \tag{7.32}$$

we are led to the following equation for the spatial part,

$$\left\{ie^{-(\beta_k+\alpha)}R^i{}_{\hat{i}}\sigma^{\hat{i}}e_i + \frac{1}{2}\tilde{F}(\alpha,\beta_+) + \frac{1}{2}e^{-\alpha}\Omega_{\hat{3}}\sigma^{\hat{3}}\right\}\Xi(\psi,\theta,\phi) = E\,\Xi(\psi,\theta,\phi). \tag{7.33}$$

As in the previous section, $N(\eta)$ satisfies the equation (7.9).

Substituting the Pauli matrices explicitly, the equation becomes

$$\begin{pmatrix} E - \frac{1}{2}\tilde{F}(\alpha,\beta_+) - ie^{-\beta_{\hat{3}}-\alpha}R^i{}_{\hat{3}}e_i - \frac{1}{2}e^{-\alpha}\Omega_{\hat{3}} & -ie^{-\beta_{\hat{1}}-\alpha}\left(R^i{}_{\hat{1}} - iR^i{}_{\hat{2}}\right)e_i \\ -ie^{-\beta_{\hat{1}}-\alpha}\left(R^i{}_{\hat{1}} + iR^i{}_{\hat{2}}\right)e_i & E - \frac{1}{2}\tilde{F}(\alpha,\beta_+) + ie^{-\beta_{\hat{3}}-\alpha}R^i{}_{\hat{3}}e_i + \frac{1}{2}e^{-\alpha}\Omega_{\hat{3}} \end{pmatrix}\Xi = 0. \tag{7.34}$$

Furthermore, recalling the relation between the left- and right-invariant bases as given by (2.24), namely

$$\tilde{e}_j = R^i{}_j e_i, \tag{7.35}$$

and the relation between the space-fixed angular momentum and the left-invariant basis given by

$$\tilde{L}_i = -i\tilde{e}_i, \tag{7.36}$$

we can express the corresponding components in the matrix equation in terms of the space-fixed angular momentum components as follows

$$
\begin{aligned}
i\left(R^i{}_{\hat{1}} - iR^i{}_{\hat{2}}\right) e_i &= i(\tilde{e}_{\hat{1}} - i\tilde{e}_{\hat{2}}) = -\tilde{L}_-, \\
i\left(R^i{}_{\hat{1}} + iR^i{}_{\hat{2}}\right) e_i &= i(\tilde{e}_{\hat{1}} + i\tilde{e}_{\hat{2}}) = -\tilde{L}_+.
\end{aligned}
\tag{7.37}
$$

For convenience, let us introduce a parameter $l_{\hat{i}} = e^{-\beta_{\hat{i}}-\alpha}$. Thus, the equation (7.34) can be written as

$$
\begin{pmatrix}
E - \frac{1}{2}\tilde{F}(\alpha,\beta_+) + l_{\hat{3}}\tilde{L}_{\hat{3}} - \frac{1}{2}e^{-\alpha}\Omega_{\hat{3}} & l_{\hat{1}}\tilde{L}_- \\
l_{\hat{1}}\tilde{L}_+ & E - \frac{1}{2}\tilde{F}(\alpha,\beta_+) - l_{\hat{3}}\tilde{L}_{\hat{3}} + \frac{1}{2}e^{-\alpha}\Omega_{\hat{3}}
\end{pmatrix} \Xi = 0. \tag{7.38}
$$

The rotating axisymmetric Bianchi IX model corresponds to the symmetric "ideal" top, whose Hamiltonian is expressed in terms of space-fixed angular momentum operators (see Sec. 6.3.3). In this case, the spinor should be expanded in terms of the basis given by (6.79). Hence, here we have

$$
\Xi_{nlm} = \begin{pmatrix} w_1 \\ w_2 \end{pmatrix} = \begin{pmatrix} f^1_{nlm}|l, m-\frac{1}{2}, n\rangle \\ f^2_{nlm}|l, m+\frac{1}{2}, n\rangle \end{pmatrix}. \tag{7.39}
$$

Recalling the eigenvalue equations for space-fixed angular momentum $\tilde{L}$ given by (6.27), we can derive the following relations:

$$
\begin{aligned}
\tilde{L}_- w_2 &= f^2_{nlm}\tilde{L}_-|l, m+\frac{1}{2}, n\rangle = f^2_{nlm}\alpha_{m+\frac{1}{2}}|l, m-\frac{1}{2}, n\rangle, \\
\tilde{L}_{\hat{3}} w_1 &= f^1_{nlm}\tilde{L}_{\hat{3}}|l, m-\frac{1}{2}, n\rangle = (m-1/2)\, f^1_{nlm}|l, m-\frac{1}{2}, n\rangle, \\
\tilde{L}_+ w_1 &= f^1_{nlm}\tilde{L}_+|l, m-\frac{1}{2}, n\rangle = f^1_{nlm}\alpha_{m+\frac{1}{2}}|l, m+\frac{1}{2}, n\rangle, \\
\tilde{L}_{\hat{3}} w_2 &= f^2_{nlm}\tilde{L}_{\hat{3}}|l, m+\frac{1}{2}, n\rangle = (m+1/2)\, f^2_{nlm}|l, m+\frac{1}{2}, n\rangle.
\end{aligned}
\tag{7.40}
$$

Expressing the matrix equation as two separate equations and substituting the above results leads to

$$
\begin{aligned}
\left(E - \frac{1}{2}\tilde{F}(\alpha,\beta_+) - \frac{1}{2}e^{-\alpha}\Omega_{\hat{3}} + l_{\hat{3}}\,(m-1/2)\right) f^1_{nlm} &= -\alpha_{m+\frac{1}{2}}\, l_{\hat{1}} f^2_{nlm}, \\
\left(E - \frac{1}{2}\tilde{F}(\alpha,\beta_+) + \frac{1}{2}e^{-\alpha}\Omega_{\hat{3}} - l_{\hat{3}}\,(m+1/2)\right) f^2_{nlm} &= -\alpha_{m+\frac{1}{2}} l_{\hat{1}} f^1_{nlm}.
\end{aligned}
\tag{7.41}
$$

Energy eigenvalues

Next, by dividing one equation by the other, we obtain

$$
\left(E - \tfrac{1}{2}\tilde{F}(\alpha,\beta_+) + \tfrac{1}{2}e^{-\alpha}\Omega_{\hat{3}} - (m+1/2)\, l_{\hat{3}}\right)\left(E - \tfrac{1}{2}\tilde{F}(\alpha,\beta_+) - \tfrac{1}{2}e^{-\alpha}\Omega_{\hat{3}} + (m-1/2)\, l_{\hat{3}}\right) = \alpha^2_{m+\frac{1}{2}} l^2_{\hat{1}}. \tag{7.42}
$$

Simplifying the equation further and setting $\beta_{\hat{1}} = \beta_{\hat{2}} = \beta_+, \quad \beta_{\hat{3}} = -2\beta_+$, leads to

$$\begin{aligned} &E^2 - \left(\tilde{F}(\alpha,\beta_+) + e^{-\alpha}e^{2\beta_+}\right) E + \frac{1}{4}\tilde{F}^2(\alpha,\beta_+) + \frac{1}{2}\tilde{F}(\alpha,\beta_+)e^{-\alpha}e^{2\beta_+} \\ &- \left(m^2 - \frac{1}{4}\right) e^{-2\alpha}e^{4\beta_+} - e^{-2\alpha}e^{-2\beta_+}\alpha^2_{m+\frac{1}{2}} + me^{-2\alpha}e^{2\beta_+}\Omega_{\hat{3}} - \frac{1}{4}e^{-2\alpha}\Omega^2_{\hat{3}} = 0. \end{aligned} \tag{7.43}$$

Then, the solutions cen be given by

$$E_{1,2} = \frac{1}{2}\left(\tilde{F}(\alpha,\beta_+) + e^{-\alpha}e^{2\beta_+}\right) \pm e^{-(\beta_+ + \alpha)}\left[m^2e^{6\beta_+} + \alpha^2_{m+\frac{1}{2}} - me^{4\beta_+}\Omega_{\hat{3}} + \frac{1}{4}e^{2\beta_+}\Omega^2_{\hat{3}}\right]^{1/2}. \tag{7.44}$$

Let us introduce functions

$$\tilde{\omega}^{\text{rot}}_{ml}(\alpha,\beta_+,\Omega_{\hat{3}}) := e^{-(\beta_+ + \alpha)}\left[m^2e^{6\beta_+} + \alpha^2_{m+\frac{1}{2}} - me^{4\beta_+}\Omega_{\hat{3}} + \frac{1}{4}e^{2\beta_+}\Omega^2_{\hat{3}}\right]^{1/2} \tag{7.45}$$

and

$$\tilde{G}^{\text{rot}}(\alpha,\beta_+) = \frac{1}{2}\left(\tilde{F}(\alpha,\beta_+) + e^{-\alpha}e^{2\beta_+}\right), \tag{7.46}$$

Then, the energy eigenvalues can be written as:

$$\begin{aligned} E_1 &= \tilde{G}^{\text{rot}}(\alpha,\beta_+) - \tilde{\omega}^{\text{rot}}_{ml}(\alpha,\beta_+,\Omega_{\hat{3}}), \\ E_2 &= \tilde{G}^{\text{rot}}(\alpha,\beta_+) + \tilde{\omega}^{\text{rot}}_{ml}(\alpha,\beta_+,\Omega_{\hat{3}}). \end{aligned} \tag{7.47}$$

It is important to note that in this case, the degeneracy of the energy values is lifted due to Coriolis or Lense-Thirring forces[35]. As seen in the corresponding formula, modes with $m > 0$ are suppressed, while modes with $m < 0$ are enhanced due to the rotation of the space.

When the universe approaches a closed FLRW form, we have $\beta_+ \to 0$ and $\Omega_3 \to 0$. Then the energy eigenvalues become

$$E_{1,2} \to e^{-\alpha}\left\{\frac{5}{4} \pm \left[m^2 + \alpha^2_{m+\frac{1}{2}}\right]^{1/2}\right\}. \tag{7.48}$$

Finally, the general solution of the Weyl equation in a rotating axisymmetric Bianchi IX model has the same form as in (7.26), with the energy eigenvalues and spinor eigenstates specific to this model.

[35] A similar situation occurs in [148], where, instead of a spatial rotation, the authors consider a spacetime rotation, imposing additional conditions to prevent the formation of closed timelike world-lines.

7.1.3 Diagonal Bianchi IX model

The inverse vierbein given by (4.21) for Bianchi IX reads

$$h_{\hat{i}}{}^{i} = (b^k)^{-1}\delta^{i}{}_{\hat{i}}, \quad h_{\hat{0}}{}^{0} = \frac{1}{N}, \quad h_{\hat{0}}{}^{i} = 0, \quad h_{\hat{i}}{}^{0} = 0, \tag{7.49}$$

with

$$b^k = e^{\beta_k+\alpha}, \quad \text{where} \quad \beta_1 = \beta_+ + \sqrt{3}\beta_-, \quad \beta_2 = \beta_+ - \sqrt{3}\beta_-, \quad \beta_3 = -2\beta_+. \tag{7.50}$$

Thus, by dropping the rotational contributions in the left-handed Weyl equation (7.1), the equation for the diagonal Bianchi IX in conformal time takes the following form:

$$\left[i\bar{\sigma}^{\hat{0}}\partial_\eta + ie^{-(\beta_{\hat{i}}+\alpha)}\bar{\sigma}^{\hat{i}}e_{\hat{i}} - \frac{3i}{2}\alpha' - \frac{1}{2}F(\alpha,\beta_+,\beta_-)\right]\Psi_L = 0. \tag{7.51}$$

Solutions in the fixed background

Considering that α and β_+ are constants at a specific moment, and using (3.8), the equation takes the form

$$i\partial_\eta\Psi_L = \left[ie^{-(\beta_{\hat{i}}+\alpha)}\sigma^{\hat{i}}e_{\hat{i}} + \frac{1}{2}F(\alpha,\beta_+,\beta_-)\right]\Psi_L. \tag{7.52}$$

Separating the temporal and spatial parts as in (7.7), the equation for the spatial part reads

$$\left[ie^{-(\beta_{\hat{i}}+\alpha)}\sigma^{\hat{i}}e_{\hat{i}} + \frac{1}{2}F(\alpha,\beta_+,\beta_-)\right]\Xi(\psi,\theta,\phi) = E\,\Xi(\psi,\theta,\phi). \tag{7.53}$$

Substituting the Pauli matrices explicitly, we obtain

$$\begin{pmatrix} ie^{-\alpha}e^{-\beta_{\hat{3}}}e_{\hat{3}} + \frac{1}{2}F(\alpha,\beta_+,\beta_-) & ie^{-\alpha}(e^{-\beta_{\hat{1}}}e_{\hat{1}} - ie^{-\beta_{\hat{2}}}e_{\hat{2}}) \\ ie^{-\alpha}(e^{-\beta_{\hat{1}}}e_{\hat{1}} + ie^{-\beta_{\hat{2}}}e_{\hat{2}}) & -ie^{-\alpha}e^{-\beta_{\hat{3}}}e_{\hat{3}} + \frac{1}{2}F(\alpha,\beta_+,\beta_-) \end{pmatrix}\Xi = E\,\Xi. \tag{7.54}$$

Expressing the right-invariant basis in terms of body-fixed angular momentum operator and using the relations

$$L_{\hat{1}} = \frac{1}{2}\left(L_- + L_+\right), \quad L_{\hat{2}} = \frac{1}{2i}\left(L_+ - L_-\right), \tag{7.55}$$

the equation can be rewritten as

$$\begin{pmatrix} \frac{1}{2}F(\alpha,\beta_\pm) + l_{\hat{3}}L_{\hat{3}} & -\frac{l_{\hat{2}}-l_{\hat{1}}}{2}L_+ + \frac{l_{\hat{2}}+l_{\hat{1}}}{2}L_- \\ \frac{l_{\hat{2}}+l_{\hat{1}}}{2}L_+ - \frac{l_{\hat{2}}-l_{\hat{1}}}{2}L_- & \frac{1}{2}F(\alpha,\beta_\pm) - l_{\hat{3}}L_{\hat{3}} \end{pmatrix}\Xi = E\,\Xi. \tag{7.56}$$

In Chapter 6, we discussed that the fixed Mixmaster or diagonal Bianchi IX universe resembles an asymmetric top. Furthermore, in Sec. 6.3.3, we constructed the eigenbasis for the "ideal" asymmetric top, as given in (6.88). Thus, any spinor field on the asymmetric top can be expanded in terms of this basis. Therefore, for the spinor Ξ, we can write the following expansion,

$$\Xi_{ml} = \begin{pmatrix} w_1 \\ w_2 \end{pmatrix} = \sum_n a^l_{mn} \begin{pmatrix} f^1_{lm}|l, m, n - \frac{1}{2}\rangle \\ f^2_{lm}|l, m, n + \frac{1}{2}\rangle \end{pmatrix}. \tag{7.57}$$

The coefficients a^l_{mn} can be determined by solving the Hamiltonian eigenvalue equation for the asymmetric "ideal" top, given by (6.69), which corresponds to the Mixmaster universe for specific values of α, β_+, and β_-. The explicit calculations of the coefficients are extremely complicated and may even be intractable. Therefore, we will not carry them out here. Instead, we will focus on obtaining the energy eigenvalues, expressed in terms of these general coefficients, in order to examine the main structure and contributions.

The matrix equation (7.56), expressed as two separate equations, can be written as

$$\left(\frac{1}{2}F(\alpha, \beta_\pm) + l_{\hat{3}}L_{\hat{3}}\right) w_1 + \left(\frac{l_{\hat{2}} + l_{\hat{1}}}{2}\, L_- - \frac{l_{\hat{2}} - l_{\hat{1}}}{2}\, L_+\right) w_2 = E w_1, \tag{7.58}$$

$$\left(\frac{l_{\hat{2}} + l_{\hat{1}}}{2}\, L_+ - \frac{l_{\hat{2}} - l_{\hat{1}}}{2}\, L_-\right) w_1 + \left(\frac{1}{2}F(\alpha, \beta_\pm) - l_{\hat{3}}L_{\hat{3}}\right) w_2 = E w_2. \tag{7.59}$$

Recalling the eigenvalue equations (6.26), we can calculate the following terms:

- For the L_3 operator acting on w_1 and w_2:

$$L_3 \sum_n a^l_{mn}\left|l, m, n + \frac{(-1)^\mu}{2}\right\rangle = \sum_n a^l_{mn}\left(n + \frac{(-1)^\mu}{2}\right)\left|l, m, n + \frac{(-1)^\mu}{2}\right\rangle \tag{7.60}$$

- For the L_+ operator acting on w_1 and w_2:

$$L_+ \sum_n a^l_{mn}\left|l, m, n + \frac{(-1)^\mu}{2}\right\rangle = \sum_n a^l_{mn}\alpha_{n + \frac{(-1)^\mu}{2} + 1}\left|l, m, n + \frac{(-1)^\mu}{2} + 1\right\rangle \tag{7.61}$$

  – $\mu = 1$

$$L_+ \sum_n a^l_{mn}\left|l, m, n - \frac{1}{2}\right\rangle = \sum_n a^l_{mn}\alpha_{n+\frac{1}{2}}\left|l, m, n + \frac{1}{2}\right\rangle \tag{7.62}$$

– $\mu = 2$

$$
\begin{aligned}
L_+ \sum_n a^l_{mn} \Big| l, m, n + \frac{1}{2} \Big\rangle &= \sum_n a^l_{mn} \alpha_{n+\frac{3}{2}} \Big| l, m, n + \frac{1}{2} + 1 \Big\rangle \\
&= \sum_k a^l_{m,(k-1)} \alpha_{k+\frac{1}{2}} \Big| l, m, k + \frac{1}{2} \Big\rangle,
\end{aligned}
\tag{7.63}
$$

where we introduced $k = n + 1$.

- For the L_- operator acting on w_1 and w_2:

$$
L_- \sum_n a^l_{mn} \Big| l, m, n + \frac{(-1)^\mu}{2} \Big\rangle = \sum_n a^l_{mn} \alpha_{n+\frac{(-1)^\mu}{2}} \Big| l, m, n + \frac{(-1)^\mu}{2} - 1 \Big\rangle \tag{7.64}
$$

– $\mu = 1$

$$
\begin{aligned}
L_- \sum_n a^l_{mn} \Big| l, m, n - \frac{1}{2} \Big\rangle &= \sum_n a^l_{mn} \alpha_{n-\frac{1}{2}} \Big| l, m, n - \frac{3}{2} \Big\rangle \\
&= \sum_p a^l_{m,(p+1)} \alpha_{p+\frac{1}{2}} \Big| l, m, p - \frac{1}{2} \Big\rangle,
\end{aligned}
\tag{7.65}
$$

where we introduced $p = n - 1$.

– $\mu = 2$

$$
L_- \sum_n a^l_{mn} \Big| l, m, n + \frac{1}{2} \Big\rangle = \sum_n a^l_{mn} \alpha_{n+\frac{1}{2}} \Big| l, m, n - \frac{1}{2} \Big\rangle. \tag{7.66}
$$

Substituting the above results into the equations (7.58) and (7.59), leads to

$$
\begin{aligned}
& f^1_{lm} \sum_n a^l_{mn} \left[E - \frac{1}{2} F(\alpha, \beta_\pm) - l_{\hat{3}} \left(n - \frac{1}{2} \right) \right] \Big| l, m, n - \frac{1}{2} \Big\rangle \\
&= f^2_{lm} \sum_n \left[\frac{l_{\hat{2}} + l_{\hat{1}}}{2} a^l_{mn} \alpha_{n+\frac{1}{2}} \Big| l, m, n - \frac{1}{2} \Big\rangle - \frac{l_{\hat{2}} - l_{\hat{1}}}{2} a^l_{m,(n-1)} \alpha_{n+\frac{1}{2}} \Big| l, m, n + \frac{1}{2} \Big\rangle \right],
\end{aligned}
\tag{7.67}
$$

and

$$
\begin{aligned}
& f^1_{lm} \left[\frac{l_{\hat{2}} + l_{\hat{1}}}{2} \sum_n a^l_{mn} \alpha_{n+\frac{1}{2}} \Big| l, m, n + \frac{1}{2} \Big\rangle - \frac{l_{\hat{2}} - l_{\hat{1}}}{2} \sum_p a^l_{m,(p+1)} \alpha_{p+\frac{1}{2}} \Big| l, m, p - \frac{1}{2} \Big\rangle \right] \\
&= f^2_{lm} \sum_n a^l_{mn} \left[E - \frac{1}{2} F(\alpha, \beta_\pm) + l_{\hat{3}} \left(n + \frac{1}{2} \right) \right] \Big| l, m, n + \frac{1}{2} \Big\rangle.
\end{aligned}
\tag{7.68}
$$

To proceed with the calculations of energy eigenvalues, let us use the orthonormalization relations (5.65). It is more convenient to rewrite it it in the following form

$$\int_0^{2\pi} d\phi \int_0^{\pi} \sin\theta d\theta \int_0^{2\pi} d\psi \left\langle l', m', n' \middle| l, m, n \right\rangle = \frac{8\pi^2}{2l+1}\delta_{ll'}\delta_{mm'}\delta_{nn'}. \tag{7.69}$$

Applying $\left\langle l', m', n' - \frac{1}{2} \right|$ to both sides of the first equation and integrating over the ranges of the Euler angles allows us to eliminate the summation, leading to the following explicit expression:

$$\begin{aligned}
&\int_0^{2\pi} d\phi \int_0^{\pi} \sin\theta d\theta \int_0^{2\pi} d\psi\, f_{lm}^1 \sum_n a_{mn}^l \left[E - \frac{1}{2}F(\alpha, \beta_\pm) - l_{\hat{3}}\left(n - \frac{1}{2}\right)\right] \\
&\qquad\qquad \times \left\langle l', m', n' - \frac{1}{2} \middle| l, m, n - \frac{1}{2} \right\rangle \\
&= \int_0^{2\pi} d\phi \int_0^{\pi} \sin\theta d\theta \int_0^{2\pi} d\psi\;\, f_{lm}^2 \sum_n \left[\frac{l_{\hat{2}} + l_{\hat{1}}}{2}\, a_{mn}^l \alpha_{n+\frac{1}{2}} \left\langle l', m', n' - \frac{1}{2} \middle| l, m, n - \frac{1}{2} \right\rangle \right. \\
&\qquad\qquad \left. - \frac{l_{\hat{2}} - l_{\hat{1}}}{2}\, a_{m,(n-1)}^l \alpha_{n+\frac{1}{2}} \left\langle l', m', n' - \frac{1}{2} \middle| l, m, n + \frac{1}{2} \right\rangle \right],
\end{aligned} \tag{7.70}$$

which leads to

$$f_{lm}^1 a_{mn}^l \left[E - \frac{1}{2}F(\alpha, \beta_\pm) - l_{\hat{3}}\left(n - \frac{1}{2}\right)\right] = f_{lm}^2 \left[\frac{l_{\hat{2}} + l_{\hat{1}}}{2}\, a_{mn}^l \alpha_{n+\frac{1}{2}} - \frac{l_{\hat{2}} - l_{\hat{1}}}{2}\, a_{m,(n-2)}^l \alpha_{n-\frac{1}{2}}\right]. \tag{7.71}$$

Similarly, for the second equation applying $\left\langle l', m', n' + \frac{1}{2} \right|$ on both sides and integrating over the ranges of the Euler angles leads to

$$f_{lm}^1 \left[\frac{l_{\hat{2}} + l_{\hat{1}}}{2}\, a_{mn}^l \alpha_{n+\frac{1}{2}} - \frac{l_{\hat{2}} - l_{\hat{1}}}{2}\, a_{m,(n+2)}^l \alpha_{n+\frac{3}{2}}\right] = f_{lm}^2 a_{mn}^l \left[E - \frac{1}{2}F(\alpha, \beta_\pm) + l_{\hat{3}}\left(n + \frac{1}{2}\right)\right]. \tag{7.72}$$

Energy eigenvalues

Afterwards, we divide the two equations by each other to eliminate the f_{lm}^1 and f_{lm}^2 coefficients. Simplifying the resulting equation further, we obtain

$$\begin{aligned}
&E^2 - \left(F(\alpha, \beta_\pm) - l_{\hat{3}}\right) E + \frac{1}{4}F^2(\alpha, \beta_\pm) - \frac{1}{2}F(\alpha, \beta_\pm) l_{\hat{3}} - l_{\hat{3}}^2\left(n^2 - \frac{1}{4}\right) \\
&- \frac{(l_{\hat{2}} + l_{\hat{1}})^2}{4}\alpha_{n+\frac{1}{2}}^2 + \frac{l_{\hat{2}}^2 - l_{\hat{1}}^2}{4}\alpha_{n+\frac{1}{2}} \left(\frac{a_{m,(n-2)}^l}{a_{mn}^l}\alpha_{n-\frac{1}{2}} + \frac{a_{m,(n+2)}^l}{a_{mn}^l}\alpha_{n+\frac{3}{2}}\right) \\
&- \frac{(l_{\hat{2}} - l_{\hat{1}})^2}{4}\frac{a_{m,(n+2)}^l}{a_{mn}^l}\frac{a_{m,(n-2)}^l}{a_{mn}^l}\alpha_{n+\frac{3}{2}}\alpha_{n-\frac{1}{2}} = 0.
\end{aligned} \tag{7.73}$$

The solutions of the above quadratic equation are given by

$$E = \frac{F(\alpha, \beta_\pm) - l_{\hat{3}}}{2} \pm \left\{ n^2 l_{\hat{3}} + \frac{(l_{\hat{2}} + l_{\hat{1}})^2}{4} \alpha^2_{n+\frac{1}{2}} - \frac{l^2_{\hat{2}} - l^2_{\hat{1}}}{4} \alpha_{n+\frac{1}{2}} \left(\frac{a^l_{m,(n-2)}}{a^l_{mn}} \alpha_{n-\frac{1}{2}} + \frac{a^l_{m,(n+2)}}{a^l_{mn}} \alpha_{n+\frac{3}{2}} \right) \right.$$
$$\left. + \frac{(l_{\hat{2}} - l_{\hat{1}})^2}{4} \frac{a^l_{m,(n+2)}}{a^l_{mn}} \frac{a^l_{m,(n-2)}}{a^l_{mn}} \alpha_{n+\frac{3}{2}} \alpha_{n-\frac{1}{2}} \right\}^{\frac{1}{2}}. \tag{7.74}$$

Introducing new functions

$$G(\alpha, \beta_+, \beta_-) := \frac{1}{2} \left[F(\alpha, \beta_\pm) - l_{\hat{3}} \right], \tag{7.75}$$

and

$$\omega_{nlm}(\alpha, \beta_+, \beta_-) = \left[n^2 l_{\hat{3}} + \frac{(l_{\hat{2}} + l_{\hat{1}})^2}{4} \alpha^2_{n+\frac{1}{2}} - \frac{l^2_{\hat{2}} - l^2_{\hat{1}}}{4} \alpha_{n+\frac{1}{2}} \left(\frac{a^l_{m,(n-2)}}{a^l_{mn}} \alpha_{n-\frac{1}{2}} + \frac{a^l_{m,(n+2)}}{a^l_{mn}} \alpha_{n+\frac{3}{2}} \right) \right.$$
$$\left. + \frac{(l_{\hat{2}} - l_{\hat{1}})^2}{4} \frac{a^l_{m,(n+2)}}{a^l_{mn}} \frac{a^l_{m,(n-2)}}{a^l_{mn}} \alpha_{n+\frac{3}{2}} \alpha_{n-\frac{1}{2}} \right]^{\frac{1}{2}}, \tag{7.76}$$

the energy eigenstates can be given by the following form

$$\begin{aligned} E_1 &= G(\alpha, \beta_+, \beta_-) - \omega_{nlm}(\alpha, \beta_+, \beta_-), \\ E_2 &= G(\alpha, \beta_+, \beta_-) + \omega_{nlm}(\alpha, \beta_+, \beta_-). \end{aligned} \tag{7.77}$$

Note that, in this case, the energy eigenvalues depend on the values of all the quantum numbers n, l and m due to the asymmetry, i.e., $l_{\hat{2}} \neq l_{\hat{1}}$, unlike in the axisymmetric case, where only n and l are involved.

When the universe approaches a closed FLRW form, we have $\beta_+ \to 0$, and $\beta_- \to 0$. Then, the energy eigenvalues become

$$E_{1,2} \to e^{-\alpha} \left\{ \frac{1}{4} \pm \left[n^2 + \alpha^2_{n+\frac{1}{2}} \right]^{1/2} \right\}, \tag{7.78}$$

which are the same as those in the axisymmetric Bianchi IX model.

General solution

In this case, the general solution can be expressed as follows:

$$\Psi_L(\eta, \psi, \theta, \phi) = \sum_{m\,l} \left[a^1_{ml} \Xi^1_{ml} e^{-iE_1\eta} + a^2_{ml} \Xi^2_{ml} e^{-iE_2\eta} \right], \tag{7.79}$$

where the sum is over m and l only.

7.1.4 Rotating Bianchi IX model

Finally, we can discuss the most general case, namely, the rotating Bianchi IX model. In conformal time, the equation of motion (7.1) takes the form

$$\left[i\bar{\sigma}^{\hat{0}}\partial_\eta + ie^{-(\beta_{\hat{i}}+\alpha)}R^i{}_{\hat{i}}\bar{\sigma}^{\hat{i}}e_i - \frac{3i}{2}\alpha' - \frac{1}{2}F(\alpha,\beta_+,\beta_-) - \frac{1}{2N}\sum_{\hat{l}}\left(1+\frac{I_{\hat{l}}}{4}\right)^{\frac{1}{2}}\Omega_{\hat{l}}\sigma^{\hat{l}}\right]\Psi_L = 0. \tag{7.80}$$

Solutions in the fixed background

Considering β_+ and α as constants given at the specific moment, the equation reads

$$i\partial_\eta\Psi_L = \left[ie^{-\alpha}e^{-\beta_k}R^i{}_{\hat{i}}\sigma^{\hat{i}}e_i + \frac{1}{2}F(\alpha,\beta_+,\beta_-) + \frac{1}{2N}\sum_{\hat{l}}\left(1+\frac{I_{\hat{l}}}{4}\right)^{\frac{1}{2}}\Omega_{\hat{l}}\sigma^{\hat{l}}\right]\Psi_L. \tag{7.81}$$

Separating the temporal and spatial variables as in previous sections, the equation for the spatial part takes the form

$$\left[ie^{-\alpha}e^{-\beta_k}R^i{}_{\hat{i}}\sigma^{\hat{i}}e_i + \frac{1}{2}F(\alpha,\beta_+,\beta_-) + \frac{1}{2N}\sum_{\hat{l}}\left(1+\frac{I_{\hat{l}}}{4}\right)^{\frac{1}{2}}\Omega_{\hat{l}}\sigma^{\hat{l}}\right]\Xi(\psi,\theta,\phi) = E\,\Xi(\psi,\theta,\phi). \tag{7.82}$$

Substituting the Pauli matrices explicitly, using the relation $\tilde{e}_j = R^i{}_j e_i$ and introducing parameters $\bar{I}_i = \left(1+\frac{I_{\hat{i}}}{4}\right)^{\frac{1}{2}}$ for shorthand notation, the equation takes the form

$$\begin{pmatrix} il_{\hat{3}}\tilde{e}_{\hat{3}} + \frac{1}{2}F(\alpha,\beta_\pm) + \frac{1}{2}e^{-\alpha}\bar{I}_3\Omega_{\hat{3}} & i\left(l_{\hat{1}}\tilde{e}_{\hat{1}} - il_{\hat{2}}\tilde{e}_{\hat{2}}\right) + \frac{1}{2}e^{-\alpha}\left(\bar{I}_1\Omega_{\hat{1}} - i\bar{I}_2\Omega_{\hat{2}}\right) \\ i\left(l_{\hat{1}}\tilde{e}_{\hat{1}} + il_{\hat{2}}\tilde{e}_{\hat{2}}\right) + \frac{1}{2}e^{-\alpha}\left(\bar{I}_1\Omega_{\hat{1}} + i\bar{I}_2\Omega_{\hat{2}}\right) & -il_{\hat{3}}\tilde{e}_{\hat{3}} + \frac{1}{2}F(\alpha,\beta_\pm) - \frac{1}{2}e^{-\alpha}\bar{I}_3\Omega_{\hat{3}} \end{pmatrix}\Xi = E\,\Xi. \tag{7.83}$$

Using $\tilde{L}_i = -i\tilde{e}_i$ and the relations (7.55) for $\tilde{L}$, then the equation can be expressed as follows:

$$\begin{pmatrix} -l_{\hat{3}}\tilde{L}_{\hat{3}} + \frac{1}{2}F(\alpha,\beta_\pm) + \frac{1}{2}e^{-\alpha}\bar{I}_3\Omega_{\hat{3}} & \frac{l_{\hat{2}}-l_{\hat{1}}}{2}\tilde{L}_+ - \frac{l_{\hat{2}}+l_{\hat{1}}}{2}\tilde{L}_- + \frac{1}{2}e^{-\alpha}\left(\bar{I}_1\Omega_{\hat{1}} - i\bar{I}_2\Omega_{\hat{2}}\right) \\ -\frac{l_{\hat{2}}+l_{\hat{1}}}{2}\tilde{L}_+ + \frac{l_{\hat{2}}-l_{\hat{1}}}{2}\tilde{L}_- + \frac{1}{2}e^{-\alpha}\left(\bar{I}_1\Omega_{\hat{1}} + i\bar{I}_2\Omega_{\hat{2}}\right) & l_{\hat{3}}\tilde{L}_{\hat{3}} + \frac{1}{2}F(\alpha,\beta_\pm) - \frac{1}{2}e^{-\alpha}\bar{I}_3\Omega_{\hat{3}} \end{pmatrix}\Xi = E\,\Xi. \tag{7.84}$$

As discussed in Sec. 6.3.3, the second-order equation for the rotating Bianchi IX model corresponds to the Hamiltonian eigenvalue equation of an asymmetric "ideal" top, expressed in terms of space-fixed angular momentum operators. In this case, the spinor field should be expanded in terms of the basis given in (6.93). Hence, we can write

$$\Xi_{nl} = \begin{pmatrix} w_1 \\ w_2 \end{pmatrix} = \sum_m \tilde{a}^l_{mn}\begin{pmatrix} f^1_{ln}|l,m-\frac{1}{2},n\rangle \\ f^2_{ln}|l,m+\frac{1}{2},n\rangle \end{pmatrix}. \tag{7.85}$$

Then, the equation (7.84) can be expressed as two equations:

$$\begin{aligned}
&\left(E-\frac{1}{2}F(\alpha,\beta_\pm)+l_{\hat{3}}\tilde{L}_{\hat{3}}-\frac{1}{2}e^{-\alpha}\bar{I}_3\Omega_{\hat{3}}\right)w_1=\left(\frac{l_{\hat{2}}-l_{\hat{1}}}{2}\tilde{L}_+-\frac{l_{\hat{2}}+l_{\hat{1}}}{2}\tilde{L}_-+\frac{1}{2}e^{-\alpha}\left(\bar{I}_1\Omega_{\hat{1}}-i\bar{I}_2\Omega_{\hat{2}}\right)\right)w_2,\\
&\left(-\frac{l_{\hat{2}}+l_{\hat{1}}}{2}\tilde{L}_++\frac{l_{\hat{2}}-l_{\hat{1}}}{2}\tilde{L}_-+\frac{1}{2}e^{-\alpha}\left(\bar{I}_1\Omega_{\hat{1}}+i\bar{I}_2\Omega_{\hat{2}}\right)\right)w_1=\left(E-\frac{1}{2}F(\alpha,\beta_\pm)-l_{\hat{3}}\tilde{L}_{\hat{3}}+\frac{1}{2}e^{-\alpha}\bar{I}_3\Omega_{\hat{3}}\right)w_2.
\end{aligned} \tag{7.86}$$

Using the eigenvalue equations 6.27, we can calculate

- For the $\tilde{L}_3$ operator acting on w_1 and w_2:

$$\tilde{L}_3\sum_m \tilde{a}^l_{mn}\Big|l,m+\frac{(-1)^\mu}{2},n\Big\rangle=\sum_m \tilde{a}^l_{mn}\left(m+\frac{(-1)^\mu}{2}\right)\Big|l,m+\frac{(-1)^\mu}{2},n\Big\rangle \tag{7.87}$$

- For the $\tilde{L}_+$ operator acting on w_1 and w_2:

$$\tilde{L}_+\sum_m \tilde{a}^l_{mn}\Big|l,m+\frac{(-1)^\mu}{2},n\Big\rangle=\sum_m \tilde{a}^l_{mn}\alpha_{m+\frac{(-1)^\mu}{2}+1}\Big|l,m+\frac{(-1)^\mu}{2}+1,n\Big\rangle \tag{7.88}$$

  - $\mu=1$

$$\tilde{L}_+\sum_m \tilde{a}^l_{mn}\Big|l,m-\frac{1}{2},n\Big\rangle=\sum_m \tilde{a}^l_{mn}\alpha_{m+\frac{1}{2}}\Big|l,m+\frac{1}{2},n\Big\rangle \tag{7.89}$$

  - $\mu=2$

$$\begin{aligned}
\tilde{L}_+\sum_m \tilde{a}^l_{mn}\Big|l,m+\frac{1}{2},n\Big\rangle&=\sum_m \tilde{a}^l_{mn}\alpha_{m+\frac{3}{2}}\Big|l,m+\frac{3}{2},n\Big\rangle\\
&=\sum_k \tilde{a}^l_{(k-1),n}\alpha_{k+\frac{1}{2}}\Big|l,k+\frac{1}{2},n\Big\rangle,
\end{aligned} \tag{7.90}$$

  where we introduced $k=m+1$.

- For the $\tilde{L}_-$ operator acting on w_1 and w_2:

$$\tilde{L}_-\sum_m \tilde{a}^l_{mn}\Big|l,m+\frac{(-1)^\mu}{2},n\Big\rangle=\sum_m \tilde{a}^l_{mn}\alpha_{m+\frac{(-1)^\mu}{2}}\Big|l,m+\frac{(-1)^\mu}{2}-1,n\Big\rangle \tag{7.91}$$

  - $\mu=1$

$$\begin{aligned}
\tilde{L}_-\sum_m \tilde{a}^l_{mn}\Big|l,m-\frac{1}{2},n\Big\rangle&=\sum_m \tilde{a}^l_{mn}\alpha_{m-\frac{1}{2}}\Big|l,m-\frac{3}{2},n\Big\rangle\\
&=\sum_p \tilde{a}^l_{(p+1),n}\alpha_{p+\frac{1}{2}}\Big|l,p-\frac{1}{2},n\Big\rangle,
\end{aligned} \tag{7.92}$$

  where we introduced $p=m-1$.

– $\mu = 2$

$$\tilde{L}_- \sum_m \tilde{a}^l_{mn} \Big| l, m + \frac{1}{2}, n \Big\rangle = \sum_m \tilde{a}^l_{mn} \alpha_{m+\frac{1}{2}} \Big| l, m - \frac{1}{2}, n \Big\rangle. \tag{7.93}$$

Substituting these relations into the above equations and proceeding as in the previous section, while omitting the explicit intermediate steps for brevity, yields

$$\begin{aligned} & f^1_{ln} \tilde{a}^l_{mn} \left(E - \frac{1}{2} F(\alpha, \beta_+, \beta_-) + l_{\hat{3}} \left(m - \frac{1}{2} \right) - \frac{1}{2} e^{-\alpha} \bar{I}_3 \Omega_{\hat{3}} \right) \\ & = f^2_{ln} \left\{ \left[\frac{l_{\hat{2}} - l_{\hat{1}}}{2} \tilde{a}^l_{(m-2),n} \alpha_{m-\frac{1}{2}} - \frac{l_{\hat{2}} + l_{\hat{1}}}{2} \tilde{a}^l_{mn} \alpha_{m+\frac{1}{2}} \right] + \frac{1}{2} e^{-\alpha} \left(\bar{I}_1 \Omega_{\hat{1}} - i \bar{I}_2 \Omega_{\hat{2}} \right) \tilde{a}^l_{(m-1),n} \right\}, \end{aligned} \tag{7.94}$$

and

$$\begin{aligned} & f^1_{ln} \left\{ \left[-\frac{l_{\hat{2}} + l_{\hat{1}}}{2} \tilde{a}^l_{mn} \alpha_{m+\frac{1}{2}} + \frac{l_{\hat{2}} - l_{\hat{1}}}{2} \tilde{a}^l_{(m+2),n} \alpha_{m+\frac{3}{2}} \right] + \frac{1}{2} e^{-\alpha} \left(\bar{I}_1 \Omega_{\hat{1}} + i \bar{I}_2 \Omega_{\hat{2}} \right) \tilde{a}^l_{m+1,n} \right\} \\ & = f^2_{ln} \tilde{a}^l_{mn} \left(E - \frac{1}{2} F(\alpha, \beta_+, \beta_-) - l_{\hat{3}} \left(m + \frac{1}{2} \right) + \frac{1}{2} e^{-\alpha} \bar{I}_3 \Omega_{\hat{3}} \right). \end{aligned} \tag{7.95}$$

Energy eigenvalues

Dividing the equations obtained above by each other and further simplifying the resulting equation leads to

$$\begin{aligned} & E^2 - (F(\alpha, \beta_+, \beta_-) + l_{\hat{3}}) E + \frac{1}{4} F^2(\alpha, \beta_+, \beta_-) + \frac{1}{2} F(\alpha, \beta_+, \beta_-) l_{\hat{3}} - l^2_{\hat{3}} \left(m^2 - \frac{1}{4} \right) \\ & + e^{-\alpha} \bar{I}_3 \Omega_{\hat{3}} l_{\hat{3}} m - \frac{1}{4} e^{-2\alpha} \bar{I}^2_3 \Omega^2_{\hat{3}} - W(\alpha, \beta_\pm, \Omega_i) = 0, \end{aligned}$$

where we introduced a function

$$\begin{aligned} W(\alpha, \beta_\pm, \Omega_i) = & \left\{ \left[\frac{l_{\hat{2}} - l_{\hat{1}}}{2} \frac{\tilde{a}^l_{m-2,n}}{\tilde{a}^l_{mn}} \alpha_{m-\frac{1}{2}} - \frac{l_{\hat{2}} + l_{\hat{1}}}{2} \alpha_{m+\frac{1}{2}} \right] + \frac{1}{2} e^{-\alpha} \left(\bar{I}_1 \Omega_{\hat{1}} - i \bar{I}_2 \Omega_{\hat{2}} \right) \frac{\tilde{a}^l_{m-1,n}}{\tilde{a}^l_{mn}} \right\} \\ \times & \left\{ \left[-\frac{l_{\hat{2}} + l_{\hat{1}}}{2} \alpha_{m+\frac{1}{2}} + \frac{l_{\hat{2}} - l_{\hat{1}}}{2} \frac{\tilde{a}^l_{m+2,n}}{\tilde{a}^l_{mn}} \alpha_{m+\frac{3}{2}} \right] + \frac{1}{2} e^{-\alpha} \left(\bar{I}_1 \Omega_{\hat{1}} + i \bar{I}_2 \Omega_{\hat{2}} \right) \frac{\tilde{a}^l_{m+1,n}}{\tilde{a}^l_{mn}} \right\}. \end{aligned} \tag{7.96}$$

We obtain the following energy eigenstates

$$E_{1,2} = \frac{(F(\alpha, \beta_+, \beta_-) + l_{\hat{3}})}{2} \pm \left[l^2_{\hat{3}} m^2 - e^{-\alpha} \bar{I}_3 \Omega_{\hat{3}} l_{\hat{3}} m + \frac{1}{4} e^{-2\alpha} \bar{I}^2_3 \Omega^2_{\hat{3}} + W(\alpha, \beta_\pm, \Omega_i) \right]^{\frac{1}{2}}. \tag{7.97}$$

Introducing functions

$$\omega_{nlm}(\alpha, \beta_+, \Omega_{\hat{i}}) := \left[l_{\hat{3}}^2 m^2 - e^{-\alpha} \bar{I}_3 \Omega_{\hat{3}} l_{\hat{3}} m + \frac{1}{4} e^{-2\alpha} \bar{I}_3^2 \Omega_{\hat{3}}^2 + W(\alpha, \beta_\pm, \Omega_i) \right]^{\frac{1}{2}}, \tag{7.98}$$

and

$$G^{\mathrm{rot}}(\alpha, \beta_+, \beta_-) := \frac{1}{2} \left[F(\alpha, \beta_\pm) - l_{\hat{3}} \right], \tag{7.99}$$

the energy eigenvalues can be expressed as follows:

$$\begin{aligned} E_1 &= G^{\mathrm{rot}}(\alpha, \beta_+, \beta_-) - \omega_{nlm}^{\mathrm{rot}}(\alpha, \beta_+, \beta_-, \Omega_{\hat{i}}), \\ E_2 &= G^{\mathrm{rot}}(\alpha, \beta_+, \beta_-) + \omega_{nlm}^{\mathrm{rot}}(\alpha, \beta_+, \beta_- i, \Omega_{\hat{i}}). \end{aligned} \tag{7.100}$$

When the universe approaches a closed FLRW form, we have $\beta_\pm \to 0$, and $\Omega_3 \to 0$. Then the energy eigenvalues become

$$E_{1,2} \to e^{-\alpha} \left\{ \frac{1}{4} \pm \left[m^2 + \alpha_{m+\frac{1}{2}}^2 \right]^{1/2} \right\}. \tag{7.101}$$

General solution

The general solution can be expressed similar to the case for diagonal Bianchi IX; however, here we sum over n and l quantum numbers instead,

$$\Psi_L(\eta, \psi, \theta, \phi) = \sum_{n\,l} \left[a_{nl}^1 \Xi_{nl}^1 e^{-iE_1\eta} + a_{nl}^2 \Xi_{nl}^2 e^{-iE_2\eta} \right]. \tag{7.102}$$

7.1.5 Fermion level crossing

In Sec. 3.3.2, we discussed various approaches to particle creation in an expanding universe, one of which involves the assumption of "in" and "out" static regions. This is the approach that we will apply in the current context. This framework considers a Bianchi IX metric that remains static for $\eta < \eta_i$, where the parameters β_+, β_-, α, and $\Omega_{\hat{i}}$ are fixed constants at a specific time. For $\eta > \eta_f$, the universe isotropizes and approaches a closed FLRW model, where the parameters β_+, β_- and $\Omega_{\hat{i}}$ decay to zero, while in the intermediate region $\eta_i < \eta < \eta_f$, the metric undergoes time-dependent variations. Under this assumption, the past and future vacuum states, $|0_{\mathrm{in}}\rangle$ and $|0_{\mathrm{out}}\rangle$, can be unambiguously defined, providing a well-structured framework for analyzing the particle creation process in an expanding Bianchi IX universe.

Let us now recall the energy eigenvalues obtained for the different universe models discussed in the previous section. These eigenvalues can be expressed in the general form as follows, which includes all the cases considered:

$$\begin{aligned} E_J^1 &= G - \omega_J, \\ E_J^2 &= G + \omega_J. \end{aligned} \tag{7.103}$$

As we have already discussed, due to the anisotropy of spacetime, there are no clearly defined positive or negative eigenvalues which correspond to antiparticles and particles correspondingly. We also obtained the energy eigenvalues in the limit where the universe approaches isotropy, i.e., when the anisotropy factors β_+, β_- and the angular velocity Ω_i approach zero. In this limit, the function G takes a constant value for a fixed value of α, which contrasts with the case of large initial anisotropy ($\beta_+ \ll -1$). In this latter case, the function G becomes very large. Hence, it is easy to realize that for some modes with two initially positive eigenvalues, i.e. a state with two antiparticles, as the anisotropic universe evolves and approaches to the isotropic state, one of the eigenvalues (i.e., E_J^1) becomes negative. This phenomena is refereed to as "level crossing". Let us also point out that, for the different models discussed, the situation differs in that the level crossing occurs for different mode values; however, the physical discussion remains the same.

To understand the physical implications of the sign flipping, let us consider the Bogoliubov transformations.

Bogoliubov transformations

Recalling the discussion on Bogoliubov transformations in Sec. 3.3, let us consider a mode J (a general label for $\{nlm\}$) in the "in" state, where both E_1 and E_2 are positive. In the "out" region, however, E_1 becomes negative.

- In the "in" state, from (7.26) it follows that for a mode J

$$\Psi_J = a_J^{\mathrm{in}\dagger} e^{-iE_1^{J^{\mathrm{in}}}\eta} \Xi_1^{J^{\mathrm{in}}} + b_J^{\mathrm{in}\dagger} e^{-iE_2^{J^{\mathrm{in}}}\eta} \Xi_2^{J^{\mathrm{in}}}. \tag{7.104}$$

  The "in" vacuum is defined by

$$a_J^{\mathrm{in}}|0\rangle = b_J^{\mathrm{in}}|0\rangle = 0. \tag{7.105}$$

  Hence, in this case, in the initial static region, both ${a^{\mathrm{in}}}^\dagger_J$ and $b_J^{\mathrm{in}\dagger}$ create antineutrinos.

- In the "out" state, the field expansion reads

$$\Psi_J = a_J^{\mathrm{out}} e^{-iE_1^{J^{\mathrm{out}}}\eta} \Xi_1^{J^{\mathrm{out}}} + b_J^{\mathrm{out}\dagger} e^{-iE_2^{J^{\mathrm{out}}}\eta} \Xi_2^{J^{\mathrm{out}}}. \tag{7.106}$$

The "out" vacuum is defined by

$$a_J^{\text{out}}|\tilde{0}\rangle = b_J^{\text{out}}|\tilde{0}\rangle = 0. \tag{7.107}$$

Since here, E_1 is negative, a_J^{out} represents the neutrino annihilation operator, and $b_J^{\text{out}\dagger}$ represents the antineutrino creation operator.

As in Sec. 3.3, we can relate the "in" and "out" creation/annihilation operators to each other as given by (3.115) and (3.116). Without deriving the details explicitly, it can be shown that the two vacua are related as described in [61], [62],

$$|0\rangle \sim a_J^{\text{out}\dagger}\,|\tilde{0}\rangle\,, \tag{7.108}$$

Therefore, at each level crossing, a single neutrino will appear in the "out" state. This phenomenon is explained in relation to the chiral anomaly and has been further explored in [149] within the context of gravitational leptogenesis. Given the fermion non-conservation observed in the Bianchi IX model, a natural question arises: can this phenomenon be related to the matter-antimatter asymmetry? As mentioned in Sec. 3.1.1, neutrinos cannot be Weyl fermions, so the above discussion does not directly contribute to the fundamental analysis of matter-antimatter asymmetry. However, the appearance of asymmetric effects motivates the next step: the study of Dirac fermions in search of spectral asymmetries. It is important to note that, unlike Weyl fermions, which are neutral, charge conservation in GR ensures that there cannot be fermion-number violation due to the particle creation process for charged Dirac fermions. Hence, the discussion of particle creation is of less significance in this context. The main focus, therefore, will be on the study of the energy spectrum of particles and antiparticles, specifically looking for asymmetries. The mathematical approaches developed through the study of Weyl fermions will be applied in the analysis of Dirac fermions in the next section.

7.2 Dirac spinor

In this section, we consider the Dirac equation in the Bianchi IX universe, as derived in Sec. 4.4 and given by (4.99). In the Weyl basis, it decomposes into two equations,

$$\left[ih_{\hat{\alpha}}{}^{\mu}\sigma^{\hat{\alpha}}e_{\mu} - \frac{3i}{2N}\dot{\alpha} + \frac{1}{2}F(\alpha,\beta_+,\beta_-) - \frac{1}{2N}\sum_{\hat{\imath}}\left(1+\frac{I_{\hat{\imath}}}{4}\right)^{\frac{1}{2}}\Omega_{\hat{\imath}}\sigma^{\hat{\imath}}\right]\Psi_R = M\Psi_L, \quad (7.109)$$

and

$$\left[ih_{\hat{\alpha}}{}^{\mu}\bar{\sigma}^{\hat{\alpha}}e_{\mu} - \frac{3i}{2N}\dot{\alpha} - \frac{1}{2}F(\alpha,\beta_+,\beta_-) - \frac{1}{2N}\sum_{\hat{\imath}}\left(1+\frac{I_{\hat{\imath}}}{4}\right)^{\frac{1}{2}}\Omega_{\hat{\imath}}\sigma^{\hat{\imath}}\right]\Psi_L = M\Psi_R. \quad (7.110)$$

7.2.1 Axisymmetric Bianchi IX model

For the axisymmetric Bianchi IX model, the equations (7.109) and (7.110) simplify to

$$\left[ih_{\hat{\alpha}}{}^{\mu}\sigma^{\hat{\alpha}}e_{\mu} - \frac{3i}{2N}\dot{\alpha} + \frac{1}{2}\tilde{F}(\alpha,\beta_+)\right]\Psi_R = M\Psi_L, \quad (7.111)$$

and

$$\left[ih_{\hat{\alpha}}{}^{\mu}\bar{\sigma}^{\hat{\alpha}}e_{\mu} - \frac{3i}{2N}\dot{\alpha} - \frac{1}{2}\tilde{F}(\alpha,\beta_+)\right]\Psi_L = M\Psi_R. \quad (7.112)$$

where the inverse vierbein is given by (7.3).

Solutions in the fixed background

Assuming α and β_+ are constants and recalling the notation from (3.8), the above equations in conformal time, expressed in terms of the Pauli matrices, take the form

$$\begin{aligned}\left[i\partial_\eta + ie^{-(\beta_{\hat{\imath}}+\alpha)}\sigma^{\hat{\imath}}e_i + \frac{1}{2}\tilde{F}(\alpha,\beta_+)\right]\Psi_R = M\Psi_L,\\ \left[i\partial_\eta - ie^{-(\beta_{\hat{\imath}}+\alpha)}\sigma^{\hat{\imath}}e_i - \frac{1}{2}\tilde{F}(\alpha,\beta_+)\right]\Psi_L = M\Psi_R.\end{aligned} \quad (7.113)$$

Let us present the temporal and spatial decomposition of the Dirac spinor field as follows:

$$\Psi = \begin{pmatrix}\Psi_L\\ \Psi_R\end{pmatrix} = N(\eta)\begin{pmatrix}w_L\\ w_R\end{pmatrix}. \quad (7.114)$$

Substituting this decomposition into the equations, the equation for the temporal part reads

$$i\frac{(\partial_\eta N(\eta))}{N(\eta)} = E \quad \rightarrow \quad N(\eta) = e^{-iE\eta}, \quad (7.115)$$

where E is a constant.

Moreover, the equations for the spatial part are given by

$$\begin{aligned} \left[E + ie^{-(\beta_{\hat{\imath}}+\alpha)}\sigma^{\hat{i}}e_i + \frac{1}{2}\tilde{F}(\alpha,\beta_+)\right] w_R &= Mw_L, \\ \left[E - ie^{-(\beta_{\hat{\imath}}+\alpha)}\sigma^{\hat{i}}e_i - \frac{1}{2}\tilde{F}(\alpha,\beta_+)\right] w_L &= Mw_R. \end{aligned} \tag{7.116}$$

Substituting the Pauli matrices explicitly and recalling the relations (7.13), the equations can be expressed in terms of the body-fixed angular momentum operator as follows:

$$\begin{pmatrix} E + \frac{1}{2}\tilde{F}(\alpha,\beta_+) + e^{-(\beta_{\hat{3}}+\alpha)}L_{\hat{3}} & e^{-(\beta_{\hat{1}}+\alpha)}L_- \\ e^{-(\beta_{\hat{1}}+\alpha)}L_+ & E + \frac{1}{2}\tilde{F}(\alpha,\beta_+) - e^{-(\beta_{\hat{3}}+\alpha)}L_{\hat{3}} \end{pmatrix} w_R = Mw_L, \tag{7.117}$$

and

$$\begin{pmatrix} E - \frac{1}{2}\tilde{F}(\alpha,\beta_+) - e^{-(\beta_{\hat{3}}+\alpha)}L_{\hat{3}} & -e^{-(\beta_{\hat{1}}+\alpha)}L_- \\ -e^{-(\beta_{\hat{1}}+\alpha)}L_+ & E - \frac{1}{2}\tilde{F}(\alpha,\beta_+) + e^{-(\beta_{\hat{3}}+\alpha)}L_{\hat{3}} \end{pmatrix} w_L = Mw_R. \tag{7.118}$$

As discussed in the previous section, each two-spinor can be expanded in terms of the eigenbasis of the symmetric "ideal" top. Specifically, we have

$$w_L^{nlm} = \begin{pmatrix} w_1 \\ w_2 \end{pmatrix} = \begin{pmatrix} f^1_{nlm}|l,m,n-\frac{1}{2}\rangle \\ f^2_{nlm}|l,m,n+\frac{1}{2}\rangle \end{pmatrix}, \tag{7.119}$$

$$w_R^{nlm} = \begin{pmatrix} w_3 \\ w_4 \end{pmatrix} = \begin{pmatrix} f^3_{nlm}|l,m,n-\frac{1}{2}\rangle \\ f^4_{nlm}|l,m,n+\frac{1}{2}\rangle \end{pmatrix}. \tag{7.120}$$

The above two matrix equations can be expressed as four separate equations. The first equation leads to

$$\begin{aligned} \left[E + \frac{1}{2}\tilde{F}(\alpha,\beta_+) + e^{-(\beta_{\hat{3}}+\alpha)}L_{\hat{3}}\right] w_3 + e^{-(\beta_{\hat{1}}+\alpha)}L_-w_4 &= Mw_1, \\ e^{-(\beta_{\hat{1}}+\alpha)}L_+w_3 + \left[E + \frac{1}{2}\tilde{F}(\alpha,\beta_+) - e^{-(\beta_{\hat{3}}+\alpha)}L_{\hat{3}}\right] w_4 &= Mw_2. \end{aligned} \tag{7.121}$$

and from the second equation, one obtains

$$\begin{aligned} \left[E - \frac{1}{2}\tilde{F}(\alpha,\beta_+) - e^{-(\beta_{\hat{3}}+\alpha)}L_{\hat{3}}\right] w_1 - e^{-(\beta_{\hat{1}}+\alpha)}L_-w_2 &= Mw_3, \\ - e^{-(\beta_{\hat{1}}+\alpha)}L_+w_1 + \left[E - \frac{1}{2}\tilde{F}(\alpha,\beta_+) + e^{-(\beta_{\hat{3}}+\alpha)}L_{\hat{3}}\right] w_2 &= Mw_4. \end{aligned} \tag{7.122}$$

Using the eigenvalue equations (6.26), we calculate the following relations

$$
\begin{aligned}
L_+ w_{1,3} &= f^{1,3}_{nlm}\, L_+ \, |l, m, n - \frac{1}{2}\rangle = f^{1,3}_{nlm} \alpha_{n+\frac{1}{2}} |l, m, n + \frac{1}{2}\rangle, \\
L_- w_{2,4} &= f^{2,4}_{nlm}\, L_- \, |l, m, n + \frac{1}{2}\rangle = f^{2,4}_{nlm} \alpha_{n+\frac{1}{2}} |l, m, n - \frac{1}{2}\rangle, \\
L_{\hat{3}} w_{1,3} &= f^{1,3}_{nlm} \left(n - \frac{1}{2}\right) |l, m, n - \frac{1}{2}\rangle, \\
L_{\hat{3}} w_{2,4} &= f^{2,4}_{nlm} \left(n + \frac{1}{2}\right) |l, m, n + \frac{1}{2}\rangle.
\end{aligned}
\tag{7.123}
$$

Substituting the above relations into equations (7.121) and (7.122) and rewriting them in matrix form, we obtain

$$
\begin{pmatrix} E + \frac{1}{2}\tilde{F}(\alpha, \beta_+) + e^{-(\beta_{\hat{3}}+\alpha)} \left(n - \frac{1}{2}\right) & \alpha_{n+\frac{1}{2}}\, e^{-(\beta_{\hat{1}}+\alpha)} \\ \alpha_{n+\frac{1}{2}}\, e^{-(\beta_{\hat{1}}+\alpha)} & E + \frac{1}{2}\tilde{F}(\alpha, \beta_+) - e^{-(\beta_{\hat{3}}+\alpha)} \left(n + \frac{1}{2}\right) \end{pmatrix} \begin{pmatrix} f^3_{nlm} \\ f^4_{nlm} \end{pmatrix} = M \begin{pmatrix} f^1_{nlm} \\ f^2_{nlm} \end{pmatrix},
\tag{7.124}
$$

and

$$
\begin{pmatrix} E - \frac{1}{2}\tilde{F}(\alpha, \beta_+) - e^{-(\beta_{\hat{3}}+\alpha)} \left(n - \frac{1}{2}\right) & -\alpha_{n+\frac{1}{2}} e^{-(\beta_{\hat{1}}+\alpha)} \\ -\alpha_{n+\frac{1}{2}} e^{-(\beta_{\hat{1}}+\alpha)} & E - \frac{1}{2}\tilde{F}(\alpha, \beta_+) + e^{-(\beta_{\hat{3}}+\alpha)} \left(n + \frac{1}{2}\right) \end{pmatrix} \begin{pmatrix} f^1_{nlm} \\ f^2_{nlm} \end{pmatrix} = M \begin{pmatrix} f^3_{nlm} \\ f^4_{nlm} \end{pmatrix}.
\tag{7.125}
$$

Energy eigenvalues

To eliminate the spinor components, we first express $\begin{pmatrix} f^1_{nlm} \\ f^2_{nlm} \end{pmatrix}$ in terms of $\begin{pmatrix} f^3_{nlm} \\ f^4_{nlm} \end{pmatrix}$ using the first equation and substitute this expression into the second equation. This leads to the following equation:

$$
\begin{aligned}
&\begin{pmatrix} E - \frac{1}{4}e^{-4\beta_+-\alpha} - ne^{2\beta_+-\alpha} & -\alpha_{n+\frac{1}{2}} e^{-(\beta_++\alpha)} \\ -\alpha_{n+\frac{1}{2}} e^{-(\beta_++\alpha)} & E - \frac{1}{4}e^{-4\beta_+-\alpha} + ne^{2\beta_+-\alpha} \end{pmatrix} \\
&\times \begin{pmatrix} E + \frac{1}{4}e^{-4\beta_+-\alpha} + ne^{2\beta_+-\alpha} & \alpha_{n+\frac{1}{2}}\, e^{-(\beta_++\alpha)} \\ \alpha_{n+\frac{1}{2}}\, e^{-(\beta_++\alpha)} & E + \frac{1}{4}e^{-4\beta_+-\alpha} - ne^{2\beta_+-\alpha} \end{pmatrix} = M^2.
\end{aligned}
\tag{7.126}
$$

Here, we have substituted $\beta_1 = \beta_2 = \beta_+$, $\beta_3 = -2\beta_+$ and the function $\tilde{F}(\alpha, \beta_+)$ as defined in (7.5). The multiplication of the matrices and further simplification leads to the following matrix equation:

$$
A := \begin{pmatrix} a_{11} & a_{12} \\ a_{21} & a_{22} \end{pmatrix} = 0,
\tag{7.127}
$$

where

$$\begin{aligned}
a_{11} &= E^2 - M^2 - e^{-2(\alpha+\beta_+)}\left[n^2 e^{6\beta_+} + \alpha^2_{n+\frac{1}{2}}\right] - \frac{1}{16}e^{-2(\alpha+4\beta_+)} - \frac{1}{2}ne^{-2(\alpha+\beta_+)},\\
a_{12} &= a_{21} = -\frac{1}{2}e^{-5\beta_+-2\alpha}\,\alpha_{n+\frac{1}{2}},\\
a_{22} &= E^2 - M^2 - e^{-2(\alpha+\beta_+)}\left[n^2 e^{6\beta_+} + \alpha^2_{n+\frac{1}{2}}\right] - \frac{1}{16}e^{-2(\alpha+4\beta_+)} + \frac{1}{2}n\,e^{-2(\alpha+\beta_+)}.
\end{aligned} \tag{7.128}$$

To solve this equation, first we need to diagonalize the matrix. Let us consider the characteristic equation

$$\det(\lambda I - A) = 0, \tag{7.129}$$

which can be written explicitly as

$$\begin{aligned}
0 = \det(\lambda I - A) &= \det\left[\begin{pmatrix}\lambda & 0\\ 0 & \lambda\end{pmatrix} - \begin{pmatrix}a_{11} & a_{12}\\ a_{21} & a_{22}\end{pmatrix}\right] = \det\left[\begin{pmatrix}\lambda - a_{11} & -a_{12}\\ -a_{21} & \lambda - a_{22}\end{pmatrix}\right]\\
&= (\lambda - a_{11})\,(\lambda - a_{22}) - a_{12}^2\\
&= \lambda^2 - (a_{11} + a_{22})\lambda + a_{11}a_{22} - a_{12}^2\\
&= (\lambda - \lambda_1)(\lambda - \lambda_2).
\end{aligned} \tag{7.130}$$

We obtain the following eigenvalues for the characteristic equation:

$$\lambda_{1,2} = E^2 - M^2 - \tfrac{1}{16}e^{-2(\alpha+4\beta_+)} - n^2 e^{-2\alpha+4\beta_+} - \alpha^2_{n+\frac{1}{2}}e^{-2(\alpha+\beta_+)} \pm \tfrac{1}{2}e^{-2\alpha-5\beta_+}\sqrt{n^2 e^{6\beta_+} + \alpha^2_{n+\frac{1}{2}}}. \tag{7.131}$$

Setting

$$\lambda_1 = 0, \quad \text{and} \quad \lambda_2 = 0, \tag{7.132}$$

we obtain the following energy eigenvalues

$$E_1^s = -\sqrt{M^2 + e^{-2(\alpha+\beta_+)}\left[\frac{1}{4}e^{-3\beta_+} \pm \sqrt{n^2 e^{6\beta_+} + \alpha^2_{n+\frac{1}{2}}}\right]^2}, \tag{7.133}$$

and

$$E_2^s = \sqrt{M^2 + e^{-2(\alpha+\beta_+)}\left[\frac{1}{4}e^{-3\beta_+} \pm \sqrt{n^2 e^{6\beta_+} + \alpha^2_{n+\frac{1}{2}}}\right]^2}, \tag{7.134}$$

where $s = 1, 2$.

Using the notations introduced in (7.21) and (7.22) from the previous section, we can express the eigenvalues in the following form

$$E_1^s = -\sqrt{M^2 + \left[\tilde{G}(\alpha, \beta_+) \pm \tilde{\omega}_{nl}(\alpha, \beta_+)\right]^2}, \tag{7.135}$$

and

$$E_2^s = \sqrt{M^2 + \left[\tilde{G}(\alpha, \beta_+) \pm \tilde{\omega}_{nl}(\alpha, \beta_+)\right]^2}. \tag{7.136}$$

The negative eigenvalues correspond to particles, representing positive-frequency solutions, and the positive eigenvalues correspond to antiparticles. Unlike the case for the Weyl spinors, for the Dirac spinors, there are clear positive and negative energy eigenvalues, therefore no level crossing is possible. This was expected of course, as the charge is conserved in curved spacetime.

An intriguing phenomenon arises when analyzing the system for different values of the spin index s. The energy eigenvalues of a given mode exhibit noticeable variations, either being enhanced or suppressed, depending on s, for both particles and antiparticles. This effect stems directly from the anisotropy of space, which induces spin-dependent modifications in the energy spectrum. Thus, the interaction between "spin orientation" and the anisotropic background leads to shifts in the energy levels.

General solution

Therefore, the general solution can be given by

$$\Psi(\eta, \psi, \theta, \phi) = \sum_{s=1,2} \sum_{n\,l\,m} \left[a^s_{nlm} \Xi^s_{nlm} e^{-iE^s_1\eta} + b^{s\dagger}_{nlm} \bar{\Xi}^s_{nlm} e^{+iE^s_1\eta}\right], \tag{7.137}$$

where Ξ^s_{nlm} and $\bar{\Xi}^s_{nlm}$ are four independent eigenspinors which are obtained from equations (7.124) and (7.125).

7.2.2 Rotating axisymmetric Bianchi IX model

Solutions in the fixed background

Following the discussion on rotating axisymmetric Bianchi IX in Sec. 7.1.2, it is easy to notice that the equations (7.109) and (7.110) take the form

$$\begin{aligned} &\left\{i\sigma^{\hat{0}}\partial_\eta + ie^{-(\beta_k+\alpha)}R^i{}_{\hat{i}}\sigma^{\hat{i}}e_i + \frac{1}{2}\tilde{F}(\alpha, \beta_+) - \frac{1}{2}e^{-\alpha}\Omega_{\hat{3}}\sigma^{\hat{3}}\right\}\Psi_R = M\Psi_L, \\ &\left\{i\sigma^{\hat{0}}\partial_\eta - ie^{-(\beta_k+\alpha)}R^i{}_{\hat{i}}\sigma^{\hat{i}}e_i - \frac{1}{2}\tilde{F}(\alpha, \beta_+) - \frac{1}{2}e^{-\alpha}\Omega_{\hat{3}}\sigma^{\hat{3}}\right\}\Psi_L = M\Psi_R. \end{aligned} \tag{7.138}$$

Using the temporal and spatial decomposition (7.114), and taking into account (7.115), the equations for the spatial part can be written as

$$\begin{aligned} &\left\{E + ie^{-(\beta_k+\alpha)}R^i{}_{\hat{i}}\sigma^{\hat{i}}e_i + \frac{1}{2}\tilde{F}(\alpha, \beta_+) - \frac{1}{2}e^{-\alpha}\Omega_{\hat{3}}\sigma^{\hat{3}}\right\}w_R = Mw_L, \\ &\left\{E - ie^{-(\beta_k+\alpha)}R^i{}_{\hat{i}}\sigma^{\hat{i}}e_i - \frac{1}{2}\tilde{F}(\alpha, \beta_+) - \frac{1}{2}e^{-\alpha}\Omega_{\hat{3}}\sigma^{\hat{3}}\right\}w_L = Mw_R. \end{aligned} \tag{7.139}$$

Substituting the Pauli matrices explicitly leads to

$$\begin{pmatrix} ie^{-\alpha}e^{-\beta_{\hat{3}}}R^i{}_{\hat{3}}e_i + E + \frac{1}{2}\tilde{F}(\alpha,\beta_+) - \frac{1}{2}e^{-\alpha}\Omega_{\hat{3}} & ie^{-\alpha}e^{-\beta_{\hat{1}}}\left(R^i{}_{\hat{1}} - iR^i{}_{\hat{2}}\right)e_i \\ ie^{-\alpha}e^{-\beta_{\hat{1}}}\left(R^i{}_{\hat{1}} + iR^i{}_{\hat{2}}\right)e_i & -ie^{-\alpha}e^{-\beta_{\hat{3}}}R^i{}_{\hat{3}}e_i + E + \frac{1}{2}\tilde{F}(\alpha,\beta_+) + \frac{1}{2}e^{-\alpha}\Omega_{\hat{3}} \end{pmatrix} w_R = Mw_L, \tag{7.140}$$

and

$$\begin{pmatrix} -ie^{-\alpha}e^{-\beta_{\hat{3}}}R^i{}_{\hat{3}}e_i + E - \frac{1}{2}\tilde{F}(\alpha,\beta_+) - \frac{1}{2}e^{-\alpha}\Omega_{\hat{3}} & -ie^{-\alpha}e^{-\beta_{\hat{1}}}\left(R^i{}_{\hat{1}} - iR^i{}_{\hat{2}}\right)e_i \\ -ie^{-\alpha}e^{-\beta_{\hat{1}}}\left(R^i{}_{\hat{1}} + iR^i{}_{\hat{2}}\right)e_i & ie^{-\alpha}e^{-\beta_{\hat{3}}}R^i{}_{\hat{3}}e_i + E - \frac{1}{2}\tilde{F}(\alpha,\beta_+) + \frac{1}{2}e^{-\alpha}\Omega_{\hat{3}} \end{pmatrix} w_L = Mw_R. \tag{7.141}$$

Expanding the spinors in terms of symmetric "ideal" top eigenbasis (6.79), we can write

$$w_L^{nlm} = \begin{pmatrix} w_1 \\ w_2 \end{pmatrix} = \begin{pmatrix} f^1_{nlm}|l, m - \frac{1}{2}, n\rangle \\ f^2_{nlm}|l, m + \frac{1}{2}, n\rangle \end{pmatrix}, \tag{7.142}$$

and

$$w_R^{nlm} = \begin{pmatrix} w_3 \\ w_4 \end{pmatrix} = \begin{pmatrix} f^3_{nlm}|l, m - \frac{1}{2}, n\rangle \\ f^4_{nlm}|l, m + \frac{1}{2}, n\rangle \end{pmatrix}. \tag{7.143}$$

Furthermore, recalling the relations (7.35), (7.36) and (7.37), the equations can be rewritten in terms of space-fixed angular momentum operator as follows:

$$\begin{pmatrix} -l_{\hat{3}}\tilde{L}_{\hat{3}} + E + \frac{1}{2}\tilde{F}(\alpha,\beta_+) - \frac{1}{2}e^{-\alpha}\Omega_{\hat{3}} & -l_{\hat{1}}\tilde{L}_- \\ -l_{\hat{1}}\tilde{L}_+ & l_{\hat{3}}\tilde{L}_{\hat{3}} + E + \frac{1}{2}\tilde{F}(\alpha,\beta_+) + \frac{1}{2}e^{-\alpha}\Omega_{\hat{3}} \end{pmatrix} \begin{pmatrix} w_3 \\ w_4 \end{pmatrix} = M \begin{pmatrix} w_1 \\ w_2 \end{pmatrix}, \tag{7.144}$$

and

$$\begin{pmatrix} l_{\hat{3}}\tilde{L}_{\hat{3}} + E - \frac{1}{2}\tilde{F}(\alpha,\beta_+) - \frac{1}{2}e^{-\alpha}\Omega_{\hat{3}} & l_{\hat{1}}\tilde{L}_- \\ l_{\hat{1}}\tilde{L}_+ & -l_{\hat{3}}\tilde{L}_{\hat{3}} + E - \frac{1}{2}\tilde{F}(\alpha,\beta_+) + \frac{1}{2}e^{-\alpha}\Omega_{\hat{3}} \end{pmatrix} \begin{pmatrix} w_1 \\ w_2 \end{pmatrix} = M \begin{pmatrix} w_3 \\ w_4 \end{pmatrix}. \tag{7.145}$$

Using the eigenvalue equations (6.27), the following relations are obtained:

$$\begin{aligned} \tilde{L}_- w_{2,4} &= f^{2,4}_{nlm}\tilde{L}_-|l, m + \frac{1}{2}, n\rangle = f^{2,4}_{nlm}\alpha_{m+\frac{1}{2}}|l, m - \frac{1}{2}, n\rangle, \\ \tilde{L}_{\hat{3}} w_{1,3} &= f^{1,3}_{nlm}\tilde{L}_{\hat{3}}|l, m - \frac{1}{2}, n\rangle = (m - 1/2)\, f^{1,3}_{nlm}|l, m - \frac{1}{2}, n\rangle, \\ \tilde{L}_+ w_{1,3} &= f^{1,3}_{nlm}\tilde{L}_+|l, m - \frac{1}{2}, n\rangle = f^{1,3}_{nlm}\alpha_{m+\frac{1}{2}}\,|l, m + \frac{1}{2}, n\rangle, \\ \tilde{L}_{\hat{3}} w_{2,4} &= f^{2,4}_{nlm}\tilde{L}_{\hat{3}}|l, m + \frac{1}{2}, n\rangle = (m + 1/2)\, f^{2,4}_{nlm}|l, m + \frac{1}{2}, n\rangle. \end{aligned} \tag{7.146}$$

Substituting the above relations into the equations (7.144) and (7.145), leads to the following matrix equations:

$$\begin{pmatrix} -l_{\hat{3}}\,(m - 1/2) + E + \frac{1}{2}\tilde{F}(\alpha,\beta_+) - \frac{1}{2}e^{-\alpha}\Omega_{\hat{3}} & -l_{\hat{1}}\alpha_{m+\frac{1}{2}} \\ -l_{\hat{1}}\alpha_{m+\frac{1}{2}} & l_{\hat{3}}\,(m + 1/2) + E + \frac{1}{2}\tilde{F}(\alpha,\beta_+) + \frac{1}{2}e^{-\alpha}\Omega_{\hat{3}} \end{pmatrix} \begin{pmatrix} f^3_{nlm} \\ f^4_{nlm} \end{pmatrix} = M \begin{pmatrix} f^1_{nlm} \\ f^2_{nlm} \end{pmatrix}, \tag{7.147}$$

and the second equation reads

$$\begin{pmatrix} l_{\hat{3}}\,(m-1/2)+E-\frac{1}{2}\tilde{F}(\alpha,\beta_+)-\frac{1}{2}e^{-\alpha}\Omega_{\hat{3}} & l_{\hat{1}}\alpha_{m+\frac{1}{2}} \\ l_{\hat{1}}\alpha_{m+\frac{1}{2}} & -l_{\hat{3}}\,(m+1/2)+E-\frac{1}{2}\tilde{F}(\alpha,\beta_+)+\frac{1}{2}e^{-\alpha}\Omega_{\hat{3}} \end{pmatrix} \begin{pmatrix} f^1_{nlm} \\ f^2_{nlm} \end{pmatrix} = M \begin{pmatrix} f^3_{nlm} \\ f^4_{nlm} \end{pmatrix}. \tag{7.148}$$

These lead to the following equation:

$$\begin{aligned} &\begin{pmatrix} m\,e^{(2\beta_+-\alpha)}+E-\tilde{G}(\alpha,\beta_+)-\frac{1}{2}e^{-\alpha}\Omega_{\hat{3}} & e^{-(\beta_++\alpha)}\alpha_{m+\frac{1}{2}} \\ e^{-(\beta_++\alpha)}\alpha_{m+\frac{1}{2}} & -m\,e^{(2\beta_+-\alpha)}+E-\tilde{G}(\alpha,\beta_+)+\frac{1}{2}e^{-\alpha}\Omega_{\hat{3}} \end{pmatrix} \\ \times &\begin{pmatrix} -m\,e^{(2\beta_+-\alpha)}+E+\tilde{G}(\alpha,\beta_+)-\frac{1}{2}e^{-\alpha}\Omega_{\hat{3}} & -e^{-(\beta_++\alpha)}\alpha_{m+\frac{1}{2}} \\ -e^{-(\beta_++\alpha)}\alpha_{m+\frac{1}{2}} & m\,e^{(2\beta_+-\alpha)}+E+\tilde{G}(\alpha,\beta_+)+\frac{1}{2}e^{-\alpha}\Omega_{\hat{3}} \end{pmatrix} = M^2, \end{aligned} \tag{7.149}$$

where we set $\beta_1 = \beta_2 = \beta_+$ and $\beta_3 = -2\beta_+$. The functions $\tilde{G}(\alpha,\beta_+)$ are given by (7.21).

Energy eigenvalues

Multiplication of the matrices leads to the following equation:

$$A := \begin{pmatrix} a_{11} & a_{12} \\ a_{21} & a_{22} \end{pmatrix} = 0, \tag{7.150}$$

where

$$\begin{aligned} a_{11} &= E^2 - M^2 + e^{-\alpha}\Omega_3 E - \tilde{G}^2(\alpha,\beta_+) - e^{-2(\alpha+\beta_+)}\left[e^{6\beta_+}m^2 + \alpha^2_{m+\frac{1}{2}}\right] \\ &\quad + 2me^{-\alpha+2\beta_+}\tilde{G}(\alpha,\beta_+) + \frac{1}{4}e^{-2\alpha}\Omega_3^2, \\ a_{12} &= e^{-\alpha-\beta_+}\left[-2\tilde{G}(\alpha,\beta_+) + e^{-\alpha}\Omega_3\right]\alpha_{m+\frac{1}{2}}, \\ a_{21} &= e^{-\alpha-\beta_+}\left[-2\tilde{G}(\alpha,\beta_+) - e^{-\alpha}\Omega_3\right]\alpha_{m+\frac{1}{2}}, \\ a_{22} &= E^2 - M^2 - e^{-\alpha}\Omega_3 E - \tilde{G}^2(\alpha,\beta_+) - e^{-2(\alpha+\beta_+)}\left[e^{6\beta_+}m^2 + \alpha^2_{m+\frac{1}{2}}\right] \\ &\quad - 2me^{-\alpha+2\beta_+}\tilde{G}(\alpha,\beta_+) + \frac{1}{4}e^{-2\alpha}\Omega_3^2. \end{aligned} \tag{7.151}$$

The eigenvalues of the characteristic equation (7.130) are

$$\begin{aligned} \lambda_{1,2} = E^2 - M^2 - \tilde{G}^2 - e^{-2(\alpha+\beta_+)}\left[e^{6\beta_+}m^2 + \alpha^2_{m+\frac{1}{2}}\right] + \frac{1}{4}e^{-2\alpha}\Omega_3^2 \\ \pm \Bigg\{ 4\tilde{G}^2 e^{-2\alpha-2\beta_+}\left[e^{6\beta_+}m^2 + \alpha^2_{m+\frac{1}{2}}\right] - e^{-4\alpha-2\beta_+}\alpha^2_{m+\frac{1}{2}}\Omega_3^2 \\ - 4me^{-2\alpha+2\beta_+}\Omega_3\tilde{G}E + e^{-2\alpha}\Omega_3^2 E^2 \Bigg\}^{\frac{1}{2}}. \end{aligned} \tag{7.152}$$

We can calculate the energy eigenvalues by setting

$$\lambda_1 = 0, \quad \text{and} \quad \lambda_2 = 0. \tag{7.153}$$

These lead to the following equation:

$$\begin{aligned}
&E^4 - 2\left(M^2 + \tilde{G}^2 + e^{-2(\alpha+\beta_+)}\left[e^{6\beta_+}m^2 + \alpha^2_{m+\frac{1}{2}}\right] + \frac{1}{4}e^{-2\alpha}\Omega_3^2\right)E^2 \\
&+ 4e^{-2\alpha+2\beta_+}m\Omega_3\tilde{G}E + \left(M^2 + \tilde{G}^2 + e^{-2(\alpha+\beta_+)}\left[e^{6\beta_+}m^2 + \alpha^2_{m+\frac{1}{2}}\right] - \frac{1}{4}e^{-2\alpha}\Omega_3^2\right)^2 \\
&- 4e^{-2\alpha-2\beta_+}\left[e^{6\beta_+}m^2 + \alpha^2_{m+\frac{1}{2}}\right]\tilde{G}^2 + e^{-4\alpha-2\beta_+}\alpha^2_{m+\frac{1}{2}}\Omega_3^2 = 0.
\end{aligned} \tag{7.154}$$

For convenience, let us introduce the following functions:

$$\begin{aligned}
a &= 2\left(M^2 + \tilde{G}^2(\alpha,\beta_+) + e^{-2(\alpha+\beta_+)}\left[e^{6\beta_+}m^2 + \alpha^2_{m+\frac{1}{2}}\right] + \frac{1}{4}e^{-2\alpha}\Omega_3^2\right), \\
b &= 4e^{-2\alpha+2\beta_+}m\Omega_3\tilde{G}(\alpha,\beta_+), \\
c &= \left(M^2 + \tilde{G}^2(\alpha,\beta_+) + e^{-2(\alpha+\beta_+)}\left[e^{6\beta_+}m^2 + \alpha^2_{m+\frac{1}{2}}\right] - \frac{1}{4}e^{-2\alpha}\Omega_3^2\right)^2 \\
&\quad - 4e^{-2\alpha-2\beta_+}\left[e^{6\beta_+}m^2 + \alpha^2_{m+\frac{1}{2}}\right]\tilde{G}^2(\alpha,\beta_+) + e^{-4\alpha-2\beta_+}\alpha^2_{m+\frac{1}{2}}\Omega_3^2.
\end{aligned} \tag{7.155}$$

Thus, the equations (7.154) can be written as

$$E^4 - aE^2 + bE + c = 0. \tag{7.156}$$

We obtain the following solutions to this equation, i.e., the energy eigenvalues[36]

$$\begin{aligned}
E_1^{s=1} &= -\left[\frac{1}{2}\sqrt{\frac{2a}{3} + q_1 + q_2} + \frac{1}{2}\sqrt{\frac{4a}{3} - q_1 - q_2 + \frac{2b}{\sqrt{\frac{2a}{3} + q_1 + q_2}}}\right], \\
E_1^{s=2} &= -\left[\frac{1}{2}\sqrt{\frac{2a}{3} + q_1 + q_2} - \frac{1}{2}\sqrt{\frac{4a}{3} - q_1 - q_2 + \frac{2b}{\sqrt{\frac{2a}{3} + q_1 + q_2}}}\right], \\
E_2^{s=1} &= \frac{1}{2}\sqrt{\frac{2a}{3} + q_1 + q_2} + \frac{1}{2}\sqrt{\frac{4a}{3} - q_1 - q_2 - \frac{2b}{\sqrt{\frac{2a}{3} + q_1 + q_2}}}, \\
E_2^{s=2} &= \frac{1}{2}\sqrt{\frac{2a}{3} + q_1 + q_2} - \frac{1}{2}\sqrt{\frac{4a}{3} - q_1 - q_2 - \frac{2b}{\sqrt{\frac{2a}{3} + q_1 + q_2}}},
\end{aligned} \tag{7.157}$$

[36] Given that the relations under the square root are always positive.

where q_1, q_2 are given by

$$\begin{aligned} q_1 &= \frac{2^{1/3}(a^2+12c)}{3\left(-2a^3+27b^2+72ac+\sqrt{-4(a^2+12c)^3+(-2a^3+27b^2+72ac)^2}\right)^{1/3}}, \\ q_2 &= \frac{\left(-2a^3+27b^2+72ac+\sqrt{-4(a^2+12c)^3+(-2a^3+27b^2+72ac)^2}\right)^{1/3}}{3\cdot 2^{1/3}}. \end{aligned} \tag{7.158}$$

The negative eigenvalues correspond to particles, while the positive eigenvalues correspond to antiparticles. Specifically, the eigenvalues $E_1^{s=1}$ are always negative, and $E_2^{s=1}$ are always positive, meaning they correspond to particle and antiparticle states, respectively.

Notably, the eigenvalues $E_1^{s=2}$ and $E_2^{s=2}$ can change their signs if the following condition is satisfied:

$$\frac{1}{2}\sqrt{\frac{4a}{3}-q_1-q_2-\frac{2b}{\sqrt{\frac{2a}{3}+q_1+q_2}}} > \frac{1}{2}\sqrt{\frac{2a}{3}+q_1+q_2}. \tag{7.159}$$

If this condition holds throughout isotropization, a level crossing occurs. However, in this case, $E_1^{s=2}$ and $E_2^{s=2}$ change their signs simultaneously, ensuring charge conservation in curved spacetime.

Another important aspect of these results is the rotational contribution to the energy eigenvalues. The terms proportional to $2b$, which scale with Ω_3, enter with a positive sign for particle eigenstates and a negative sign for antiparticle eigenstates. Consequently, for $s=1$, the energy of the particle states increases due to the rotational contribution, while the energy of the antiparticle states decreases.

In contrast, for $s=2$, the eigenvalue $E_1^{s=2}$ is suppressed, whereas $E_2^{s=2}$ is enhanced, assuming that the first square root term is always smaller than the second one. This is due to the spin-angular velocity interaction term, and the results can be understood roughly as follows: if the spin is aligned with the angular velocity, the energy gets enhanced; if the spin is anti-aligned, the energy is suppressed.

For the previous case, we noticed that the energy eigenvalues could either be enhanced or suppressed, depending on s, for both particles and antiparticles. This effect stems directly from the anisotropy of space, which induces spin-dependent modifications in the energy spectrum. In contrast, here, the addition of the spin-angular velocity coupling leads to more complex energy modifications depending on the alignment of the two.

General solution

The general solution can be given as follows:

$$\Psi(\eta,\psi,\theta,\phi) = \sum_{s=1,2}\sum_{n\,l\,m}\left[a^s_{nlm}\Xi^s_{nlm}e^{-iE^s_{\hat{1}}\eta} + b^{s\dagger}_{nlm}\bar{\Xi}^s_{nlm}e^{-iE^s_{\hat{2}}\eta}\right], \tag{7.160}$$

where $E_2^{s=2} > 0$ and $E_1^{s=2} < 0$.

7.2.3 Diagonal Bianchi IX model

Solutions in the fixed background

In conformal time, the equations (7.109) and (7.110) for diagonal Bianchi IX at a fixed time take the form

$$\begin{aligned}\left[i\sigma^{\hat{0}}\partial_\eta + ie^{-(\beta_{\hat{i}}+\alpha)}\sigma^{\hat{i}}e_i + \frac{1}{2}F(\alpha,\beta_\pm)\right]\Psi_R = M\Psi_L,\\ \left[i\sigma^{\hat{0}}\partial_\eta - ie^{-(\beta_{\hat{i}}+\alpha)}\sigma^{\hat{i}}e_i - \frac{1}{2}F(\alpha,\beta_\pm)\right]\Psi_L = M\Psi_R.\end{aligned} \tag{7.161}$$

Substituting the temporal and spatial decomposition (7.114) into the equations and taking into account (7.115), the equations for the spatial part are written by

$$\begin{aligned}\left[E + ie^{-(\beta_{\hat{i}}+\alpha)}\sigma^{\hat{i}}e_i + \frac{1}{2}F(\alpha,\beta_\pm)\right]w_R = Mw_L,\\ \left[E - ie^{-(\beta_{\hat{i}}+\alpha)}\sigma^{\hat{i}}e_i - \frac{1}{2}F(\alpha,\beta_\pm)\right]w_L = Mw_R.\end{aligned} \tag{7.162}$$

Substituting the Pauli matrices, the first equation can be given by

$$\begin{pmatrix} E + \frac{1}{2}F(\alpha,\beta_\pm) + ie^{-\alpha}e^{-\beta_{\hat{3}}}e_{\hat{3}} & ie^{-\alpha}(e^{-\beta_{\hat{1}}}e_{\hat{1}} - ie^{-\beta_{\hat{2}}}e_{\hat{2}}) \\ ie^{-\alpha}(e^{-\beta_{\hat{1}}}e_{\hat{1}} + ie^{-\beta_{\hat{2}}}e_{\hat{2}}) & E + \frac{1}{2}F(\alpha,\beta_\pm) - ie^{-\alpha}e^{-\beta_{\hat{3}}}e_{\hat{3}} \end{pmatrix} w_R = Mw_L; \tag{7.163}$$

and the second equation reads

$$\begin{pmatrix} E - \frac{1}{2}F(\alpha,\beta_\pm) - ie^{-\alpha}e^{-\beta_{\hat{3}}}e_{\hat{3}} & -ie^{-\alpha}(e^{-\beta_{\hat{1}}}e_{\hat{1}} - ie^{-\beta_{\hat{2}}}e_{\hat{2}}) \\ -ie^{-\alpha}(e^{-\beta_{\hat{1}}}e_{\hat{1}} + ie^{-\beta_{\hat{2}}}e_{\hat{2}}) & E - \frac{1}{2}F(\alpha,\beta_\pm) + ie^{-\alpha}e^{-\beta_{\hat{3}}}e_{\hat{3}} \end{pmatrix} w_L = Mw_R. \tag{7.164}$$

Using the relations in (7.55) and $l_i = e^{-\beta_{\hat{i}}-\alpha}$, the equations can be rewritten in terms of body-fixed angular momentum operator, i.e.

$$\begin{pmatrix} E + \frac{1}{2}F(\alpha,\beta_\pm) + l_{\hat{3}}L_{\hat{3}} & \frac{l_{\hat{1}}-l_{\hat{2}}}{2}L_+ + \frac{l_{\hat{1}}+l_{\hat{2}}}{2}L_- \\ \frac{l_{\hat{1}}+l_{\hat{2}}}{2}L_+ + \frac{l_{\hat{1}}-l_{\hat{2}}}{2}L_- & E + \frac{1}{2}F(\alpha,\beta_\pm) - l_{\hat{3}}L_{\hat{3}} \end{pmatrix} w_R = Mw_L, \tag{7.165}$$

the second equation reads

$$\begin{pmatrix} E - \frac{1}{2}F(\alpha,\beta_\pm) - l_{\hat{3}}L_{\hat{3}} & \frac{l_{\hat{2}}-l_{\hat{1}}}{2}L_+ - \frac{l_{\hat{1}}+l_{\hat{2}}}{2}L_- \\ -\frac{l_{\hat{1}}+l_{\hat{2}}}{2}L_+ + \frac{l_{\hat{2}}-l_{\hat{1}}}{2}L_- & E - \frac{1}{2}F(\alpha,\beta_\pm) + l_{\hat{3}}L_{\hat{3}} \end{pmatrix} w_L = M w_R. \tag{7.166}$$

As already explained in Sec. 7.1.3, the spinor fields can be expanded as follows:

$$w_L = \begin{pmatrix} w_1 \\ w_2 \end{pmatrix} = \sum_n b^l_{mn} \begin{pmatrix} f^1_{lm}|l,m,n-\frac{1}{2}\rangle \\ f^2_{lm}|l,m,n+\frac{1}{2}\rangle \end{pmatrix}, \tag{7.167}$$

and

$$w_R = \begin{pmatrix} w_3 \\ w_4 \end{pmatrix} = \sum_n c^l_{mn} \begin{pmatrix} f^3_{lm}|l,m,n-\frac{1}{2}\rangle \\ f^4_{lm}|l,m,n+\frac{1}{2}\rangle \end{pmatrix} \tag{7.168}$$

The matrix equations (7.165) and (7.166) can be written as four separate equations. The first equation leads to

$$\begin{aligned} &\left(E + \frac{1}{2}F(\alpha,\beta_\pm) + l_{\hat{3}}L_{\hat{3}}\right) w_3 + \left(\frac{l_{\hat{1}}-l_{\hat{2}}}{2}L_+ + \frac{l_{\hat{1}}+l_{\hat{2}}}{2}L_-\right) w_4 = M w_1, \\ &\left(\frac{l_{\hat{1}}+l_{\hat{2}}}{2}L_+ + \frac{l_{\hat{1}}-l_{\hat{2}}}{2}L_-\right) w_3 + \left(E + \frac{1}{2}F(\alpha,\beta_\pm) - l_{\hat{3}}L_{\hat{3}}\right) w_4 = M w_2, \end{aligned} \tag{7.169}$$

and the second one

$$\begin{aligned} &\left(E - \frac{1}{2}F(\alpha,\beta_\pm) - l_{\hat{3}}L_{\hat{3}}\right) w_1 + \left(\frac{l_{\hat{2}}-l_{\hat{1}}}{2}L_+ - \frac{l_{\hat{1}}+l_{\hat{2}}}{2}L_-\right) w_2 = M w_3, \\ &\left(-\frac{l_{\hat{1}}+l_{\hat{2}}}{2}L_+ + \frac{l_{\hat{2}}-l_{\hat{1}}}{2}L_-\right) w_1 + \left(E - \frac{1}{2}F(\alpha,\beta_\pm) + l_{\hat{3}}L_{\hat{3}}\right) w_2 = M w_4. \end{aligned} \tag{7.170}$$

Using the eigenvalue equations (6.26), we obtain the following relations:

- The operator L_3 acting on $w_{1,3}$ and $w_{2,4}$:

$$L_3 \sum_n a^l_{mn}\Big|l,m,n+\frac{(-1)^\mu}{2}\Big\rangle = \sum_n a^l_{mn}\left(n+\frac{(-1)^\mu}{2}\right)\Big|l,m,n+\frac{(-1)^\mu}{2}\Big\rangle \tag{7.171}$$

where $\mu = 1,2,3,4$.

- The operator L_2 acting on $w_{1,3}$ and $w_{2,4}$:

$$L_+ \sum_n a^l_{mn}\Big|l,m,n+\frac{(-1)^\mu}{2}\Big\rangle = \sum_n a^l_{mn}\alpha_{n+\frac{(-1)^\mu}{2}+1}\Big|l,m,n+\frac{(-1)^\mu}{2}+1\Big\rangle \tag{7.172}$$

  - $\mu = 1,3$

$$L_+ \sum_n a^l_{mn}\Big|l,m,n-\frac{1}{2}\Big\rangle = \sum_n a^l_{mn}\alpha_{n+\frac{1}{2}}\Big|l,m,n+\frac{1}{2}\Big\rangle \tag{7.173}$$

– $\mu = 2, 4$

$$L_+ \sum_n a^l_{mn} \Big| l, m, n + \frac{1}{2} \Big\rangle = \sum_n a^l_{mn} \alpha_{n+\frac{3}{2}} \Big| l, m, n + \frac{1}{2} + 1 \Big\rangle$$
$$= \sum_k a^l_{m,(k-1)} \alpha_{k+\frac{1}{2}} \Big| l, m, k + \frac{1}{2} \Big\rangle, \tag{7.174}$$

where we introduced $k = n + 1$.

- The operator L_- acting on $w_{1,3}$ and $w_{2,4}$:

$$L_- \sum_n a^l_{mn} \Big| l, m, n + \frac{(-1)^\mu}{2} \Big\rangle = \sum_n a^l_{mn} \alpha_{n+\frac{(-1)^\mu}{2}} \Big| l, m, n + \frac{(-1)^\mu}{2} - 1 \Big\rangle \tag{7.175}$$

– $\mu = 1, 3$

$$L_- \sum_n a^l_{mn} \Big| l, m, n - \frac{1}{2} \Big\rangle = \sum_n a^l_{mn} \alpha_{n-\frac{1}{2}} \Big| l, m, n - \frac{3}{2} \Big\rangle$$
$$= \sum_p a^l_{m,(p+1)} \alpha_{p+\frac{1}{2}} \Big| l, m, p - \frac{1}{2} \Big\rangle, \tag{7.176}$$

where we introduced $p = n - 1$.

– $\mu = 2, 4$

$$L_- \sum_n a^l_{mn} \Big| l, m, n + \frac{1}{2} \Big\rangle = \sum_n a^l_{mn} \alpha_{n+\frac{1}{2}} \Big| l, m, n - \frac{1}{2} \Big\rangle. \tag{7.177}$$

Then, we substitute these relations into the above-mentioned four equations. The equations in (7.169) take the forms

$$\begin{aligned} & f^3_{lm} \sum_n c^l_{mn} \left[E + \frac{1}{2} F(\alpha, \beta_\pm) + l_{\hat{3}} \left(n - \frac{1}{2} \right) \right] \Big| l, m, n - \frac{1}{2} \Big\rangle \\ & + f^4_{lm} \sum_n \left[\frac{l_{\hat{1}} - l_{\hat{2}}}{2} c^l_{m,(n-1)} \alpha_{n+\frac{1}{2}} \Big| l, m, n + \frac{1}{2} \Big\rangle + \frac{l_{\hat{1}} + l_{\hat{2}}}{2} c^l_{mn} \alpha_{n+\frac{1}{2}} \Big| l, m, n - \frac{1}{2} \Big\rangle \right] \\ & = f^1_{lm} M \sum_n b^l_{mn} | l, m, n - \frac{1}{2} \rangle, \end{aligned} \tag{7.178}$$

and

$$\begin{aligned} & f^3_{lm} \sum_n \left[\frac{l_{\hat{1}} + l_{\hat{2}}}{2} c^l_{mn} \alpha_{n+\frac{1}{2}} \Big| l, m, n + \frac{1}{2} \Big\rangle + \frac{l_{\hat{1}} - l_{\hat{2}}}{2} c^l_{m,(n+1)} \alpha_{n+\frac{1}{2}} \Big| l, m, n - \frac{1}{2} \Big\rangle \right] \\ & + f^4_{lm} \sum_n c^l_{mn} \left[E + \frac{1}{2} F(\alpha, \beta_\pm) - l_{\hat{3}} \left(n + \frac{1}{2} \right) \right] \Big| l, m, n + \frac{1}{2} \Big\rangle \\ & = M f^2_{lm} \sum_n b^l_{mn} | l, m, n + \frac{1}{2} \rangle. \end{aligned} \tag{7.179}$$

Next, the equations in (7.170) lead to

$$
\begin{aligned}
&f^1_{lm}\sum_n b^l_{mn}\left[E-\frac{1}{2}F(\alpha,\beta_\pm)-l_{\hat{3}}\left(n-\frac{1}{2}\right)\right]\Big|l,m,n-\frac{1}{2}\Big\rangle\\
&+f^2_{lm}\sum_n\left[\frac{l_{\hat{2}}-l_{\hat{1}}}{2}b^l_{m,(n-1)}\alpha_{n+\frac{1}{2}}\Big|l,m,n+\frac{1}{2}\Big\rangle-\frac{l_{\hat{1}}+l_{\hat{2}}}{2}b^l_{mn}\alpha_{n+\frac{1}{2}}\Big|l,m,n-\frac{1}{2}\Big\rangle\right]\\
&=Mf^3_{lm}\sum_n c^l_{mn}\Big|l,m,n-\frac{1}{2}\Big\rangle,
\end{aligned}
\tag{7.180}
$$

and

$$
\begin{aligned}
&f^1_{lm}\sum_n\left[-\frac{l_{\hat{1}}+l_{\hat{2}}}{2}b^l_{mn}\alpha_{n+\frac{1}{2}}\Big|l,m,n+\frac{1}{2}\Big\rangle+\frac{l_{\hat{2}}-l_{\hat{1}}}{2}b^l_{m,(n+1)}\alpha_{n+\frac{1}{2}}\Big|l,m,n-\frac{1}{2}\Big\rangle\right]\\
&+f^2_{lm}\sum_n b^l_{mn}\left[E-\frac{1}{2}F(\alpha,\beta_\pm)+l_{\hat{3}}\left(n+\frac{1}{2}\right)\right]\Big|l,m,n+\frac{1}{2}\Big\rangle\\
&=Mf^4_{lm}\sum_n c^l_{mn}|l,m,n+\frac{1}{2}\rangle.
\end{aligned}
\tag{7.181}
$$

After lengthy, yet straightforward calculations, following the same steps described in Sec. 7.1.3, we obtain the following equation:

$$
\begin{aligned}
&\begin{pmatrix}
c^l_{mn}\left[E+\frac{1}{2}F(\alpha,\beta_\pm)+l_{\hat{3}}\left(n-\frac{1}{2}\right)\right] & \left[\frac{l_{\hat{1}}-l_{\hat{2}}}{2}c^l_{m,(n-2)}\alpha_{n-\frac{1}{2}}+\frac{l_{\hat{1}}+l_{\hat{2}}}{2}c^l_{mn}\alpha_{n+\frac{1}{2}}\right]\\
\left[\frac{l_{\hat{1}}+l_{\hat{2}}}{2}c^l_{mn}\alpha_{n+\frac{1}{2}}+\frac{l_{\hat{1}}-l_{\hat{2}}}{2}c^l_{m,(n+2)}\alpha_{n+\frac{3}{2}}\right] & c^l_{mn}\left[E+\frac{1}{2}F(\alpha,\beta_\pm)-l_{\hat{3}}\left(n+\frac{1}{2}\right)\right]
\end{pmatrix}
\begin{pmatrix} f^3_{lm}\\ f^4_{lm}\end{pmatrix}\\
&=Mb^l_{mn}\begin{pmatrix} f^1_{lm}\\ f^2_{lm}\end{pmatrix},
\end{aligned}
\tag{7.182}
$$

and

$$
\begin{aligned}
&\begin{pmatrix}
b^l_{mn}\left[E-\frac{1}{2}F(\alpha,\beta_\pm)-l_{\hat{3}}\left(n-\frac{1}{2}\right)\right] & \left[\frac{l_{\hat{2}}-l_{\hat{1}}}{2}b^l_{m,(n-2)}\alpha_{n-\frac{1}{2}}-\frac{l_{\hat{1}}+l_{\hat{2}}}{2}b^l_{mn}\alpha_{n+\frac{1}{2}}\right]\\
\left[-\frac{l_{\hat{1}}+l_{\hat{2}}}{2}b^l_{mn}\alpha_{n+\frac{1}{2}}+\frac{l_{\hat{2}}-l_{\hat{1}}}{2}b^l_{m,(n+2)}\alpha_{n+\frac{3}{2}}\right] & b^l_{mn}\left[E-\frac{1}{2}F(\alpha,\beta_\pm)+l_{\hat{3}}\left(n+\frac{1}{2}\right)\right]
\end{pmatrix}
\begin{pmatrix} f^1_{lm}\\ f^2_{lm}\end{pmatrix}\\
&=Mc^l_{mn}\begin{pmatrix} f^3_{lm}\\ f^4_{lm}\end{pmatrix}.
\end{aligned}
\tag{7.183}
$$

The energy eigenvalues can be determined by solving the equation

$$
\begin{aligned}
&\begin{pmatrix}
E-\frac{1}{2}F(\alpha,\beta_\pm)-l_{\hat{3}}\left(n-\frac{1}{2}\right) & \frac{l_{\hat{2}}-l_{\hat{1}}}{2}\frac{b^l_{m,(n-2)}}{b^l_{mn}}\alpha_{n-\frac{1}{2}}-\frac{l_{\hat{1}}+l_{\hat{2}}}{2}\alpha_{n+\frac{1}{2}}\\
-\frac{l_{\hat{1}}+l_{\hat{2}}}{2}\alpha_{n+\frac{1}{2}}+\frac{l_{\hat{2}}-l_{\hat{1}}}{2}\frac{b^l_{m,(n+2)}}{b^l_{mn}}\alpha_{n+\frac{3}{2}} & E-\frac{1}{2}F(\alpha,\beta_\pm)+l_{\hat{3}}\left(n+\frac{1}{2}\right)
\end{pmatrix}\\
&\times\begin{pmatrix}
E+\frac{1}{2}F(\alpha,\beta_\pm)+l_{\hat{3}}\left(n-\frac{1}{2}\right) & \frac{l_{\hat{1}}-l_{\hat{2}}}{2}\frac{c^l_{m,(n-2)}}{c^l_{mn}}\alpha_{n-\frac{1}{2}}+\frac{l_{\hat{1}}+l_{\hat{2}}}{2}\alpha_{n+\frac{1}{2}}\\
\frac{l_{\hat{1}}+l_{\hat{2}}}{2}\alpha_{n+\frac{1}{2}}+\frac{l_{\hat{1}}-l_{\hat{2}}}{2}\frac{c^l_{m,(n+2)}}{c^l_{mn}}\alpha_{n+\frac{3}{2}} & E+\frac{1}{2}F(\alpha,\beta_\pm)-l_{\hat{3}}\left(n+\frac{1}{2}\right)
\end{pmatrix}=M^2.
\end{aligned}
\tag{7.184}
$$

Due to the complexity of the obtained expressions, interpreting the final results remains challenging without assigning specific values to the unknown parameters. Consequently, the calculations are halted at this stage. Beyond this point, the remaining steps proceed analogously to those in previous models, yielding eigenvalues with a structure similar to those in (7.135) and (7.136), albeit with significantly more intricate expressions. However, since no qualitatively new physical insights would emerge, the key aspects can be sufficiently discussed within the axisymmetric case.

7.2.4 Rotating Bianchi IX model

Solutions in the fixed background

In conformal time, setting $N = e^{\alpha}$, the equations (7.109) and (7.110) take the form

$$\begin{aligned}
&\left[i\sigma^{\hat{0}}\partial_\eta + ie^{-\alpha}e^{-\beta_k}R^{i}{}_{\hat{i}}\sigma^{\hat{i}}e_i + \frac{1}{2}F(\alpha,\beta_\pm) - \frac{1}{2}e^{-\alpha}\sum_{\hat{l}}\left(1+\frac{I_{\hat{l}}}{4}\right)^{\frac{1}{2}}\Omega_{\hat{l}}\sigma^{\hat{l}}\right]\Psi_R = M\Psi_L,\\
&\left[i\sigma^{\hat{0}}\partial_\eta - ie^{-\alpha}e^{-\beta_k}R^{i}{}_{\hat{i}}\sigma^{\hat{i}}e_i - \frac{1}{2}F(\alpha,\beta_\pm) - \frac{1}{2}e^{-\alpha}\sum_{\hat{l}}\left(1+\frac{I_{\hat{l}}}{4}\right)^{\frac{1}{2}}\Omega_{\hat{l}}\sigma^{\hat{l}}\right]\Psi_L = M\Psi_R.
\end{aligned} \tag{7.185}$$

Decomposing the spinor field into temporal and spatial parts as in previous sections leads to the following spatial equations:

$$\begin{aligned}
&\left[E + ie^{-\alpha}e^{-\beta_k}R^{i}{}_{\hat{i}}\sigma^{\hat{i}}e_i + \frac{1}{2}F(\alpha,\beta_\pm) - \frac{1}{2}e^{-\alpha}\sum_{\hat{l}}\left(1+\frac{I_{\hat{l}}}{4}\right)^{\frac{1}{2}}\Omega_{\hat{l}}\sigma^{\hat{l}}\right]w_R = Mw_L,\\
&\left[E - ie^{-\alpha}e^{-\beta_k}R^{i}{}_{\hat{i}}\sigma^{\hat{i}}e_i - \frac{1}{2}F(\alpha,\beta_\pm) - \frac{1}{2}e^{-\alpha}\sum_{\hat{l}}\left(1+\frac{I_{\hat{l}}}{4}\right)^{\frac{1}{2}}\Omega_{\hat{l}}\sigma^{\hat{l}}\right]w_L = Mw_R.
\end{aligned} \tag{7.186}$$

For shorthand notation, we introduce $\bar{I}_{\hat{i}} = \left(1+\frac{I_{\hat{i}}}{4}\right)^{\frac{1}{2}}$ and $l_{\hat{i}} = e^{\beta_{\hat{i}}+\alpha}$. Substituting the Pauli matrices explicitly and utilizing the relation between the right- and left-invariant bases, the equations can be rewritten as follows:

$$\begin{pmatrix} E+\frac{1}{2}F(\alpha,\beta_\pm)+il_{\hat{3}}\tilde{e}_{\hat{3}}-\frac{1}{2}e^{-\alpha}\bar{I}_3\Omega_{\hat{3}} & i(l_{\hat{1}}\tilde{e}_{\hat{1}}-il_{\hat{2}}\tilde{e}_{\hat{2}})-\frac{1}{2}e^{-\alpha}\left(\bar{I}_1\Omega_{\hat{1}}-i\bar{I}_2\Omega_{\hat{2}}\right) \\ i(l_{\hat{1}}\tilde{e}_{\hat{1}}+il_{\hat{2}}\tilde{e}_{\hat{2}})-\frac{1}{2}e^{-\alpha}\left(\bar{I}_1\Omega_{\hat{1}}+i\bar{I}_2\Omega_{\hat{2}}\right) & E+\frac{1}{2}F(\alpha,\beta_\pm)-il_{\hat{3}}\tilde{e}_{\hat{3}}+\frac{1}{2}e^{-\alpha}\bar{I}_3\Omega_{\hat{3}} \end{pmatrix} w_R = Mw_L, \tag{7.187}$$

and

$$\begin{pmatrix} E-\frac{1}{2}F(\alpha,\beta_\pm)-il_{\hat{3}}\tilde{e}_{\hat{3}}-\frac{1}{2}e^{-\alpha}\bar{I}_3\Omega_{\hat{3}} & -i(l_{\hat{1}}\tilde{e}_{\hat{1}}-il_{\hat{2}}\tilde{e}_{\hat{2}})-\frac{1}{2}e^{-\alpha}\left(\bar{I}_1\Omega_{\hat{1}}-i\bar{I}_2\Omega_{\hat{2}}\right) \\ -i(l_{\hat{1}}\tilde{e}_{\hat{1}}+il_{\hat{2}}\tilde{e}_{\hat{2}})-\frac{1}{2}e^{-\alpha}\left(\bar{I}_1\Omega_{\hat{1}}+i\bar{I}_2\Omega_{\hat{2}}\right) & E-\frac{1}{2}F(\alpha,\beta_\pm)+il_{\hat{3}}\tilde{e}_{\hat{3}}+\frac{1}{2}e^{-\alpha}\bar{I}_3\Omega_{\hat{3}} \end{pmatrix} w_L = Mw_R. \tag{7.188}$$

Using the relation between the left-invariant basis and the space-fixed angular momentum operator, given by $\tilde{L}_i = -i\tilde{e}_i$, and recalling the relations from (7.55), the equations can be given by

$$\begin{pmatrix} E + \frac{1}{2}F(\alpha,\beta_\pm) - l_{\hat{3}}\tilde{L}_{\hat{3}} - \frac{1}{2}e^{-\alpha}\bar{I}_3\Omega_{\hat{3}} & \frac{l_{\hat{2}}-l_{\hat{1}}}{2}\tilde{L}_+ - \frac{l_{\hat{1}}+l_{\hat{2}}}{2}\tilde{L}_- - \frac{1}{2}e^{-\alpha}\left(\bar{I}_1\Omega_{\hat{1}} - i\bar{I}_2\Omega_{\hat{2}}\right) \\ -\frac{l_{\hat{1}}+l_{\hat{2}}}{2}\tilde{L}_+ + \frac{l_{\hat{2}}-l_{\hat{1}}}{2}\tilde{L}_- - \frac{1}{2}e^{-\alpha}\left(\bar{I}_1\Omega_{\hat{1}} + i\bar{I}_2\Omega_{\hat{2}}\right) & E + \frac{1}{2}F(\alpha,\beta_\pm) + l_{\hat{3}}\tilde{L}_{\hat{3}} + \frac{1}{2}e^{-\alpha}\bar{I}_3\Omega_{\hat{3}} \end{pmatrix} \begin{pmatrix} w_3 \\ w_4 \end{pmatrix} = M \begin{pmatrix} w_1 \\ w_2 \end{pmatrix}, \tag{7.189}$$

and

$$\begin{pmatrix} E - \frac{1}{2}F(\alpha,\beta_\pm) + l_{\hat{3}}\tilde{L}_{\hat{3}} - \frac{1}{2}e^{-\alpha}\bar{I}_3\Omega_{\hat{3}} & \frac{l_{\hat{1}}-l_{\hat{2}}}{2}\tilde{L}_+ + \frac{l_{\hat{1}}+l_{\hat{2}}}{2}\tilde{L}_- - \frac{1}{2}e^{-\alpha}\left(\bar{I}_1\Omega_{\hat{1}} - i\bar{I}_2\Omega_{\hat{2}}\right) \\ \frac{l_{\hat{1}}+l_{\hat{2}}}{2}\tilde{L}_+ + \frac{l_{\hat{1}}-l_{\hat{2}}}{2}\tilde{L}_- - \frac{1}{2}e^{-\alpha}\left(\bar{I}_1\Omega_{\hat{1}} + i\bar{I}_2\Omega_{\hat{2}}\right) & E - \frac{1}{2}F(\alpha,\beta_\pm) - l_{\hat{3}}\tilde{L}_{\hat{3}} + \frac{1}{2}e^{-\alpha}\bar{I}_3\Omega_{\hat{3}} \end{pmatrix} \begin{pmatrix} w_1 \\ w_2 \end{pmatrix} = M \begin{pmatrix} w_3 \\ w_4 \end{pmatrix}. \tag{7.190}$$

The spinor field can be expanded in terms of the eigenbasis of asymmetric “ideal” top (related to the space-fixed Hamiltonian), given by (6.93). Hence, we have

$$w_L^{nl} = \begin{pmatrix} w_1 \\ w_2 \end{pmatrix} = \sum_m \tilde{b}^l_{mn} \begin{pmatrix} f^1_{ln}|l, m-\frac{1}{2}, n\rangle \\ f^2_{ln}|l, m+\frac{1}{2}, n\rangle \end{pmatrix}, \tag{7.191}$$

and

$$w_R^{nl} = \begin{pmatrix} w_3 \\ w_4 \end{pmatrix} = \sum_m \tilde{c}^l_{mn} \begin{pmatrix} f^3_{ln}|l, m-\frac{1}{2}, n\rangle \\ f^4_{ln}|l, m+\frac{1}{2}, n\rangle \end{pmatrix}. \tag{7.192}$$

Next, we substitute these expansions into (7.189)and (7.190) and simplify the resulting equations, following the same steps as in the previous sections. The detailed calculations are omitted here, as they closely mirror those presented earlier.

We obtain the following equations

$$\begin{pmatrix} b_{11} & b_{12} \\ b_{21} & b_{22} \end{pmatrix} \begin{pmatrix} f^3_{ln} \\ f^4_{ln} \end{pmatrix} = M\tilde{b}^l_{mn} \begin{pmatrix} f^1_{ln} \\ f^2_{ln} \end{pmatrix}, \tag{7.193}$$

where

$$\begin{aligned} b_{11} &= \tilde{c}^l_{mn}\left(E + \frac{1}{2}F(\alpha,\beta_\pm) - l_{\hat{3}}\left(m - \frac{1}{2}\right) - \frac{1}{2}e^{-\alpha}\bar{I}_3\Omega_{\hat{3}}\right), \\ b_{12} &= \frac{l_{\hat{2}}-l_{\hat{1}}}{2}\tilde{c}^l_{m-2,n}\alpha_{m-\frac{1}{2}} - \frac{l_{\hat{1}}+l_{\hat{2}}}{2}\tilde{c}^l_{mn}\alpha_{m+\frac{1}{2}} - \frac{1}{2}e^{-\alpha}\left(\bar{I}_1\Omega_{\hat{1}} - i\bar{I}_2\Omega_{\hat{2}}\right)\tilde{c}^l_{m-1,n}, \\ b_{21} &= -\frac{l_{\hat{1}}+l_{\hat{2}}}{2}\tilde{c}^l_{mn}\alpha_{m+\frac{1}{2}} + \frac{l_{\hat{2}}-l_{\hat{1}}}{2}\tilde{c}^l_{m+2,n}\alpha_{m+\frac{3}{2}} - \frac{1}{2}e^{-\alpha}\left(\bar{I}_1\Omega_{\hat{1}} + i\bar{I}_2\Omega_{\hat{2}}\right)\tilde{c}^l_{m+1,n}, \\ b_{22} &= \tilde{c}^l_{mn}\left(E + \frac{1}{2}F(\alpha,\beta_\pm) + l_{\hat{3}}\left(m + \frac{1}{2}\right) + \frac{1}{2}e^{-\alpha}\bar{I}_3\Omega_{\hat{3}}\right), \end{aligned} \tag{7.194}$$

and

$$\begin{pmatrix} c_{11} & c_{12} \\ c_{21} & c_{22} \end{pmatrix} \begin{pmatrix} f^1_{ln} \\ f^2_{ln} \end{pmatrix} = \tilde{c}^l_{mn}M \begin{pmatrix} f^3_{ln} \\ f^4_{ln} \end{pmatrix}, \tag{7.195}$$

where

$$
\begin{aligned}
c_{11} &= \tilde{b}^l_{mn}\left(E - \frac{1}{2}F(\alpha,\beta_\pm) + l_{\hat{3}}\left(m - \frac{1}{2}\right) - \frac{1}{2}e^{-\alpha}\bar{I}_3\Omega_{\hat{3}}\right), \\
c_{12} &= \left[\frac{l_{\hat{1}} - l_{\hat{2}}}{2}\tilde{b}^l_{m-2,n}\alpha_{m-\frac{1}{2}} + \frac{l_{\hat{1}} + l_{\hat{2}}}{2}\tilde{b}^l_{mn}\alpha_{m+\frac{1}{2}} - \frac{1}{2}e^{-\alpha}\left(\bar{I}_1\Omega_{\hat{1}} - i\bar{I}_2\Omega_{\hat{2}}\right)\tilde{b}^l_{m-1,n}\right], \\
c_{21} &= \left[\frac{l_{\hat{1}} + l_{\hat{2}}}{2}\tilde{b}^l_{mn}\alpha_{m+\frac{1}{2}} + \frac{l_{\hat{1}} - l_{\hat{2}}}{2}\tilde{b}^l_{m+2,n}\alpha_{m+\frac{3}{2}} - \frac{1}{2}e^{-\alpha}\left(\bar{I}_1\Omega_{\hat{1}} + i\bar{I}_2\Omega_{\hat{2}}\right)\tilde{b}^l_{m+1,n}\right], \\
c_{22} &= \tilde{b}^l_{mn}\left(E - \frac{1}{2}F(\alpha,\beta_\pm) - l_{\hat{3}}\left(m + \frac{1}{2}\right) + \frac{1}{2}e^{-\alpha}\bar{I}_3\Omega_{\hat{3}}\right).
\end{aligned}
\tag{7.196}
$$

The energy eigenvalues can be determined by solving the equation

$$
\begin{pmatrix} c_{11} & c_{12} \\ c_{21} & c_{22} \end{pmatrix}\begin{pmatrix} b_{11} & b_{12} \\ b_{21} & b_{22} \end{pmatrix} = M^2. \tag{7.197}
$$

Here as well, due to the complexity of the obtained expressions, we conclude the calculations at this stage. However, we note that for the rotating Bianchi IX model, the energy eigenvalues will have a structure similar to those in (7.157) for the axisymmetric Bianchi IX case, though with significantly more intricate expressions.

7.3 Discussion of results

Thus, in this section, we discussed the solutions of the Dirac field equations for a range of Bianchi IX models in a fixed background. For the axisymmetric Bianchi IX model, we showed that, unlike the case for Weyl spinors, Dirac spinors have clear positive and negative energy eigenvalues corresponding to particles and antiparticles, meaning that level crossing does not occur (as expected due to charge conservation). Interestingly, we observe that for both particles and antiparticles, the energy eigenvalues differ between the two spin states, with one state being enhanced and the other suppressed due to geometric anisotropy. In other words, the anisotropy of space induces spin-dependent modifications in the energy spectrum. Furthermore, for the rotating axisymmetric Bianchi IX model, the situation becomes even more complex. In addition to the energy difference arising from spin states due to anisotropy (i.e., anisotropy factors), the rotational contribution to the energy eigenvalues enters with a positive sign for particle eigenstates and a negative sign for antiparticle eigenstates. As a result, we obtain four distinct eigenvalues corresponding to particles and antiparticles, with two spin states each. In addition, the final results for the diagonal and rotating Bianchi IX models are not calculated explicitly due to the appearance of terms that can only be determined by solving the second-order equation for the Dirac spinor field in Bianchi IX model, as discussed in Sec. 6.3. However, it is important to note that these more complicated cases do not introduce any new physical phenomena of interest in the context of matter-antimatter asymmetry.

Finally, one could draw an analogy between these results and the Zeeman effect in quantum mechanics, where atomic energy levels split in the presence of an external magnetic field. This splitting arises due to the interaction between the magnetic field and the magnetic moment of an atomic electron, which is a consequence of its orbital motion and spin. The energy separation between levels occurs as a result of the alignment of the magnetic moment with the external field, with the separation proportional to the strength of the magnetic field. In our case, the "angular velocity" of the universe plays a similar role to the magnetic field, influencing different energy eigenstates in distinct ways and causing a "splitting" of energy levels—an effect absent in isotropic models.

8 Conclusion and outlook

This thesis set out to explore a potential resolution to the matter-antimatter asymmetry in the Universe within a homogeneous and anisotropic geometric background. Specifically, the Weyl and Dirac spinor fields were studied in the context of the Bianchi IX universe. The choice of the Bianchi IX model was motivated by its role in the dynamics of the early universe, as described by the BKL conjecture, and its potential contribution to angular momentum generation in a cosmological setting. The analysis was conducted in a fixed background as an initial step toward understanding the fundamental features of the particle spectrum in such spacetimes. This approach provides a foundation for future refinements using the adiabatic approximation and further developments based on the WKB approximation. The study demonstrated that the anisotropies of the Bianchi IX model induce an asymmetry in the energy spectrum of particles and antiparticles, highlighting the potential significance of geometric effects in addressing matter-antimatter asymmetry.

We extended the discussion of Weyl spinors, initially explored by Gibbons for the axisymmetric Bianchi IX model, to a broader range of models, beginning with the simplest cases. We demonstrated that the fermion level crossing observed in the simplest model also appears across the entire set of models considered. However, the specific mode values at which the level crossing occurs vary between models, while the underlying physical interpretation remains consistent. The phenomenon of level crossing arises due to the anisotropy of spacetime, as in such geometries, the energy eigenvalues do not exhibit clearly defined positive or negative signs corresponding to antiparticles and particles, a feature that is absent in isotropic spacetimes. Although neutrinos cannot be Weyl fermions, the discussion of level crossing remains relevant, as it contributes to ongoing investigations within the context of gravitational leptogenesis [149].

We analyzed the solutions of the Dirac field equations in a range of Bianchi IX models under the assumption of a fixed background. For the axisymmetric Bianchi IX model, we demonstrated that, in contrast to Weyl spinors, Dirac spinors exhibit well-defined positive and negative energy eigenvalues corresponding to particles and antiparticles, preventing level crossing as expected from charge conservation. Notably, we found that energy eigenvalues differ between spin states for both particles and antiparticles, with one state being enhanced and the other suppressed due to geometric anisotropy. This indicates that spatial anisotropy induces spin-dependent modifications in the energy spectrum. For the rotating axisymmetric Bianchi IX model, the situation becomes even more intricate. Beyond the energy differences arising from anisotropy, rotational effects introduce an additional contribution to the energy eigenvalues, due to spin-angular velocity coupling, appearing with a positive sign for particle eigenstates and a negative sign for antiparticle eigenstates. Consequently, four distinct eigenvalues emerge, corresponding to particles and antiparticles with two spin states each. The final results for the general diagonal and rotating Bianchi IX models are not computed explicitly due to the complexity of the expressions, which require solving second-order equations for the Dirac spinor field. However, these cases do not introduce any qualitatively new physical phenomena.

Therefore, these results highlight the significance of background anisotropies in the search for an explanation of the matter-antimatter asymmetry and encourage further investigation in this direction. This work serves as an initial step, utilizing the simplified and somewhat unrealistic fixed-background approximation. As noted earlier, the next logical step is to apply the adiabatic approximation to refine these results and bring the model closer to more realistic conditions. Additionally, our analysis has focused on the free field, but to explore annihilation processes and the anisotropic effects of the Bianchi IX model on these processes, it will be necessary to extend the study to Quantum Electrodynamics (QED).

Since baryons are the primary contributors to the matter density of the Universe, a complete analysis of baryon asymmetry due to geometric anisotropies requires studying Quantum Chromodynamics (QCD) in the Bianchi IX model. In this framework, one must also consider sphaleron processes and CP-violating effects within the Standard Model, to assess whether these effects in an anisotropic universe could be more significant than in FLRW models. If so, this could provide an explanation for the matter-antimatter asymmetry in terms of geometric effects, without the need to invoke physics beyond the Standard Model.

Finally, anisotropic universe models present a potential explanation for the observed CMB anomalies [89], [90]. Studies on dark matter and matter-antimatter asymmetry within the ΛCDM framework highlight the need for extending beyond the Standard Model of particle physics. Furthermore, the challenges associated with the cold dark matter (CDM) model emphasize the limitations of the ΛCDM model, suggesting the need for revisions to its highly symmetric assumptions, as well as to the current Standard Model of particle physics. The work presented in this thesis lays the foundation for addressing these cosmic puzzles within a geometric framework, without relying on beyond Standard Model physics. Given that the highly symmetric, homogeneous, and isotropic universe we observe today is unlikely to have been the initial state of the Universe's evolution, the exploration of anisotropic models offers a more realistic approach.

A Appendix

A.1 Euler angles

In classical mechanics, the motion of a rigid body is studied by considering either the rotation of the body itself or the rotation of the coordinate system. When the coordinate system is rotated counterclockwise, it corresponds to a clockwise rotation of the body relative to the new frame. This type of transformation, where the coordinate system is rotated, is called a *passive* transformation. Conversely, when the transformation is applied directly to the body while keeping the coordinate system fixed, it is referred to as an *active* transformation. In this discussion, we will use the rotation of the coordinate system.

To specify the orientation of a rigid body with respect to the fixed coordinate system, three independent parameters are needed. The *Euler angles* can be used as such parameters [126], [143], [144]. These angles are the angles of three successive rotations required to carry a set of movable coordinates (attached to the rigid body) from an initial orientation, coinciding with the x, y, z fixed coordinate system, to a final orientation, coinciding with the x', y', z' system. Thus, the three Euler angles, θ, ϕ, ψ, completely define the orientation of the x', y', z' axes with respect to a set of fixed axes x, y, z.

The rotations of one coordinate system relative to another are described by orthogonal matrices with a determinant of $+1$. These matrices can be expressed in terms of Euler angles.

The choice of the sequence of rotations around different axes is arbitrary. The only constraint is that after the initial rotation (about any of the three Cartesian axes), the following two rotations must not be around the same axis. Based on this, there are 12 possible conventions for defining Euler angles. Additionally, some authors use a left-handed coordinate system, creating further variations in the literature, which can cause inconvenience when working across different branches of physics.

The three most frequently used conventions are zxz, zyz, and xyz. As their names suggest, the first two differ only in the choice of the axis for the second rotation, while the first and third rotations are performed around the z-axis.

The zxz-convention is often used in Classical Mechanics to describe the motion of a rigid body. In Quantum Mechanics, Quantum Field Theory, Nuclear Physics, and Particle Physics, the zyz-convention is the most common choice. In engineering, the xyz-convention is used, where rotations are performed around three different axes. In this case, the angles are also known as Tait-Bryan angles.

Details of these conventions are provided in the following subsections.

zyz-convention

As demonstrated in Fig. 3, the three successive rotations described by the Euler angles are as follows:

- Rotate the initial system of axes, x, y, z, *counterclockwise* about the z-axis by an angle ϕ $(0 \leq \phi \leq 2\pi)$, into new axes labeled by ξ, η, ζ.

- Rotate the axes ξ, η, ζ about the η-axis *counterclockwise* by and angle θ $(0 \leq \theta \leq \pi)$, to produce another intermediate set of axes ξ', η', ζ'. The line of intersections of the two planes x, y and ξ', η' is called the line of nodes. It coincides with η'.

- Rotate the axes ξ', η', ζ' about the ξ'-axis *counterclockwise* by an angle ψ $(0 \leq \psi \leq 2\pi)$, which finally leads to the x', y', z' system of axes.

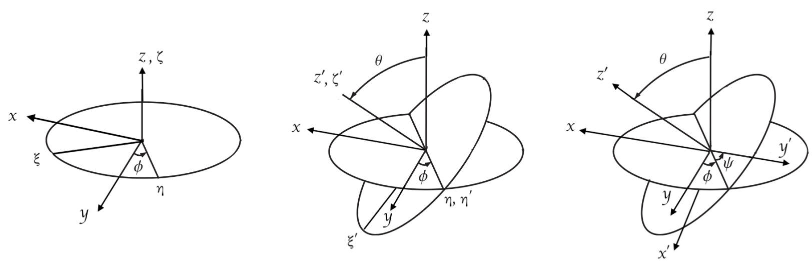

Figure 3: Euler angles.

Let us now present the matrices corresponding to the three rotations described above. The first rotation, about the z-axis, is given by the following matrix:

$$R_z(\phi) = \begin{pmatrix} \cos\phi & \sin\phi & 0 \\ -\sin\phi & \cos\phi & 0 \\ 0 & 0 & 1 \end{pmatrix}, \tag{A.1}$$

Next, the matrix for a rotation about the intermediate y-axis (i.e., η') is as follows:

$$R_y(\theta) = \begin{pmatrix} \cos\theta & 0 & -\sin\theta \\ 0 & 1 & 0 \\ \sin\theta & 0 & \cos\theta \end{pmatrix}, \tag{A.2}$$

Finally, the rotation about the z' leads to:

$$R_z(\psi) = \begin{pmatrix} \cos\psi & \sin\psi & 0 \\ -\sin\psi & \cos\psi & 0 \\ 0 & 0 & 1 \end{pmatrix}. \tag{A.3}$$

Thus, the rotation describing the transformation from the x, y, z axes to the x', y', z' axes is given by

$$\mathbf{x}' = R\,\mathbf{x}, \quad \text{where} \quad R = R_z(\psi)R_y(\theta)R_z(\phi), \tag{A.4}$$

which reads explicitly

$$R = \begin{pmatrix} \cos\theta\cos\phi\cos\psi - \sin\phi\sin\psi & \cos\theta\cos\psi\sin\phi + \cos\phi\sin\psi & -\cos\psi\sin\theta \\ -\cos\psi\sin\phi - \cos\theta\cos\phi\sin\psi & \cos\phi\cos\psi - \cos\theta\sin\phi\sin\psi & \sin\theta\sin\psi \\ \cos\phi\sin\theta & \sin\theta\sin\phi & \cos\theta \end{pmatrix}. \tag{A.5}$$

The inverse transformation, from body coordinates to space axes, is given by

$$\mathbf{x} = R^{-1}\mathbf{x}', \tag{A.6}$$

where

$$R^{-1} = \begin{pmatrix} \cos\theta\cos\phi\cos\psi - \sin\phi\sin\psi & -\cos\psi\sin\phi - \cos\theta\cos\phi\sin\psi & \cos\phi\sin\theta \\ \cos\theta\cos\psi\sin\phi + \cos\phi\sin\psi & \cos\phi\cos\psi - \cos\theta\sin\phi\sin\psi & \sin\theta\sin\phi \\ -\cos\psi\sin\theta & \sin\theta\sin\psi & \cos\theta \end{pmatrix}. \tag{A.7}$$

zxz-convention

In this convention, the only difference from zyz-convention is that the second rotation is about an intermediate x-axis (or ξ') instead. Hence, the two matrices that describe rotations around the z-axis are the same.

Thus, the rotation matrices in zxz-convention are given by

$$R_z(\phi) = \begin{pmatrix} \cos\phi & \sin\phi & 0 \\ -\sin\phi & \cos\phi & 0 \\ 0 & 0 & 1 \end{pmatrix}, \tag{A.8}$$

for the rotation about intermediate x-axis (i.e., ξ') is

$$R_x(\theta) = \begin{pmatrix} 1 & 0 & 0 \\ 0 & \cos\theta & \sin\theta \\ 0 & -\sin\theta & \cos\theta \end{pmatrix}, \tag{A.9}$$

and

$$R_z(\psi) = \begin{pmatrix} \cos\psi & \sin\psi & 0 \\ -\sin\psi & \cos\psi & 0 \\ 0 & 0 & 1 \end{pmatrix}. \tag{A.10}$$

The matrix of the complete transformation is given by

$$R = \begin{pmatrix} \cos\psi\cos\phi - \cos\theta\sin\phi\sin\psi & \cos\psi\sin\phi + \cos\theta\cos\phi\sin\psi & \sin\psi\sin\theta \\ -\sin\psi\cos\phi - \cos\theta\sin\phi\cos\psi & -\sin\psi\sin\phi + \cos\theta\cos\phi\cos\psi & \cos\psi\sin\theta \\ \sin\theta\sin\phi & -\sin\theta\cos\phi & \cos\theta \end{pmatrix}. \tag{A.11}$$

The inverse rotation matrix is

$$R^{-1} = \begin{pmatrix} \cos\psi\cos\phi - \cos\theta\sin\phi\sin\psi & -\sin\psi\cos\phi - \cos\theta\sin\phi\cos\psi & \sin\theta\sin\phi \\ \cos\psi\sin\phi + \cos\theta\cos\phi\sin\psi & -\sin\psi\sin\phi + \cos\theta\cos\phi\cos\psi & -\sin\theta\cos\phi \\ \sin\theta\sin\psi & \sin\theta\cos\psi & \cos\theta \end{pmatrix}. \tag{A.12}$$

xyz-convention

Here, the rotations are performed around three different axes: first, a rotation about the z-axis by an angle ϕ, then a rotation about an intermediate y-axis by an angle θ, and finally, a rotation about the final x-axis by an angle ψ.

The rotation matrices in the xyz-convention read

$$R_z(\phi) = \begin{pmatrix} \cos\phi & \sin\phi & 0 \\ -\sin\phi & \cos\phi & 0 \\ 0 & 0 & 1 \end{pmatrix}, \tag{A.13}$$

for the rotation about the intermediate y-axis

$$R_y(\theta) = \begin{pmatrix} \cos\theta & 0 & -\sin\theta \\ 0 & 1 & 0 \\ \sin\theta & 0 & \cos\theta \end{pmatrix}, \tag{A.14}$$

and for the rotation abound x-axis

$$R_x(\psi) = \begin{pmatrix} 1 & 0 & 0 \\ 0 & \cos\psi & \sin\psi \\ 0 & -\sin\psi & \cos\psi \end{pmatrix}. \tag{A.15}$$

Hence, the complete rotation matrix takes the form

$$R = \begin{pmatrix} \cos\theta\cos\phi & \cos\theta\sin\phi & -\sin\theta \\ \sin\psi\sin\theta\cos\phi - \cos\psi\sin\phi & \sin\psi\sin\theta\sin\phi + \cos\psi\cos\phi & \cos\theta\sin\psi \\ \cos\psi\sin\theta\cos\phi + \sin\psi\sin\theta & \cos\psi\sin\theta\sin\phi - \sin\psi\cos\phi & \cos\theta\cos\psi \end{pmatrix}. \tag{A.16}$$

Also, the inverse of it is given by

$$R^{-1} = \begin{pmatrix} \cos\theta\cos\phi & \sin\psi\sin\theta\cos\phi - \cos\psi\sin\phi & \cos\psi\cos\phi\sin\theta + \sin\psi\sin\phi \\ \cos\theta\sin\phi & \sin\psi\sin\theta\sin\phi + \cos\psi\cos\phi & \cos\psi\sin\theta\sin\phi - \sin\psi\cos\phi \\ -\sin\theta & \cos\theta\sin\psi & \cos\theta\cos\psi \end{pmatrix}. \tag{A.17}$$

A.2 Invariant basis of Bianchi IX

To construct the invariant basis $\{e_i\}$ for the Bianchi type-IX model, we follow the approach outlined in [150]. The basis will be expressed in terms of the Euler angles in the zyz-convention[37].

The general rotation $R \in SO(3)$ is a product of three successive rotation matrices, as given by (5.4). Explicitly, it takes the form

$$R = \begin{pmatrix} \cos\theta\cos\phi\cos\psi - \sin\phi\sin\psi & \cos\theta\cos\psi\sin\phi + \cos\phi\sin\psi & -\cos\psi\sin\theta \\ -\cos\psi\sin\phi - \cos\theta\cos\phi\sin\psi & \cos\phi\cos\psi - \cos\theta\sin\phi\sin\psi & \sin\theta\sin\psi \\ \cos\phi\sin\theta & \sin\theta\sin\phi & \cos\theta \end{pmatrix}. \tag{A.18}$$

The rotation group $SO(3)$ is a smooth manifold, with points corresponding to all 3×3 rotation matrices R. To construct an invariant basis, we consider curves $C(\lambda)$ passing through $C(0) = I \in SO(3)$, and calculate the tangent vectors of these curves at $\lambda = 0$. These tangent vectors will serve as the generators of rotations about the x, y, and z axes, denoted by e_1, e_2, and e_3, respectively. Therefore, we consider the following curves in terms of the parameter λ:

- For the rotation about the z-axis

$$C(\lambda) = R_z(\lambda)R, \tag{A.19}$$

- For the rotation about the x-axis

$$C(\lambda) = R_x(\lambda)R, \tag{A.20}$$

- For the rotation about the y-axis

$$C(\lambda) = R_y(\lambda)R, \tag{A.21}$$

On the other hand, we can express the curves as

$$C(\lambda) = R_z(\psi(\lambda))R_y(\theta(\lambda))R_z(\phi(\lambda)), \tag{A.22}$$

where $\psi(\lambda)$, $\theta(\lambda)$ and $\phi(\lambda)$ are functions that describe the curve. For the first curve, we have

$$C(\lambda) = R_z(\lambda)R_z(\psi)R_y(\theta)R_z(\phi) = R_z(\lambda + \psi)R_y(\theta)R_z(\phi). \tag{A.23}$$

[37]Note that in [150], the zxz-convention of Euler angles is used. Therefore, the invariant basis obtained here is different from the one calculated in the book.

Comparing this to (A.22), we obtain

$$\psi(\lambda) = \psi + \lambda, \quad \theta(\lambda) = \theta, \quad \phi(\lambda) = \phi. \tag{A.24}$$

The tangent vector of the curve at $\lambda = 0$ is given by

$$\frac{d}{d\lambda} C(\lambda)\Big|_{\lambda=0} = \left[\frac{d\psi(\lambda)}{d\lambda} \frac{\partial}{\partial\psi} + \frac{d\theta(\lambda)}{d\lambda} \frac{\partial}{\partial\theta} + \frac{d\phi(\lambda)}{d\lambda} \frac{\partial}{\partial\phi} \right] C(\lambda)\Big|_{\lambda=0}. \tag{A.25}$$

Therefore, we obtain

$$e_3 = \frac{\partial}{\partial\psi}. \tag{A.26}$$

Next, we consider the curve

$$C(\lambda) = R_x(\lambda)\mathcal{P} = R_x(\lambda)R_z(\psi)R_y(\theta)R_z(\phi). \tag{A.27}$$

For small λ, the matrix $R_x(\lambda)$ reads

$$R_x(\lambda) = \begin{pmatrix} 1 & 0 & 0 \\ 0 & 1 & \lambda \\ 0 & -\lambda & 1 \end{pmatrix}. \tag{A.28}$$

By calculating $C(\lambda)$ explicitly and comparing the resulting matrix with (A.22), we obtain the following relations:

$$\psi(\lambda) = \arcsin\left(\frac{\lambda\cos\theta + \sin\theta\sin\psi}{\sin\theta(\lambda)}\right), \quad \theta(\lambda) = \arccos\left(\cos\theta - \lambda\sin\theta\sin\psi\right), \tag{A.29}$$

and

$$\phi(\lambda) = \arcsin\left(\frac{\sin\theta\sin\phi - \lambda(\cos\phi\cos\psi - \cos\theta\sin\phi\sin\psi)}{\sin\theta(\lambda)}\right). \tag{A.30}$$

This leads to

$$\frac{d\psi(\lambda)}{d\lambda}\Big|_{\lambda=0} = \cot\theta\cos\psi, \quad \frac{d\theta(\lambda)}{d\lambda}\Big|_{\lambda=0} = \frac{\sin\psi\sin\theta}{\sqrt{1-(\cos\theta - \lambda\sin\psi\sin\theta)^2}}\Big|_{\lambda=0} = \sin\psi, \tag{A.31}$$

and

$$\frac{d\phi(\lambda)}{d\lambda}\Big|_{\lambda=0} = -\frac{\cos\psi}{\sin\theta}. \tag{A.32}$$

Substitute the above results into (A.25), we obtain

$$e_1 = \sin\psi\frac{\partial}{\partial\theta} + \cos\psi\left(\cot\theta\frac{\partial}{\partial\psi} - \frac{1}{\sin\theta}\frac{\partial}{\partial\phi}\right). \tag{A.33}$$

Finally, let us consider the the last curve, which reads

$$C(\lambda) = R_y(\lambda)R = R_y(\lambda)R_z(\psi)R_y(\theta)R_z(\phi). \tag{A.34}$$

For small λ, the matrix $R_y(\lambda)$ is given by

$$R_y(\lambda) = \begin{pmatrix} 1 & 0 & -\lambda \\ 0 & 1 & 0 \\ \lambda & 0 & 1 \end{pmatrix}, \tag{A.35}$$

By calculating $C(\lambda)$ explicitly and comparing it with (A.22), we obtain

$$\psi(\lambda) = \arccos\left(\frac{\lambda\cos\theta + \cos\psi\sin\theta}{\sin\theta(\lambda)}\right), \quad \theta(\lambda) = \arccos\left(\cos\theta - \lambda\cos\psi\sin\theta\right), \tag{A.36}$$

and

$$\phi(\lambda) = \arcsin\left(\frac{\sin\theta\sin\phi + \lambda(\cos\theta\cos\psi\sin\phi + \cos\phi\sin\psi)}{\sin\theta(\lambda)}\right). \tag{A.37}$$

Furthermore, at $\lambda = 0$ we get

$$\frac{d\psi(\lambda)}{d\lambda}\bigg|_{\lambda=0} = -\cot\theta\sin\psi, \quad \frac{d\theta(\lambda)}{d\lambda}\bigg|_{\lambda=0} = \frac{\cos\psi\sin\theta}{\sqrt{1-(\cos\theta - \lambda\cos\psi\sin\theta)^2}}\bigg|_{\lambda=0} = \cos\psi, \tag{A.38}$$

and

$$\frac{d\phi(\lambda)}{d\lambda}\bigg|_{\lambda=0} = \frac{\sin\psi}{\sin\theta}. \tag{A.39}$$

Substituting these relations into the (A.25), leads to

$$e_2 = \cos\psi\frac{\partial}{\partial\theta} - \sin\psi\left(\cot\theta\frac{\partial}{\partial\psi} - \frac{1}{\sin\theta}\frac{\partial}{\partial\phi}\right). \tag{A.40}$$

Hence, all three basis vectors in terms of Euler angles (in the zyz-convention) are given by

$$\begin{aligned} e_1 &= \sin\psi\frac{\partial}{\partial\theta} + \cos\psi\left(\cot\theta\frac{\partial}{\partial\psi} - \frac{1}{\sin\theta}\frac{\partial}{\partial\phi}\right), \\ e_2 &= \cos\psi\frac{\partial}{\partial\theta} - \sin\psi\left(\cot\theta\frac{\partial}{\partial\psi} - \frac{1}{\sin\theta}\frac{\partial}{\partial\phi}\right), \\ e_3 &= \frac{\partial}{\partial\psi}. \end{aligned} \tag{A.41}$$

By calculating the commutation relations of these vectors, we can see that the obtained basis is indeed right-invariant, i.e., it satisfies the relation (2.22).

A.3 Derivation of an auxiliary quantity for spinor Lagrangian

In this section, we derive the auxiliary quantity $\frac{i}{2}\kappa_{\hat{\alpha}\hat{\beta}\hat{\rho}}\gamma^{\hat{\rho}}\Sigma^{\hat{\alpha}\hat{\beta}}$ that appears in the Dirac Lagrangian (4.55). Let us recall the equations derived in Sec. 4.2.2, which will be instrumental in carrying out the calculation:

$$\gamma^{\hat{0}}{}_{\hat{\beta}\hat{\gamma}} = 0 \quad \text{for any } \hat{\beta}, \hat{\gamma}, \tag{A.42}$$

$$\gamma^{\hat{i}}{}_{\hat{l}\hat{j}} = b^n (b^m)^{-1} (b^k)^{-1} \varepsilon_{\hat{i}\hat{j}\hat{l}}, \tag{A.43}$$

and

$$\gamma^{\hat{i}}{}_{\hat{0}\hat{l}} = \frac{(b^k)^{-1}}{N}\left[b^n R^{\hat{i}}{}_q (\mathcal{J}_j)^q{}_l N^j - \left(\dot{b}^n R^{\hat{i}}{}_l + b^n \dot{R}^{\hat{i}}_l\right)\right] R^l{}_{\hat{l}}, \tag{A.44}$$

where $n = \hat{i},\ m = \hat{j},\ k = \hat{l}$.

Using these equations, we proceed with the calculation of the auxiliary quantity, step by step, as outlined below.

First, we recall $\kappa_{\hat{\alpha}\hat{\beta}\hat{\rho}}$ given by (4.60)

$$\kappa_{\hat{\alpha}\hat{\beta}\hat{\rho}} = \frac{1}{2}(\gamma_{\hat{\rho}\hat{\alpha}\hat{\beta}} + \gamma_{\hat{\beta}\hat{\alpha}\hat{\rho}} - \gamma_{\hat{\alpha}\hat{\beta}\hat{\rho}}), \tag{A.45}$$

where

$$\gamma_{\hat{\alpha}\hat{\beta}\hat{\gamma}} = \eta_{\hat{\alpha}\hat{\sigma}}\gamma^{\hat{\sigma}}{}_{\hat{\beta}\hat{\gamma}} = \delta_{\hat{\alpha}\hat{0}}\gamma^{\hat{0}}{}_{\hat{\beta}\hat{\gamma}} + \delta_{\hat{\alpha}\hat{i}}\gamma^{\hat{i}}{}_{\hat{\beta}\hat{\gamma}}. \tag{A.46}$$

Considering the gauge $N^i = 0$, the calculation of all the components gives the following results:

For $\hat{\alpha} = 0$,

$$\begin{aligned}\kappa_{\hat{0}\hat{\beta}\hat{\rho}} &= \frac{1}{2}(\gamma_{\hat{\rho}\hat{0}\hat{\beta}} + \gamma_{\hat{\beta}\hat{0}\hat{\rho}}) \\ &= -\frac{1}{2N}\left[\left(b^{\hat{\beta}}\right)^{-1}\left(\dot{b}^{\hat{\rho}}\delta_{\hat{\rho}\hat{\beta}} + b^{\hat{\rho}}\omega^{\hat{\rho}}{}_{\hat{\beta}}\right) + \left(b^{\hat{\rho}}\right)^{-1}\left(\dot{b}^{\hat{\beta}}\delta_{\hat{\beta}\hat{\rho}} + b^{\hat{\beta}}\omega^{\hat{\beta}}{}_{\hat{\rho}}\right)\right].\end{aligned} \tag{A.47}$$

Recalling

$$b^k = e^{\tilde{\beta}_k/2}, \quad \tilde{\beta}_k = 2(\beta_k + \alpha), \tag{A.48}$$

with

$$\beta_1 = \beta_+ + \sqrt{3}\beta_-, \quad \beta_2 = \beta_+ - \sqrt{3}\beta_-, \quad \beta_3 = -2\beta_+, \tag{A.49}$$

and using the property $\omega^{\hat{i}}{}_{\hat{\rho}} = -\omega^{\hat{\rho}}{}_{\hat{i}}$, leads to:

- For $\hat{\beta} = 1$

$$\kappa_{\hat{0}\hat{1}\hat{0}} = 0, \quad \kappa_{\hat{0}\hat{1}\hat{1}} = -\frac{1}{N}\left(\dot{\beta}_+ + \sqrt{3}\dot{\beta}_- + \dot{\alpha}\right), \quad \kappa_{\hat{0}\hat{1}\hat{2}} = -\frac{1}{N}\sinh\left(2\sqrt{3}\beta_-\right)\omega^{\hat{1}}{}_{\hat{2}}, \tag{A.50}$$

and

$$\kappa_{\hat{0}\hat{1}\hat{3}} = \frac{1}{N}\sinh\left(3\beta_+ + \sqrt{3}\beta_-\right)\omega^{\hat{3}}{}_{\hat{1}}. \tag{A.51}$$

- For $\hat{\beta} = 2$

$$\kappa_{\hat{0}\hat{2}\hat{0}} = 0, \quad \kappa_{\hat{0}\hat{2}\hat{1}} = -\frac{1}{N}\sinh(2\sqrt{3}\beta_-)\omega^{\hat{1}}{}_{\hat{2}}, \quad \kappa_{\hat{0}\hat{2}\hat{2}} = -\frac{1}{N}\left(\dot{\beta}_+ - \sqrt{3}\dot{\beta}_- + \dot{\alpha}\right), \tag{A.52}$$

and

$$\kappa_{\hat{0}\hat{2}\hat{3}} = -\frac{1}{N}\sinh\left(3\beta_+ - \sqrt{3}\beta_-\right)\omega^{\hat{2}}{}_{\hat{3}}. \tag{A.53}$$

- For $\hat{\beta} = 3$

$$\kappa_{\hat{0}\hat{3}\hat{0}} = 0, \quad \kappa_{\hat{0}\hat{3}\hat{1}} = \frac{1}{N}\sinh\left(3\beta_+ + \sqrt{3}\beta_-\right)\omega^{\hat{3}}{}_{\hat{1}}, \quad \kappa_{\hat{0}\hat{3}\hat{2}} = -\frac{1}{N}\sinh\left(3\beta_+ - \sqrt{3}\beta_-\right)\omega^{\hat{2}}{}_{\hat{3}}, \tag{A.54}$$

and

$$\kappa_{\hat{0}\hat{3}\hat{3}} = -\frac{1}{N}\left(-2\dot{\beta}_+ + \dot{\alpha}\right). \tag{A.55}$$

For $\hat{\alpha} = 1$

$$\kappa_{\hat{1}\hat{\beta}\hat{\rho}} = \frac{1}{2}(\gamma_{\hat{\rho}\hat{1}\hat{\beta}} + \gamma_{\hat{\beta}\hat{1}\hat{\rho}} - \gamma_{\hat{1}\hat{\beta}\hat{\rho}}), \tag{A.56}$$

- For $\hat{\beta} = 2$

$$\kappa_{\hat{1}\hat{2}\hat{\rho}} = \frac{1}{2}(\gamma_{\hat{\rho}\hat{1}\hat{2}} + \gamma_{\hat{2}\hat{1}\hat{\rho}} - \gamma_{\hat{1}\hat{2}\hat{\rho}}), \tag{A.57}$$

which for $\hat{\rho} = 0$, using $\gamma_{abc} = -\gamma_{acb}$, takes the form

$$\begin{aligned} \kappa_{\hat{1}\hat{2}\hat{0}} &= \frac{1}{2}(-\gamma_{\hat{2}\hat{0}\hat{1}} + \gamma_{\hat{1}\hat{0}\hat{2}}) \\ &= -\frac{1}{N}\cosh\left(2\sqrt{3}\beta_-\right)\omega^{\hat{1}}{}_{\hat{2}}. \end{aligned} \tag{A.58}$$

Next, using

$$\gamma_{\hat{p}\hat{j}\hat{l}} = \delta_{\hat{p}\hat{i}}\gamma^{\hat{i}}{}_{\hat{j}\hat{l}} = \delta_{\hat{p}\hat{i}}\varepsilon_{\hat{i}\hat{j}\hat{l}}e^{\left(\tilde{\beta}_{\hat{i}} - \tilde{\beta}_{\hat{j}} - \tilde{\beta}_{\hat{l}}\right)/2}, \tag{A.59}$$

we get

$$\kappa_{\hat{1}\hat{2}\hat{\rho}} = \frac{1}{2}(\gamma_{\hat{\rho}\hat{1}\hat{2}} + \gamma_{\hat{2}\hat{1}\hat{\rho}} - \gamma_{\hat{1}\hat{2}\hat{\rho}})$$
$$= \frac{1}{2}\left(\delta_{\hat{\rho}\hat{i}}\varepsilon_{\hat{i}\hat{1}\hat{2}}e^{\left(\tilde{\beta}_{\hat{i}}-\tilde{\beta}_{\hat{1}}-\tilde{\beta}_{\hat{2}}\right)/2} + \delta_{\hat{2}\hat{i}}\varepsilon_{\hat{i}\hat{1}\hat{\rho}}e^{\left(\tilde{\beta}_{\hat{i}}-\tilde{\beta}_{\hat{1}}-\tilde{\beta}_{\hat{\rho}}\right)/2} - \delta_{\hat{1}\hat{i}}\varepsilon_{\hat{i}\hat{2}\hat{\rho}}e^{\left(\tilde{\beta}_{\hat{i}}-\tilde{\beta}_{\hat{2}}-\tilde{\beta}_{\hat{\rho}}\right)/2}\right), \tag{A.60}$$

which leads to

$$\kappa_{\hat{1}\hat{2}\hat{1}} = 0, \quad \kappa_{\hat{1}\hat{2}\hat{2}} = 0, \quad \kappa_{\hat{1}\hat{2}\hat{3}} = \frac{1}{2}e^{-\alpha}e^{(-4\beta_+)} - e^{(2\beta_+)}e^{-\alpha}\cosh\left(2\sqrt{3}\beta_-\right). \tag{A.61}$$

- For $\hat{\beta} = 3$, following the same steps as before, we obtain

$$\kappa_{\hat{1}\hat{3}\hat{0}} = \frac{1}{N}\cosh\left(3\beta_+ + \sqrt{3}\beta_-\right)\omega^{\hat{3}}{}_{\hat{1}}, \quad \kappa_{\hat{1}\hat{3}\hat{1}} = 0, \tag{A.62}$$

and

$$\kappa_{\hat{1}\hat{3}\hat{2}} = \frac{1}{2}e^{(-4\beta_+)} + e^{(2\beta_+)}\sinh\left(2\sqrt{3}\beta_-\right), \quad \kappa_{\hat{1}\hat{3}\hat{3}} = 0. \tag{A.63}$$

- For $\hat{\alpha} = 2$, $\hat{\beta} = 3$

$$\kappa_{\hat{2}\hat{3}\hat{\rho}} = \frac{1}{2}(\gamma_{\hat{\rho}\hat{2}\hat{3}} + \gamma_{\hat{3}\hat{2}\hat{\rho}} - \gamma_{\hat{2}\hat{3}\hat{\rho}}), \tag{A.64}$$

which leads to

$$\kappa_{\hat{2}\hat{3}\hat{0}} = -\frac{1}{N}\cosh\left(3\beta_+ - \sqrt{3}\beta_-\right)\omega^{\hat{2}}{}_{\hat{3}}, \quad \kappa_{\hat{2}\hat{3}\hat{1}} = -\frac{1}{2}e^{-\alpha}e^{(-4\beta_+)} + e^{(2\beta_+)}e^{-\alpha}\sinh\left(2\sqrt{3}\beta_-\right), \tag{A.65}$$

and

$$\kappa_{\hat{2}\hat{3}\hat{2}} = 0, \quad \kappa_{\hat{2}\hat{3}\hat{3}} = 0. \tag{A.66}$$

Next, using the Lorentz generators in Weyl (or chiral) representation given by

$$\Sigma^{0i} = -\frac{1}{2}\begin{pmatrix} \sigma^i & 0 \\ 0 & -\sigma^i \end{pmatrix}, \quad \Sigma^{ij} = -\frac{i}{2}\epsilon^{ijk}\begin{pmatrix} \sigma^k & 0 \\ 0 & \sigma^k \end{pmatrix}, \tag{A.67}$$

we can calculate $\gamma^{\hat{\rho}}\Sigma^{\hat{\alpha}\hat{\beta}}$ matrices. We get the following results

$$\gamma^{\hat{i}}\Sigma^{\hat{0}\hat{j}} = \frac{1}{2}\begin{pmatrix} 0 & \delta_{ij}I + i\varepsilon_{ijk}\sigma_k \\ \delta_{ij}I + i\varepsilon_{ijk}\sigma_k & 0 \end{pmatrix}, \tag{A.68}$$

which leads to

$$\gamma^{\hat{1}}\Sigma^{\hat{0}\hat{1}} = \gamma^{\hat{2}}\Sigma^{\hat{0}\hat{2}} = \gamma^{\hat{3}}\Sigma^{\hat{0}\hat{3}} = \frac{1}{2}\gamma^{\hat{0}}. \tag{A.69}$$

Next, we obtain

$$\gamma^{\hat{0}}\Sigma^{\hat{i}\hat{j}} = -\gamma^{\hat{i}}\Sigma^{\hat{0}\hat{j}} = -\frac{i}{2}\varepsilon^{ijk}\begin{pmatrix} 0 & \sigma_k \\ \sigma_k & 0 \end{pmatrix}, \quad \text{for} \quad i \neq j, \tag{A.70}$$

and

$$\gamma^{\hat{j}}\Sigma^{\hat{0}\hat{i}} = -\gamma^{\hat{i}}\Sigma^{\hat{0}\hat{j}}. \tag{A.71}$$

Furthermore, we calculate

$$\gamma^{\hat{l}}\Sigma^{\hat{i}\hat{j}} = \frac{i}{2}\varepsilon^{\hat{l}\hat{i}\hat{j}}\begin{pmatrix} 0 & -I \\ I & 0 \end{pmatrix}. \tag{A.72}$$

Let us note, that

$$\gamma^{\hat{1}}\Sigma^{\hat{2}\hat{3}} = -\gamma^{\hat{2}}\Sigma^{\hat{1}\hat{3}} = \gamma^{\hat{3}}\Sigma^{\hat{1}\hat{2}}. \tag{A.73}$$

Finally, it can be shown that the only non-vanishing contributions are

$$\begin{aligned} \frac{i}{2}\kappa_{\hat{\alpha}\hat{\beta}\hat{\rho}}\gamma^{\hat{\rho}}\Sigma^{\hat{\alpha}\hat{\beta}} = {}& \frac{i}{2}\left(\kappa_{\hat{0}\hat{1}\hat{1}} + \kappa_{\hat{0}\hat{2}\hat{2}} + \kappa_{\hat{0}\hat{3}\hat{3}}\right)\gamma^{\hat{0}} + i\left(\kappa_{\hat{1}\hat{2}\hat{3}} - \kappa_{\hat{1}\hat{3}\hat{2}} + \kappa_{\hat{2}\hat{3}\hat{1}}\right)\gamma^{\hat{1}}\Sigma^{\hat{2}\hat{3}} \\ & + i\left(\kappa_{\hat{1}\hat{2}\hat{0}}\gamma^{\hat{0}}\Sigma^{\hat{1}\hat{2}} + \kappa_{\hat{1}\hat{3}\hat{0}}\gamma^{\hat{0}}\Sigma^{\hat{1}\hat{3}} + \kappa_{\hat{2}\hat{3}\hat{0}}\gamma^{\hat{0}}\Sigma^{\hat{2}\hat{3}}\right). \end{aligned} \tag{A.74}$$

Thus, by substituting all the terms into the relation above, we obtain the following result

$$\begin{aligned} \frac{i}{2}\kappa_{\hat{\alpha}\hat{\beta}\hat{\rho}}\gamma^{\hat{\rho}}\Sigma^{\hat{\alpha}\hat{\beta}} = {}& -\frac{3i}{2N}\dot{\alpha}\gamma^{\hat{0}} + \frac{i}{2}e^{-\alpha}\left[e^{-4\beta_+} + e^{2\beta_+ + 2\sqrt{3}\beta_-} + e^{2\beta_+ - 2\sqrt{3}\beta_-}\right]\gamma^{\hat{1}}\Sigma^{\hat{2}\hat{3}} \\ & - \frac{i}{N}\Big[\cosh\left(2\sqrt{3}\beta_-\right)\omega^{\hat{1}}{}_{\hat{2}}\gamma^{\hat{0}}\Sigma^{\hat{1}\hat{2}} + \cosh\left(3\beta_+ + \sqrt{3}\beta_-\right)\omega^{\hat{3}}{}_{\hat{1}}\gamma^{\hat{0}}\Sigma^{\hat{3}\hat{1}} \\ & + \cosh\left(3\beta_+ - \sqrt{3}\beta_-\right)\omega^{\hat{2}}{}_{\hat{3}}\gamma^{\hat{0}}\Sigma^{\hat{2}\hat{3}}\Big]. \end{aligned} \tag{A.75}$$

References

[1] LIGO Scientific Collaboration and Virgo Collaboration, *Observation of Gravitational Waves from a Binary Black Hole Merger*, Phys. Rev. Lett. **116**, 061102 (2016).

[2] The Event Horizon Telescope Collaboration et al., *First M87 Event Horizon Telescope Results. I. The Shadow of the Supermassive Black Hole*, ApJL **875** L1 (2019).

[3] S. Hawking and R. Penrose, *The Nature of Space and Time* (Princeton University Press, Princeton, 1996).

[4] S. W. Hawking and G. F. R. Ellis, *The Large Scale Structure of Space-Time* (Cambridge University Press, Cambridge, 1973).

[5] C. Kiefer, *Quantum Gravity*, 3rd ed. (Oxford University Press, Oxford, 2012).

[6] N. D. Birrell and P. C. W. Davies, *Quantum Fields in Curved Space* (Cambridge University Press, Cambridge, 1982).

[7] C. Bennett et al. (WMAP), *The Microwave Anisotropy Probe Mission*, Astrophys. J. **583**, 1 (2003), arXiv:astro-ph/0301158.

[8] Planck Collaboration, *Planck 2018 results. VI. Cosmological parameters*, Astron. Astrophys. **641**, A6 (2020), arXiv:1807.06209; Erratum: Astron. Astrophys. **652**, C4 (2021).

[9] J. K. Adelman-McCarthy et al., *The Fourth Data Release of the Sloan Digital Sky Survey*, Astrophys. J. Suppl. **162**, 38–48 (2006), arXiv:astro-ph/0507711.

[10] P. J. E. Peebles, *Principles of Physical Cosmology* (Princeton University Press, Princeton, 1993).

[11] A. A. Starobinsky, *Spectrum of relict gravitational radiation and the early state of the universe*, JETP Lett. **30**, 682–685 (1979).

[12] A. Guth, *The Inflationary Universe: A Possible Solution to the Horizon and Flatness Problems*, Phys. Rev. D **23**, 347–356 (1981).

[13] A. D. Linde, *A New Inflationary Universe Scenario: A Possible Solution of the Horizon, Flatness, Homogeneity, Isotropy and Primordial Monopole Problems*, Phys. Lett. B **108**, 389–393 (1982).

[14] D. J. Schwarz, C. J. Copi, D. Huterer and G. D. Starkman, *CMB Anomalies after Planck*, Class. Quant. Grav. **33**, 18, 184001 (2016).

[15] A. G. Riess et al., *A 2.4% Determination of the Local Value of the Hubble Constant*, ApJ **826** 1, 56 (2016).

[16] E. Abdalla et al., *Cosmology intertwined: a review of the particle physics, astrophysics, and cosmology associated with the cosmological tensions and anomalies*, JHEAp **34**, 49–211 (2022).

[17] E. Di Valentino, O. Mena, S. Pan, L. Visinelli, W. Yang, A. Melchiorri, D.F. Mota, A.G. Riess and J. Silk, *In the realm of the Hubble tension—a review of solutions*, Class. Quant. Grav. **38**, 15, 153001 (2021).

[18] S. Weinberg, *Cosmology* (Oxford University Press, Oxford, 2008).

[19] E. W. Kolb and M. S. Turner, The Early Universe (Addison-Wesley, Reading, MA, 1990).

[20] S. Dodelson, *Modern Cosmology* (Academic Press, San Diego, CA, 2003).

[21] V. Mukhanov, *Physical Foundations of Cosmology* (Cambridge University Press, Cambridge, 2005).

[22] R. A. Alpher, H. Bethe, and G. Gamow, *The origin of chemical elements*, Phys. Rev. **73**, 803–804 (1948).

[23] A. A. Penzias and R. W. Wilson, *A measurement of excess antenna temperature at 4080 Mc/s*, ApJ **142**, 419–421 (1965).

[24] J. C. Mather et al., *A Preliminary Measurement of the Cosmic Microwave Background Spectrum by the Cosmic Background Explorer (COBE) Satellite*, ApJ Lett. **354**, L37 (1990).

[25] L. Perivolaropoulos and F. Skara, *Challenges for ΛCDM: An update*, New Astron. Rev. **95**, 101659 (2022).

[26] C. J. Copi, D. Huterer, D. J. Schwarz and G. D. Starkman, *Large-angle anomalies in the CMB*, Adv. Astron. **2010**, 847541 (2010), arXiv:1004.5602v2.

[27] D. Baumann, *TASI Lectures on Inflation*, arXiv:0907.5424 (2009).

[28] P. Peter and J.-P. Uzan, *Primordial Cosmology* (Oxford University Press, Oxford, 2009).

[29] C. J. Copi, D. Huterer, G. D. Starkman, *Multipole vectors - A New representation of the CMB sky and evidence for statistical anisotropy or non-Gaussianity at* $2 \leq l \leq 8$, Phys. Rev. D **70**, 043515 (2004).

[30] C. L. Bennett, R. S. Hill, G. Hinshaw, D. Larson, K. M. Smith, J. Dunkley et al., *Seven-year Wilkinson Microwave Anisotropy Probe (WMAP) Observations: Are There Cosmic Microwave Background Anomalies?*, Astrophys. J. Supp. **192**, 17 (2011), arXiv:1001.4758v2.

[31] D. Blas, *Introduction to dark matter* (Durham University, 2019), available at `https://conference.ippp.dur.ac.uk/event/1291/attachments/6076/8176/DM_Blas1.pdf`.

[32] K. Freese, *Review of Observational Evidence for Dark Matter in the Universe and in Upcoming Searches for Dark Stars*, EAS Publ. Ser. **36**, 113–126 (2009), arXiv:0812.4005.

[33] V. Rubin and W. Ford, *Rotation of the Andromeda Nebula from a Spectroscopic Survey of Emission Regions*, ApJ **159**, 379 (1970).

[34] K. Freese, *Status of Dark Matter in the Universe*, Int. J. Mod. Phys. **1**, 06, 325-355 (2017).

[35] V. A. Rubakov and D. S. Gorbunov, *Introduction to the Theory of the Early Universe: Cosmological Perturbations and Inflationary Theory* (World Scientific, Singapore, 2011).

[36] L. Bergström, *Non-baryonic dark matter: Observational evidence and detection methods*, Rept. Prog. Phys. **63**, 793 (2000).

[37] A. Arbey and F. Mahmoudi, *Dark matter and the early Universe: a review*, Prog. Part. Nucl. Phys. **119**, 103865 (2021).

[38] K. Arun, S. B. Gudennavar and C. Sivaram, *Dark matter, dark energy, and alternate models: A review*, Adv. Space Res. **60**, 166–186 (2017).

[39] M. Viel, G. D. Becker, J. S. Bolton and M. G. Haehnelt, *Warm dark matter as a solution to the small scale crisis: New constraints from high redshift Lyman-α forest data*, Phys. Rev. D **88**, 043502 (2013).

[40] G. Bertone, D. Hooper and J. Silk, *Particle dark matter: Evidence, candidates and constraints*, Phys. Rept. **405**, 279–390 (2005).

[41] B. Famaey and S. McGaugh, *Modified Newtonian Dynamics (MOND): Observational Phenomenology and Relativistic Extensions*, Living Rev. Rel. **15**, 10 (2012).

[42] A. D. Popolo and M. Le Delliou, *Small scale problems of the ΛCDM Model: A short review*, Galaxies **5**, 1, 17 (2017), arXiv:1606.07790v3.

[43] J.S. Bullock and M. Boylan-Kolchin, *Small-Scale Challenges to the ΛCDM Paradigm*, Ann. Rev. Astron. Astrophys. **55**, 343–387 (2017), arXiv:1707.04256v2.

[44] W. Hu, R. Barkana and A. Gruzinov, *Cold and fuzzy dark matter*, Phys. Rev. Lett. **85**, 1158–1161 (2000).

[45] F. C. van den Bosch, A. Burkert and R. A. Swaters, *The angular momentum content of dwarf galaxies: new challenges for the theory of galaxy formation*, Mon. Not. Roy. Astron. Soc. **326**, 1205 (2001).

[46] G. Steigman, *Observational tests of antimatter cosmologies*, Ann. Rev. Astron. Astrophys. **14**, 339 (1976).

[47] G. Steigman, *When Clusters Collide: Constraints On Antimatter On The Largest Scales*, JCAP **0810**, 001 (2008), arXiv:0808.1122.

[48] V. A. Rubakov and D. S. Gorbunov, *Introduction to the Theory of the Early Universe: Hot Big Bang Theory*, 2nd ed. (World Scientific, Singapore, 2017).

[49] L. Canetti, M. Drewes and M. Shaposhnikov, *Matter and Antimatter in the Universe*, New J. Phys. **14**, 095012 (2012), arXiv:1204.4186v2.

[50] G. Steigman, *Primordial Nucleosynthesis: The Predicted and Observed Abundances and Their Consequences*, PoS NICXI 001 (2010), arXiv:1008.4765.

[51] E. Komatsu et al. (WMAP), *Seven-Year Wilkinson Microwave Anisotropy Probe (WMAP) Observations: Cosmological Interpretation*, Astrophys. J. Suppl. **192**, 18 (2011), arXiv:1001.4538.

[52] A. D. Sakharov, *Violation of CP Invariance, C asymmetry, and baryon asymmetry of the universe*, Pisma Zh. Eksp. Teor. Fiz. **5**, 32 (1967); JETP Lett. **6**, 24 (1967).

[53] V. A. Kuzmin, V. A. Rubakov and M. E. Shaposhnikov, *On anomalous electroweak baryon-number non-conservation in the early universe*, Phys. Lett. B **155**, 36 (1985).

[54] G. 't Hooft, *Symmetry Breaking Through Bell-Jackiw Anomalies*, Phys. Rev. Lett. **37**, 8 (1976).

[55] M. Kobayashi and T. Maskawa, *CP-Violation in the Renormalizable Theory of Weak Interaction*, Prog. Theor. Phys. **49**, 652 (1973).

[56] M. Dine and A. Kusenko, *The Origin of the matter-antimatter asymmetry*, Rev. Mod. Phys. **76**, 1 (2003).

[57] H. Davoudiasl, R. Kitano, G. D. Kribs, H. Murayama, and P. J. Steinhardt, *Gravitational Baryogenesis*, Phys. Rev. Lett. **93**, 201301 (2004), arXiv:hep-ph/0403019.

[58] V. A. Rubakov and M. E. Shaposhnikov, *Electroweak baryon number nonconservation in the early universe and in high-energy collisions*, Usp. Fiz. Nauk **166**, 493–537 (1996); Phys. Usp. **39**, 461–502 (1996).

[59] A. Riotto, M. Trodden, *Recent progress in baryogenesis*, Ann. Rev. Nucl. Part. Sci. **49**, 35–75 (1999).

[60] G. F. R. Ellis, R. Maartens and M. A. H. MacCallum, *Relativistic Cosmology* (Cambridge University Press, Cambridge, 2012).

[61] G. W. Gibbons, *Cosmological fermion-number non-conservation*, Phys. Lett. B **84**, 431–434 (1979).

[62] G. W. Gibbons, *Spectral Asymmetry and Quantum Field Theory in Curved Spacetime*, Ann. Phys. **125**, 98 (1980).

[63] L. D. Landau and E. M. Lifshitz, *The Classical Theory of Fields*, 4th ed. (Pergamon Press, Oxford, 1975).

[64] E. Lifshitz, *On the gravitational stability of the expanding universe*, J. Phys. (USSR) **10**, 116 (1946). Republished as a Golden Oldie in: Gen. Relativ. Gravit. **49**, 18 (2017), with an editorial note by G.F.R. Ellis.

[65] V.A. Belinskii, I.M. Khalatnikov, E.M. Lifshitz, *Oscillatory approach to a singular point in the relativistic cosmology*, Adv. Phys. **19**, 525 (1970).

[66] V.A. Belinskii, I.M. Khalatnikov, E.M. Lifshitz, *A general solution of the Einstein equations with a time singularity*, Adv. Phys. **31**, 639 (1982).

[67] C. W. Misner, *Mixmaster universe*, Phys. Rev. Lett. **22**, 1071 (1969).

[68] M. P. Ryan, *Qualitative Cosmology: Diagrammatic Solutions for Bianchi Type IX Universes with Expansion, Rotation, and Shear. I. The Symmetric Case*, Ann. Phys. **65**, 506–537 (1971).

[69] M. P. Ryan, *Qualitative Cosmology: Diagrammatic Solutions for Bianchi Type IX Universes with Expansion, Rotation, and Shear. II. The General Case*, Ann. Phys. **68**, 541–555 (1971).

[70] C. Kiefer, N. Kwidzinski and W. Piechocki, *On the dynamics of the general Bianchi IX spacetime near the singularity*, Eur. Phys. J. C **78**, 9, 691 (2018).

[71] M. Bojowald, *Loop Quantum Cosmology and Singularities*, Living Rev. Relativ. **11**, 4 (2008).

[72] R. van den Hoogen and I. Olasagasti, *Isotropization of scalar field Bianchi type-IX models with an exponential potential*, Phys. Rev. D **59**, 107302 (1999).

[73] G. W. Gibbons and S. W. Hawking, *Cosmological event horizons, thermodynamics, and particle creation*, Phys. Rev. D **15**, 2738 (1977).

[74] S. W. Hawking and I. G. Moss, *Supercooled phase transitions in the very early universe*, Phys. Lett. **110B**, 35 (1982).

[75] R. M. Wald, *Asymptotic behavior of homogeneous cosmological models in the presence of a positive cosmological constant*, Phys. Rev. D 28, 2118 (1983).

[76] C. Kiefer, L. Chataignier and M. Tyagi, *Time and its arrow from quantum geometrodynamics?*, J. Phys. Conf. Ser. **2883**, 1, 012008 (2024).

[77] B. L. Hu and L. Parker, *Anisotropy damping through quantum effects in the early universe*, Phys. Rev. D **17**, 933 (1978); Erratum: Phys. Rev. D **17**, 3292 (1978).

[78] LX Li, *Effect of the Global Rotation of the Universe on the Formation of Galaxies*, Gen. Rel. Grav. **30**, 497–507 (1998).

[79] P. J. E. Peebles, *The large-scale structure of the universe* (Princeton University Press, Princeton, 1980).

[80] G. Gamow, *Rotating Universe?*, Nature **158**, 549 (1946).

[81] K. Gödel, in *Kurt Gödel: Collected Works, Volume II*, edited by S. Feferman et al. (Oxford University Press, Oxford, 1990).

[82] C. B. Collins and S. W. Hawking, *The rotation and distortion of the universe*, Mon. Not. R. Astron. Soc. **162**, 307 (1973).

[83] Y. N. Obukhov, *On Physical Foundations and Observational Effects of Cosmic Rotation*, in *Colloquium on Cosmic Rotation*, edited by M. Scherfner, T. Chrobok, and M. Shefaat (Wissenschaft und Technik Verlag, Berlin, 2000), pp. 23–96; arXiv:astro-ph/0008106.

[84] W. Godłowski, M. Szydłowski, P. Flin, and M. Biernacka, *Rotation of the Universe and the Angular Momenta of Celestial Bodies*, Gen. Rel. and Grav. **35**, 907–913 (2003).

[85] W. Godłowski, *Global and Local Effects of Rotation: Observational Aspects*, Int. J. Mod. Phys. D **20**, 1643–1673 (2011).

[86] P. Wang, N. I. Libeskind, E. Tempel, X. Kang and Q. Guo, *Possible observational evidence for cosmic filament spin*, Nature Astron. **5**, 8, 839–845 (2021); Erratum: Nature Astron. **5**, 10, 1077 (2021).

[87] H. S. Hwang, M. Gyoon Lee,*Searching for rotating galaxy clusters in SDSS and 2dFGRS*, Astrophys. J. **662**, 236-249 (2007).

[88] I. Ciufolini and J. A. Wheeler, *Gravitation and Inertia* (Princeton University Press, Princeton, 1995).

[89] A. Pontzen, *Rogues' gallery: the full freedom of the Bianchi CMB anomalies*, Phys. Rev. D **79**, 103518 (2009), arXiv:0901.2122.

[90] P. Sundell and T. Koivisto, *Anisotropic cosmology and inflation from tilted Bianchi IX model*, Phys. Rev. D **92** 12, 123529 (2015).

[91] A. Yu. Kamenshchik and O. V. Teryaev, *Chaotic spin precession in anisotropic universes and fermionic dark matter*, Phys. Part. Nucl. Lett. **13**, 3, 298-302 (2016).

[92] M. P. Ryan and L. C. Shepley, *Homogeneous Relativistic Cosmologies* (Princeton University Press, Princeton, 1975)

[93] J. Wainwright and G. F. R. Ellis, *Dynamical Systems in Cosmology*, (Cambridge University Press, Cambridge, 1997).

[94] G. F. R. Ellis and H. van Elst, *Cosmological models: Cargese lectures 1998*, NATO Sci. Ser. C **541**, 1–116 (1999).

[95] R. T. Jantzen, *Spatially Homogeneous Dynamics: A Unified Picture*, arXiv:gr-qc/0102035; originally published in *Proceedings of the International School Enrico Fermi, Course LXXXVI (1982) on Gamov Cosmology*, edited by R. Ruffini and F. Melchiorri (North Holland, Amsterdam, 1987), pp. 61–147.

[96] R. T. Jantzen and C. Uggla, *The kinematical role of automorphisms in the orthonormal frame approach to Bianchi cosmology*, J. Math. Phys. **40**, 353–368 (1999).

[97] R. T. Jantzen, *The Dynamical Degrees of Freedom in Spatially Homogeneous Cosmology*, Commun. math. Phys. **64**, 211–232 (1979).

[98] A. Krasinski, C. G. Behr, E. Schücking et al., *The Bianchi Classification in the Schücking-Behr Approach*, Gen. Rel. Grav. **35**, 475–489 (2003).

[99] F. B. Estabrook, H. D. Wahlquist and C. G. Behr, *Dyadic Analysis of Spatially Homogeneous World Models*, J. Math. Phys. **9**, 497 (1968).

[100] M. P. Ryan, *Hamiltonian Cosmology* (Springer, Berlin, 1972).

[101] R. T. Jantzen, *Perfect Fluid Sources for Spatially Homogeneous Spacetimes*, Ann. Phys. **145**, 378–388 (1983).

[102] C. W. Misner, *The isotropy of the universe*, Astrophys. J. **151**, 431 (1968).

[103] D. H. King, *Gravity-wave insights to Bianchi type-IX universes*, Phys. Rev. D **44**, 2356 (1991).

[104] A. Zee, *Quantum Field Theory in a Nutshell*, 2nd ed. (Princeton University Press, Princeton, 2010).

[105] M. D. Schwarz, *Quantum Field Theory and the Standard Model* (Cambridge University Press, Cambridge, 2014).

[106] M. Peskin and D. Schroeder, *An Introduction to Quantum Field Theory* (Westview Press, Chicago, 1995).

[107] D. Tong, *Lectures on Quantum Field Theory*, available at `https://www.damtp.cam.ac.uk/user/tong/qft.html`.

[108] M. S. Swanson, *Path Integrals and Quantum Processes*, 1st ed. (Academic Press, San Diego, 1992).

[109] J. D. Bjorken and S. D. Drell, *Relativistic quantum fields* (International series in pure and applied physics, McGraw-Hill, New York, 1965).

[110] L. E. Parker and D. J. Toms, *Quantum Field Theory in Curved Spacetime* (Cambridge University Press, Cambridge, 2009).

[111] P. B. Pal, *Dirac, Majorana and Weyl fermions*, Am. J. Phys. **79**, 485–498 (2011), arXiv:1006.1718v2.

[112] M. Srednicki, *Quantum Field Theory*, 1st ed. (Cambridge University Press, Cambridge, 2007).

[113] A. A. Grib, S. G. Mamaev and V. M. Mostepanenko, *Vacuum Quantum Effects in Strong Fields* (Friedmann Laboratory Publishing, St. Petersburg, 1994).

[114] A. A. Saharian, *Lectures on Quantum Fields in Curved Space*, available at `http://training.hepi.tsu.ge/rtn/activities/sources/LectQFTrev.pdf`.

[115] S. A. Fulling, *Aspects of Quantum Field Theory in Curved Space-Time* (Cambridge University Press, Cambridge, 1989).

[116] S. W. Hawking, *Black hole explosions?*, Nature **248**, 30 (1974).

[117] S. W. Hawking, *Particle creation by black holes,* Commun. math. Phys. **43**, 199–220 (1975); Erratum: Commun. math. Phys. **46**, 206 (1976).

[118] L. Parker, *Particle creation in expanding universes*, Phys. Rev. Lett. **21**, 562 (1968).

[119] L. Parker, *Quantized fields and particle creation in expanding universes. I*, Phys. Rev. **183**, 1057 (1969).

[120] S. A. Fulling, *Remarks on positive frequency and Hamiltonians in expanding universes*, Gen. Relat. Gravit. **10**, 807–824 (1979).

[121] B. L. Hu, *Scalar waves in the mixmaster universe. II. Particle creation*, Phys. Rev. D **9**, 3263–3281 (1974).

[122] B. L. Hu, S. A. Fulling and L. Parker, *Quantized scalar fields in a closed anisotropic universe*, Phys. Rev. D **8**, 2377–2385 (1973).

[123] O. Obregon and M. Ryan, *Bianchi type IX cosmological models with spinor fields*, J. Math. Phys. **22**, 623 (1981).

[124] T. Damour and P. Spindel, *Quantum Einstein-Dirac Bianchi universes*, Phys. Rev. D **83**, 123520 (2011).

[125] L. Parker, *Quantized fields and particle creation in expanding universes. II*, Phys. Rev. D **3**, 346 (1971).

[126] G. B. Arfken, H. J. Weber and F. E. Harris, *Mathematical Methods for Physicists*, 7th. ed. (Academic Press, New York, 2012).

[127] A. Zee, *Group Theory in a Nutshell for Physicists* (Princeton University Press, Princeton, 2016).

[128] I. M. Gel'fand, R. A. Minlos, Z. Ya. Shapiro, *Representations of the rotation and Lorentz groups and their applications* (Pergamon Press, New York, 1963); translated from *Predstavleniya gruppy vrashchenii i gruppy Lorentsa*, originally published by Fizmatgiz, Moscow, 1958.

[129] E. P. Wigner, *Group Theory and its Application to the Quantum Mechanics of Atomic Spectra* (Academic Press, New York, 1959).

[130] R. U. Sexl and H. K. Urbantke, *Relativity, Groups, Particles: Special Relativity and Relativistic Symmetry in Field and Particle Physics* (Springer, Vienna, 2012).

[131] L. H. Ryder, *Quantum field theory*, 2nd ed. (Cambridge University Press, Cambridge, 1996).

[132] E. C. Kemble, *The fundamental principles of quantum mechanics* (McGraw-Hill, New York And London, 1937).

[133] J. N. Goldberg, A. J. Macfarlane, E. T. Newman, F. Rohrlich and E. C. G. Sudarshan, *Spin-s Spherical Harmonics and ð*, J. Math. Phys. **8**, 2155–2161 (1967).

[134] M. Tinkham, *Group Theory and Quantum Mechanics* (Dover Publications, Mineola, NY, 2003).

[135] A. S. Davydov, *Quantum Mechanics*, translated by D. Ter Haar (Pergamon Press, Oxford, 1965).

[136] L. D. Landau and E. M. Lifshitz, *Quantum Mechanics: Non-Relativistic Theory*, 3rd ed., Vol. 3, *Course of Theoretical Physics* (Butterworth-Heinemann, Oxford, 1981).

[137] J. J. Sakurai, *Modern Quantum Mechanics*, Revised ed. (Addison-Wesley, Boston, 1993).

[138] A. R. Edmonds, *Angular Momentum in Quantum Mechanics* (Princeton University Press, Princeton, NJ, 1957).

[139] B. L. Hu, *Scalar waves in the mixmaster Universe. I. The Helmholtz equation in a fixed background*, Phys. Rev. D **8**, 1048–1060 (1973).

[140] C. Van Winter, *The asymmetric rotator in quantum mechanics*, Physica **20**, 274–292 (1954).

[141] P. Atkins and R. Friedman, *Molecular Quantum Mechanics*, 3rd ed. (Oxford University Press, Oxford, 1999).

[142] J. S. Dowker and D. F. Pettengill, *The quantum mechanics of the ideal asymmetric top with spin*, J. Phys. A **7**, 1527–1536 (1974).

[143] H. Goldstein, *Classical Mechanics*, 2nd ed. (Addison-Wesley, 1980).

[144] L. D. Landau and E. M. Lifshitz, *Mechanics*, 3rd ed., Vol. 1, *Course of Theoretical Physics* (Butterworth-Heinemann, Oxford, 1976).

[145] G. W. King, R. M. Hainer and P. C. Crossl, *The Asymmetric Rotor I. Calculation and Symmetry Classification of Energy Levels*, J. Chem. Phys. **11**, 27–42 (1943).

[146] R. S. Mulliken, *Species classification and rotational energy level patterns of non-linear triatomic molecules*, Phys. Rev. **59**, 873, (1941).

[147] J. H. Van Vleck, *On σ-Type Doubling and Electron Spin in the Spectra of Diatomic Molecules*, Phys. Rev. **33**, 467 (1929).

[148] G. W. Gibbons and J. Richer, *Gravitational Creation of Odd Numbers of Fermions*, Phys. Lett. B **89**, 338–340 (1980).

[149] K. Kamada and J. Kume, *On the inefficiency of fermion level-crossing under the parity-violating spin-2 gravitational field*, arXiv:2404.19726.

[150] C. W. Misner, K. S. Thorne and J. A. Wheeler, *Gravitation* (Freeman, San Francisco, 1973).